Synthetic Strategies Toward Heterocyclic Seven Membered Ring Systems: Building Libraries of Privileged Scaffolds for Medicinal Chemistry and Forensic Analysis

A Dissertation
Presented to
The Academic Faculty

by

Ariel N. Parker

In Partial Fulfillment
of the Requirements for the Degree
Doctor of Philosophy in the
School of Chemistry and Biochemistry

Georgia Institute of Technology
December 2021

Synthetic Strategies Toward Heterocyclic Seven Membered Ring Systems: Building Libraries of Privileged Scaffolds for Medicinal Chemistry and Forensic Analysis

Approved by:

Dr. Stefan France, Advisor
School of Chemistry and Biochemistry
Georgia Institute of Technology

Dr. Will Gutekunst
School of Chemistry and Biochemistry
Georgia Institute of Technology

Dr. David Collard
School of Chemistry and Biochemistry
Georgia Institute of Technology

Dr. Elsa Reichmanis
Chemical and Biomolecular Engineering
Lehigh University

Dr. M.G. Finn
School of Chemistry and Biochemistry
Georgia Institute of Technology

Date Approved: December 02, 2021

This thesis is dedicated to my grandfather, the late Harold Cleveland. Although he wasn't a man of many words, in his own special way, he always let me know that he was proud. I wish he was here to witness and celebrate this accomplishment with me, but I just know he is smiling down from heaven. I pray that you are resting in the sweetest of heavenly peace.

ACKNOWLEDGEMENTS

It is a genuine pleasure to express my deep sense of thanks and gratitude to everyone who has contributed to this thesis. To my research advisor, Dr. Stefan France. I couldn't have asked for a better boss. During my time at tech, he has pushed me to "make it happen" and given me the space to explore new ideas and go after whatever professional opportunity I desired. Through his one-of-a-kind mentorship style, he has cultivated a highly supportive, respectful, fun, and diverse lab environment. It has truly been a privilege to be a part of the France lab. It is my hope that the France lab continues to thrive.

Next, I would like to thank my thesis committee, Dr. M.G. Finn, Dr, David Collard, Dr. Elsa Reichmanis, and Dr. Will Gutekunst, who have challenged me, helped me through scientific discussion, and ensured that I knew what was needed to succeed. In addition, I would like to express my thanks to the Georgia Tech NMR center staff, Dr. Leslie Gelbaum and Dr. Johannes Leisen for keeping the instruments in excellent condition and helping me troubleshoot experiments.

I would also like to express my gratitude to my lab mates, both past and present. To Dr. Ray Shenje and Dr. Cynthia Martin, I am grateful for their scientific contributions on the work we published together. I also would like to thank Dr. Corey Williams, Dr. Evelyn Ligon, Dr. Matthew Sandridge, Dr. George Ward, and Dr. Brett McLarney for their leadership, training, and answering all my questions during their time in the France lab. To the present members of the France lab Meghan Benda, Gabriel Faura, and Doris Chen, Elizabeth Jones, Nima Ronaghi, Shaoren Yuan, and Caria Evans, without each of you I don't know how I would have made it. The study sessions, the late nights spent in lab, the

scientific discussions, the lunches and dinners, the singing and dancing, and all the other highs and lows of graduate school would not have been the same without each of them. They have not only been amazing lab mates, but also friends. It has been a genuine pleasure working alongside them and witnessing their growth as chemists. I wish each of them the very best in their future endeavors.

Finally, I would like to thank my parents, Judge and Telida Parker, for the values they instilled in me that have enabled me to succeed. Their unconditional love, support, and encouragement have carried me not only throughout this journey, but also life. I cannot thank them enough for the sacrifices they have made for our family. To the rest of my family and friends, who have called, texted, feed, motivated, supported, and encouraged me throughout this journey, I sincerely thank you.

TABLE OF CONTENTS

LIST OF TABLES

LIST OF FIGURES

LIST OF SCHEMES

LIST OF SYMBOLS AND ABBREVIATIONS

$(COCl)_2$	oxalyl chloride
^{13}C	Carbon-13
^{19}F	Fluorine-19
^{1}H	Hydrogen-1
α	Alpha
Ac	Acetate
Ac_2O	Acetic anhydride
AcOH	Acetic acid
Ag_2CO_3	silver(I) carbonate
AgOTf	silver(I) trifluoromethanesulfonate
$Al(OTf)_3$	Aluminum(III) trifluoromethanesulfonate
aq	Aqueous
Ar	Aryl
Au	Gold
AuCl	Gold Chloride
β	Beta
$B(OH)_2$	boronic acid
Br	bromo

C	Carbon
$Ca(NTf_2)_2$	Calcium(II) bis(trifluoromethanesulfonimide)
CCK-A	Cholecystokinin receptor A
CH_2Cl_2	Dichloromethane
CH_3CN	Acetonitrile
Cl	Chloro
CO	Carbon monoxide
COOEt	Ethyl ester
$CuCl_2$	Copper (II) Chloride
$Cu(OAc)_2$	Copper(II) acetate
DCM	Dichloromethane
DMF	Dimethylformamide
Et	Ethyl
eq.	Equivalent
EWG	Electron withdrawing group
$Ga(OTf)_3$	Gallium(III) trifluoromethanesulfonate
H	Hydrogen
h	hour
HCl	Hydrochloric Acid

$Hf(OTf)_4$	Hafnium(IV) trifluoromethanesulfonate
IR	Infrared spectroscopy
L	Ligand
LC	Liquid Chromatography
LHMDS	Lithium bis(trimethylsilyl)amide
M	Metal
M	Molar
m	*meta*
Me	Methyl
MeOAc	Methyl Acetate
$Mg(OTf)_2$	Magnesium(II) trifluoromethanesulfonate
mol %	Mole percent
MS	Mass Spectroscopy
MW	Microwave
n-Bu_4NPF_6	Tetrabutylammoniumhexafluorophosphate
NaOH	Sodium hydroxide
NMR	Nuclear magnetic resonance
o	ortho
OMe	Methoxy

p	*para*
p-TsOH	*p*-Toluenesulfonic acid
p-QMs	*Para*-quinone methide
PG	Protecting group
Ph	Phenyl
Pd	Palladium
PPh_3	Triphenylphosphine
RCM	Ring-closing metathesis
rt	Room temperature
$Sc(OTf)_3$	Scandium(III) trifluoromethanesulfonate
TFA	Trifluoroacetic acid
THF	Tetrahydrofuran
$Yb(OTf)_3$	Ytterbium(III) trifluoromethanesulfonate
$Zn(OTf)_2$	Zinc(II) trifluoromethanesulfonate

SUMMARY

Natural products are often the inspiration for many pharmaceutical compounds as they are found to have drug-like properties. Many times, these compounds exhibit structural commonalities and are therefore referred to as "privileged structures." Synthetic organic chemists have devoted significant time and effort into developing efficient methods to access these privileged scaffolds for the construction of diverse libraries. This thesis explores novel synthetic strategies to access the privileged scaffolds: cyclohepta[*b*]indole and the 1,4-benzodiazepine, flubromazepam. The protocols designed to access these heterocyclic seven-membered ring systems include: 1) a formal [5+2] cycloaddition between alkenes and indole fused alkylidenes, 2) a Friedel-Crafts transformation and 3) a nucleophilic arylation. Additionally, through the development of these modular protocols new discoveries were made providing new insights in medicinal chemistry and forensic analysis.

CHAPTER 1. INTRODUCTION

1.1 Privileged Scaffolds

Small organic molecules have proven to be influential tools in biology and medicine by functioning as both therapeutics and probes that help explain the macromolecules regulating biological processes.[1] Often times, therapeutics are designed based off of natural products, or the secondary metabolites that are produced as a result of biological processes in living organisms. Natural products are frequently extracted from the cells, tissues, and secretions of microorganisms, as well as plants and animals and are believed to be evolutionary designed defense mechanisms against competing organisms. Typically, these natural products extracted from their respective sources contain a range of structurally diverse and novel chemical compounds providing scientists with a host of molecules with drug-like properties such as anti-bacterial, anti-cancer, anti-inflammatory, anti-parasitic, and anti-viral. Structurally, these compounds are also known to contain particularly complex molecular scaffolds, multiple and biologically important stereocenters, and a host of functional groups which covers a wide range of chemical space. Factors such as structural complexity, toxicity, and adverse pharmacokinetics often limit the clinical potential of natural products on their own and, therefore, structural modification is often required.[2] To this end, synthetic chemist often design libraries of compounds based off natural products in search of new drug candidates.[3] Furthermore, examination of libraries of natural products that have been isolated and characterized often reveals structural commonalities that are referred to as "privileged structures[4]."

The term "privileged structures" was first proposed by Evans and co-workers[5] in 1988 as a single molecular framework "capable of providing useful ligands for more than one receptor." Originally, Evans linked this concept to benzodiazepines and their ability to bind to the cholecystokinin (CCK-A) receptor A[6]. Since then, this term has taken on a different meaning than the original concept and now often refers to multiple molecules with the same scaffold having biological activity. There are many examples of privileged structures that include: β-lactams[7], flavonoids[8], chalcones[9], benzodiazepines[10], indoles[11], biaryls[12], and quinolines[13]. This list is by no means exhaustive as scientist have only discovered a fraction of chemical space and new structures are being identified every day. Thus, chemists have taken advantage of the unknown chemical space surrounding the principle of privileged scaffolds through the isolation and synthesis of natural products in addition to altering these scaffolds to create new analogues that impart improved bioactivity. This expansion of the idea of privileged structures has led to the construction of libraries based off privileged scaffolds that not only introduce new technologies and reactions of broad scope but also take into consideration drug-like parameters, the structure activity relationship of the scaffold, and effective screening test.

1.2 This Thesis: Featured Heteroaromatic Privileged Scaffold

This thesis will explore synthetic strategies established to access the privileged scaffolds: cyclohepta[*b*]indole and the 1,4-benzodiazepine, flubromazepam. These targets are considered privileged as they are known to interact directly with some specific binding site within the active site. Although biologically active, these heteroaromatic systems present unique synthetic challenges centered around construction of the seven membered ring. This introductory chapter will provide a brief a summary of the methods previously

established toward synthesizing these targets whereas the remaining chapters will investigate novel strategies used to build libraries pertaining to these privileged structures for the purposes of medicinal chemistry and forensic analysis.

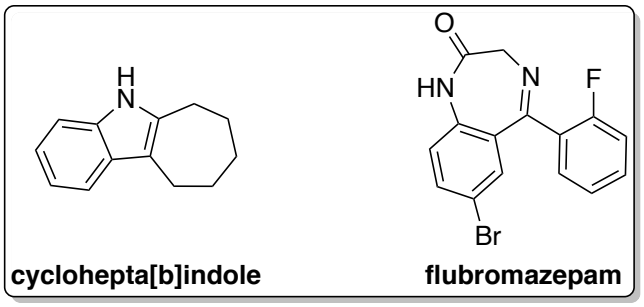

Figure 1.1 Featured Privileged Scaffolds

1.3 Cyclohepta[*b*]indole

The cyclohepta[*b*]indole motif is an indole alkaloid that represents a privileged scaffold in medicinal chemistry for its broad spectrum of biological activity. The intricate architecture of cyclohepta[*b*]indole natural products as well as their pharmaceutical derivatives has inspired the development of synthetic methods aimed at creating libraries of structurally diverse cyclohepta[*b*]indole analogues. Here, a variety of methods targeting cyclohepta[*b*]indoles published throughout the literature will be discussed while Chapter 2 will focus on the synthetic development of [5+2] cycloaddition reactions regarding the privileged scaffold.

1.3.1 Synthetic Approaches Toward Cyclohepta[b]indoles

So-called common rings sizes (three to six membered rings) have been extensively studied throughout history and thus have general methods for their construction. Contrarily,

due to entropy and enthalpy factors it is harder to predict reactivity and find reaction synthons to construct seven membered rings.[14] Consequently, many methods associated with the construction of seven-membered rings are specific to the cycloheptanoid system being investigated, as in the case of cyclohepta[*b*]indoles. Synthetic chemists have found that approaches such as metal-mediated intramolecular cyclization cascades, olefin metathesis, [3,3]-sigmatropic rearrangements with divinylcyclopropanes, and [4+3]-cycloadditions have been useful and efficient procedures to construction cyclohepta[*b*]indoles.

1.3.1.1 Metal-mediated Intramolecular Cyclization Cascades Toward Cyclohepta[*b*]indoles

Widenhoefer and co-workers[15] utilized a metal-mediated intramolecular cyclization cascade through the palladium (II)-catalyzed tandem cyclization/carboalkoxylation of alkenyl indoles to produce the cyclohepta[b]indole motif in 74% yield (Scheme 1.1A). This reaction is proposed to proceed through coordination of the palladium species with the alkenyl indole **1** to form complex **2** followed by subsequent loss of HCl to form palladium alkyl intermediate **3**. Alpha-migratory insertion of CO into the Pd-C bond leads to the formation of halo acylpalladium species **4** which is then undergoes methanolysis to give the cyclohepta[*b*]indole product **5** and regenerate the Pd-catalyze upon addition of $CuCl_2$. Another example of this method can be seen in Ishikura and Kato's[16] development of cycloalkyl[*b*]indoles **7** through a Pd-catalyzed intramolecular cyclization via the alkyl migration process in indolylborates **6** (Scheme 1.1B). Unfortunately, these methods aren't solely focused and building libraries of

cyclohepta[*b*]indoles and only showcase their synthesis as a complement to the general method.

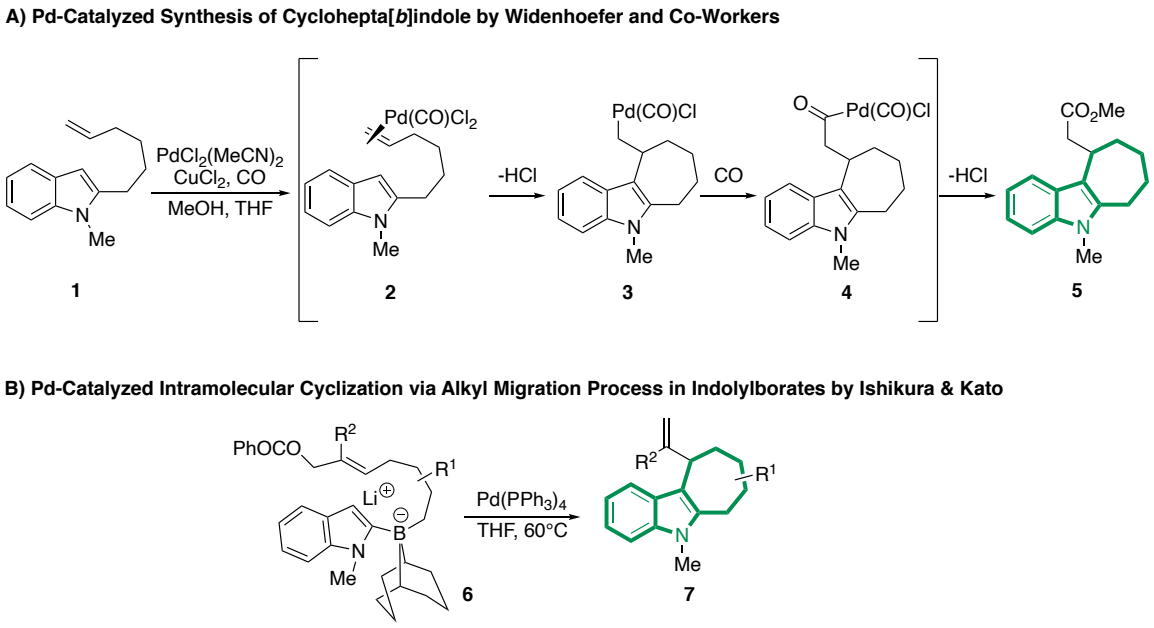

Scheme 1.1 Representative Examples of Pd-Catalyzed Syntheses Toward Cyclohepta[*b*]indole

1.3.1.2 Ring-Closing Metathesis Toward Cyclohepta[*b*]indoles

Ring-closing metathesis (RCM) reactions are powerful tools used to access carbocyclic and heterocyclic compounds of many ring sizes.[17] RCM reactions are generally Ru-catalyzed and proceed through a metallacyclobutane. This method tends to circumvent the entropy and enthalpy factors that limit seven membered ring syntheses. Thus, the RCM reaction has been found to be useful in building cyclohepta[*b*]indoles. One example of this method was established by Ramasastry and co-workers[18] where they generated indolyl diene **8** via a two-step process and used Grubbs I catalyst to catalyze the RCM producing tetrahydrocyclohepta[*b*]indoles **9** (Scheme 1.2A). In route to the tetracyclic ring system of the cyclohepta[*b*]indole natural product, ervitsine, Alonso and co-workers[19] demonstrated

an indole-templated ring closing metathesis to construct the seven-membered ring segment followed by a vinyl halide Heck reaction to generate the piperidine ring (Scheme 1.2B). These two examples show the power and simplicity of the RCM reaction to efficiently generate the seven-membered ring of the cyclohepta[*b*]indole. However, this method tends to generate cyclohepta[*b*]indoles that lack functionality around the seven-membered ring.

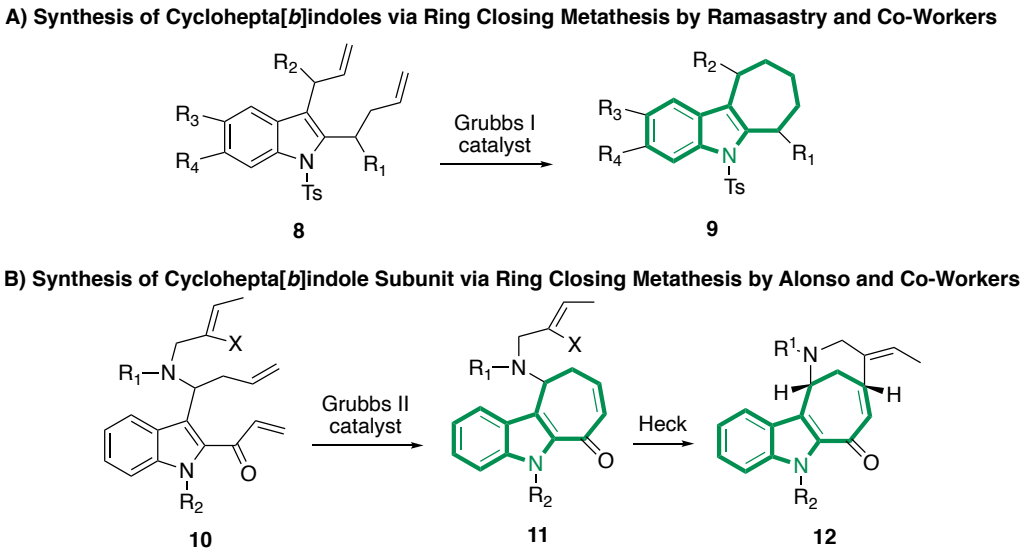

Scheme 1.2 Representative Examples Cyclohepta[*b*]indole Synthesis via RCM

1.3.1.3 Cyclohepta[*b*]indoles via Sigmatropic Rearrangements

The construction of seven-membered rings within natural products via divinylcyclopropane rearrangements have been used considerably throughout the literature.[20] Sinha and co-workers[21] took advantage of this method and adapted it to the formation of cyclohepta[*b*]indoles. A mixture of 2,3-disubstituted indoles **14** was formed from the reaction of alkynylaniline **13** with 3,4-dichloro-1-butene in the presence of a Pd(II)-catalyst. When R^x is an alkyl group, treatment of **14** with NaOH lead to the *in situ* generation of divinylcyclopropane intermediate **I**. Finally, subsequent thermal [3,3]-

sigmatropic rearrangement of **I** provided 8 examples in up to 81% yield of tetrahydrocyclohepta[*b*]indole derivatives **15**. To complement this method, Gaich and co-workers[22], developed a similar approach accessing the divinylcyclopropane intermediate **II** through the oxidation and olefination of indolyl chiral cyclopropyl alcohol **16**. With the addition of heat, rearrangement occurred and produced (S)-SIRT1-inhibitor IV, a pharmaceutically relevant cyclohepta[*b*]indole.

A) Synthesis of Cyclohepta[*b*]indoles via *In Situ* Generated Divinylcyclopropane Intermediates by Sinha and Co-Workers

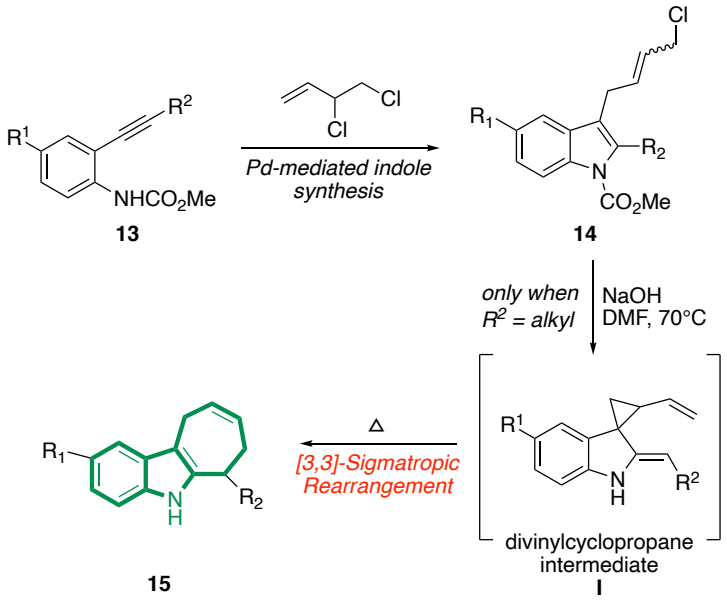

B) Enantioselective Synthesis of Cyclohepta[*b*]indoles via *In Situ* Generated Divinylcyclopropane Intermediates by Gaich and Co-Workers

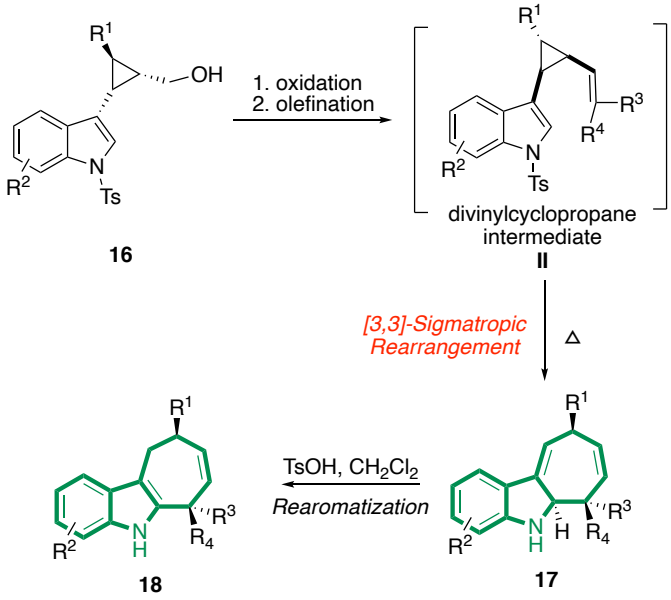

Scheme 1.3 Cyclohepta[*b*]indole Synthesis via Divinylcyclopropane Intermediates

1.3.1.4 [4+3]-Cycloaddition Reactions Toward Cyclohepta[*b*]indoles

Of the methods mentioned, cycloaddition reactions toward seven-membered rings have proven to be the most efficient and atom-economical as it allows the simultaneous or nearly simultaneous formation of two C-C bonds in a single step with regio- and/or diastereoselective control. Generating 4-carbon and 3-carbon synthons for this transformation is generally much easier than finding suitable 5-carbon and 2-carbon synthons for [5+2]-cycloadditions, thus methods directed at cyclohepta[*b*]indoles through [4+3]-cycloadditions have been studied more extensively. [4+3]-cycloaddition methods developed toward the synthesis of cyclohepta[*b*]indoles generally involve *in situ* generated highly reactive intermediates such as indolyl carbocations,[23a,d,e,h] oxyallyl cations,[23f] and metal carbenes (Scheme 1.4).[23b,c,g] As shown in numerous examples throughout the literature, indolyl carbocations are commonly formed through the acid catalyzed dehydration of indolyl alcohols and subsequently treated with a 4-carbon synthons such as dienes and, in a special case, Nazarov reagents. Oxyallyl cations are used to a lesser extent, however, Hsung and co-workers[23f] were able to generate this intermediate starting with *N*-arylallenamides. Upon treatment with Murray's reagent and zinc chloride the oxyallyl cation is formed and reacted with furan to make the cycloadduct. This adduct undergoes cyclization and elimination to give the desired cyclohepta[*b*]indole product. Lastly, the use of metal carbene intermediates toward the synthesis of cyclohepta[*b*]indoles typically involve the use of vinyl metal carbenes (derived from vinyl diazo compounds), vinyl Fischer carbenes and vinyl gold carbene (derived from propargylic esters and/or propargylic) reacted with a diene. These recent examples show the synthetic power of cycloaddition reactions toward constructing seven-membered rings as in

cyclohepta[*b*]indoles. Chapter 2 will further investigate the formal [5+2]-cycloaddition reaction toward the synthesis of highly functionalized cyclohepta[b]indoles.

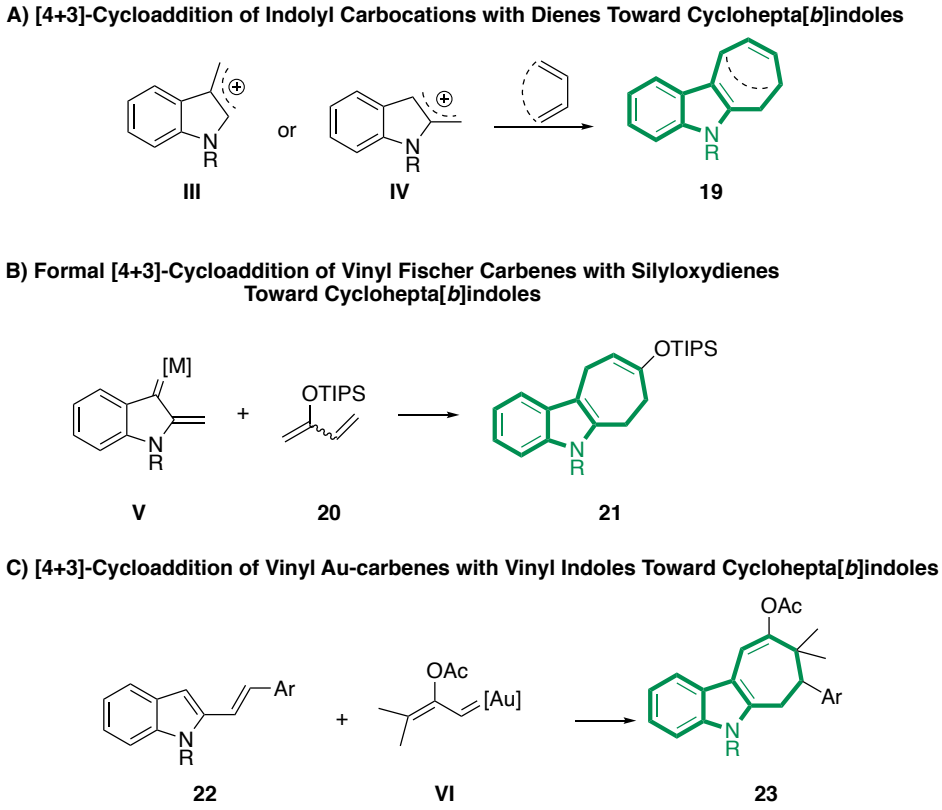

Scheme 1.4 [4+3]-Cycloaddition Examples Toward Cyclohepta[*b*]indoles

1.4 Flubromazepam: A Synthetic 1,4-benzodiazepine

The well-established utility of 1,4-benzodiazepines as privileged scaffolds in medicinal chemistry has raised a need for preparative methods that allow access to large numbers of structurally diverse compounds suitable for drug discovery.[10] As a result, many research facilities and pharmaceutical companies have synthesized various benzodiazepine analogues as drug candidates as well as published their syntheses and basic animal testing data in the literature.[24] With no approved medicinal use and no federal regulations,

benzodiazepines such as flubromazepam was one of the first designer benzodiazepines on the recreational drug market.

The most extensively used method for preparing flubromazepam and other 1,4-benzodiazepines was established by Sternbach and coworkers[25] in 1962 through *ortho*-aminobenzophenone (Scheme 1.5). Their synthesis showcased the formation of *ortho*-aminobenzophenone intermediates through the Friedel-Crafts acylation of *p*-substituted anilines with *o*-substituted benzoyl chlorides. Once formed, the respective *ortho*-aminobenzophenone was treated with haloacetyl halide to afford the amide followed by addition of ammonia to first displace the halide giving the glycinamide, then cyclization by imine formation giving the respective benzodiazepine. This study also proved that benzodiazepines could be formed via a one pot reaction upon treatment of *ortho*-aminobenzophenone with glycine ester hydrochloride in pyridine.

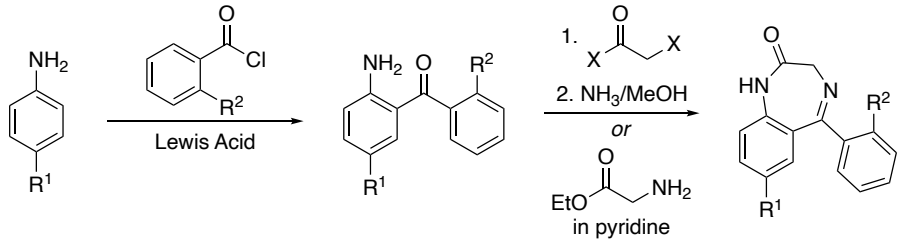

Scheme 1.5 Sternbach's Synthesis of Benzodiazepines

Although this method allowed Sternbach and coworkers to produce a library of 50 benzodiazepine derivatives, the Friedel-Crafts chemistry failed to give any further structural diversity due to the electronic preferences that the 4-EWG-substituted anilines impose on the acylation. As a result, the key *ortho*-aminobenzophenone intermediate is often limited to EWGs (bromo-, chloro-, and nitro-substituents) in the *para* position which

structurally restricts the 1,4-benzodiazepines to only a few substitution patterns and regio- or positional isomers. The challenges associated with accessing structurally diverse 1,4-benzodiazepines through Sternbach and coworker's Friedel-Crafts method has created room for additional methods to access the key *ortho*-aminobenzophenone intermediate that tolerate diverse functionality and positional isomers of 1,4-benzodiazepines.

1.4.1 Alternative Routes to the Key Benzophenone Intermediate

Previously in the France lab[26], several alternative approaches to access the key benzophenone intermediate for the synthesis of the twelve positional isomers of flubromazepam were attempted. The first approach was inspired by Li and Kwong's[27] Pd-catalyzed oxidative C-H bond coupling of acetanilides and aldehydes. This methodology showcased 9 examples of the benzophenone products with halogenated substituents in the *ortho*- and *meta*- positions. Attempts to extend this methodology to access the 12 positional isomers of flubromazepam failed when using the corresponding bromoanilines and fluorobenzaldehydes likely due to the deactivation of the system by the additional bromine.

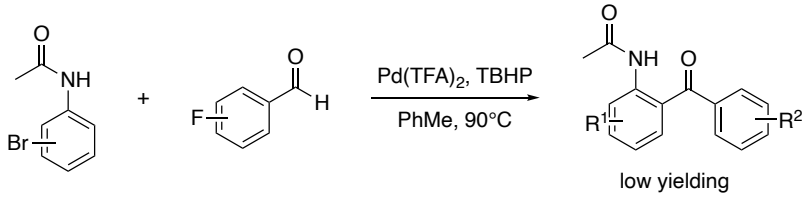

Scheme 1.6 Attempted Pd-catalyzed Oxidative C-H bond Coupling of Acetanilides and Aldehydes

Another attempted synthesis was motivated by Qi and co-worker's[28] successful Ag-catalyzed decarboxylative acylation of arylglyoxylic acids with arylboronic acids producing unsymmetrical benzophenones. It was envisioned that respective bromoisatin

precursor could be hydrolyzed to the corresponding glyoxylic acid then subsequently treated with the correctly substituted arylboronic acid to access the key aminobenzophenone intermediates. This strategy was particularly chosen based off of the methods tolerance for both halo and amino-substituted phenylglyoxylic acids and boronic acids, but unfortunately no desired product was formed.

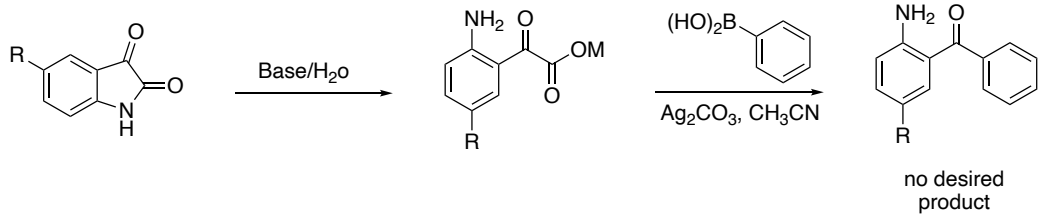

Scheme 1.7 Attempted Ag-catalyzed Decarboxylative Acylation of Arylglyoxylic Acids with Arylboronic Acids

Following the previous failed attempts, a new strategy was devised involving the benzoylation of *in situ* generated fluoro-substituted phenyl-lithium reagents with 2-amino-X-bromo-*N*-methoxy *N*-methylbenzamides. This strategy will be discussed in greater detail in Chapter 3 but was successful in accessing the 2-amino-X-bromo-X′-fluorobenzophenone precursors in up to 78% yield for nine of the twelve positional isomers of flubromazepam. Chapter 3 will focus on the synthetic strategy toward the key benzophenone intermediate for the remaining three (6,X')-flubromazepam positional isomers to complete the set and set the stage for forensic analysis.

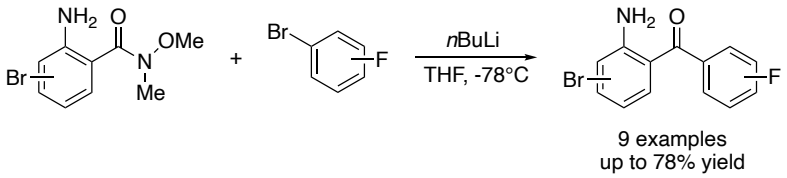

Scheme 1.8 Successful Synthesis of 2-amino-X-bromo-X′-fluorobenzophenone Precursors via Benzoylation

1.5 Thesis Outline

This thesis consists of synthetic strategies established to access a library of privileged scaffolds pertaining to the heterocyclic seven-membered ring systems of the cyclohepta[*b*]indole and the 1,4-benzodiazepine, flubromazepam. Previously established approaches to these privileged scaffolds have been highlighted along with the advantages and disadvantages of each method. Hypotheses and synthetic strategies will be discussed as well as experimental challenges and ways to circumvent each issue.

Chapter 2 will focus on the importance and synthesis of the cyclohepta[*b*]indole motif. A literature survey shows a variety of general methods to access this core structure but lacks in [5+2]-cycloaddition examples. We address this issue by investigating indolyl alkylidene β-ketoesters as potential building blocks based off of an analogous system used in our successful synthesis of azepino[1,2-*a*]indoles. This study was found to provide access to the cyclohepta[*b*]indole scaffold through the calcium-catalyzed, formal [5 + 2] cycloaddition of indolyl alkylidene β-ketoesters with mono- and disubstituted aryl olefins. Unanticipated chemodivergence with phenyl vinyl sulfide/ether revealed a double [5 + 2] cycloaddition cascade providing ethano-bridged cyclohepta[b]indoles. Overall, the method's highlights include: (1) use of a green, calcium-based catalyst (2.5 mol %

loading); (2) reaction times under 1 h; (3) mild reaction conditions; (4) substrate-derived chemodivergence; (5) functional group tolerance; and (6) examples of derivatization.

Chapter 3 will address the mounting concern among forensic examiners regarding the emergence of positional isomers as technically legal alternatives to scheduled benzodiazepines such as flubromazepam. Flubromazepam was identified by the Drug Enforcement Administration for future scheduling and has encouraged the preemptive synthesis of analogs as standards. Thus, nine of the twelve possible flubromazepam isomers were synthesized, however, the three (6,X')-isomers proved inaccessible via that approach. Through a redesigned synthetic approach, the remaining three isomers were obtained; thus, completing the set and enabling future forensic analysis.

In Chapter 4, traditional forensic analysis techniques such as liquid chromatography-mass spectroscopy (LC-MS), infrared spectroscopy (IR), and proton, carbon, and fluorine nuclear magnetic resonance (^{1}H, ^{13}C, ^{19}F NMR) were used for the structural identification and validation of the three newly synthesized (6,X')-flubromazepam isomers. The characterization data of the 3 isomers were also to compared to the parent in hopes that each isomer presents a unique analytical profile for the purpose of differentiation.

Finally, Chapter 5 will summarize the findings of each chapter and offer future outlooks based off results obtain throughout this work.

1.6 References

(1) (a) Newman, D. J.; Cragg, G. M. Natural Products as Sources of New Drugs from 1981 to 2014. *J. Nat. Prod.* **2016**, *79* (3), 629–661. (b) Lachance, H.; Wetzel, S.; Kumar, K.; Waldmann, H. Charting, Navigating, and Populating Natural Product Chemical Space for Drug Discovery. *J. Med. Chem.* **2012**, *55* (13), 5989–6001. (c) Stockwell, B. R. Exploring Biology with Small Organic Molecules. *Nature* **2004**, *432* (7019), 846–854.

(2) Gerry, C. J.; Schreiber, S. L. Chemical Probes and Drug Leads from Advances in Synthetic Planning and Methodology. *Nat. Rev. Drug Discov.* **2018**, *17* (5), 333–352.

(3) Quinn, R. J.; Carroll, A. R.; Pham, N. B.; Baron, P.; Palframan, M. E.; Suraweera, L.; Pierens, G. K.; Muresan, S. Developing a Drug-like Natural Product Library. *J. Nat. Prod.* **2008**, *71* (3), 464–468.

(4) Welsch, M. E.; Snyder, S. A.; Stockwell, B. R. Privileged Scaffolds for Library Design and Drug Discovery. *Curr. Opin. Chem. Biol.* **2010**, *14* (3), 347–361.

(5) Evans, B. E.; Rittle, K. E.; Bock, M. G.; DiPardo, R. M.; Freidinger, R. M.; Whitter, W. L.; Lundell, G. F.; Veber, D. F.; Anderson, P. S.; Chang, R. S. L.; et al. Methods for Drug Discovery: Development of Potent, Selective, Orally Effective Cholecystokinin Antagonists. *J. Med. Chem.* **1988**, *31* (12), 2235–2246.

(6) Evans, B. E.; Bock, M. G.; Rittle, K. E.; DiPardo, R. M.; Whitter, W. L.; Veber, D. F.; Anderson, P. S.; Freidinger, R. M. Design of Potent, Orally Effective,

Nonpeptidal Antagonists of the Peptide Hormone Cholecystokinin. *Proc. Natl. Acad. Sci. U. S. A.* **1986**, *83* (13), 4918–4922.

(7) Fisher, J. F.; Mobashery, S. Chapter 3 The β-Lactam (Azetidin-2-One) as a Privileged Ring in Medicinal Chemistry. In *Privileged Scaffolds in Medicinal Chemistry: Design, Synthesis, Evaluation*; The Royal Society of Chemistry, 2016; pp 64–97.

(8) Boniface, P. K.; Elizabeth, F. I. Flavones as a Privileged Scaffold in Drug Discovery: Current Developments. *Curr. Org. Synth.* **2019**, *16* (7), 968–1001. (b) Singh, M.; Kaur, M.; Silakari, O. Flavones: An Important Scaffold for Medicinal Chemistry. *Eur. J. Med. Chem.* **2014**, *84*, 206–239.

(9) Zhuang, C.; Zhang, W.; Sheng, C.; Zhang, W.; Xing, C.; Miao, Z. Chalcone: A Privileged Structure in Medicinal Chemistry. *Chem. Rev.* **2017**, *117* (12), 7762–7810.

(10) (a) Smith, S. G.; Sanchez, R.; Zhou, M.-M. Privileged Diazepine Compounds and Their Emergence as Bromodomain Inhibitors. *Chem. Biol.* **2014**, *21* (5), 573–583. (b) Bunin, B. A.; Plunkett, M. J.; Ellman, J. A. The Combinatorial Synthesis and Chemical and Biological Evaluation of a 1,4-Benzodiazepine Library. *Proc. Natl. Acad. Sci.* **1994**, *91* (11), 4708 LP – 4712. (c) Kaur, N.; Kishore, D. Synthetic Strategies Applicable in the Synthesis of Privileged Scaffold: 1,4-Benzodiazepine. *Synth. Commun.* **2014**, *44* (10), 1375–1413.

(11) (a) Wan, Y.; Li, Y.; Yan, C.; Yan, M.; Tang, Z. Indole: A Privileged Scaffold for the Design of Anti-Cancer Agents. *Eur. J. Med. Chem.* **2019**, *183*, 111691. (b) Sravanthi, T. V; Manju, S. L. Indoles — A Promising Scaffold for Drug Development. *Eur. J. Pharm. Sci.* **2016**, *91*, 1–10.

(12) (a) Sahn, J. J.; Su, J. Y.; Martin, S. F. Facile and Unified Approach to Skeletally Diverse, Privileged Scaffolds. *Org. Lett.* **2011**, *13* (10), 2590–2593. (b) Yuan, S.; Chang, J.; Yu, B. Construction of Biologically Important Biaryl Scaffolds through Direct C–H Bond Activation: Advances and Prospects. *Top. Curr. Chem.* **2020**, *378* (2), 23.

(13) (a) Musiol, R. An Overview of Quinoline as a Privileged Scaffold in Cancer Drug Discovery. *Expert Opin. Drug Discov.* **2017**, *12* (6), 583–597. (b) Yadav, P.; Shah, K. Quinolines, a Perpetual, Multipurpose Scaffold in Medicinal Chemistry. *Bioorg. Chem.* **2021**, *109*, 104639.

(14) de Oliveira, K. T.; Servilha, B. M.; de C. Alves, L.; Desiderá, A. L.; Brocksom, T. J. Chapter 14 - The Synthesis of Seven-Membered Rings in Natural Products; Atta-ur-Rahman, B. T.-S. in N. P. C., Ed.; Elsevier, 2014; Vol. 42, pp 421–463.

(15) Liu, C.; Widenhoefer, R. A. Palladium-Catalyzed Cyclization/Carboalkoxylation of Alkenyl Indoles. *J. Am. Chem. Soc.* **2004**, *126* (33), 10250–10251.

(16) Ishikura, M.; Kato, H. A Synthetic Use of the Intramolecular Alkyl Migration Process in Indolylborates for Intramolecular Cyclization: A Novel Construction of Carbazole Derivatives. *Tetrahedron* **2002**, *58* (49), 9827–9838.

(17) General reviews, see: (a)Handbook of Metathesis; Grubbs, R. H., Ed.; Wiley-VCH: Weinheim, 2003; Vol. 2; (b) Deiters, A.; Martin, S. F. Chem. Rev. **2004**, *104*, 2199-2238.

(18) Mishra, U. K.; Yadav, S.; Ramasastry, S. S. V. One-Pot Multicatalytic Approaches for the Synthesis of Cyclohepta[b]Indoles, Indolotropones, and Tetrahydrocarbazoles. *J. Org. Chem.* **2017**, *82* (13), 6729–6737.

(19) Bennasar, M. L.; Zulaica, E.; Solé, D.; Alonso, S. Sequential Ring-Closing Metathesis-Vinyl Halide Heck Cyclization Reactions: Access to the Tetracyclic Ring System of Ervitsine. *Tetrahedron* **2012**, *68* (24), 4641–4648.

(20) Krüger, S.; Gaich, T. Recent Applications of the Divinylcyclopropane–Cycloheptadiene Rearrangement in Organic Synthesis. *Beilstein J. Org. Chem. 1014* **2014**, *10* (1), 163–193.

(21) Chakraborty, A.; Goswami, K.; Adiyala, A.; Sinha, S. Syntheses of Spiro[Cyclopent[3]Ene-1,3′-Indole]s and Tetrahydrocyclohepta[b]Indoles from 2,3-Disubstituted Indoles through Sigmatropic Rearrangement. *European J. Org. Chem.* **2013**, *2013* (31), 7117–7127.

(22) Gritsch, P. J.; Stempel, E.; Gaich, T. Enantioselective Synthesis of Cyclohepta[b]indoles: Gram-Scale Synthesis of (S)-SIRT1-Inhibitor IV. Org. Lett. 2013, 15, 5472−5475.

(23) For examples of [4 + 3] cycloadditions toward cyclohepta[b] indoles: (a) Gelis, C.; Levitre, G.; Merad, J.; Retailleau, P.; Neuville, L.; Masson, G. Highly Diastereo- and

Enantioselective Synthesis of Cyclohepta[*b*]Indoles by Chiral-Phosphoric-Acid-Catalyzed (4+3) Cycloaddition. *Angew. Chemie - Int. Ed.* **2018**, *57* (37), 12121–12125. (b) Xu, G.; Chen, L.; Sun, J. Rhodium-Catalyzed Asymmetric Dearomative [4 + 3]-Cycloaddition of Vinylindoles with Vinyldiazoacetates: Access to Cyclohepta[b]Indoles. *Org. Lett.* **2018**, *20* (11), 3408–3412. (c) Li, Y.; Zhu, C. Z.; Zhang, J. Gold-Catalyzed [4+3] Cycloaddition/C–H Functionalization Cascade: Regio- and Diastereoselective Route to Cyclohepta[*b*]Indoles. *European J. Org. Chem.* **2017**, *2017* (45), 6609–6613. (d) Zhang, H. H.; Zhu, Z. Q.; Fan, T.; Liang, J.; Shi, F. Intermediate-Dependent Unusual [4+3], [3+2] and Cascade Reactions of 3-Indolylmethanols: Controllable Chemodivergent and Stereoselective Synthesis of Diverse Indole Derivatives. *Adv. Synth. Catal.* **2016**, *358* (8), 1259–1288. (e) Zhang, J.; Shao, J.; Xue, J.; Wang, Y.; Li, Y. One Pot Hydroamination/[4 + 3] Cycloaddition: Synthesis towards the Cyclohepta[*b*]Indole Core of Silicine and Ervatamine. *RSC Adv.* **2014**, *4* (109), 63850–63854. (f) He, S.; Hsung, R. P.; Presser, W. R.; Ma, Z. X.; Haugen, B. J. An Approach to Cyclohepta[b]Indoles through an Allenamide (4 + 3) Cycloaddition-Grignard Cyclization-Chugaev Elimination Sequence. *Org. Lett.* **2014**, *16* (8), 2180–2183. (g) Shu, D.; Song, W.; Li, X.; Tang, W. Rhodium- and Platinum-Catalyzed [4+3] Cycloaddition with Concomitant Indole Annulation: Synthesis of Cyclohepta[*b*]Indoles. *Angew. Chemie Int. Ed.* **2013**, *52* (11), 3237–3240. (h) Han, X.; Li, H.; Hughes, R. P.; Wu, J. Gallium(III)-Catalyzed Three-Component (4+3) Cycloaddition Reactions. *Angew. Chemie - Int. Ed.* **2012**, *51* (41), 10390–10393.

(24) Moosmann, B.; King, L. A.; Auwärter, V. Designer Benzodiazepines: A New Challenge. *World Psychiatry*. 2015, p 248.

(25) Sternbach, L. H.; Fryer, R. I.; Metlesics, W.; Reeder, E.; Sach, G.; Saucy, G.; Stempel, A. Quinazolines and 1, 4-Benzodiazepines. VI. 1a Halo-, Methyl-, and Methoxy-Substituted 1, 3-Dihydro-5-Phenyl-2H-1, 4-Benzodiazepin-2-Ones1b, C. *J. Org. Chem.* **1962**, *27* (11), 3788–3796.

(26) Ligon, E. S.; Nawyn, J.; Jones, L. V; Allred, B. M.; Reinhardt, D. V; France, S. Synthesis of Flubromazepam Positional Isomers for Forensic Analysis. *J. Org. Chem.* **2019**, *84* (16), 10280–10291.

(27) Wu, Y.; Li, B.; Mao, F.; Li, X.; Kwong, F. Y. Palladium- Catalyzed Oxidative C−H Bond Coupling of Steered Acetanilides and Aldehydes: A Facile Access to ortho-Acylacetanilides. Org. Lett. 2011, 13, 3258−3261.

(28) Cheng, K.; Zhao, B.; Qi, C. Silver-catalyzed Decarboxylative Acylation of Arylglyoxylic Acids with Arylboronic Acids. RSC Adv. 2014, 4, 48698−48702.

CHAPTER 2. FORMAL [5+2] CYCLOADDITION TOWARD HIGHLY FUNCTIONALIZED CYCLOHEPTA[*B*]INDOLE DERIVATIVES[*†]

2.1 Significance of Cyclohepta[*b*]indole Framework

The cyclohepta[*b*]indole is a 6,5,7-tricyclic indole-fused seven-membered ring system that represents a "privileged scaffold" in the chemical and pharmaceutical industries (Figure 1).[1] The cyclohepta[*b*]indole motif is a common core found in a number of bioactive naturally occurring indole alkaloids such as actinophyllic acid **2** (fibrinolysis inhibitor),[2] exotine B **5** (inhibitor of liposaccharide-induced nitric oxide production),[3] and methuenine **6** (anticholinergic agent).[4] The pharmaceutical industry has also targeted this privileged scaffold in a series of molecular targets that show inhibitory biological activity against histone deacetylase SIRT **3**,[5] adipocyte fatty-acid binding protein **4**,[6] and leukotriene B4 production **7**.[7] Due to a wide array of biological activities that cyclohepta[*b*]indole-containing molecules possess, significant interest from both medicinal and synthetic organic chemists has resulted in numerous patents being issued within the past decade as well as a number of synthetic approaches to the scaffold being reported.[8]

[*]Work on the catalytic formal [5+2]-cycloaddition approach for the synthesis of cyclohepta[*b*]indoles was performed in collaboration with Ray Shenje and Cynthia Martin.
[†] Published in Org. Lett. **2019**, 21, 18, 7268–7273

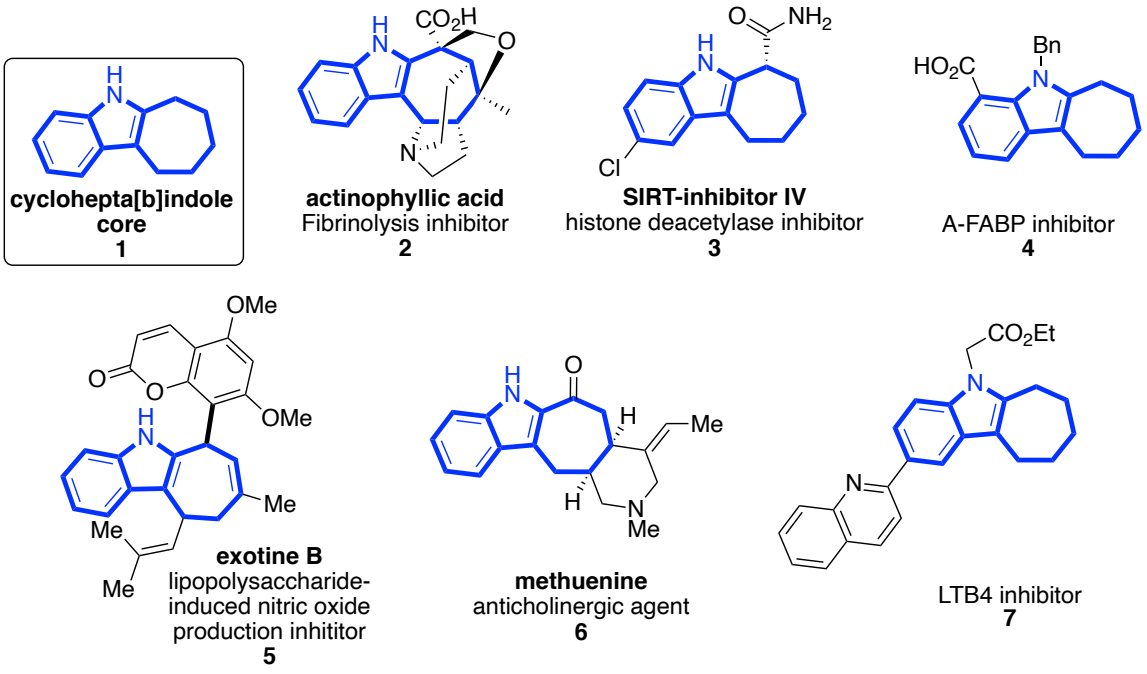

Figure 2.1: Representative Cyclohepta[*b*]indole-containing Compounds

2.2 Previous Synthetic Approaches Accessing the Cyclohepta[*b*]indoles Motif

Over the past decade, tremendous effort has been dedicated to developing general protocols to access the cyclohepta[*b*]indole motif. Although successful in achieving the motif, preparing cyclohepta[*b*]indoles that are differentially functionalized on the seven membered ring has proven to be difficult due to limitations including lack of functional group tolerance, harsh reaction conditions, low atom economy, and multiple steps to generate the necessary starting precursors. For example, historically, the Fischer indolization was the primary method used to prepare the motif.[9] While efficient in the formation of indoles, this method is limited in producing highly functionalized, unsymmetrical cyclohepta[*b*]indoles due to the need of a pre-functionalized cycloheptyl ring.[10] As a result, alternative approaches were sought such as metal-mediated intramolecular cyclization cascades,[11] olefin metathesis,[12] [3,3]-sigmatropic

rearrangements with divinylcyclopropanes,[13] [4+3]-cycloadditions,[14] and [5+2]-cycloadditions. Of the previous methods mentioned, [4+3]- and [5+2]-cycloaddition reactions have proven to be the most efficient, atom economical, and elegant approaches toward the cyclohepta[*b*]indole framework as it constructs the seven-membered ring in a single step with simultaneous or nearly simultaneous formation of two C-C bonds in a regio- and/or diastereoselective manner.

Previously reported [4+3] cycloaddition reactions utilize *in situ* generated highly reactive intermediates such as indolyl carbocations,[14a,d,e,h] oxyallyl cations,[14f] and metal carbenes.[14b,c,g] While [4+3] cycloaddition approaches toward cyclohepta[*b*]indole are found abundantly throughout the literature, there are currently only a few known examples of [5+2] cycloaddition reactions toward the targeted motif. As shown in Scheme 2.1, the first [5+2] cycloaddition method was reported in 2014 by Li et al.[15] and furnished oxacyclohepta[*b*]indoles **9** through an intramolecular dearomative indole [5+2] cycloaddition via an oxidopyrylium ylide. In 2017, Ohno et al.[16] described the synthesis of dihydrocyclohepta[*b*]indoles **12** through an Au(I)-catalyzed intermolecular [5+2] cycloaddition of diyne **11** and unsubstituted indole **10**. Later in 2018, Nishida et al.[17] developed an indium catalyzed intermolecular [5+2] cycloaddition of alkynes **14** and 2-((1*H*-indol-2-yl)methyl)- acrylates **13** where the In(III)-catalyst served a dual purpose, acting as a π-Lewis acid and σ-Lewis acid to activate both the alkyne and enoate moiety, respectively. Again in 2018, Haak et al.[18] disclosed the synthesis of hexahydrocyclohepta[*b*]indole **19** from a Ru(0)-catalyzed annulation and subsequent [5+2] cycloaddition of indole **16** and secondary alkenylpropargyl alcohols **17** in a one pot process. Also in that same year, Anand et al.[19] reported the synthesis of tetra- and

pentacyclic cyclohepta[*b*]indole derivatives **21** through a Au-catalyzed intermolecular [5+2] cycloaddition of indole **19** and alkynylated *p*-quinone methides (*p*-QMs) **20**.

Unfortunately, these [5+2] cycloaddition routes toward cyclohepta[*b*]indoles suffer from one of the following limitations: 1) high catalyst loading, 2) low functional group tolerance, and/or 3) multiple steps to generate the cycloaddition precursor/reactive intermediate, which limits the functionality on the cycloheptanoid ring. Thus, we sought to design a versatile protocol toward highly functionalized cyclohepta[*b*]indoles.

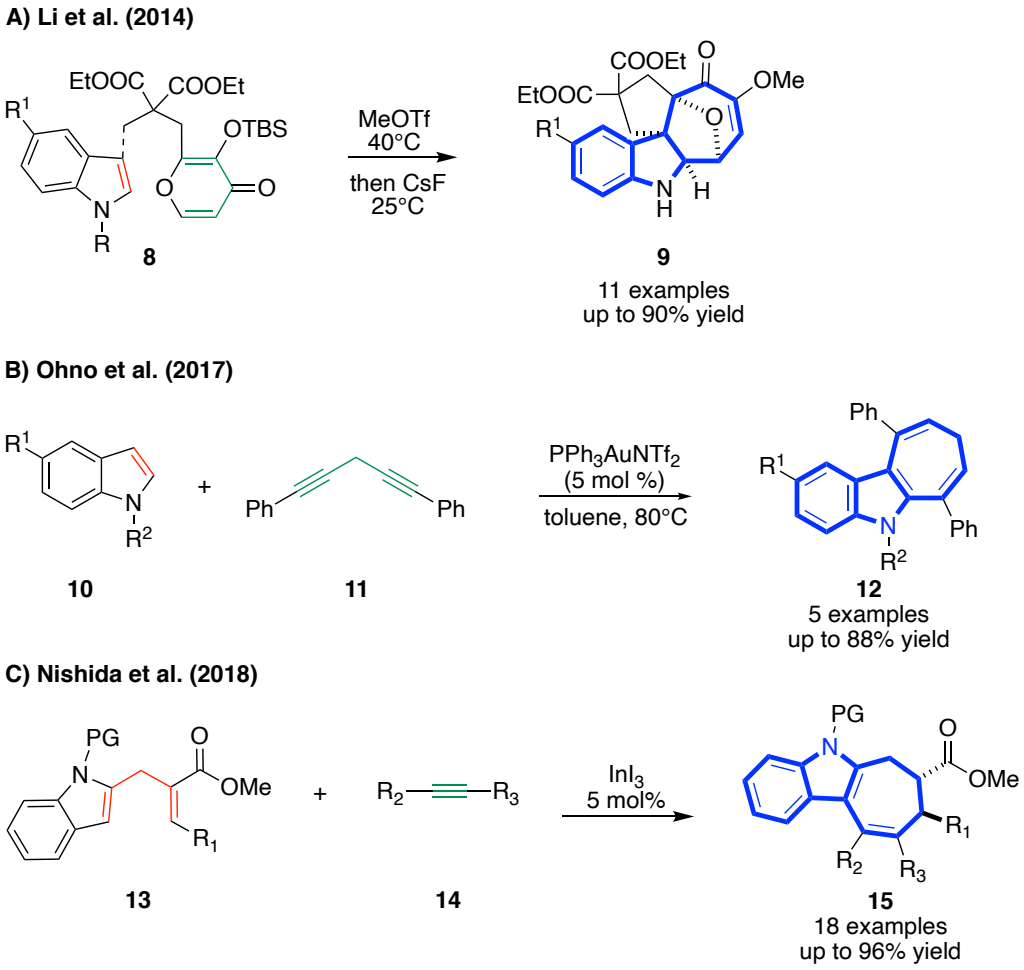

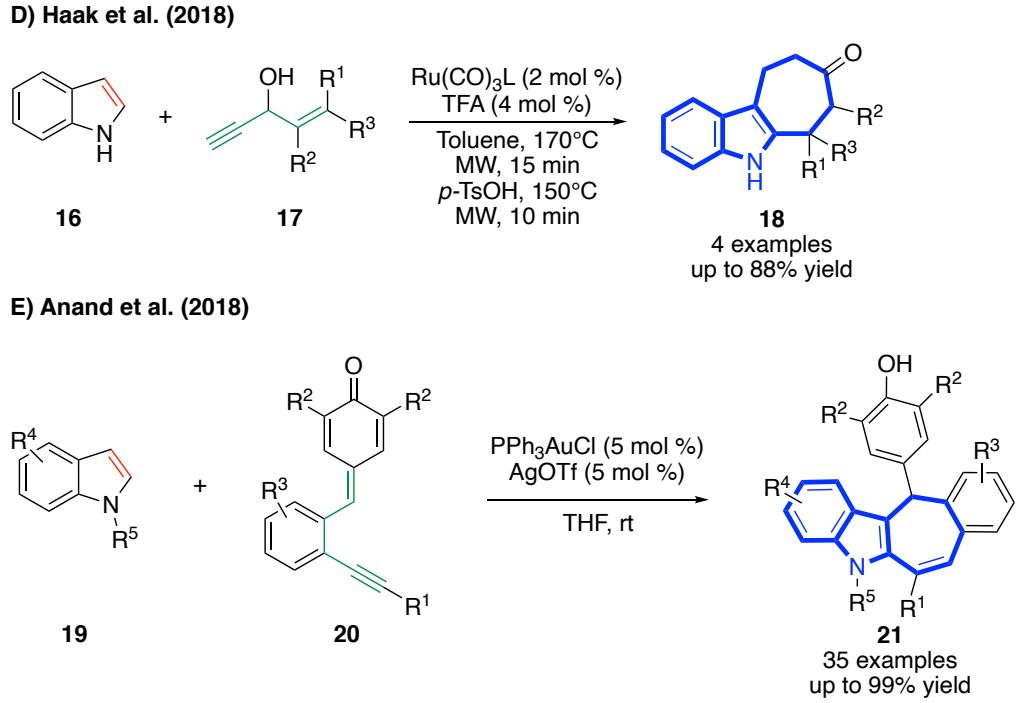

Scheme 2.1 Previously Established [5+2] Cycloadditions Toward Cyclohepta[*b*]indole Derivatives

2.3 The Development of a Formal [5+2] Cycloaddition Toward Cyclohepta[*b*]indoles

2.3.1 Project Justification and Rationale

The development of an approach toward cyclohepta[*b*]indoles was inspired by our report on the Lewis acid catalyzed formal [5+2] cycloaddition of *N*-indolyl alkylidene β-amide esters with substituted olefins **23** to form azepine [1,2-*a*]indoles (Scheme 2.2A).[20] This transformation proceeded through a formal [2+2] cycloaddition to give cyclobutane intermediate **25** which then undergoes ring-opening and subsequent Friedel-Crafts-type cyclization to form the desired azepinoindole **27**. It was also discovered that the choice of Lewis acid determined which competing pathway would take precedent ([5+2] vs. [2+2]).

Given the versatility of the indole moiety, we sought to extend the formal [5+2]-cycloaddition chemistry to access the cyclohepta[*b*]indole framework by employing the analogous *C*-acylated indolyl alkylidene β-ketoester **24** (Scheme 2.2B).

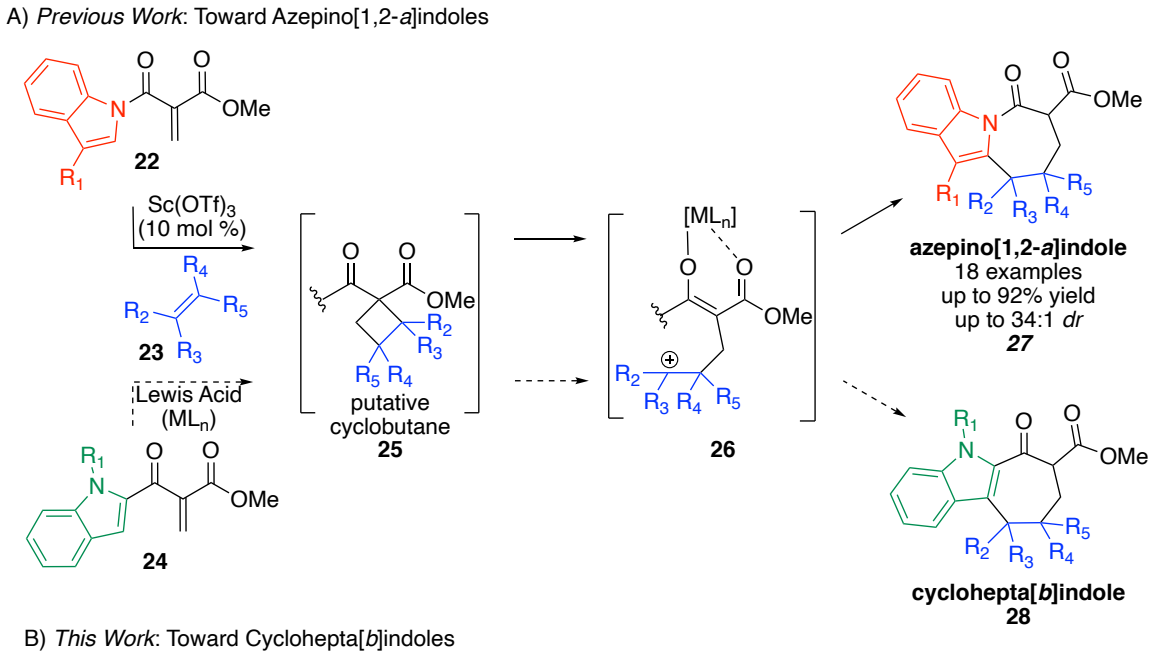

Scheme 2.2 Formal [5+2] Cycloadditions of Indolyl Alkylidene β-ketoesters and Olefins

2.3.2 Reaction Design

While the formal [5+2] cycloaddition transformation has been demonstrated to work well with *N*-acylated indolyl alkylidene β-ketoesters to produce azepino [1,2-*a*]indoles, producing cyclohepta[*b*]indoles through this transformation with the homologous *C*-acylated indolyl alkylidene β-ketoesters poses several difficulties. First, the formation of 7-membered rings is less entropically favoured compared to smaller ring sizes. Secondly, compared to the *N*-acylated indolyl alkylidene β-ketoesters which are stable and easily synthesized due to the less polarizing amide bond, the *C*-acylated

homolog has the potential to be more electrophilic due to the strong polarization of the enone moiety and thus more susceptible to degradation pathways and side products. Finally, once the intended ring opening occurs to form zwitterionic intermediate **I**, it is crucial that π-attack from the heteroaromatic system occurs immediately to mitigate side reactions such as E1 elimination **30**. However, the chosen indole π-nucleophile is suitable for this transformation since the C3 position of the indole is known to be the most nucleophilic site (Scheme 2.3).

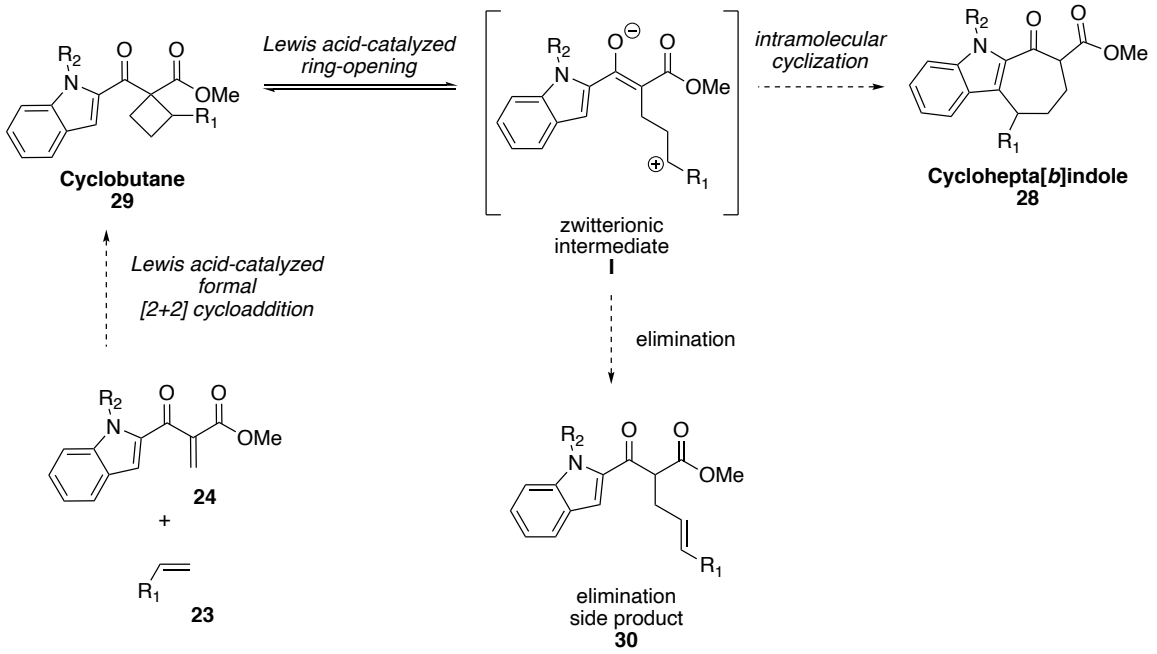

Scheme 2.3 Proposed Strategy Toward Cyclohepta[*b*]indoles

2.3.3 Model Substrate Synthesis

The alkylidene precursor **33** was synthesized through a 3-step sequence in which commercially available 1-methylindole-2-carboxylic acid **31** was transformed into the acid chloride *in situ* then reacted with the enolate of methyl acetate to form β-ketoester **32**.

Subsequently, β-ketoester **32** underwent a $Cu(OAc)_2$ catalyzed condensation with formaldehyde to afford alkylidene **33** (Scheme 2.4).

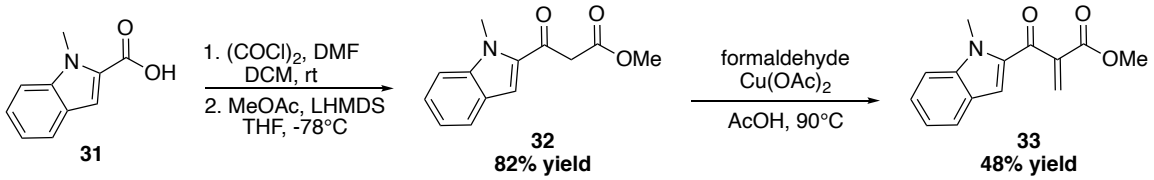

Scheme 2.4 Synthesis of Model Substrate

2.3.4 Proof of Concept

The study began by subjecting alkylidene **33** and α-methyl styrene **23a** to the optimized conditions used in the synthesis of azepino[1,2-*a*]indole (10 mol % of $Sc(OTf)_3$, 5 eq. alkene, in 0.1M DCM at rt). Gratifyingly, these conditions provided cyclohepta[*b*]indole **28aa** as a complex keto-enol mixture in 51% yield (Scheme 2.5). This result proved that the formal [5+2] cycloaddition strategy not only provides the azepino[1,2-*a*]indole framework, but also can be applied to the analogous cyclohepta[*b*]indole framework .

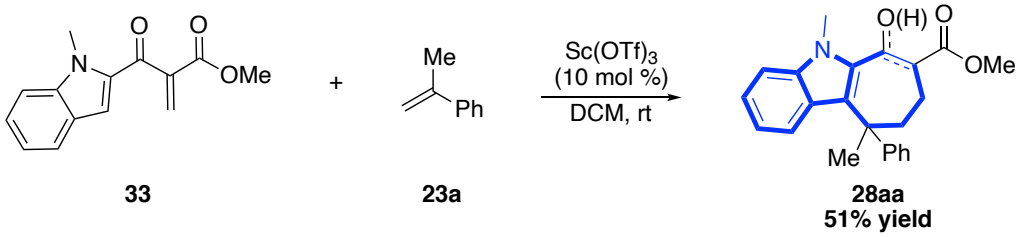

Scheme 2.5 Initial Test Reaction for the Synthesis of Cyclohepta[*b*]indoles

2.3.5 Reaction Optimization

After proof of concept was established, numerous efforts were made to further optimize the reaction (Table 2.1). An improved yield (65%) was obtained when the reaction was conducted at reflux (entry 2). Decreasing the catalyst loadings to 5 mol % and 2.5 mol % afforded the desired product 28aa with the same 66% yield (entries 3 and 4). At this point, other Lewis acids were screened at 2.5 mol % loading in hopes of both improving reaction yields and identifying any selective conditions for cyclobutane formation. $Ga(OTf)_3$ led to the cyclohepta[*b*]indole product mixture in 67% yield without any cyclobutane formation (entry 5). $Zn(OTf)_2$ similarly generated a 44% yield of only cyclohepta[*b*]indole 28aa (entry 6). $Yb(OTf)_3$, which selectively afforded cyclobutane in our previous report, gave only cyclohepta[*b*]indole in 51% yield (entry 7). No desired products were obtained with $Mg(OTf)_2$ (entry 8). Both $Al(OTf)_3$ and $Hf(OTf)_4$ raised the cyclohepta[*b*]indole product yield to 73% (entries 9 and 10). Next, we employed the Niggemann's Lewis acidic calcium complex[21] due its success in our previous intramolecular cyclizations, the complex which consist of $Ca(NTf_2)_2$ with *n*-Bu_4NPF_6 as an additive produced the best yield of cyclohepta[*b*]indole 4aa at 98% (entry 11). Consistent with the observed results with $Sc(OTf)_3$, reduced yields were obtained upon performing the calcium reaction at room temperature (entry 12). It is important to note that the cyclobutane was never detected under any of the reaction conditions, which is in sharp contrast with the azepino system.

To ensure that the catalysis is due to the calcium−additive complex and not from its individual components, a series of control reactions were conducted. Performing the reaction without the additive, *n*-Bu_4NPF_6, afforded no desired product (entry 13). In contrast, while the reaction did not proceed to any appreciable degree without $Ca(NTf_2)_2$

present (entry 14) , the Brønsted acid $HNTf_2$ gave 64% yield of the desired product. Given this result, a synergistic Lewis and Brønsted acid effect between the formed calcium complex and $HNTf_2$ cannot be ruled out. Further efforts in optimizing temperature, solvent, and concentration led to no improvements in yield. Thus, the optimized reaction conditions for the above transformation were 2.5 mol % of $Ca(NTf_2)_2$ and 2.5 mol % of *n*-Bu_4NPF_6 in CH_2Cl_2 (0.1M) with 5.0 eq. of alkene.

Table 2.1 Lewis Acid Screen for Formal [5+2] Cycloaddition[a]

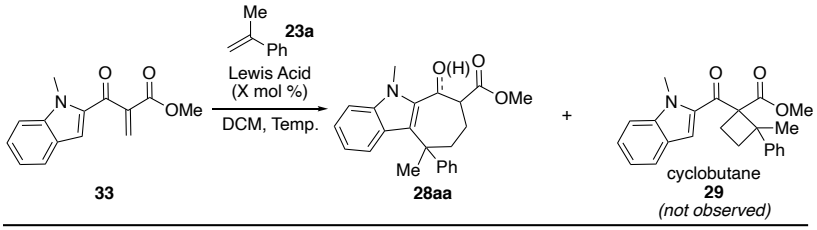

Entry	Lewis Acid (mol %)	Time (h)	Yield (%)[b]
1[c]	$Sc(OTf)_3$ (10)	1.0	51
2	$Sc(OTf)_3$ (10)	0.5	65
3	$Sc(OTf)_3$ (5)	1.0	66
4	$Sc(OTf)_3$ (2.5)	1.0	66
5	$Ga(OTf)_3$ (2.5)	1.0	67
6	$Zn(OTf)_2$ (2.5)	0.5	44
7	$Yb(OTf)_3$ (2.5)	1.0	51
8	$Mg(OTf)_2$ (2.5)	1.5	0[d]
9	$Al(OTf)_3$ (2.5)	1.0	73
10	$Hf(OTf)_4$ (2.5)	0.5	73
11	$Ca(NTf_2)_2$ (2.5) n-Bu_4NPF_6 (2.5)	0.5	98
12[c]	$Ca(NTf_2)_2$ (2.5) n-Bu_4NPF_6 (2.5)	0.5	73
13	$Ca(NTf_2)_2$ (2.5)	24.0	0[d]
14	n-Bu_4NPF_6 (2.5)	24.0	0[e]
15	$HNTf_2$ (2.5)	1.5	64

[a]Reaction performed with alkylidene **33**, α-methylstyrene (**23a**, 5 equiv), and indicated acid catalyst in CH_2Cl_2 (0.1 M) at 40 °C. [b]Isolated yield of **28aa** after column chromatography. [c]Reaction performed at room temperature. [d]No desired products obtained. [e]No reaction.

2.3.6 Examination of the Substrate Scope

With the promising results from the model system, the cycloaddition study was expanded to explore the substrate scope and general limitations (Scheme 2.6). First, changes to the indole moiety were somewhat tolerated. Both the *N*-benzyl and N-H (unprotected) alkylidenes (**33b** and **33c**) gave their cycloaddition products **28ba** and **28ca** with α-methylstyrene (**23a**) in 56% and 53% yield, respectively. Similarly, the 5-bromoindolyl alkylidene **33d** provided the cyclohepta[*b*]indole **28da** in 75% yield. To our dismay, no products (**28ea** or **28fa**) were obtained when α-methylstyrene was reacted with either the 3- acyl indolyl alkylidene **33e** (only degradation observed) or the methyl-substituted alkylidene **33f** (only competing Nazarov cyclization product formed).[23]

Next, other 1,1-disubstituted olefins were employed. As with α-methylstyrene, 4-methoxy-α-methylstyrene (**23b**) and 2-(prop-1-en-2-yl)thiophene (**23c**) each gave their respective cycloaddition products **28ab** and **28ac** in 93% and 84% yield. Methylene cyclohexane **23d**, a 1,1-dialkyl olefin, also afforded the expected cycloheptyl product **28ad** in 12% yield. The low yield is likely a result of the 1,1-dialkyl olefin being a much weaker nucleophile when compared to the α-substituted styrenes.

Monosubstituted olefins were subsequently examined. Electron-rich styrenes, such as **23e** (*p*-methoxy substituent) and **23f** (*p*-methyl substituent), provided their respective products **28ae** and **28af** in 63% and 48% yield. While styrene (**23g**) gave its product **28ag** in 20% yield, only 5% yield of product **28ah** could be isolated with the more electron-poor substrate, *p*-chlorostyrene **23h**. 2-Vinylnaphthalene **23i** generated 60% of the cycloaddition product **28ai**. In contrast, when 1-hexene (**23j**, unactivated) or TMS

allylsilane (**23k**, activated) was employed, no reaction was detected, and only starting materials were recovered.

1,2-Disubstituted olefins were then evaluated. Indene **23l** provided cycloaddition product **28al** in 57% yield, while *p*-methoxy-β-methylstyrene **23m** afforded cyclohepta[*b*]indole **28am** in 71% yield. Conversely, 1,1,2-trisubstituted olefins (**23n** and **23o**) proved untenable as complex mixtures were obtained or olefin polymerization/degradation (likely due to the presence of $HNTf_2$) was observed under the reaction conditions.

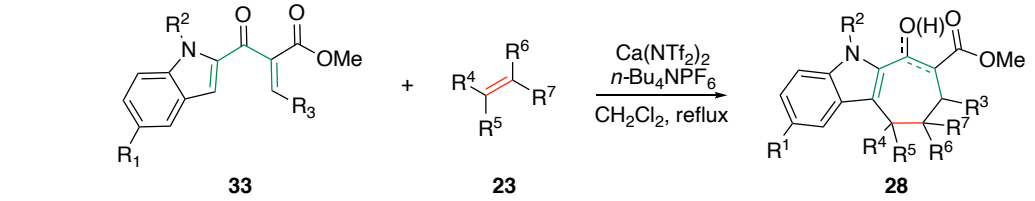

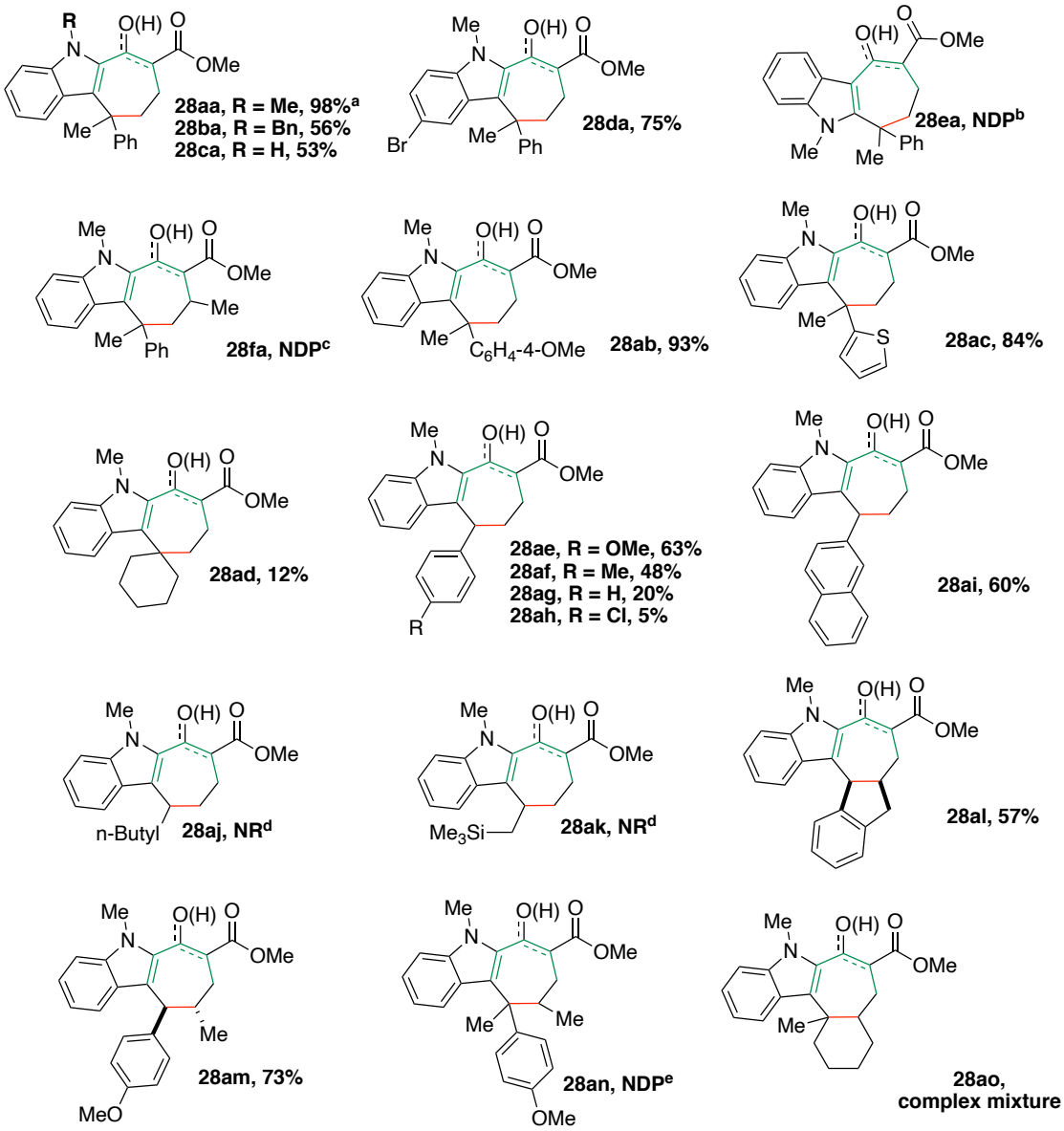

[a]Numbers represent isolated yields of **28** following column chromatography. [b]No desired product formed due to extensive degradation of alkylidene. [c]No desired product formed due to the formation of Nazarov cyclization byproduct. [d]No reaction. Only starting materials recovered. [e]No desired product formed due to alkene degradation.

Scheme 2.6: Exploration of Reaction Scope

2.3.7 Chemodivergent Pathway

Interestingly, when phenyl vinyl sulfide (**23p**) was reacted with alkylidene **33a**, the anticipated cyclohepta[*b*]indole product **28ap** was not observed (Scheme 2.7A). Instead, the bicyclic cyclohepta[*b*]indole framework **34ap** was isolated in 50% yield as a single diastereomer and confirmed by X-ray crystallography (Scheme 2.7B). **34ap** contains an indole ring fused to a bicyclo[3.2.2]nonene moiety and represents an unprecedented cyclohepta[*b*]indole framework. A similar bicyclic product **34aq** was formed with phenyl vinyl ether **23q**, albeit with lower yield (41%) and diastereoselectivity (3.6:1 dr).

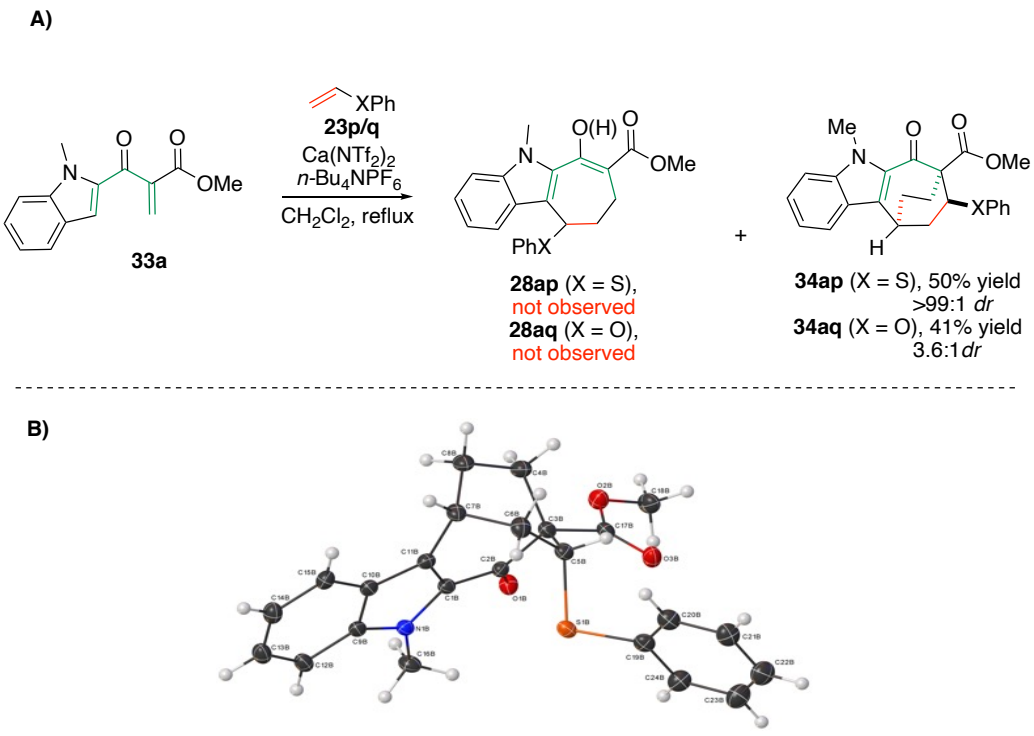

Scheme 2.7: (A) Unexpected Bicyclic Byproduct with Vinyl Sulfide and Ether (B) Crystal Structure of 34ap Drawn at the 50% Probability Level

To further explore this chemodivergent pathway, other hetero-alkene such as cyclic/acyclic alkyl enol ethers and enamides were examined, but neither

cyclohepta[*b*]indole product was obtained. This lack of reactivity is presumably due to the presence of $HNTf_2$, which appears to catalyze polymerization of the alkyl enol ethers and hydrolysis of the enamides. In comparison, **23p** and **23q** are less susceptible to acid catalysis and, thus, are amenable to the reaction conditions.

2.3.8 Reaction Mechanism

Adapted from our mechanistic understanding for the formation of the azepino[1,2-*a*]indole framework, the formal [5+2] cycloaddition between *C*-acylated indolyl alkylidene β-ketoesters **24** and alkenes **23** is presumed to occur through Lewis acid activation of the alkylidene followed by Michael addition type intermolecular attack of the alkene to form intermediate **I** (Scheme 2.8). Intermediate **I** then undergoes a Friedel Crafts type ring closure to form the desired cyclohepta[*b*]indole products **28** (pathway a). Although cyclobutane **29** formation through a formal [2+2] cycloaddition (pathway b) is a viable option considering the results from the formation of the azepino[1,2-*a*]indole framework, no cyclobutane product **29** was detected under any reaction conditions for the formation of cyclohepta[*b*]indoles.

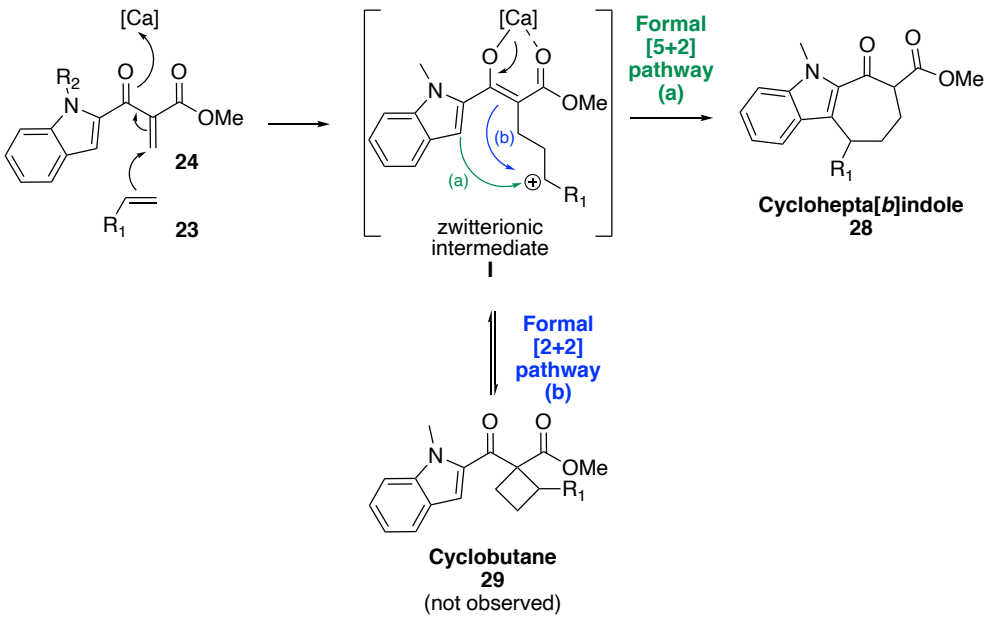

Scheme 2.8: Reaction Mechanism for the Formation of Cyclohepta[*b*]indoles

The bicyclic cyclohepta[*b*]indole derivative **34ap** is proposed to form through a cascade sequence that starts with the formation of the expected formal [5 + 2] cycloaddition product **28ap** (Scheme 2.9). Lewis acid activation of the phenyl sulfide is assumed to facilitate C−X bond cleavage to provide the cationic, resonance-stabilized divinyl iminium intermediate **II** and PhS^-. *In situ* generation of PhS^- is supported by the formation of **35**, the Michael addition product of phenyl sulfide, and the starting alkylidene **33a**. Finally, a subsequent [5 + 2] cycloaddition of intermediate **II** with another molecule of phenyl vinyl sulfide **23p** affords the observed bicyclic product **34ap**. This transformation is particularly interesting as, to the best of our knowledge, [5 + 2] cycloadditions involving divinyl iminium intermediates have not been previously reported in the literature.

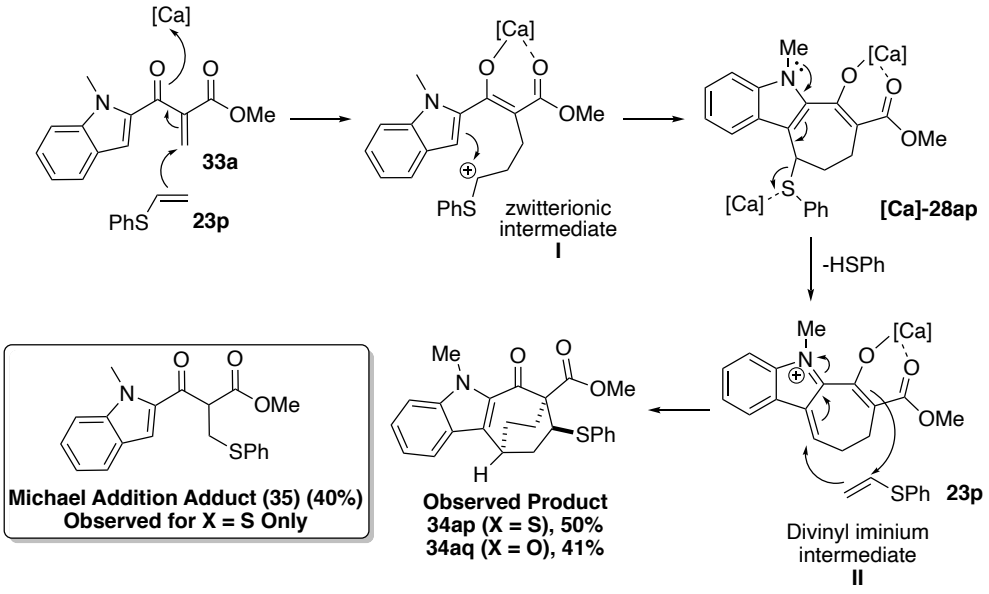

Scheme 2.9: Proposed Mechanism for Cascade Formation of Bicyclic Cyclohepta[*b*]indole 34ap/q

2.3.9 Derivatization

Given that the [5 + 2] cycloaddition transformation resulted in the formation of a complex keto−enol mixture of the cyclohepta[*b*]indole products, Krapcho decarbalkoxylation[22] was employed to simplify NMR analysis and validate product formation (Scheme 2.10). Treatment of each resulting keto-enol cyclohepta[*b*]indole product **28** with NaCl in wet DMSO at 150 °C afforded decarbalkoxylated cyclohepta[*b*]indole products **36** in 50-87% yield. It is also important to note that one diastereomer for **28al** and **28am** were isolated in each case (Scheme 2.10).

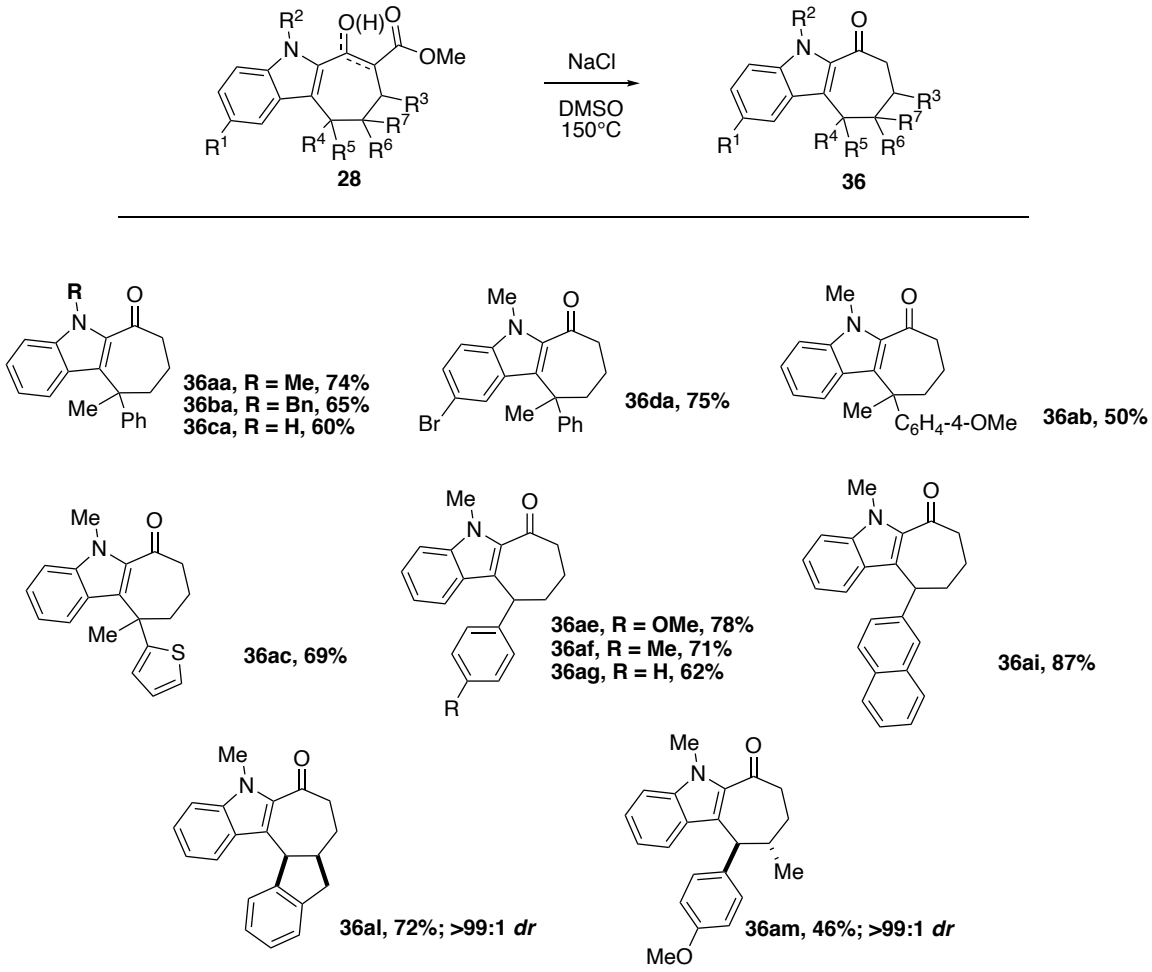

Scheme 2.10: Krapcho Decarbalkoxylation

Beyond decarbalkoxylation, the keto−enol mixtures of the cyclohepta[*b*]indole products can be readily derivatized (Scheme 2.11). For example, treatment of **28aa** with NaH and Tf_2O afforded the corresponding enol triflate **37aa** in 50% yield. To highlight the versatility of this intermediate, **37aa** was then subjected to Pd-catalyzed Sonogashira coupling[24] with phenylacetylene to provide enyne **40aa** in 66% yield. Similarly, methylation[25] of cyclohepta[*b*]indole **28aa** with K_2CO_3 and Me_2SO_4 resulted in 51% of the *C*-methylated product **38aa** (as a 1.2:1 diastereomeric mixture) and 27% of the *O*-methylated product **39aa**.

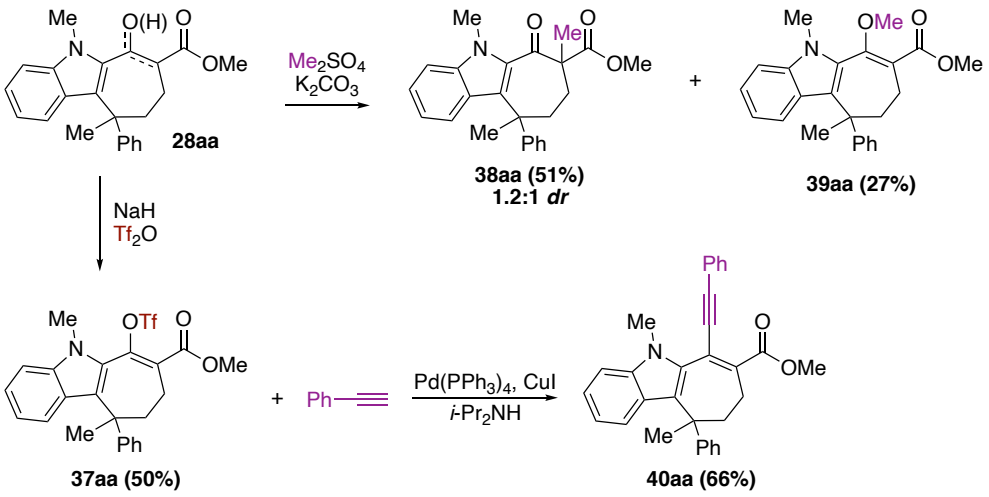

Scheme 2.11:Facile Derivatization of Cyclohepta[*b*]indole

2.4 Summary

We describe in this chapter a formal [5+2] cycloaddition strategy accessing highly functionalized cyclohepta[*b*]indoles which are found in a variety of natural products with suitable bioactive properties (Scheme 2.12). To affect the formal [5+2] transformation we were able to use a low loading (2.5 mol %) of a green calcium-based catalyst, readily accessible olefins and *C*-acylated indolyl α-alkylidene β- ketoesters in <1 h to provide the desired substituted cycloheptyl rings. Competing cyclobutane formation ([2 + 2] cycloaddition) is not observed, whereas Nazarov cyclization is only observed (no [5 + 2]) with substituted alkylidenes (R≠H). Various 2-acyl indoles are tolerated, thus allowing for tunable substitution about the cyclohepta[*b*]indole framework. Mono- and disubstituted aryl alkenes are particularly compatible with the method and give products in up to 98% yield. Interestingly, when either phenyl vinyl sulfide or ether are employed, an unanticipated chemodivergence was observed affording ethano-bridged cyclohepta[*b*]indoles in up to 50% yield. These products presumably formed from the

expected [5 + 2] cycloaddition product following PhXH elimination to form a divinyl iminium intermediate, which undergoes an unprecedented [5 + 2] cycloaddition. Finally, examples of cyclohepta[*b*]indole product derivatization highlight the general practicality of this method.

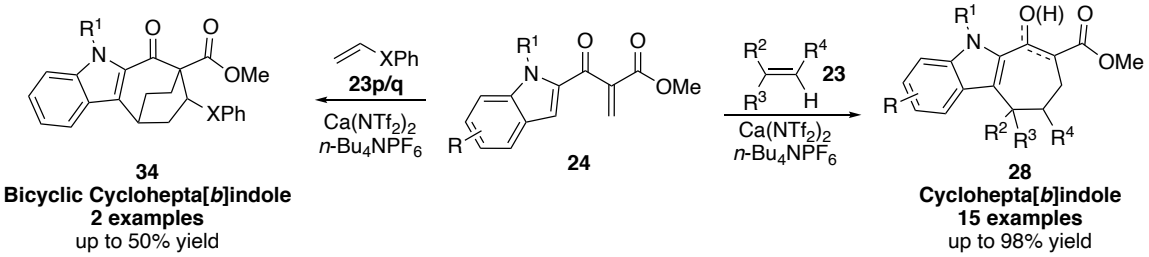

Scheme 2.12: Chemodivergent Synthesis of Highly Functionaly Cyclohepta[*b*]indole Derivatives

2.5 Experimental

2.5.1 General Methods

Chromatographic purification was performed as flash chromatography with Silicycle SiliaFlash P60 silica gel (40-63μm) or preparative thin-layer chromatography (prep-TLC) using silica gel F254 (1000 μm) plates and solvents indicated as eluent with 0.1-0.5 bar pressure. For quantitative flash chromatography, technical grades solvents were utilized. Analytical thin-layer chromatography (TLC) was performed on Silicycle SiliaPlate TLC silica gel F254 (250 μm) TLC glass plates. Visualization was accomplished with UV light. Infrared (IR) spectra were obtained via attenuated total reflection (ATR) with a diamond plate using a Bruker ALPHA Fourier-transform infrared spectrophotometer. The IR bands are characterized as broad (br), weak (w), medium (m), and strong (s). Proton and carbon nuclear magnetic resonance spectra (^{1}H NMR and ^{13}C NMR) were recorded on a Varian

Mercury Vx 300 MHz spectrometer or a Bruker 500 MHz spectrometer with solvent resonances as the internal standard (^{1}H NMR: $CDCl_3$ at 7.26 ppm or DMSO-d_6 at 2.50; 13C NMR: CDCl3 at 77.0 ppm or DMSO-d_6 at 39.5). 1 H NMR data are reported as follows: chemical S-1 shift (ppm), multiplicity (s = singlet, d = doublet, dd = doublet of doublets, dt = doublet of triplets, ddd = doublet of doublet of doublets, t = triplet, m = multiplet, br = broad), coupling constants (Hz), and integration. Mass spectra were obtained through EI on a Micromass AutoSpec machine or through ESI on a Thermo Orbitrap XL. The accurate mass analyses run in EI mode were at a mass resolution of 10,000 and were calibrated using PFK (perfluorokerosene) as an internal standard. The accurate mass analyses run in EI mode were at a mass resolution of 30,000 using the calibration mixture supplied by Thermo. Uncorrected melting points were measured with a digital melting point apparatus (DigiMelt MPA 160).

2.5.2 Experimental Procedures

2.5.2.1 Synthesis of Carboxylic Acids

Synthesis of 5-bromo-1-methyl-1*H*-Indole-2-carboxylic acid (31b):

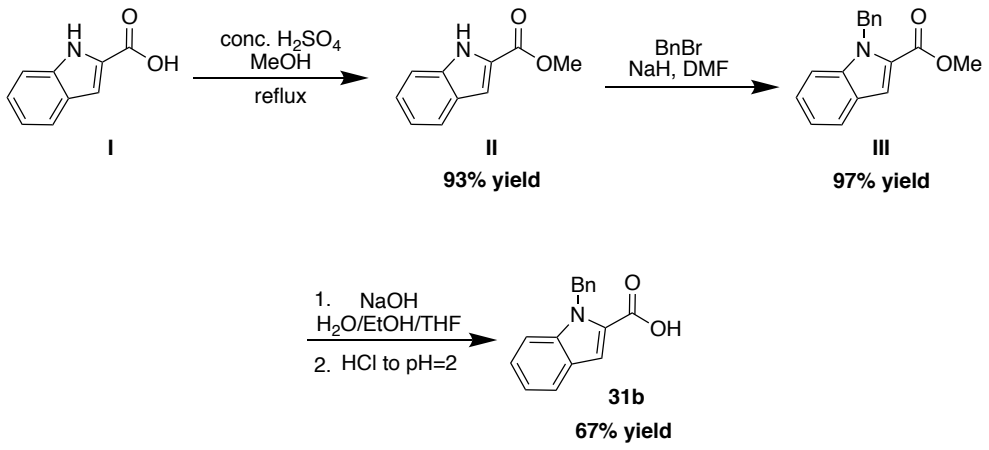

I **II** **III**

93% yield **97% yield**

31b

67% yield

The 1-benzyl-1*H*-indole-2-carboxylic acid **31b** was prepared according to literature procedure with slight modifications to the esterification of indole-2-carboxylic acid, N-protection, and hydrolysis of the ester. To a dry flask charged with a stir bar and indole-2-carboxylic acid **I** (1.00 g, 6.21 mmol) under nitrogen was added dry methanol (5 mL) to make a 1.3 M solution. Catalytic concentrated H_2SO_4 (3 drops) was then added. The reaction was then stirred at reflux overnight, concentrated down, diluted with DCM, and washed with water followed by brine. The organic layer was dried over Na_2SO_4, filtered and concentrated by rotary evaporation to give ester **II** as a white solid (1.02 g, 93% yield). Characterizations were consistent with previously reported literature.[26]

Without purification a solution of N-H ester **II** (4.20 g, 24 mmol) in DMF (48 mL) was added dropwise to a solution of NaH (1.92 g, 48 mmol, 60% in mineral oil) in DMF (69 mL) at 0°C. After, a solution of BnBr (8.20 g, 48 mmol) in DMF (32 mL) was added dropwise. The mixture was stirred at 0°C for 30 minutes, then room temperature overnight. The reaction mixture was quenched with water and extracted with ethyl acetate. The organic layer was dried over Na_2SO_4, filtered and concentrated by rotary evaporation to produce Bn-protected ester **III** as a yellow solid (6.15 g, 97% yield). Characterizations were consistent with previously reported literature.[27]

The N-Benzylindole-2-carboxylate **III** (5.00 g, 18.8 mmol) was added to a solution of NaOH (3.01 g, 75.4 mmol) in H_2O/EtOH/THF (1:1:1) and stirred for 4 hours at room temperature. The solution was then cooled to 0°C and acidified by concentrated HCl to a pH of 2. The solution was extracted with ethyl acetate and washed with brine. The organic layer was dried over Na_2SO_4, filtered and concentrated by rotary evaporation to give the

title compound **31b** as a white solid (3.27 g, 67% yield). Characterizations were consistent with previously reported literature.[28]

Synthesis of 5-bromo-1-methyl-1*H*-Indole-2-carboxylic acid (31d):

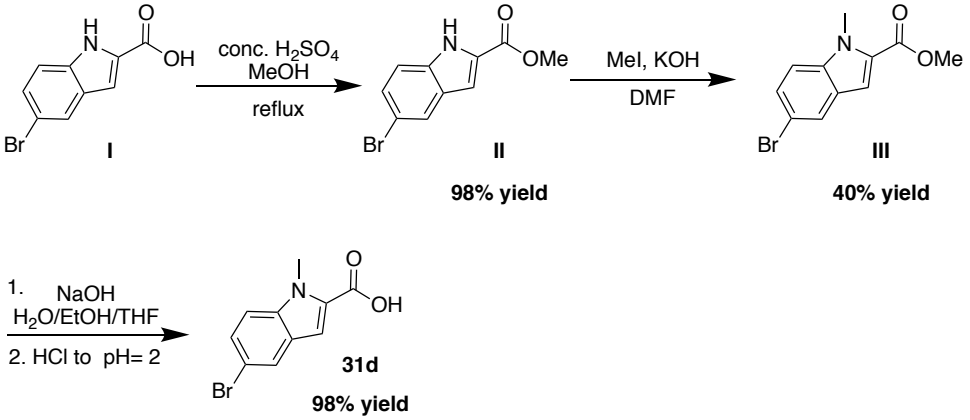

The 5-bromo-1-methyl-1*H*-Indole-2-carboxylic acid **31d** was prepared from the esterification of 5-bromo indole-2-carboxylic acid **I**, methylation, and hydrolysis of the ester. To a dry flask charged with a stir bar and 5-bromo-indole-2-carboxylic acid (2.04 g, 8.33 mmol) under nitrogen was added dry methanol (7 mL) to make a 1.27 M solution. Catalytic concentrated H_2SO_4 (5 drops) was then added. The reaction was then stirred at reflux overnight, concentrated down, diluted with DCM, and washed with water followed by brine. The organic layer was dried over Na_2SO_4, filtered and concentrated by rotary evaporation to give ester **II** as a white solid (2.11 g, 98% yield). Characterizations were consistent with previously reported literature.[29]

Without purification, a flask was charged with N-H ester **II** (2.11 g, 8.30 mmol), KOH (2.74 g, 41.5 mmol), DMF (28 mL), and MeI (1.23 mL, 19.7 mmol) and stirred at room temperature for 20 minutes. The reaction was then filtered through a plug of silica gel to

remove excess KOH and water was added to the filtrate and the solution was extracted with DCM. The organic layer was dried over Na_2SO_4, filtered and concentrated by rotary evaporation to give **methyl 5-bromo-1-methyl-1*H*-indole-2-carboxylate III** as a white solid (0.896 g, 40% yield). **^{1}H NMR** (500 MHz, $CDCl_3$) δ = 7.81 (dd, *J* = 1.9, 0.9 Hz, 1H), 7.43 (ddd, *J* = 8.9, 1.9, 0.8 Hz, 1H), 7.28 (s, 1H), 7.22 (d, *J* = 1.0 Hz, 1H), 4.07 (d, *J* = 1.1 Hz, 3H), 3.93 (s, 3H). **^{13}C NMR** (500 MHz, $CDCl_3$) δ = 162.29, 138.14, 128.63, 127.89, 127.33, 124.84, 113.73, 111.79, 109.31, 77.29, 77.04, 76.78, 51.80, 31.81. **IR** 3027 (w), 2925 (w), 1645 (s), 702 (m), 698 (m) cm^{-1}. **HRMS (EI)** *m/z:* $[M]^+$ Calcd. for $C_{21}H_{10}NO_2Br$, 266.9895; Found, 266.9907.

The methyl 5-bromo-1-methyl-1*H*-indole-2-carboxylate **III** (0.858 g, 3.20 mmol) was added to a solution of NaOH (0.511 g, 12.8 mmol) in H_2O/EtOH/THF (1:1:1) and stirred for 4 hours at room temperature. The solution was then cooled to 0°C and acidified by concentrated HCl to a pH of 2. The solution was extracted with ethyl acetate and washed with brine. The organic layer was dried over Na_2SO_4, filtered and concentrated by rotary evaporation to give the title compound **31d** as a white solid (0.793 g, 98% yield). **^{1}H NMR** (500 MHz, DMSO-d_6) 7.88 (dd, *J* = 2.0, 0.6 Hz, 1H), 7.56 (dt, *J* = 8.8, 0.8 Hz, 1H), 7.42 (dd, *J* = 8.9, 2.0 Hz, 1H), 7.19 (d, *J* = 0.9 Hz, 1H), 4.01 (s, 3H). **^{13}C NMR** (500 MHz, DMSO-d_6) 163.11, 138.25, 130.20, 127.46, 124.70, 113.52, 113.19, 109.14, 32.18. **IR HRMS (ESI)** *m/z:* $[M+H]^+$ calc. for $C_{10}H_9NO_2Br$, 253.9811; Found, 253.9806.

2.5.2.2 Synthesis of β-Keto Esters

General Procedure A for β-ketoesters: To a dry flask charged with a stir bar and the starting aryl carboxylic acid (1.00 equiv.) under nitrogen was added dry CH_2Cl_2 to make a

0.5 M solution. The solution was then cooled to 0˚C. Catalytic DMF (few drops) was then added. Oxalyl chloride (1.20 equiv.) was added over 1 min with stirring at 0˚C with a needle used to vent into a balloon. After 15 min, the reaction was allowed to warm to room temperature with continued stirring. The reaction was monitored by TLC until complete conversion of the carboxylic acid was observed. Upon completion, the reaction was concentrated under reduced pressure, the generated acid chloride was re-dissolved in dry THF to make a 1 M solution, and the solution was added slowly to the prepared enolate at -78˚C. The enolate was prepared by first adding LHMDS (1 M in THF, 2.10 equiv.) to a dry flask charged with a stir bar under nitrogen and cooling to -78˚C. MeOAc (1.05 equiv.) was added to the solution of LHMDS in one shot and stirred for 45 min at -78˚C. The reaction was monitored by TLC until complete conversion of the acid chloride was observed. Upon completion, the reaction was quenched with NH_4Cl (aq.) at -78˚C, extracted with EtOAc three times, dried using Na_2SO_4, and filtered through celite. The combined organic layers were concentrated under reduced pressure and purified by flash chromatography on silica gel using EtOAc/Hexanes as the mobile phase.

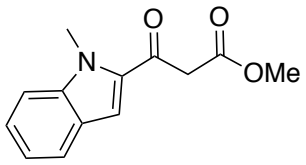

Methyl-3-(1-methyl-1H-indol-2-yl)-3-oxopropanoate 32a: Prepared following general procedure A using 1-Methylindole-2-carboxylic acid (0.635 g, 3.57 mmol) in CH_2Cl_2 (7 mL), oxalyl chloride (0.544 g, 4.28 mmol), and catalytic DMF (few drops) stirred at room temperature for 3 h to generate the acid chloride. The enolate was generated using LHMDS (1M in THF, 7.5 mL) and MeOAc (0.278 g, 3.75 mmol) and the generated acid chloride in

THF (4 mL) was added at -78˚C and stirred for 30 min. After work-up, the residue was purified by flash chromatography on silica gel (20% EtOAc/Hexanes, Rf = 0.36) to afford compound 12a as a pale yellow solid (0.405 g, 82% yield). Characterizations were consistent with previously reported literature.[26]

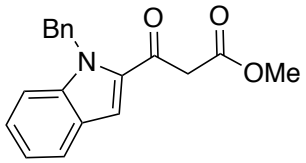

Methyl 3-(1-benzyl-1H-indol-2-yl)-3-oxopropanoate 32b: Prepared following general procedure A using 1-benzyl-1H-indole-2-carboxylic acid (3.27 g, 13.0 mmol) in CH_2Cl_2 (26 mL), oxalyl chloride (1.97 g, 15.6 mmol), and 1mL of DMF stirred at room temperature for 3 hours to generate the acid chloride. The enolate was generated using LHMDS (1M in THF, 25 mL) and MeOAc (0.942 g, 12.7 mmol) and the generated acid chloride in THF (12 mL) was added at -78°C and stirred for 30 minutes. After work-up, the residue was purified by flash chromatography on silica gel (5% EtOAc/Hexanes) to afforded compound **12b** as a pale yellow solid (2.66 g, 67% yield) **^{1}H NMR** (300 MHz, $CDCl_3$) δ = 7.74 (dt, *J* = 8.1, 1.0 Hz, 1H), 7.40 (d, *J* = 0.5 Hz, 1H), 7.38 – 7.35 (m, 2H), 7.25 – 7.15 (m, 4H), 7.05 (ddt, *J* = 7.9, 1.5, 0.8 Hz, 2H), 5.85 (s, 2H), 3.99 (s, 2H), 3.72 (s, 3H). **^{13}C NMR** (500 MHz, $CDCl_3$) δ = 185.00, 167.98, 140.44, 137.98, 133.39, 128.55, 127.19, 126.95, 126.47, 125.98, 123.30, 121.35, 113.87, 111.08, 77.32, 77.07, 76.81, 52.57, 48.24, 47.05. **IR** 2357 (w), 1730 (s), 1664 (s), 726 (m) cm^{-1}. **HMRS (ESI)** *m/z:* $[M+Na]^+$ calc. for $C_{19}H_{17}NO_3Na$, 330.1101; Found, 330.1093.

Synthesis of Methyl 3-(1*H*-indol-2-yl)-3-oxopropanoate 32c:

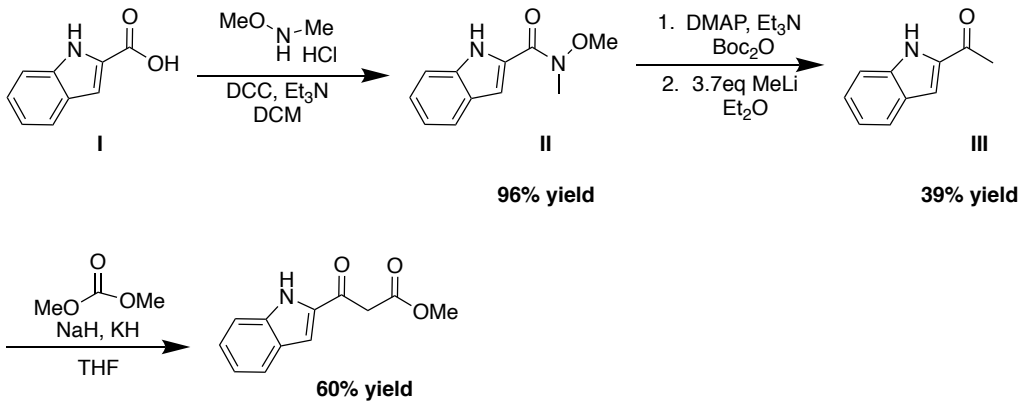

Weinreb amide formation was conducted according to the method of Dodd.[30] Protection of the indole with Boc-anhydride was prepared following the general procedure of Grieco.[31] and the resulting Boc protected indole was used crude for the alkylation with MeLi according to the method of Frontier.[32] During the course of this reaction the Boc protecting group was cleaved to give methyl ketone **III** which was then condensed with dimethylcarbonate to give the desired β-keto ester.[32]

***N*-methoxy-*N*-methyl-1*H*-indole-2-carboxamide:** Prepared following a general procedure employed by the Dodd lab.[30] To a solution of indole-2-carboxylic acid (5.0 g, 31.0 mmol) in dry CH_2Cl_2 (155 mL) was added N,O-dimethylhydroxylamine hydrochloride (3.03 g, 31.0 mmol) and triethylamine (4.32 mL, 31.0 mmol). The mixture was stirred for 5 minutes before dicyclohexylcarbodiimide (6.40 g, 31.0 mmol) was added and continued stirring for 3 hours. The reaction mixture was then concentrated by rotary evaporation. The residue was then suspended in a minimum amount of acetone and the insoluble white solid was removed by filtration. The filtrate was evaporated to dryness and the process was repeated twice to remove traces of urea. Compound **II** was obtained as a

white powder (6.17 g, 96% yield). Characterizations were consistent with previously reported literature.[30]

***Tert*-butyl 2-(methoxy(methyl)carbamoyl)-1*H*-indole-1-carboxylate:** Procedure adapted from the Grieco lab.[31] To a 0.5M solution of *N*-methoxy-*N*-methyl-1*H*-indole-2-carboxamide (4.80 g, 23.5 mmol) in CH_2Cl_2 (47 mL) were added triethylamine (3.28 mL, 23.5 mmol), di-*tert*-butyl decarbonate (10.3 g, 47.0 mmol), and 4-(dimethylamino)pyridine (2.87 g, 23.5 mmol). The solution was stirred for 7 hours at 25°C under nitrogen. The volatiles were removed, and the crude residue was carried forward.

1-(1*H*-indol-2-yl)ethan-1-one: The Boc-protected amide (5 g, 16.4 mmol) in 41 mL of dry Et_2O, under nitrogen was cooled to 78°C. Methyl lithium (1.6 M, 38 mL, 60.8 mmol) was added dropwise in 3 portions over the course of an hour. After the starting material was consumed, the reaction was allowed to come to room temperature. The reaction was then slowly quenched with NH_4Cl and extracted with EtOAc. The organic layer was washed with water followed by brine, dried with $MgSO_4$, filtered, and concentrated. The residue was dissolved in a minimum amount of EtOAc and passed over a plug of silica. The filtrate was concentrated to afford methyl ketone **III** (1.05 g, 39% yield) which was used without further purification. Characterizations were consistent with previously reported literature.[32]

Methyl 3-(1*H*-indol-2-yl)-3-oxopropanoate (32c): A flask was charged with NaH (60% dispersion in mineral oil, 0.329 g, 6.32 mmol), and KH (30% dispersion in mineral oil, 1.10 g, 8.22 mmol) and flushed with nitrogen. The hydrides were washed with dry hexanes and then suspended in dry THF (205 mL). The flask was then cooled to 0°C and a solution

of ketone (1.0 g, 6.32 mmol) and dimethylcarbonate (1.99 g, 22.1 mmol) in dry THF (27 mL) was added with stirring. The reaction was warmed to 40°C where it then took on a deep red coloration. Upon consumption of starting ketone (4 hours) the reaction was cooled to room temperature, quenched with H_2O, and extracted with EtOAc. The organic layer was washed with brine, dried with $MgSO_4$, filtered, and concentrated. After work-up, the residue was purified by flash chromatography on silica gel (EtOAc/Hexanes) to afforded compound **32c** as a yellow solid (0.813 g, 60% yield). Characterizations were consistent with previously reported literature.[32]

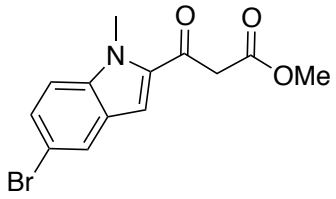

Methyl 3-(5-bromo-1-methyl-1*H*-indol-2-yl)-3-oxopropanoate (12d): Prepared following general procedure A using 5-bromo-1-methyl-1*H*-Indole-2-carboxylic acid **31b** (1.13 g, 4.46 mmol) in CH_2Cl_2 (9 mL), oxalyl chloride (0.453 mL, 5.35 mmol), and catalytic DMF (5 drops) stirred at room temperature for 3 hours to generate the acid chloride. The enolate was generated using LHMDS (1 M in THF, 8.7 mL) and MeOAc (0.347 mL, 4.36 mmol) and the generated acid chloride in THF (4 mL) was added at -78°C and stirred for 30 minutes. After work-up, the residue was purified by flash chromatography on silica gel (5% EtOAc/Hexanes) to afforded compound **32d** as a pale yellow solid (0.440 g, 32% yield). **^{1}H NMR** (300 MHz, $CDCl_3$) δ = 7.83 (dd, *J* = 1.9, 0.6 Hz, 1H), 7.47 (dd, *J* = 8.9, 1.9 Hz, 1H), 7.29 (d, *J* = 0.8 Hz, 1H), 7.22 (d, *J* = 0.8 Hz, 1H), 4.06 (s, 3H), 3.98 (s, 2H), 3.76 (s, 3H). **^{13}C NMR** (500 MHz, $CDCl_3$) δ = 185.32, 167.79,

138.96, 134.50, 129.47, 127.17, 125.36, 114.12, 112.04, 111.71, 77.28, 77.02, 76.77, 52.61, 46.97, 32.45. **IR** 2923 (w), 2363 (m), 1719 (s), 1652 (s) cm^{-1}. **HMRS (ESI)** *m/z:* $[M+Na]^+$ calc. for $C_{13}H_{12}NO_3BrNa$, 331.9893; Found, 331.9886.

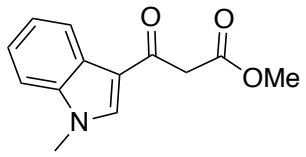

Methyl 3-(1-methyl-1*H*-indol-3-yl)-3-oxopropanoate (32e): Prepared following general procedure A using 2-carboxylic acid (2.90 g, 16.6 mmol) in CH_2Cl_2 (33 mL), oxalyl chloride (1.71 mL, 19.9 mmol), and catalytic DMF (0.5 mL) stirred at room temperature for 3 hours to generate the acid chloride. The enolate was generated using LHMDS (1 M in THF, 35 mL) and MeOAc (1.38 mL, 17.4 mmol) and the generated acid chloride in THF (17 mL) was added at -78°C and stirred for 30 min. After work-up, the residue was purified by flash chromatography on silica gel (5% EtOAc/Hexanes) to afforded compound **12e** as a yellow solid (1.60 g, 42% yield). **^{1}H NMR** (300 MHz, $CDCl_3$) δ = 8.39 – 8.33 (m, 1H), 7.77 (s, 1H), 7.36 – 7.29 (m, 3H), 3.86 (d, *J* = 6.2 Hz, 5H), 3.74 (s, 3H). **^{13}C NMR** (500 MHz, $CDCl_3$) δ = 185.95, 168.60, 137.53, 136.44, 126.32, 123.76, 123.02, 122.62, 115.90, 109.72, 77.29, 77.03, 76.78, 52.46, 47.27, 33.69. **IR** 2924 (w), 2360 (w), 1730 (s), 1639 (s), 744 (s) cm^{-1}. **HRMS (ESI)** *m/z:* $[M+Na]^+$ calc. for $C_{13}H_{13}NO_3Na$, 254.0788; Found, 254.0782.

2.5.2.3 Synthesis of Alkylidenes

General Procedure B for Alkylidene Synthesis*:* Synthesis via conditions established by France.[20] To a round bottom flask charged with $Cu(OAc)_2$ (10 mol %) and a magnetic stir bar was added a 0.2 M solution of β-keto ester (1.0 equiv.) in AcOH. A solution of 37 wt % formaldehyde in water (1.0 equiv.) was added to the reaction mixture. The mixture was stirred at 90°C for 1 hour and then AcOH was removed under reduced pressure. The resulting oil was dissolved in DCM and washed with distilled water in separatory funnel. The organic layer was separated, dried with $MgSO_4$, filtered and then concentrated under reduced pressure. The residue was purified by silica gel flash chromatography (eluting with EtOAc:Hexane) to isolate the product.

General Procedure C for Alkylidene Synthesis[20]: A round bottom flask was charged with β-keto ester (1.0 equiv.) and THF. After cooling the solution to 0°C, titanium(IV) chloride tetrahydrofuran complex (0.5 equiv.) and dry CCl_4 (0.5 equiv.) were added to the reaction vessel and allowed to stir for 1 hour at 0 °C. Aldehyde (1.0 equiv.) was added slowly, and the reaction was stirred at 0 °C for 1 hour. Then pyridine (4.0 equiv.) was slowly added to the solution. The reaction mixture was warmed to room temperature and allowed to stir overnight. The reaction was quenched with water and the organic layer was collected. The aqueous layer was extracted with ether, and the combined organic layers were washed with saturated $NaHCO_3$ and brine and dried over $MgSO_4$. The organic layer was concentrated, and purified by silica gel column chromatography eluting with EtOAc:Hexane.

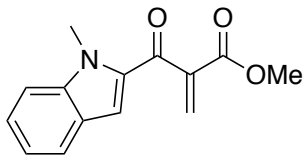

Methyl 2-(1-methyl-1*H*-indole-2-carbonyl)acrylate (33a): Prepared following general procedure B using β-keto ester **32a** (0.250 g, 1.08 mmol) in AcOH (5.4 mL), formaldehyde (0.864 g, 1.08 mmol) and $Cu(OAc)_2$ (0.0390 g, 0.216 mmol (20 mol %)). After 0.5 hours, the reaction was concentrated under reduced pressure and column chromatography afforded alkylidene **33a** as a yellow solid (0.129 g, 48% yield). Characterizations were consistent with previously reported literature.[20]

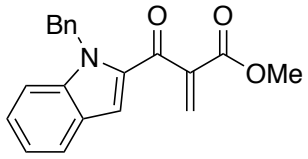

Methyl 2-(1-benzyl-1*H*-indole-2-carbonyl)acrylate (33b): Prepared following general procedure B using β-keto ester **32b** (0.250 g, 0.813 mmol) in AcOH (4.1 mL), formaldehyde (0.814 g, 0.813 mmol) and $Cu(OAc)_2$ (0.0148 g, 0.0810 mmol (10 mol %)). After 1 hour, the reaction was concentrated under reduced pressure and column chromatography afforded alkylidene **33b** as a pale yellow solid (0.139 g, 47% yield). **^{1}H NMR** (500 MHz, $CDCl_3$) δ = 7.70 (dt, *J* = 8.1, 1.0 Hz, 1H), 7.42 – 7.34 (m, 2H), 7.24 (dd, *J* = 7.0, 1.2 Hz, 2H), 7.23 – 7.15 (m, 3H), 7.10 (ddt, *J* = 7.3, 1.4, 0.7 Hz, 2H), 6.69 (d, *J* = 0.8 Hz, 1H), 6.08 (d, *J* = 0.7 Hz, 1H), 5.89 (s, 2H), 3.76 (s, 3H). **^{13}C NMR** (500 MHz, $CDCl_3$) δ = 185.23, 164.92, 141.31, 140.80, 138.01, 133.89, 130.89, 128.56, 127.25, 127.02, 126.60, 125.98, 123.40, 121.33, 116.33, 111.09, 77.30, 77.05, 76.80, 52.56, 48.17**.**

IR 3032 (w), 2951 (w), 2360 (w), 1726 (s), 1645 (s), 723 (s) cm^{-1}. **HMRS (ESI)** *m/z:* $[M+Na]^+$ calc. for $C_{20}H_{17}NO_3Na$, 342.1084; Found, 342.1092.

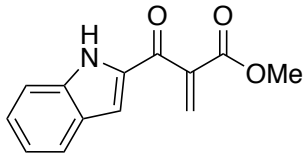

Methyl 2-(1*H*-indole-2-carbonyl)acrylate (33c): Prepared following general procedure A using β-keto ester **32c** (0.250 g, 1.15 mmol) in AcOH (5.8 mL), formaldehyde (0.0934 g, 1.15 mmol) and $Cu(OAc)_2$ (0.0209 g, 0.115 mmol (10 mol %)). After 1 hour, the reaction was concentrated under reduced pressure and column chromatography afforded alkylidene **33c** as a pale yellow solid (0.100 g, 37% yield). **^{1}H NMR** (300 MHz, $CDCl_3$) δ = 9.11 (s, 1H), 7.70 (dq, *J* = 8.1, 1.0 Hz, 1H), 7.48 – 7.34 (m, 2H), 7.17 (ddd, *J* = 8.1, 6.7, 1.3 Hz, 1H), 7.09 (dd, *J* = 2.2, 0.9 Hz, 1H), 6.78 (d, *J* = 0.7 Hz, 1H), 6.24 (d, *J* = 0.8 Hz, 1H), 3.83 (s, 3H). **^{13}C NMR** (500 MHz, $CDCl_3$) δ = 184.46, 164.80, 139.80, 138.65, 134.42, 132.08, 127.33, 127.20, 123.37, 121.25, 113.52, 112.66, 77.41, 77.16, 76.90, 52.70. **IR** 3308 (m), 2362 (m), 1729 (s), 1615 (s), 1124 (m) cm^{-1}. **HRMS (ESI)** *m/z:* $[M+H]^+$ calc. for $C_{13}H_{12}NO_3$, 230.0812; Found, 230.0806.

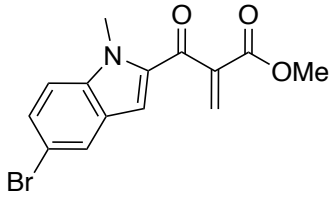

Methyl 2-(5-bromo-1-methyl-1*H*-indole-2-carbonyl)acrylate (33d): Prepared following general procedure B using β-keto ester **32d** (0.250 g, 0.806 mmol) in AcOH (4 mL), formaldehyde (0.0654 g, 0.806 mmol) and $Cu(OAc)_2$ (0.0146 g, 0.0810 mmol (10

mol %)). After 1 hour, the reaction was concentrated under reduced pressure and column chromatography afforded alkylidene **33d** as a yellow solid (0.143 g, 55% yield). **^{1}H NMR** (500 MHz, $CDCl_3$) δ = 7.79 (dd, *J* = 1.9, 0.7 Hz, 1H), 7.47 (dd, *J* = 8.9, 1.9 Hz, 1H), 7.29 (dt, *J* = 8.9, 0.7 Hz, 1H), 7.03 (d, *J* = 0.9 Hz, 1H), 6.72 (d, *J* = 0.7 Hz, 1H), 6.12 (d, *J* = 0.7 Hz, 1H), 4.10 (s, 3H), 3.81 (s, 3H). **^{13}C NMR** (500 MHz, $CDCl_3$) δ = 185.29, 164.77, 141.18, 139.38, 134.88, 131.15, 129.58, 127.12, 125.48, 114.16, 112.02, 77.29, 77.03, 76.78, 52.61, 32.33, 29.71. **IR** 2949 (w), 1715 (s), 1639 (s), 1249 (s), 750 (m), 737 (m) cm^{-1}. **HRMS (ESI)** *m/z:* $[M+Na]^+$ calc. for $C_{14}H_{12}NO_3BrNa$, 343.9893; Found, 343.9887.

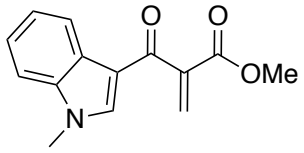

Methyl 2-(1-methyl-1*H*-indole-3-carbonyl)acrylate (33e): Prepared following general procedure A using β-keto ester **32e** (1.00 g, 4.32 mmol) in AcOH (4 mL), formaldehyde (0.32 mL, 4.32 mmol) and $Cu(OAc)_2$ (0.0785 g, 0.432 mmol). After 2 hours, the reaction was concentrated under reduced pressure and column chromatography afforded alkylidene **33e** as a red-brown oil (0.366 g, 35% yield).). **^{1}H NMR** (500 MHz, $CDCl_3$) δ = 8.43 – 8.38 (m, 1H), 7.55 (s, 1H), 7.36 – 7.29 (m, 3H), 6.62 (d, *J* = 1.0 Hz, 1H), 5.99 (d, *J* = 1.0 Hz, 1H), 3.81 (s, 3H), 3.78 (s, 3H). **^{13}C NMR** (500 MHz, $CDCl_3$) δ = 186.86, 165.36, 141.98, 138.20, 137.85, 129.18, 126.42, 123.93, 123.09, 122.71, 115.96, 109.82, 77.35, 77.10, 76.84, 52.48, 33.68. **IR** 3119 (w), 2952 (w), 1722 (s), 1604 (m), 1525 (m), 1220 (m), 747 (m) cm^{-1}. **HRMS (ESI)** *m/z:* $[M+Na]^+$ calc. for $C_{14}H_{13}NO_3Na$, 266.0788; Found, 266.0790.

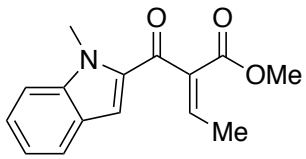

Methyl (*Z*)-2-(1-methyl-1*H*-indole-2-carbonyl)but-2-enoate (33f): According to the general procedure C, titanium(IV) chloride tetrahydrofuran complex (0.205 g, 1.08 mmol) and CCl_4 (0.1 mL, 1.08 mmol) were added to a solution of β-keto ester **32a** (0.500 g, 2.16 mmol) in THF (6 mL). After 1 hour, acetaldehyde (0.1 mL, 2.16 mmol) was added followed by pyridine (0.7 mL, 8.65 mmol). The reaction was quenched after stirring overnight and purified via column chromatography to afford alkylidene **33f** (0.337 g, 60 % yield) as a yellow solid. **^{1}H NMR** (300 MHz, $CDCl_3$) δ =7.67 (dt, *J* = 8.1, 1.0 Hz, 1H), 7.44 – 7.37 (m, 2H), 7.32 – 7.22 (m, 1H), 7.22 – 7.12 (m, 1H), 7.12 – 7.10 (m, 1H), 4.17 (s, 3H), 4.07 (d, *J* = 4.0 Hz, 1H), 3.76 (s, 1H), 3.72 (s, 3H), 1.86 (d, *J* = 7.3 Hz, 3H). **^{13}C NMR** (500 MHz, $CDCl_3$) δ = 186.69, 185.59, 165.89, 165.14, 145.62, 142.85, 140.86, 140.58, 136.35, 135.28, 134.86, 134.66, 126.64, 126.24, 125.96, 125.78, 123.30, 123.19, 123.11, 121.02, 120.93, 120.87, 114.91, 113.84, 112.94, 110.49, 110.38, 77.32, 77.07, 76.82, 52.55, 52.26, 52.03, 46.94, 32.14, 31.96, 15.75, 15.62. **IR** 2949 (w), 1715 (s), 1639 (s), 1249 (s), 750 (m), 737 (m) cm^{-1}. **HRMS (ESI)** *m/z:* $[M+Na]^+$ calc. for $C_{15}H_{15}NO_3Na$, 280.0944; Found, 280.0937.

2.5.2.4 Synthesis of alkens

General Procedure D Synthesis of alkene: nBuLi (2.5 M in hexane, 1.5 equiv.) was added to a stirred suspension of alkyltriphenylphosphonium bromide (1.5 equiv.) in dry ether. After 30 minutes, ketone (1.0 equiv.) was added and the mixture was stirred overnight at room temperature. The reaction was quenched with water and extracted with diethyl ether.

The combined organic layers were dried over $MgSO_4$ and the resulting filtrate was concentrated, and purified by silica gel column chromatography eluting with EtOAc:Hexane.

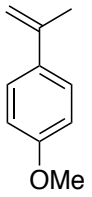

1-methoxy-4-(prop-1-en-2-yl)benzene (23b): The general procedure was followed using nBuLi (4 mL, 15.1 mmol), methyltriphenylphosphonium bromide (5.38 g, 15.1 mmol), and ether (47 mL). After 30 minutes, 1-(4-methoxyphenyl)ethan-1-one (1.50 g, 10.1 mmol) was added and the mixture was stirred overnight at room temperature. The reaction was quenched with water and extracted with diethyl ether. The combined organic layers were dried over $MgSO_4$ and the resulting filtrate was concentrated, and purified by silica gel column chromatography eluting with EtOAc:Hexanes to afford alkene **23b** as a white solid (0.978 g, 66% yield). Characterizations were consistent with previously reported literature.[33]

2.5.2.5 Synthesis of Cyclohepta[*b*]indoles

General Procedure E Synthesis of Cyclohepta[b]indoles: To a round bottom flask charged with $Ca(NTf_2)_2$ (2.5 mol%) and (n-Bu_4N)(PF_6) (2.5 mol%) in CH_2Cl_2 at 40°C and a magnetic stir bar was added a solution of alkylidene (1.0 equiv.) and alkene (5.0 equiv.) in CH_2Cl_2 (0.10 M). After complete consumption of the starting alkylidene, the reaction mixture was concentrated under reduced pressure and purified by silica gel flash chromatography eluting with EtOAc:Hexanes.

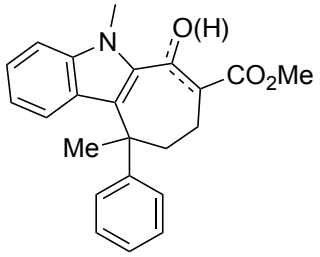

Methyl-5,10-dimethyl-6-oxo-10-phenyl-5,6,7,8,9,10-hexahydrocyclohepta[*b*]indole-7-carboxylate (28aa): The general procedure was followed using alkylidene **33a** (0.100 g, 0.411 mmol), α-methylstyrene **23a** (0.27 mL, 2.05 mmol), $Ca(NTf_2)_2$ (6.17 mg, 0.0100 mmol), (n-Bu_4N)(PF_6) (3.98 mg, 0.0100 mmol) and CH_2Cl_2 (4.11 mL) at 40°C. After 30 minutes, the reaction was allowed to cool to room temperature, then concentrated under reduced pressure, and column chromatography (EtOAc/hexane) afforded cyclohepta[*b*]indole **28aa** as a yellow solid keto-enol mixture (0.1559g, 98% yield). **^{1}H NMR** (500 MHz, $CDCl_3$) δ = 13.40 (s, 0.32H), 7.39 – 7.31 (m, 6H), 7.31 – 7.27 (m, 7H), 7.26 – 7.10 (m, 15H), 6.95 – 6.79 (m, 6H), 3.98 (s, 1H), 3.94 – 3.90 (m, 2H), 3.86 (d, J = 4.2 Hz, 11H), 3.82 (d, J = 6.4 Hz, 2H), 3.75 (s, 5H), 3.70 (s, 5H), 2.37 – 2.06 (m, 11H), 2.05 – 2.00 (m, 3H), 1.99 (s, 6H), 1.85 (s, 5H).**^{13}C NMR** (500 MHz, $CDCl_3$) δ = 193.88, 193.51, 173.30, 171.03, 170.96, 163.55, 150.64, 148.46, 147.80, 139.88, 139.72, 134.20, 129.73, 129.00, 128.73, 128.30, 128.13, 127.99, 127.39, 127.36, 126.80, 126.58, 126.30, 126.14, 126.11, 125.62, 125.39, 125.30, 125.28, 125.23, 124.17, 123.98, 123.95, 123.51, 119.77, 119.57, 119.01, 110.37, 110.35, 109.92, 105.26, 77.49, 77.07, 76.64, 60.37, 60.01, 52.41, 51.98, 47.48, 45.13, 43.86, 42.72, 33.91, 31.87, 31.80, 29.60, 29.49, 28.45, 22.24, 21.36, 19.18. **IR** 2923 (w), 2363 (m), 1739 (s), 1652 (s), 743 (s), 699 (s) cm^{-1}. **HRMS (ESI)** *m/z:* $[M+Na]^+$ calc. for $C_{22}H_{23}NO_3Na$, 384.1570; Found, 384.1565.

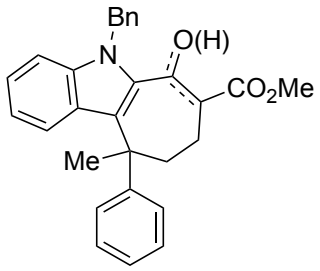

Methyl 5-benzyl-10-methyl-6-oxo-10-phenyl-5,6,7,8,9,10-hexahydrocyclohepta[*b*]indole-7-carboxylate (28ba): The general procedure was followed using alkylidene **33a** (0.100 g, 0.313 mmol), α-methylstyrene **23a** (0.204 mL, 1.57 mmol), $Ca(NTf_2)_2$ (4.70 mg, 0.00800 mmol), (n-Bu_4N)(PF_6) (3.03 mg, 0.00800 mmol) and CH_2Cl_2 (3.13 mL) at 40°C. After 30 minutes, the reaction was allowed to cool to room temperature, then concentrated under reduced pressure and column chromatography (EtOAc/hexanes) afforded cyclohepta[*b*]indole **28ba** as a yellow solid keto-enol mixture (0.0792 g, 56 % yield). **^{1}H NMR** (500 MHz, $CDCl_3$) δ = 13.37 (s, 1H), 7.39 – 7.27 (m, 24H), 7.26 – 7.08 (m, 16H), 7.02 (dt, J = 8.2, 1.0 Hz, 1H), 6.99 – 6.93 (m, 2H), 6.88 (dddd, J = 13.8, 8.0, 6.8, 1.0 Hz, 2H), 5.76 (s, 1H), 5.63 – 5.58 (m, 4H), 3.91 (dd, J = 10.0, 7.1 Hz, 1H), 3.82 – 3.79 (m, 3H), 3.58 (s, 3H), 3.52 (s, 3H), 2.62 (ddd, J = 15.6, 8.0, 1.9 Hz, 1H), 2.48 (ddd, J = 15.6, 8.5, 2.0 Hz, 1H), 2.39 – 2.17 (m, 6H), 2.16 – 2.03 (m, 8H), 2.01 (s, 3H), 1.94 (s, 3H). **^{13}C NMR** (500 MHz, $CDCl_3$) δ = 193.64, 193.43, 173.20, 170.62, 170.55, 163.29, 150.62, 148.11, 148.02, 140.07, 139.80, 139.65, 139.17, 138.52, 138.39, 133.99, 133.90, 129.91, 129.84, 129.72, 128.59, 128.58, 128.47, 128.43, 128.27, 128.16, 128.10, 127.99, 127.92, 127.90, 127.85, 127.29, 127.13, 127.05, 126.89, 126.85, 126.80, 126.71, 126.64, 126.60, 126.39, 126.32, 126.24, 126.21, 126.17, 125.80, 125.73, 125.61, 125.58, 124.31, 124.25, 124.20, 123.72, 120.18, 120.01, 119.47, 111.11, 110.71, 105.41, 77.12, 76.87, 60.57, 59.93, 52.31, 52.28, 52.00, 50.04, 48.17, 48.10, 47.57, 45.33, 45.28,

45.20, 43.69, 42.80, 29.65, 29.18, 29.06, 22.14, 21.38, 19.20. **IR** 3027 (w), 2928 (w), 1740 (s), 1654 (m), 703 (m), 701 (m) cm^{-1}. **HRMS (ESI)** *m/z:* $[M+Na]^+$ calc. for $C_{29}H_{27}NO_3Na$, 460.1883; Found, 460.1867.

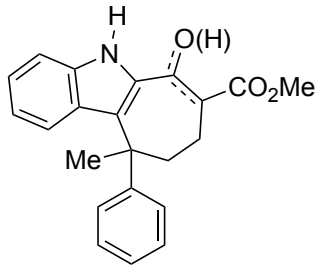

Methyl 10-methyl-6-oxo-10-phenyl-5,6,7,8,9,10-hexahydrocyclohepta[*b*]indole-7-carboxylate (28ca): The general procedure was followed using alkylidene **33c** (0.100 g, 0.436 mmol), α-methylstyrene **23a** (0.284 mL , 2.18 mmol), $Ca(NTf_2)_2$ (6.55 mg, 0.0110 mmol), (n-Bu_4N)(PF_6) (4.23 mg, 0.0110 mmol) and CH_2Cl_2 (4.36 mL) at 40°C. After 30 minutes, the reaction was allowed to cool to room temperature, then concentrated under reduced pressure and column chromatography (EtOAc/hexanes) afforded cyclohepta[*b*]indole **28ca** as a yellow solid keto-enol mixture (0.0826 g, 53 % yield). **^{1}H NMR:** (500 MHz, $CDCl_3$) δ = 13.39 (s, 1H), 9.17 (s, 1H), 9.00 (s, 1H), 7.36 (dd, *J* = 13.9, 7.7 Hz, 2H), 7.30 – 7.27 (m, 4H), 7.26 – 7.22 (m, 5H), 7.17 (qd, *J* = 6.0, 2.9 Hz, 2H), 6.97 (d, *J* = 8.2 Hz, 2H), 6.92 (d, *J* = 8.3 Hz, 1H), 6.83 (ddd, *J* = 18.4, 9.4, 7.0 Hz, 2H), 3.89 – 3.85 (m, 1H), 3.82 (d, *J* = 4.9 Hz, 5H), 3.73 (s, 1H), 2.60 (ddd, *J* = 16.8, 9.9, 1.3 Hz, 1H), 2.50 – 2.32 (m, 2H), 2.31 – 2.03 (m, 6H), 1.98 (s, 2H), 1.93 (d, *J* = 8.9 Hz, 5H). **^{13}C NMR** (500 MHz, $CDCl_3$) δ = 190.81, 190.72, 173.45, 171.35, 171.24, 161.47, 149.93, 149.41, 148.70, 137.48, 137.44, 135.96, 131.67, 131.44, 130.61, 130.35, 128.37, 128.31, 128.13, 127.99, 127.59, 127.21, 127.11, 127.03, 127.01, 126.96, 126.67, 126.59, 126.57, 126.23,

126.20, 125.78, 124.87, 124.71, 124.14, 123.23, 119.93, 119.90, 119.29, 112.00, 111.98, 111.38, 102.84, 77.31, 77.06, 76.80, 59.44, 58.76, 52.51, 52.49, 52.04, 45.35, 45.24, 45.18, 45.16, 44.43, 43.82, 29.05, 28.80, 27.88, 22.28, 21.83, 19.82. **IR** 3342 (w), 2928 (w), 2365 (m), 1733 (s), 1622 (s), 746 (m), 701 (m) cm^{-1}. **HRMS (ESI)** *m/z:* $[M+Na]^+$ calc. for $C_{22}H_{21}NO_3Na$, 370.1414; Found, 370.1406.

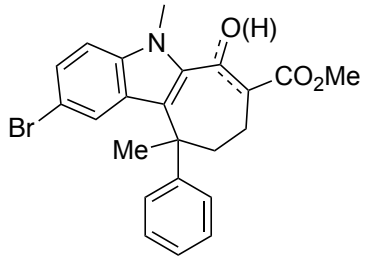

Methyl 2-bromo-5,10-dimethyl-6-oxo-10-phenyl-5,6,7,8,9,10-hexahydrocyclohepta[*b*]indole-7-carboxylate (28da): The general procedure was followed using alkylidene **33d** (0.0989 g, 0.307 mmol), α-methylstyrene **23a** (0.2 mL, 1.54 mmol), $Ca(NTf_2)_2$ (4.61 mg, 0.00800 mmol), (n-Bu_4N)(PF_6) (2.97 mg, 0.00800 mmol) and CH_2Cl_2 (3.10 mL) at reflux. After 24 hours, the reaction was allowed to cool to room temperature, then concentrated under reduced pressure and column chromatography (EtOAc/hexanes) afforded cyclohepta[*b*]indole **28da** as a yellow solid keto-enol mixture (0.101 g, 75 % yield). **^{1}H NMR:** (500 MHz, $CDCl_3$) δ = 13.35 (s, 0.34H), 7.36 (ddd, J = 2.6, 1.8, 0.7 Hz, 1H), 7.33 (ddd, J = 2.6, 1.8, 0.7 Hz, 1H), 7.30 – 7.12 (m, 19H), 7.05 – 7.02 (m, 0.39H), 6.99 (dd, J = 1.9, 0.7 Hz, 1H), 3.96 – 3.86 (m, 3H), 3.85 – 3.79 (m, 8H), 3.74 (d, J = 0.7 Hz, 3H), 3.70 (d, J = 0.7 Hz, 3H), 2.60 (ddd, J = 15.8, 7.1, 2.9 Hz, 0.48H), 2.44 (ddd, J = 15.6, 7.5, 2.8 Hz, 1H), 2.37 – 1.96 (m, 10H), 1.95 (s, 3H), 1.90 (s, 1H), 1.81 (d, J = 0.8 Hz, 3H). **^{13}C NMR:** (500 MHz, $CDCl_3$) δ = 193.88, 193.51, 170.88, 170.72,

162.86, 149.97, 147.67, 147.10, 138.39, 138.33, 138.12, 134.94, 134.93, 128.47, 128.29, 128.18, 128.13, 128.03, 127.87, 127.76, 127.26, 126.93, 126.81, 126.67, 126.56, 126.46, 126.43, 126.38, 126.16, 126.00, 125.90, 125.56, 112.95, 112.71, 112.20, 111.91, 111.89, 111.42, 108.35, 105.91, 77.28, 77.03, 76.77, 60.21, 59.79, 52.47, 52.08, 47.39, 45.00, 44.98, 43.70, 42.63, 34.07, 31.96, 31.91, 29.72, 29.51, 29.47, 29.38, 28.62, 22.71, 22.24, 21.29, 19.17, 14.15. **IR** 2941 (w), 2359 (w), 1739 (s), 1654 (s), 701 (s) cm^{-1}. **HRMS (ESI)** *m/z:* $[M+H]^+$ calc. for $C_{23}H_{23}NO_3Br$, 440.0856; Found, 440.0844.

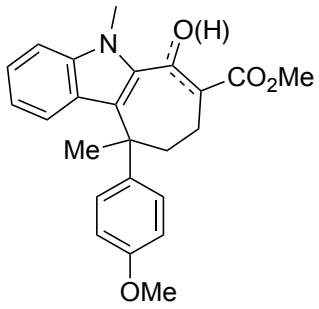

Methyl 10-(4-methoxyphenyl)-5,10-dimethyl-6-oxo-5,6,7,8,9,10-hexahydrocyclohepta[*b*]indole-7-carboxylate (4ab): The general procedure was followed using alkylidene **33a** (0.181 g, 0.743 mmol), alkene **3b** (0.439 g, 3.72 mmol), $Ca(NTf_2)_2$ (11.2 mg, 0.0190 mmol), (n-Bu_4N)(PF_6) (7.20 mg, 0.0190 mmol) and CH_2Cl_2 (7.43 mL) at 40°C. After 30 minutes, the reaction was allowed to cool to room temperature, then concentrated under reduced pressure and column chromatography (EtOAc/hexane) afforded cyclohepta[*b*]indole **28ab** as a yellow solid keto-enol mixture (0.270 g, 93% yield). **^{1}H NMR** (500 MHz, $CDCl_3$) δ = 13.41 (s, 0.23H), 7.37 – 7.33 (m, 3H), 7.31 – 7.26 (m, 3H), 7.24 – 7.21 (m, 3H), 7.17 (dt, *J* = 8.3, 1.0 Hz, 2H), 7.15 – 7.11 (m, 3H), 6.98 – 6.86 (m, 5H), 6.83 – 6.75 (m, 6H), 3.98 (s, 1H), 3.85 (d, *J* = 4.5 Hz, 9H), 3.83 (s, 1H), 3.79 (s, 4H), 3.75 (d, *J* = 6.6 Hz, 9H), 3.70 (s, 4H), 2.58 (ddd, *J* = 15.6, 7.4, 2.6 Hz, 0.23H), 2.47

(ddd, J = 15.7, 7.7, 2.7 Hz, 0.24H), 2.34 – 1.97 (m, 12H), 1.96 (s, 5H), 1.91 (s, 1H), 1.82 (s, 4H). **^{13}C NMR** (500MHz, $CDCl_3$) δ = 193.97, 193.58, 173.33, 171.07, 171.00, 163.55, 157.79, 157.72, 157.38, 142.91, 140.60, 139.89, 139.73, 134.11, 134.08, 129.62, 129.28, 128.99, 128.45, 127.84, 127.64, 127.59, 126.34, 125.42, 125.32, 125.29, 125.23, 124.28, 124.08, 123.94, 123.67, 119.74, 119.54, 118.97, 113.56, 113.38, 113.24, 110.36, 110.34, 109.91, 105.30, 77.31, 77.06, 76.80, 60.42, 60.01, 55.18, 55.15, 52.42, 51.99, 47.61, 44.56, 44.49, 43.96, 42.80, 34.15, 33.92, 31.86, 31.79, 29.86, 29.73, 29.67, 28.66, 22.37, 22.27, 21.37, 19.16, 14.10. **IR** 2928 (w), 1734 (s), 1654 (s), 1508 (s), 827 (m), 727 (m) cm^{-1}. **HRMS (ESI)** *m/z:* $[M+Na]^+$ calc. for $C_{24}H_{25}NO_4Na$, 414.1676; Found, 414.1671.

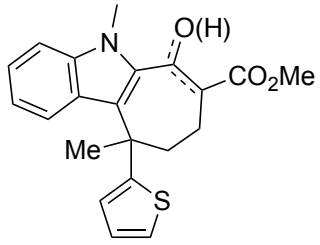

Methyl 5,10-dimethyl-6-oxo-10-(thiophen-2-yl)-5,6,7,8,9,10-hexahydrocyclohepta[*b*]indole-7-carboxylate (28ac): The general procedure was followed using alkylidene **33a** (0.100 g, 0.411 mmol), 2-(prop-1-en-2-yl)thiophene **23c** (2.55 g, 2.05 mmol), $Ca(NTf_2)_2$ (6.17 mg, 0.0100 mmol), (n-Bu_4N)(PF_6) (3.98 mg, 0.0100 mmol) and CH_2Cl_2 (4.11 mL) at 40°C. After the consumption of the starting material, the reaction was allowed to cool to room temperature, then concentrated under reduced pressure and column chromatography (EtOAc/hexane) afforded cyclohepta[*b*]indole **28ac** as a yellow solid keto-enol mixture (0.138 g, 84% yield). **^{1}H NMR** (500 MHz, $CDCl_3$) δ = 13.36 (s, 0.13H), 7.35 (ddt, J = 8.4, 3.3, 1.0 Hz, 2H), 7.31 – 7.27 (m, 2H), 7.26 – 7.23 (m, 2H), 7.19 (dd, J = 5.1, 2.9 Hz, 1H), 7.16 (dd, J = 5.0, 3.0 Hz, 0.25H), 7.05 (dt, J = 8.3, 1.0

Hz, 1H), 6.98 – 6.91 (m, 5H), 6.82 (dd, *J* = 5.0, 1.4 Hz, 1H), 3.97 (s, 1H), 3.90 (ddd, *J* = 11.7, 9.9, 6.9 Hz, 2H), 3.84 (d, *J* = 3.4 Hz, 6H), 3.75 (s, 2H), 3.70 (s, 3H), 2.55 – 2.50 (m, 0.35H), 2.35 – 2.25 (m, 2H), 2.24 – 2.09 (m, 4H), 2.08 – 2.00 (m, 1H), 1.99 – 1.93 (m, 4H), 1.90 (s, 1H), 1.82 (s, 3H). **^{13}C NMR** (500MHz, $CDCl_3$) δ = 193.91, 193.50, 170.99, 170.95, 150.09, 149.33, 139.76, 139.64, 133.50, 133.47, 132.36, 128.44, 128.29, 127.35, 127.24, 127.04, 127.00, 126.41, 125.58, 125.36, 125.34, 125.31, 125.22, 123.94, 123.76, 121.47, 120.10, 120.02, 119.82, 119.63, 110.36, 77.29, 77.03, 76.78, 60.38, 60.06, 52.42, 51.98, 43.18, 42.97, 42.80, 41.79, 31.82, 31.71, 30.25, 30.17, 28.90, 27.58, 22.11, 21.62. **IR** 2940 (w), 1734 (s), 1652 (s), 742 (m) cm^{-1}. **HRMS (ESI)** *m/z:* $[M+Na]^+$ calc. for $C_{21}H_{21}NO_3Na$, 390.1134; Found, 390.1130.

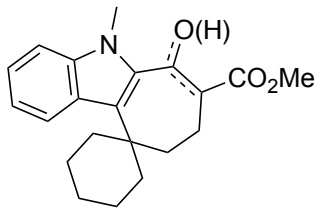

Methyl 5-methyl-6-oxo-6,7,8,9-tetrahydro-5*H*-spiro[cyclohepta[*b*]indole-10,1'-cyclohexane]-7-carboxylate (28ad): The general procedure was followed using alkylidene **33a** (0.100 g, 0.411 mmol), methylenecyclohexane **23d** (0.247 mL, 2.05 mmol), $Ca(NTf_2)_2$ (6.17 mg, 0.0100 mmol), (n-Bu_4N)(PF_6) (3.98 mg, 0.0100 mmol) and CH_2Cl_2 (4.11 mL) at 40°C. After 30 minutes, the reaction was allowed to cool to room temperature, then concentrated under reduced pressure and column chromatography (EtOAc/hexanes) afforded cyclohepta[*b*]indole **28ad** as a yellow solid keto-enol mixture (0.0176 g, 12 % yield). **^{1}H NMR** (500MHz, $CDCl_3$) δ = 13.04 (s, 0.22H), 8.05 (d, *J* = 8.3 Hz, 2H), 7.94 – 7.87 (m, 1H), 7.39 – 7.30 (m, 6H), 7.11 (tdd, *J* = 12.9, 5.3, 1.8 Hz, 3H), 3.94 – 3.79 (m,

7H), 3.78 – 3.65 (m, 17H), 2.61 – 2.36 (m, 10H), 2.24 – 2.14 (m, 5H), 1.89 – 1.80 (m, 5H), 1.75 – 1.69 (m, 4H), 1.69 – 1.60 (m, 7H), 1.60 – 1.55 (m, 10H), 1.55 – 1.38 (m, 10H). **^{13}C NMR** (500MHz, $CDCl_3$) δ = 194.80, 194.75, 170.93, 170.90, 139.85, 133.46, 130.35, 125.06, 124.87, 124.80, 124.57, 123.95, 123.87, 119.43, 119.36, 119.28, 110.81, 110.69, 110.36, 77.29, 77.04, 76.78, 60.44, 60.08, 53.79, 52.40, 52.38, 52.36, 51.95, 51.90, 40.45, 37.75, 37.65, 33.27, 33.23, 31.75, 31.69, 31.42, 30.96, 29.92, 29.75, 29.72, 29.68, 29.29, 25.97, 25.92, 22.09, 21.97, 21.87, 21.77, 20.87, 19.71. **IR** 2923 (w), 1733 (s), 1652 (s), 740 (s) cm^{-1}. **HRMS (ESI)** m/z: $[M+Na]^+$ calc. for $C_{21}H_{25}NO_3Na$ 362.1727; Found, 362.1720.

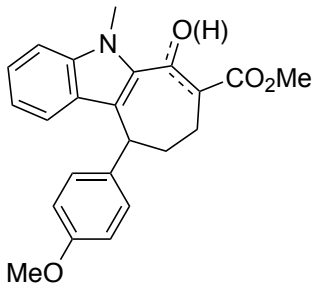

Methyl 10-(4-methoxyphenyl)-5-methyl-6-oxo-5,6,7,8,9,10-hexahydrocyclohepta[*b*]indole-7-carboxylate (28ae): The general procedure was followed using alkylidene **33a** (0.100 g, 0.411 mmol), 4-methoxystyrene **23e** (0.273 mL, 2.05 mmol), $Ca(NTf_2)_2$ (6.17 mg, 0.0100 mmol), (n-Bu_4N)(PF_6) (3.98 mg, 0.0100 mmol) and CH_2Cl_2 (4.11 mL) at 40°C. After 30 minutes, the reaction was allowed to cool to room temperature, then concentrated under reduced pressure and column chromatography (EtOAc/hexanes) afforded cyclohepta[*b*]indole **28ae** as a yellow solid keto-enol mixture (0.113 g, 63 % yield). **^{1}H NMR** (500 MHz, $CDCl_3$) δ = 13.32 (s, 0.22H), 7.41 – 7.28 (m, 9H), 7.13 (dt, J = 8.1, 1.0 Hz, 1H), 7.10 – 6.98 (m, 9H), 6.97 – 6.92 (m, 1H), 6.82 – 6.74 (m, 7H), 4.80 (dd, J = 6.5, 3.8 Hz, 2H), 4.75 (t, J = 4.8 Hz, 1H), 4.62 (dd, J = 9.4, 8.0 Hz,

0.25H), 3.98 (s, 1H), 3.96 (s, 6H), 3.93 (s, 3H), 3.87 – 3.82 (m, 3H), 3.78 (s, 3H), 3.76 – 3.74 (m, 10H), 3.71 (s, 6H), 2.72 – 2.66 (m, 0.32H), 2.43 – 2.19 (m, 10H), 2.13 – 1.95 (m, 4H). **^{13}C NMR** (500MHz, $CDCl_3$) δ = 192.66, 192.17, 173.51, 171.29, 170.75, 163.93, 158.06, 158.03, 157.75, 139.56, 139.24, 136.41, 134.63, 134.56, 134.25, 129.20, 128.72, 128.58, 126.38, 126.07, 126.03, 125.97, 125.89, 124.84, 124.13, 122.10, 121.41, 120.92, 120.33, 120.21, 119.46, 113.96, 113.82, 113.73, 110.29, 110.19, 109.66, 104.40, 77.30, 77.04, 76.79, 60.86, 58.53, 55.22, 55.19, 52.35, 52.30, 51.97, 43.11, 41.96, 40.65, 39.13, 34.55, 33.12, 32.34, 32.14, 31.89, 22.91, 22.33, 21.77. **IR** 2940 (w), 2365 (m), 1741 (s), 1652 (s) 1246 (m) cm^{-1}. **HRMS (ESI)** *m/z:* $[M+Na]^+$calc. for $C_{23}H_{23}NO_4Na$, 400.1519; Found, 400.1510.

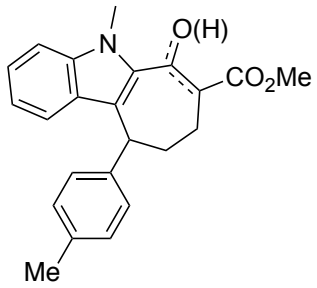

Methyl 5-methyl-6-oxo-10-(*p*-tolyl)-5,6,7,8,9,10-hexahydrocyclohepta[*b*]indole-7-carboxylate (28af): The general procedure was followed using alkylidene **33a** (0.100 g, 0.411 mmol), 4-methylstyrene **23f** (0.271 mL, 2.05 mmol), $Ca(NTf_2)_2$ (6.17 mg, 0.0100 mmol), (n-Bu_4N)(PF_6) (3.98 mg, 0.0100 mmol) and CH_2Cl_2 (4.11 mL) at 40°C. After 30 minutes, the reaction was allowed to cool to room temperature, then concentrated under reduced pressure and column chromatography (EtOAc/hexanes) afforded cyclohepta[*b*]indole **28af** as a yellow solid keto-enol mixture (0.0797 g, 48 % yield). **^{1}H NMR** (500 MHz, $CDCl_3$) δ = 13.34 (s, 0.21H), 7.41 – 7.29 (m, 6H), 7.09 – 6.90 (m, 12H),

4.83 (dd, *J* = 6.6, 3.8 Hz, 1H), 4.77 (t, *J* = 4.8 Hz, 1H), 4.65 (dd, *J* = 9.4, 8.1 Hz, 0.23H), 3.98 (d, *J* = 7.7 Hz, 5H), 3.94 (d, *J* = 4.1 Hz, 2H), 3.90 – 3.82 (m, 3H), 3.79 (s, 2H), 3.71 (s, 4H), 2.73 (ddd, *J* = 15.1, 8.4, 1.8 Hz, 0.33H), 2.53 – 2.47 (m, 1H), 2.46 – 2.20 (m, 16H), 2.15 – 1.94 (m, 3H). **^{13}C NMR** (500MHz, $CDCl_3$) δ = 192.67, 192.18, 173.52, 171.30, 170.77, 163.96, 143.45, 141.27, 139.57, 139.53, 139.25, 139.19, 135.91, 135.41, 134.63, 134.32, 129.94, 129.32, 129.21, 129.17, 129.09, 128.15, 127.67, 127.51, 127.22, 126.43, 126.08, 126.04, 126.02, 125.81, 124.69, 124.15, 122.74, 122.08, 121.42, 120.88, 120.34, 120.21, 119.48, 110.29, 110.19, 109.66, 104.42, 77.32, 77.07, 76.81, 60.93, 58.55, 52.35, 52.30, 51.98, 43.59, 42.41, 41.09, 39.11, 34.50, 33.15, 32.37, 32.09, 31.91, 22.94, 22.36, 21.82, 21.04, 21.03, 21.01. **IR** 2925 (w), 1741 (s), 1654 (s), 744 (s) cm^{-1}. **HRMS (ESI)** *m/z:* $[M+H]^+$ calc. for $C_{23}H_{24}NO_3$, 362.1751; Found, 362.1747.

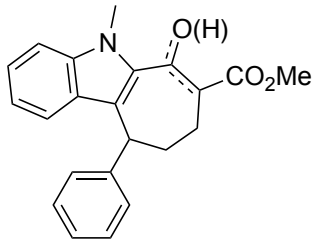

Methyl 5-methyl-6-oxo-10-phenyl-5,6,7,8,9,10-hexahydrocyclohepta[*b*]indole-7-carboxylate (28ag): The general procedure was followed using alkylidene **33a** (0.100 g, 0.411mmol), styrene **23g** (0.591 g, 2.05 mmol), $Ca(NTf_2)_2$ (6.17 mg, 0.0100 mmol), (*n*-$Bu_4N)(PF_6)$ (3.98 mg, 0.0100 mmol) and CH_2Cl_2 (4.11 mL) at 40°C. After 30 minutes, the reaction was allowed to cool to room temperature, concentrated under reduced pressure, and purified by column chromatography (EtOAc/hexanes) to afford cyclohepta[*b*]indole **38ah** as a yellow solid keto-enol mixture (0.0715 g, 20 % yield). **^{1}H NMR** (500 MHz, $CDCl_3$) δ = 13.32 (s, 0.15H), 7.40 – 7.29 (m, 6H), 7.26 – 7.23 (m, 3H), 7.21 – 7.14 (m,

3H), 7.14 – 7.06 (m, 4H), 7.04 (ddd, *J* = 8.1, 6.7, 1.5 Hz, 1H), 6.93 (dddd, *J* = 15.0, 8.0, 6.7, 1.1 Hz, 1H), 4.85 (dd, *J* = 6.6, 3.9 Hz, 1H), 4.79 (t, *J* = 4.9 Hz, 0.47H), 4.72 – 4.65 (m, 0.19H), 3.99 (s, 1H), 3.97 (s, 3H), 3.94 (s, 2H), 3.88 – 3.81 (m, 2H), 3.78 (s, 1H), 3.70 (s, 3H), 2.79 – 2.68 (m, 0.28H), 2.56 – 2.47 (m, 0.35H), 2.44 – 2.21 (m, 5H), 2.14 – 1.92 (m, 2H). **^{13}C NMR** (500MHz, $CDCl_3$) δ = 192.62, 192.17, 173.49, 171.25, 170.72, 163.92, 146.44, 144.27, 142.67, 139.55, 139.25, 134.68, 134.38, 128.62, 128.49, 128.39, 128.27, 127.78, 127.63, 126.42, 126.39, 126.38, 126.08, 126.04, 125.99, 125.98, 125.42, 125.34, 124.41, 124.16, 122.46, 122.03, 121.38, 120.80, 120.35, 120.23, 119.50, 110.31, 110.21, 109.68, 104.44, 77.29, 77.04, 76.79, 60.86, 58.57, 52.37, 52.31, 51.98, 44.01, 42.82, 41.53, 39.07, 34.45, 33.14, 32.36, 32.10, 31.90, 22.94, 22.39, 21.83. **IR** 2920 (w), 2849 (w), 1740 (s), 1652 (s), 740 (s), 699 (s) cm^{-1}. **HRMS (ESI)** *m/z:* $[M+Na]^+$ calc. for $C_{22}H_{21}NO_3Na$, 370.1414; Found, 370.1406.

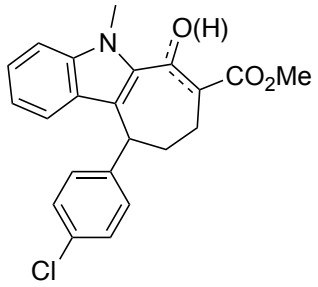

Methyl 10-(4-chlorophenyl)-5-methyl-6-oxo-5,6,7,8,9,10-hexahydrocyclohepta[*b*]indole-7-carboxylate (28ah): The general procedure was followed using alkylidene **33a** (0.100 g, 0.411 mmol), 4-chlorostyrene **23h** (0.247 mL, 2.05 mmol), $Ca(NTf_2)_2$ (6.17 mg, 0.0100 mmol), (*n*-Bu_4N)(PF_6) (3.98 mg, 0.0100 mmol) and CH_2Cl_2 (4.11 mL) at 40°C. After 30 minutes, the reaction was allowed to cool to room temperature, then concentrated under reduced pressure and column chromatography

(EtOAc/hexane) afforded cyclohepta[*b*]indole **28ah** as a yellow solid keto-enol mixture (0.00950 g, 5 % yield). **^{1}H NMR** (500 MHz, $CDCl_3$) δ = 13.35 (s, 0.19H), 7.41 – 7.30 (m, 4H), 7.24 – 7.17 (m, 3H), 7.14 – 7.09 (m, 1H), 7.08 – 7.01 (m, 4H), 6.96 (dddd, *J* = 16.0, 8.0, 6.6, 1.2 Hz, 1H), 4.81 (t, *J* = 5.3 Hz, 1H), 4.78 (t, *J* = 4.9 Hz, 0.41H), 4.70 – 4.63 (m, 0.21H), 3.99 (d, *J* = 2.7 Hz, 1H), 3.97 (s, 3H), 3.94 (s, 1H), 3.85 – 3.77 (m, 3H), 3.72 (s, 3H), 2.80 – 2.69 (m, 0.22H), 2.49 (dtd, *J* = 13.9, 8.3, 1.6 Hz, 0.21H), 2.45 – 2.31 (m, 3H), 2.31 – 2.17 (m, 2H), 2.12 – 1.99 (m, 1H), 1.93 (dtd, *J* = 13.8, 9.7, 1.8 Hz, 0.25H). **^{13}C NMR** (500MHz, $CDCl_3$) δ = 192.49, 192.03, 173.43, 171.14, 170.56, 163.76, 145.02, 142.85, 141.36, 139.56, 139.24, 139.17, 134.66, 134.35, 132.19, 131.60, 129.59, 129.12, 129.01, 128.93, 128.79, 128.65, 128.54, 126.22, 126.18, 126.15, 125.80, 124.55, 124.32, 123.57, 121.81, 121.75, 121.20, 120.60, 120.52, 120.42, 119.67, 110.42, 110.35, 109.81, 104.44, 77.34, 77.09, 76.83, 60.82, 58.61, 52.43, 52.36, 52.04, 43.41, 42.26, 41.13, 38.92, 34.29, 33.20, 32.38, 32.12, 31.91, 22.88, 22.26, 21.73. **IR** 2925 (w), 2357 (w), 1737 (s), 1651 (s), 742 (m) cm^{-1}. **HRMS (ESI)** *m/z:* $[M+Na]^+$ calc. for $C_{22}H_{20}NO_3ClNa$, 404.1024; Found, 404.1016.

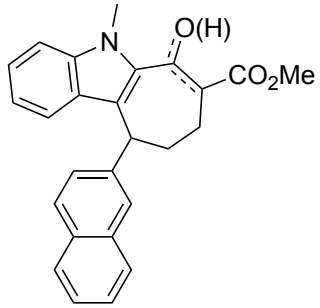

Methyl 5-methyl-10-(naphthalen-2-yl)-6-oxo-5,6,7,8,9,10-hexahydrocyclohepta[*b*]indole-7-carboxylate (28ai): The general procedure was followed using alkylidene **33a** (0.100 g, 0.411 mmol), 2-vinylnaphthalene **23i** (0.317 g,

2.05 mmol), $Ca(NTf_2)_2$ (12.3 mg, 0.0210 mmol), (n-Bu_4N)(PF_6) (7.96 mg, 0.0210 mmol) and CH_2Cl_2 (4.11 mL) at 40°C. After 30 minutes, the reaction was allowed to cool to room temperature, then concentrated under reduced pressure and column chromatography (EtOAc/hexane) afforded cyclohepta[*b*]indole **28ai** as a yellow solid keto-enol mixture (0.117 g, 60 % yield). **^{1}H NMR** (500 MHz, $CDCl_3$) δ 13.39 (s, 0.23H), 7.82 – 7.62 (m, 10H), 7.50 – 7.28 (m, 20H), 7.12 (t, J = 7.3 Hz, 1H), 7.01 (t, J = 7.4 Hz, 2H), 6.91 – 6.83 (m, 1H), 5.01 (dd, J = 6.8, 3.9 Hz, 2H), 4.96 (t, J = 5.0 Hz, 1H), 4.86 (t, J = 8.8 Hz, 0.26H), 4.00 (d, J = 14.7 Hz, 9H), 3.90 (dd, J = 9.6, 6.1 Hz, 2H), 3.84 (s, 1H), 3.77 (s, 2H), 3.70 (s, 6H), 2.83 – 2.75 (m, 0.28H), 2.51 (tdd, J = 10.2, 7.6, 4.6 Hz, 3H), 2.40 (ddt, J = 14.9, 11.1, 3.8 Hz, 2H), 2.29 (ddt, J = 14.4, 9.5, 4.7 Hz, 3H), 2.15 – 1.98 (m, 3H). **^{13}C NMR** (500MHz, $CDCl_3$) δ 192.62, 192.19, 171.24, 170.66, 141.87, 140.27, 139.62, 139.31, 134.82, 133.48, 133.39, 132.21, 128.41, 128.26, 128.18, 127.88, 127.79, 127.56, 126.85, 126.67, 126.43, 126.17, 126.12, 126.07, 126.02, 125.63, 125.59, 125.26, 124.24, 123.20, 122.09, 121.43, 120.42, 120.29, 119.58, 112.94, 110.48, 110.35, 110.24, 77.30, 77.05, 76.79, 60.92, 58.65, 52.35, 52.31, 43.09, 41.86, 34.36, 32.43, 32.16, 31.97, 29.74, 23.06, 22.44. **IR** 2924 (w), 2362 (m), 1739 (s) cm^{-1}. **HRMS (ESI)** *m/z:* $[M+Na]^+$ calc. for $C_{26}H_{23}NO_3Na$, 420.1570; Found, 420.1563.

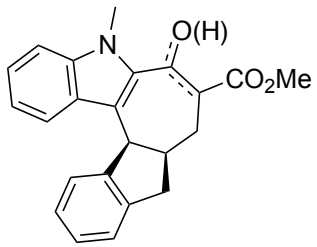

Methyl (8a*S*,13b*S*)-5-methyl-6-oxo-6,7,8,8a,9,13b-hexahydro-5*H*-benzo[2,3]azuleno[5,4-*b*]indole-7-carboxylate (28al): The general procedure was

followed using alkylidene **33a** (0.100 g, 0.411 mmol), indene **23l** (0.240 mL, 2.05 mmol), $Ca(NTf_2)_2$ (6.17 mg, 0.0100 mmol), (n-Bu_4N)(PF_6) (3.98 mg, 0.0100 mmol) and CH_2Cl_2 (4.11 mL) at 40°C. After 30 minutes, the reaction was allowed to cool to room temperature, then concentrated under reduced pressure and column chromatography (EtOAc/hexanes) afforded cyclohepta[*b*]indole **28al** as a yellow solid keto-enol mixture (0.933 g, 57 % yield). **^{1}H NMR** (500 MHz, $CDCl_3$) δ = 12.45 (s, 1H), 7.86 – 7.79 (m, 3H), 7.52 – 7.36 (m, 9H), 7.26 – 7.13 (m, 8H), 7.12 – 6.89 (m, 9H), 6.56 – 6.49 (m, 3H), 5.34 – 5.29 (m, 2H), 5.08 – 4.92 (m, 2H), 4.04 (s, 4H), 4.01 – 3.95 (m, 1H), 3.90 (d, *J* = 12.0 Hz, 6H), 3.84 – 3.76 (m, 7H), 3.74 (s, 4H), 3.66 – 3.59 (m, 2H), 3.56 (d, *J* = 12.5 Hz, 1H), 3.34 – 3.19 (m, 6H), 3.12 – 3.04 (m, 2H), 2.97 – 2.88 (m, 2H), 2.78 – 2.65 (m, 3H), 2.56 – 2.49 (m, 1H), 2.39 (ddd, *J* = 15.6, 10.7, 5.2 Hz, 2H), 2.28 – 2.17 (m, 3H). **^{13}C NMR** (500MHz, $CDCl_3$) δ = 192.01, 173.41, 171.68, 164.24, 145.82, 141.99, 139.53, 138.30, 130.34, 127.18, 127.15, 126.76, 126.34, 125.62, 124.00, 123.83, 123.60, 122.89, 120.75, 118.85, 110.51, 109.87, 54.22, 52.22, 52.04, 51.76, 44.19, 39.72, 38.06, 37.51, 33.91, 32.55, 31.70, 29.72. **IR** 2923 (w), 2360 (m), 1740 (s), 1651 (s), 743 (m) cm^{-1}. **HRMS (ESI)** *m/z:* $[M+Na]^+$ calc. for $C_{23}H_{21}NO_3Na$, 382.1414; Found, 382.1409.

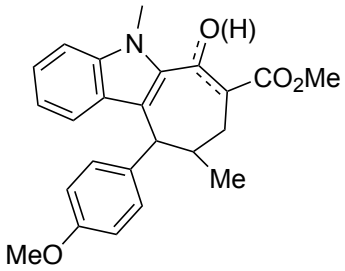

Methyl-10-(4-methoxyphenyl)-5,9-dimethyl-6-oxo-5,6,7,8,9,10-hexahydrocyclohepta[*b*]indole-7-carboxylate (28am): The general procedure was

followed using alkylidene **33a** (0.100 g, 0.411 mmol), anethole **23m** (0.988 mL, 2.05 mmol), $Ca(NTf_2)_2$ (6.17 mg, 0.0100 mmol), (n-Bu_4N)(PF_6) (3.98 mg, 0.0100 mmol) and CH_2Cl_2 (4.11 mL) at 40°C. After 30 minutes, the reaction was allowed to cool to room temperature, then concentrated under reduced pressure and column chromatography (EtOAc/hexanes) afforded cyclohepta[*b*]indole **28am** as a yellow solid keto-enol mixture (0.118 g, 73 % yield). **^{1}H NMR** (500MHz, $CDCl_3$) δ = 13.16 (s, 1H), 7.42 – 7.28 (m, 7H), 7.24 – 7.09 (m, 9H), 7.05 – 6.84 (m, 10H), 6.79 – 6.71 (m, 4H), 4.70 – 4.25 (m, 3H), 3.96 – 3.92 (m, 6H), 3.85 (s, 5H), 3.83 – 3.79 (m, 10H), 3.72 (d, *J* = 7.0 Hz, 8H), 3.20 (dd, *J* = 10.3, 8.3 Hz, 1H), 2.70 – 2.48 (m, 3H), 2.41 – 2.09 (m, 7H), 1.91 (ddd, *J* = 14.8, 6.8, 4.2 Hz, 1H), 1.37 – 1.01 (m, 12H), 1.01 – 0.86 (m, 5H). **^{13}C NMR** (500MHz, $CDCl_3$) δ = 193.13, 192.84, 173.63, 173.56, 171.59, 171.14, 171.10, 163.79, 158.00, 157.98, 157.86, 157.76, 157.66, 139.73, 139.61, 138.97, 137.99, 136.82, 136.75, 136.53, 136.40, 133.54, 133.07, 130.42, 129.97, 129.68, 129.48, 129.25, 129.05, 129.00, 128.84, 128.71, 128.64, 127.69, 127.55, 127.15, 127.00, 126.86, 126.66, 126.12, 125.94, 125.05, 124.59, 124.04, 123.86, 123.84, 123.12, 121.82, 121.58, 120.36, 120.25, 120.23, 120.21, 119.87, 119.50, 118.86, 114.21, 114.11, 113.81, 113.77, 113.75, 113.63, 113.61, 113.56, 112.87, 112.39, 112.24, 110.25, 110.21, 110.16, 109.60, 109.42, 103.11, 102.72, 77.31, 77.06, 76.80, 58.98, 58.73, 58.51, 56.35, 55.31, 55.28, 55.24, 55.21, 55.19, 55.17, 52.34, 52.30, 51.99, 51.96, 51.20, 50.95, 50.53, 50.16, 49.64, 49.34, 45.27, 44.77, 37.96, 37.72, 36.86, 33.37, 33.06, 32.65, 32.61, 32.59, 32.34, 31.85, 31.84, 30.29, 29.74, 29.27, 29.15, 29.05, 28.72, 28.63, 22.29, 22.18, 22.16, 21.82, 19.91, 19.54, 19.13, 14.65, 12.85. **IR** 2954 (w), 1610 (s), 1509 (m), 1241 (m), 824 (m), 753 (m) cm^{-1}. **HRMS (ESI)** *m/z:* $[M+Na]^+$ calc. for $C_{24}H_{25}NO_4Na$, 414.1676; Found, 414.1665.

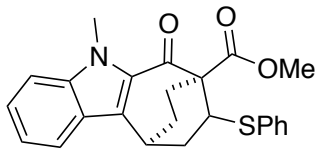

Methyl (7*S*,10*S*)-5-methyl-6-oxo-8-(phenylthio)-6,8,9,10-tetrahydro-7,10-ethanocyclohepta[*b*]indole-7(5*H*)-carboxylate (34ap): The general procedure was followed using alkylidene **33a** (0.100 g, 0.411 mmol), phenyl vinyl sulfide **23p** (0.269 mL, 2.06 mmol), $Ca(NTf_2)_2$ (6.17 mg, 0.0100 mmol), (n-Bu_4N)(PF_6) (3.98 mg, 0.0100 mmol) and CH_2Cl_2 (4.11 mL) at 40°C. After 1 hour, the reaction was allowed to cool to room temperature, then concentrated under reduced pressure and column chromatography (EtOAc/hexane) afforded cyclohepta[*b*]indole **34ap** as a yellow solid solid (0.0845 g, 50 % yield). **^{1}H NMR** (500MHz, $CDCl_3$) δ = 7.71 (d, J = 8.1 Hz, 1H), 7.46 – 7.37 (m, 4H), 7.24 – 7.15 (m, 4H), 4.14 (s, 3H), 4.03 (dd, J = 9.1, 3.0 Hz, 1H), 3.79 (s, 4H), 2.59 (ddd, J = 14.2, 9.2, 3.7 Hz, 1H), 2.42 (t, J = 10.5 Hz, 1H), 2.23 (dq, J = 14.0, 2.9 Hz, 1H), 2.10 – 2.01 (m, 2H), 1.74 (tdd, J = 10.6, 6.9, 4.6 Hz, 1H). **^{13}C NMR** (500MHz, $CDCl_3$) δ = 190.43, 172.71, 140.09, 136.59, 132.78, 132.13, 132.00, 128.70, 126.96, 126.73, 124.04, 120.85, 120.16, 110.46, 77.28, 77.03, 76.78, 52.45, 45.98, 37.94, 31.95, 29.72, 28.85, 27.19, 27.03. **IR** 2927 (w), 2363 (m), 1737 (s), 1652 (s), 746 (m) cm^{-1}. **HRMS (ESI)** *m/z:* $[M+H]^+$ calc. for $C_{24}H_{24}NO_3S$, 406.1471; Found, 406.1460.

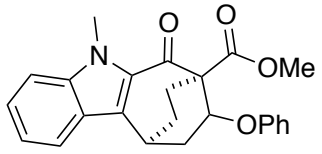

Methyl (7*S*,10*S*)-5-methyl-6-oxo-8-phenoxy-6,8,9,10-tetrahydro-7,10-ethanocyclohepta[*b*]indole-7(5*H*)-carboxylate (34aq): The general procedure was

followed using alkylidene **33a** (0.100 g, 0.411 mmol), phenyl vinyl ether **23q** (0.253 mL, 2.06 mmol), $Ca(NTf_2)_2$ (6.17 mg, 0.0100 mmol), (n-Bu_4N)(PF_6) (3.98 mg, 0.0100 mmol) and CH_2Cl_2 (4.11 mL) at 40°C. After 1 hour, the reaction was allowed to cool to room temperature, then concentrated under reduced pressure and column chromatography (EtOAc/hexanes) afforded cyclohepta[*b*]indole **34ap** as an a yellow solid (0.697 g, 41% yield). **^{1}H NMR** (500MHz, $CDCl_3$) δ = 7.70 (dt, J = 8.1, 0.9 Hz, 1H), 7.42 (dt, J = 4.0, 0.9 Hz, 2H), 7.22 – 7.15 (m, 3H), 6.88 (dddd, J = 7.8, 7.1, 1.4, 0.8 Hz, 2H), 6.80 – 6.75 (m, 2H), 5.16 (dd, J = 8.5, 2.0 Hz, 1H), 4.17 (d, J = 0.6 Hz, 3H), 3.81 (d, J = 0.6 Hz, 4H), 2.56 – 2.34 (m, 2H), 2.14 – 1.96 (m, 3H). **^{13}C NMR** (500MHz, $CDCl_3$) δ = 190.02, 172.79, 157.28, 139.75, 132.54, 132.11, 129.20, 126.54, 123.95, 120.91, 120.64, 120.02, 116.08, 110.33, 77.25, 76.99, 76.74, 73.91, 64.62, 52.40, 35.62, 32.03, 29.00, 26.44, 24.05. **IR** 2921 (w), 1730 (s), 1645 (m), 1225 (m), 736 (m) cm^{-1}. **HRMS (ESI)** *m/z:* $[M+H]^+$ calc. for $C_{24}H_{24}NO_4$, 390.1700; Found, 390.1692.

2.5.2.6 Krapcho Decarboxylation

General Procedure F Krapcho Decarboxylation Derivatization*:* To a round bottom flask charged with cyclohepta[*b*]indole (1 equiv.) in DMSO (0.1 M) and a magnetic stir bar was added sodium chloride (2 equiv.) in water (few drops) and refluxed at 150°C. After 4 hours, the reaction was quenched with water and the organic layer was collected. The aqueous layer was extracted with EtOAc, and the combined organic layers were washed with brine and dried over $MgSO_4$. The organic layer was concentrated, and purified by prep-TLC (EtOAc:Hexanes).

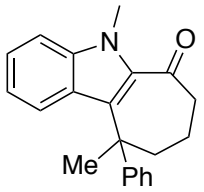

5,10-dimethyl-10-phenyl-7,8,9,10-tetrahydrocyclohepta[*b*]indol-6(5*H*)-one (36aa): The general procedure was followed using cyclohepta[*b*]indole **28aa** (0.100 g, 0.277 mmol), sodium chloride (0.323 g, 0.553 mmol), water (2 drops), and DMSO (2.8 mL). After refluxing for 4 hours at 150°C the reaction was quenched with water and the organic layer was collected. The aqueous layer was extracted with EtOAc, and the combined organic layers were washed with brine and dried over $MgSO_4$. The organic layer was concentrated and purified by prep-TLC (EtOAc:Hexanes) to afford decarboxylated cyclohepta[*b*]indole **36aa** as a yellow solid (0.0634 g, 74 % yield). **^{1}H NMR** (500 MHz, $CDCl_3$) δ = 7.35 (dt, *J* = 8.4, 0.9 Hz, 1H), 7.31 – 7.26 (m, 4H), 7.26 – 7.24 (m, 1H), 7.22 – 7.17 (m, 1H), 7.00 (dt, *J* = 8.3, 1.0 Hz, 1H), 6.86 (ddd, *J* = 8.1, 6.8, 1.1 Hz, 1H), 3.90 (s, 3H), 2.89 (td, *J* = 6.7, 2.7 Hz, 2H), 2.22 – 2.15 (m, 1H), 2.12 – 2.05 (m, 1H), 1.94 (s, 3H), 1.91 (tdd, *J* = 6.8, 5.4, 4.0 Hz, 2H). **^{13}C NMR** (500MHz, $CDCl_3$) δ = 198.41, 149.22, 139.68, 134.45, 129.37, 128.12, 126.94, 125.92, 125.54, 125.09, 124.28, 119.47, 110.28, 77.32, 77.07, 76.81, 45.62, 45.53, 45.31, 32.29, 29.03, 18.03. **IR** 2934 (w), 1645 (s), 739 (s), 698 (s) cm^{-1}. **HRMS (EI)** *m/z:* $[M]^+$ Calcd. for $C_{21}H_{21}NO$, 303.1623; Found, 303.1624.

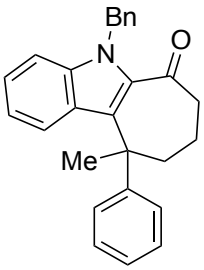

5-benzyl-10-methyl-10-phenyl-7,8,9,10-tetrahydrocyclohepta[*b*]indol-6(5*H*)-one (36ba): The general procedure was followed using cyclohepta[*b*]indole **28ba** (0.0728 g, 0.166 mmol), sodium chloride (0.0195 g, 0.333 mmol), water (2 drops), and DMSO (1.66 mL). After refluxing for 4 hours at 150°C the reaction was quenched with water and the organic layer was collected. The aqueous layer was extracted with EtOAc, and the combined organic layers were washed with brine and dried over $MgSO_4$. The organic layer was concentrated and purified by prep-TLC (EtOAc:Hexane) to afford decarboxylated cyclohepta[*b*]indole **36ba** as a yellow solid (0.0409 g, 65 % yield). **^{1}H NMR** (500MHz, $CDCl_3$) δ = 7.35 (dt, *J* = 8.5, 0.9 Hz, 1H), 7.32 – 7.26 (m, 6H), 7.25 – 7.19 (m, 3H), 7.07 – 7.02 (m, 3H), 6.89 (ddd, *J* = 8.1, 6.9, 1.0 Hz, 1H), 5.69 – 5.60 (m, 2H), 2.79 – 2.66 (m, 2H), 2.21 – 2.05 (m, 2H), 1.97 (s, 3H), 1.85 (dtdd, *J* = 9.9, 7.2, 4.6, 2.0 Hz, 2H). **^{13}C NMR** (500MHz, $CDCl_3$) δ = 198.56, 149.02, 139.72, 138.79, 134.13, 130.14, 128.55, 128.19, 127.09, 126.94, 126.35, 125.99, 125.82, 125.29, 124.36, 119.80, 110.78, 77.33, 77.07, 76.82, 48.10, 45.43, 45.37, 45.30, 28.98, 17.84. **IR** 3056 (w), 2935 (w), 1648 (s), 743 (s), 699 (s) cm^{-1}. **HRMS (ESI)** *m/z:* $[M+H]^+$ calc. for $C_{27}H_{26}NO$, 380.2009; Found, 380.1997.

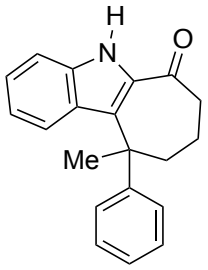

10-methyl-10-phenyl-7,8,9,10-tetrahydrocyclohepta[*b*]indol-6(5*H*)-one (36ca): The general procedure was followed using cyclohepta[*b*]indole **28ca** (0.0826 g, 0.238 mmol), sodium chloride (0.0278 g, 0.476 mmol), water (2 drops), and DMSO (2.38 mL). After

refluxing for 4 hours at 150°C the reaction was quenched with water and the organic layer was collected. The aqueous layer was extracted with EtOAc, and the combined organic layers were washed with brine and dried over $MgSO_4$. The organic layer was concentrated and purified by prep-TLC (EtOAc:Hexanes) to afford decarboxylated cyclohepta[*b*]indole **36ca** as a yellow solid (0.0342 g, 60 % yield). **^{1}H NMR** (500MHz, $CDCl_3$) δ = 9.15 (s, 1H), 7.34 (d, *J* = 8.3 Hz, 1H), 7.31 – 7.26 (m, 3H), 7.26 – 7.09 (m, 3H), 6.94 (d, *J* = 8.3 Hz, 1H), 6.81 (t, *J* = 7.6 Hz, 1H), 2.89 (qdt, *J* = 12.7, 8.3, 4.3 Hz, 2H), 2.22 (ddd, *J* = 46.6, 14.6, 9.1 Hz, 2H), 2.02 – 1.83 (m, 5H). **^{13}C NMR** (500MHz, $CDCl_3$) δ = 195.75, 149.66, 137.06, 132.22, 129.89, 128.20, 127.19, 126.86, 126.08, 126.00, 124.79, 119.62, 111.87, 77.30, 77.04, 76.79, 47.43, 45.29, 43.90, 28.59, 18.23. **IR** 3329 (br), 3056 (w), 2934 (w), 1710 (m), 1618 (s), 702 (s), 699 (s) cm^{-1}. **HRMS (ESI)** *m/z:* $[M+H]^+$ calc. for $C_{20}H_{20}NO$, 290.1539; Found, 290.1532.

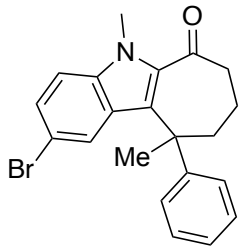

2-bromo-5,10-dimethyl-10-phenyl-7,8,9,10-tetrahydrocyclohepta[*b*]indol-6(5*H*)-one (36da): The general procedure was followed using cyclohepta[*b*]indole **28da** (0.0750 g, 0.170 mmol), sodium chloride (0.0199 g, 0.341 mmol), water (2 drops), and DMSO (1.70 mL). After refluxing for 4 hours at 150°C the reaction was quenched with water and the organic layer was collected. The aqueous layer was extracted with EtOAc, and the combined organic layers were washed with brine and dried over $MgSO_4$. The organic layer was concentrated and purified by prep-TLC (EtOAc:Hexane) to afford decarboxylated

cyclohepta[*b*]indole **36da** as a yellow solid (0.0472 g, 70 % yield). **^{1}H NMR** (500MHz, $CDCl_3$) δ = 7.30 (dt, *J* = 8.9, 1.4 Hz, 1H), 7.27 – 7.22 (m, 3H), 7.22 – 7.16 (m, 3H), 7.08 (t, *J* = 1.4 Hz, 1H), 3.83 (s, 3H), 2.84 (td, *J* = 7.0, 1.9 Hz, 2H), 2.20 – 1.99 (m, 2H), 1.91 – 1.82 (m, 5H). **^{13}C NMR** (500MHz, $CDCl_3$) δ = 98.29, 148.43, 138.08, 135.22, 128.49, 128.28, 127.96, 127.10, 126.80, 126.28, 126.20, 112.62, 111.81, 77.30, 77.05, 76.79, 45.40, 45.37, 45.16, 32.36, 29.06, 18.06. **IR** 2940 (w), 1649 (s), 698 (s) cm^{-1}. **HRMS (ESI)** *m/z:* $[M+H]^+$ calc. for $C_{21}H_{21}NOBr$, 382.0801; Found, 382.0790.

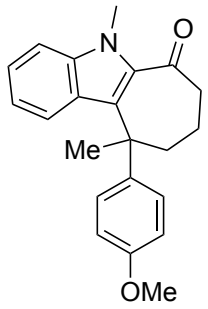

10-(4-methoxyphenyl)-5,10-dimethyl-7,8,9,10-tetrahydrocyclohepta[*b*]indol-6(5*H*)-one (36ab): The general procedure was followed using cyclohepta[*b*]indole **28ab** (0.100 g, 0.255 mmol), sodium chloride (0.0299 g, 0.511 mmol), water (2 drops), and DMSO (2.55 mL). After refluxing for 4 hours at 150°C the reaction was quenched with water and the organic layer was collected. The aqueous layer was extracted with EtOAc, and the combined organic layers were washed with brine and dried over $MgSO_4$. The organic layer was concentrated and purified by prep-TLC (EtOAc:Hexanes) to afford decarboxylated cyclohepta[*b*]indole **36ab** as a yellow solid (0.0500 g, 50 % yield). **^{1}H NMR** (500 MHz, $CDCl_3$) 7.37 (s, 1H), 7.32 – 7.27 (m, 1H), 7.24 – 7.19 (m, 2H), 7.06 (d, *J* = 8.2 Hz, 1H), 6.92 – 6.87 (m, 1H), 6.84 – 6.79 (m, 2H), 3.91 (d, *J* = 1.2 Hz, 3H), 3.80 (d, *J* = 1.1 Hz, 3H), 2.96 – 2.85 (m, 2H), 2.21 – 2.04 (m, 2H), 1.96 – 1.86 (m, 5H). **^{13}C NMR** (500MHz,

$CDCl_3$) δ = 198.49, 157.60, 141.37, 139.68, 134.34, 129.60, 127.97, 125.56, 125.07, 124.38, 119.43, 113.37, 110.25, 77.32, 77.07, 76.81, 55.18, 45.70, 45.55, 44.68, 32.26, 29.23, 18.00. **IR** 2920 (w), 1637 (s), 828 (m), 739 (m) cm^{-1}. **HRMS (EI)** *m/z:* $[M]^+$ Calcd. for $C_{22}H_{23}NO_2$, 333.1729; Found, 333.1727.

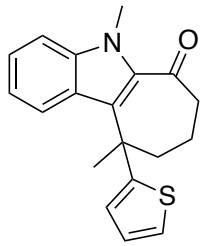

5,10-dimethyl-10-(thiophen-2-yl)-7,8,9,10-tetrahydrocyclohepta[*b*]indol-6(5*H*)-one (36ac): The general procedure was followed using cyclohepta[*b*]indole **28ac** (0.100 g, 0.272 mmol), sodium chloride (0.0318 g, 0.544 mmol), water (2 drops), and DMSO (2.72 mL). After refluxing for 4 hours at 150°C the reaction was quenched with water and the organic layer was collected. The aqueous layer was extracted with EtOAc, and the combined organic layers were washed with brine and dried over $MgSO_4$. The organic layer was concentrated and purified by prep-TLC (EtOAc:Hexanes) to afford decarboxylated cyclohepta[*b*]indole **36ac** as a yellow solid (0.0579 g, 69 % yield). **^{1}H NMR** (500 MHz, $CDCl_3$) δ = 7.34 (d, *J* = 8.4 Hz, 1H), 7.30 – 7.27 (m, 1H), 7.20 (td, *J* = 3.5, 3.0, 1.7 Hz, 1H), 7.11 (d, *J* = 8.3 Hz, 1H), 6.95 (dd, *J* = 2.9, 1.4 Hz, 1H), 6.93 – 6.88 (m, 2H), 3.87 (d, *J* = 1.0 Hz, 3H), 2.89 (q, *J* = 6.2 Hz, 2H), 2.24 – 2.16 (m, 1H), 2.07 – 2.00 (m, 1H), 1.99 – 1.87 (m, 5H). **^{13}C NMR** (500MHz, $CDCl_3$) δ = 198.45, 150.82, 139.54, 133.72, 128.81, 127.37, 125.55, 125.21, 125.09, 123.99, 120.29, 119.53, 110.27, 77.30, 77.05, 76.79, 45.55, 44.49, 43.19, 32.21, 29.54, 18.04. **IR** 2931 (w), 1642 (s), 740 (s) cm^{-1}. **HRMS (EI)** *m/z:* $[M]^+$ Calc. for $C_{19}H_{19}NOS$, 309.1187; Found, 309.1195.

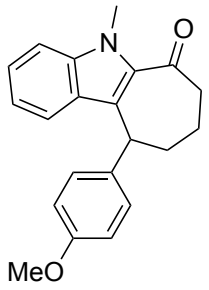

10-(4-methoxyphenyl)-5-methyl-7,8,9,10-tetrahydrocyclohepta[*b*]indol-6(5*H*)-one (36ae): The general procedure was followed using cyclohepta[*b*]indole **28ae** (0.105 g, 0.278 mmol), sodium chloride (0.0325 g, 0.556 mmol), water (2 drops), and DMSO (2.78 mL). After refluxing for 4 hours at 150°C the reaction was quenched with water and the organic layer was collected. The aqueous layer was extracted with EtOAc, and the combined organic layers were washed with brine and dried over $MgSO_4$. The organic layer was concentrated and purified by prep-TLC (EtOAc:Hexanes) to afford decarboxylated cyclohepta[*b*]indole **36ae** as a yellow solid (0.0695 g, 78 % yield). **^{1}H NMR** (500 MHz, $CDCl_3$) δ = 7.39 – 7.30 (m, 3H), 7.03 (dd, *J* = 16.8, 8.2 Hz, 3H), 6.79 (d, *J* = 8.2 Hz, 2H), 4.84 (t, *J* = 5.1 Hz, 1H), 3.99 (s, 3H), 3.76 (s, 3H), 2.90 – 2.68 (m, 2H), 2.33 (dddd, *J* = 45.8, 14.3, 9.8, 5.1 Hz, 2H), 1.89 (ttq, *J* = 14.3, 9.1, 5.0 Hz, 2H). **^{13}C NMR** (500MHz, $CDCl_3$) δ = 197.14, 157.89, 139.14, 135.86, 134.90, 128.80, 126.48, 125.89, 125.76, 121.57, 120.09, 113.77, 110.19, 77.33, 77.08, 76.82, 55.22, 44.77, 41.13, 34.53, 32.20, 19.52. **IR** 2930 (w), 1645 (s), 1508 (s), 1241 (s), 824 (m), 740 (m) cm^{-1}. **HRMS (EI)** *m/z:* $[M]^+$ Calcd. for $C_{21}H_{21}NO_2$, 319.1572; Found, 319.1573.

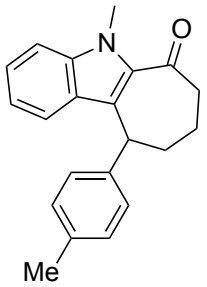

5-methyl-10-(*p*-tolyl)-7,8,9,10-tetrahydrocyclohepta[*b*]indol-6(5*H*)-one (36af): The general procedure was followed using cyclohepta[*b*]indole **28af** (0.0695 g, 0.192 mmol), sodium chloride (0.0225 g, 0.385 mmol), water (2 drops), and DMSO (1.92 mL). After refluxing for 4 hours at 150°C the reaction was quenched with water and the organic layer was collected. The aqueous layer was extracted with EtOAc, and the combined organic layers were washed with brine and dried over $MgSO_4$. The organic layer was concentrated and purified by prep-TLC (EtOAc:Hexanes) to afford decarboxylated cyclohepta[*b*]indole **36af** as a yellow solid (0.0413 g, 71 % yield). **^{1}H NMR** (500 MHz, $CDCl_3$) δ = 7.34 (dd, *J* = 13.6, 7.2 Hz, 3H), 7.09 – 6.98 (m, 5H), 4.85 (t, *J* = 5.1 Hz, 1H), 3.99 (s, 3H), 2.79 (dddd, *J* = 49.8, 14.8, 7.8, 5.5 Hz, 2H), 2.40 (dq, *J* = 15.6, 5.5 Hz, 1H), 2.30 (s, 4H), 1.89 (dtt, *J* = 19.0, 10.0, 5.1 Hz, 2H). **^{13}C NMR** (500MHz, $CDCl_3$) δ 197.13, 140.69, 139.13, 135.64, 134.95, 129.12, 127.73, 126.52, 125.82, 125.75, 121.54, 120.08, 110.17, 77.31, 77.06, 76.80, 44.77, 41.53, 34.42, 32.21, 21.01, 19.55. **IR** 2925 (w), 1647 (s), 811 (m), 740 (m) cm^{-1}. **HRMS (EI)** *m/z:* $[M]^+$ Calcd. for $C_{21}H_{21}NO$, 303.1623; Found, 303.1620.

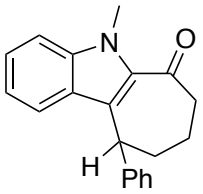

5-methyl-10-phenyl-7,8,9,10-tetrahydrocyclohepta[*b*]indol-6(5*H*)-one (36ag): The general procedure was followed using cyclohepta[*b*]indole **28ag** (0.0922 g, 0.265 mmol), sodium chloride (0.0310 g, 0.531 mmol), water (2 drops), and DMSO (2.65 mL). After refluxing for 4 hours at 150°C the reaction was quenched with water and the organic layer was collected. The aqueous layer was extracted with EtOAc, and the combined organic layers were washed with brine and dried over $MgSO_4$. The organic layer was concentrated and purified by prep-TLC (EtOAc:Hexanes) to afford decarboxylated cyclohepta[*b*]indole **36ag** as a yellow solid (0.0473 g, 62 % yield). **^{1}H NMR** (500 MHz, $CDCl_3$) δ = 7.35 (dt, *J* = 23.0, 8.2 Hz, 3H), 7.25 (t, *J* = 7.5 Hz, 2H), 7.16 (dd, *J* = 24.6, 7.4 Hz, 3H), 7.01 (t, *J* = 7.4 Hz, 1H), 4.89 (t, *J* = 5.1 Hz, 1H), 4.00 (s, 3H), 2.89 – 2.71 (m, 2H), 2.47 – 2.27 (m, 2H), 1.89 (tq, *J* = 10.3, 4.9 Hz, 2H). **^{13}C NMR** (500MHz, $CDCl_3$) δ = 197.08, 143.77, 139.13, 135.00, 128.43, 127.86, 126.49, 126.16, 125.77, 125.51, 121.51, 120.11, 110.20, 77.31, 77.06, 76.80, 44.75, 41.95, 34.42, 32.22, 19.56. **IR** 2928 (w), 1645 (s), 737 (m), 742 (m) cm^{-1}. **HRMS (EI)** *m/z:* $[M]^+$ Calcd. for $C_{20}H_{19}NO$, 289.1467; Found, 289.1463.

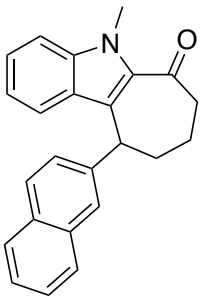

5-methyl-10-(naphthalen-2-yl)-7,8,9,10-tetrahydrocyclohepta[*b*]indol-6(5*H*)-one (36ai): The general procedure was followed using cyclohepta[*b*]indole **28ai** (0.0881 g, 0.222 mmol), sodium chloride (0.0259 g, 0.443 mmol), water (2 drops), and DMSO (2.22 mL). After refluxing for 4 hours at 150°C the reaction was quenched with water and the organic layer was collected. The aqueous layer was extracted with EtOAc, and the combined organic layers were washed with brine and dried over $MgSO_4$. The organic layer was concentrated and purified by prep-TLC (EtOAc:Hexanes) to afford decarboxylated cyclohepta[*b*]indole **36ai** as a yellow solid (0.0654 g, 87 % yield). **^{1}H NMR** (500 MHz, $CDCl_3$) δ = 7.82 – 7.73 (m, 2H), 7.68 (dd, *J* = 6.3, 3.4 Hz, 1H), 7.48 (s, 1H), 7.44 – 7.29 (m, 6H), 6.97 (t, *J* = 7.5 Hz, 1H), 5.04 (t, *J* = 5.2 Hz, 1H), 4.03 (s, 3H), 2.92 – 2.85 (m, 1H), 2.80 – 2.72 (m, 1H), 2.55 – 2.47 (m, 1H), 2.37 (ddt, *J* = 13.8, 9.1, 4.4 Hz, 1H), 1.90 (qq, *J* = 9.3, 3.9 Hz, 2H). **^{13}C NMR** (500MHz, $CDCl_3$) δ = 197.10, 141.35, 139.19, 135.10, 133.42, 132.11, 128.15, 127.76, 127.54, 126.51, 126.38, 126.31, 125.97, 125.80, 125.48, 125.32, 121.55, 120.16, 110.23, 77.29, 77.04, 76.78, 44.80, 42.24, 34.45, 32.28, 19.61. **IR** 2923 (w), 1645 (s), 817 (m), 743 (m) cm^{-1}. **HRMS (EI)** *m/z:* $[M]^+$ Calcd. for $C_{24}H_{21}NO$, 339.1623; Found, 339.1627.

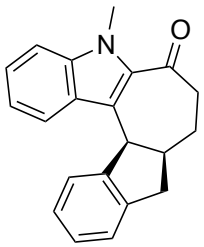

(8a*S*,13b*S*)-5-methyl-5,7,8,8a,9,13b-hexahydro-6*H*-benzo[2,3]azuleno[5,4-*b*]indol-6-one (36al): The general procedure was followed using cyclohepta[*b*]indole **28al** (0.0804 g, 0.222 mmol), sodium chloride (0.0260 g, 0.445 mmol), water (2 drops), and DMSO

(2.22 mL). After refluxing for 4 hours at 150°C the reaction was quenched with water and the organic layer was collected. The aqueous layer was extracted with EtOAc, and the combined organic layers were washed with brine and dried over $MgSO_4$. The organic layer was concentrated and purified by prep-TLC (EtOAc:Hexanes) to afford decarboxylated cyclohepta[*b*]indole **36al** as a yellow solid (0.0503 g, 72 % yield). **^{1}H NMR** (500MHz, $CDCl_3$) δ = 7.81 (d, *J* = 8.1 Hz, 1H), 7.49 (d, *J* = 3.3 Hz, 2H), 7.27 (ddd, *J* = 16.0, 9.3, 4.9 Hz, 2H), 7.17 (t, *J* = 7.5 Hz, 1H), 7.02 (t, *J* = 7.5 Hz, 1H), 6.58 (d, *J* = 7.4 Hz, 1H), 5.29 (d, *J* = 8.3 Hz, 1H), 4.15 – 4.04 (m, 3H), 3.57 (td, *J* = 17.4, 16.9, 7.7 Hz, 1H), 3.19 (tt, *J* = 8.9, 4.6 Hz, 1H), 2.94 (d, *J* = 16.4 Hz, 1H), 2.58 (ddd, *J* = 17.2, 8.0, 2.4 Hz, 1H), 2.44 – 2.32 (m, 1H), 2.12 (td, *J* = 13.4, 11.8, 5.1 Hz, 1H), 1.97 (ddd, *J* = 14.8, 8.0, 3.4 Hz, 1H). **^{13}C NMR** (500MHz, $CDCl_3$) δ = 197.40, 146.60, 142.56, 139.23, 131.93, 127.38, 126.88, 126.79, 126.17, 125.13, 124.05, 123.55, 120.71, 120.43, 110.41, 44.48, 39.94, 39.85, 39.39, 32.27, 29.87. **IR** 3020 (w), 2927 (w), 1644 (s), 737 (s) cm^{-1}. **HRMS (EI)** *m/z:* $[M]^+$ Calcd. for $C_{21}H_{19}NO$, 301.1467; Found, 301.1468.

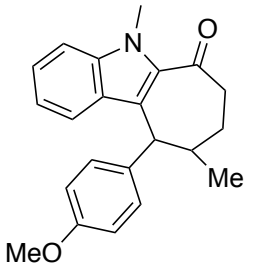

10-(4-methoxyphenyl)-5,9-dimethyl-7,8,9,10-tetrahydrocyclohepta[*b*]indol-6(5*H*)-one (36am): The general procedure was followed using cyclohepta[*b*]indole **28am** (0.0893 g, 0.228 mmol), sodium chloride (0.0266 g, 0.456 mmol), water (2 drops), and DMSO (2.28 mL). After refluxing for 4 hours at 150°C the reaction was quenched with water and

the organic layer was collected. The aqueous layer was extracted with EtOAc, and the combined organic layers were washed with brine and dried over $MgSO_4$. The organic layer was concentrated and purified by prep-TLC (EtOAc:Hexanes) to afford decarboxylated cyclohepta[*b*]indole **36am** as a yellow solid (0.0352 g, 46 % yield). **^{1}H NMR** (300MHz, $CDCl_3$) δ = 7.41 – 7.28 (m, 3H), 7.03 – 6.96 (m, 3H), 6.78 – 6.72 (m, 2H), 4.50 (d, *J* = 5.3 Hz, 1H), 3.97 (d, *J* = 1.1 Hz, 3H), 3.73 (d, *J* = 1.0 Hz, 3H), 2.88 – 2.72 (m, 2H), 2.47 – 2.39 (m, 1H), 1.99 (ddt, *J* = 15.2, 7.9, 3.7 Hz, 1H), 1.77 – 1.67 (m, 1H), 1.19 – 1.13 (m, 3H). **^{13}C NMR** (500MHz, $CDCl_3$) δ =197.84, 157.81, 139.48, 137.19, 134.00, 128.96, 127.09, 125.74, 123.45, 121.44, 120.01, 113.64, 110.14, 77.29, 77.03, 76.78, 48.96, 41.82, 38.08, 32.20, 27.23, 20.96. **IR** 2930 (w), 1648 (s), 1508 (s), 1244 (s), 827 (m), 742 (m) cm^{-1}. **HRMS (ESI)** *m/z:* $[M+H]^+$ calc. for $C_{22}H_{24}NO_2$, 334.1802; Found, 334.1800.

2.5.2.7 Characterization of Michael Addition Adduct 35

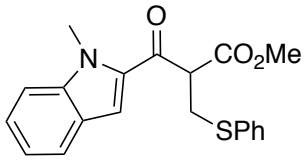

methyl 3-(1-methyl-1*H*-indol-2-yl)-3-oxo-2-((phenylthio)methyl)propanoate (35ap): **^{1}H NMR** (500MHz, $CDCl_3$) δ = 7.65 (dt, *J* = 8.1, 0.9 Hz, 1H), 7.43 – 7.36 (m, 4H), 7.34 – 7.26 (m, 3H), 7.18 – 7.14 (m, 2H), 4.53 (t, *J* = 7.3 Hz, 1H), 4.05 (s, 3H), 3.70 (s, 3H), 3.60 – 3.50 (m, 2H). **^{13}C NMR** (500 MHz, $CDCl_3$) δ = 186.45, 169.11, 140.72, 134.66, 133.91, 131.00, 129.16, 127.12, 126.82, 125.69, 123.33, 121.02, 113.53, 110.49, 77.31, 77.05, 76.80, 54.98, 52.85, 33.38, 32.35**. IR** 3053 (w), 2949 (w), 1737 (s), 1656 (s), 737 (m), 730

(m) cm^{-1}. **HRMS (ESI)** *m/z:* $[M+Na]^+$ calc. for $C_{20}H_{19}NO_3NaS$, 376.0978; Found, 376.0978.

2.5.2.8 Methylation of cyclohepta[*b*]indole 28aa

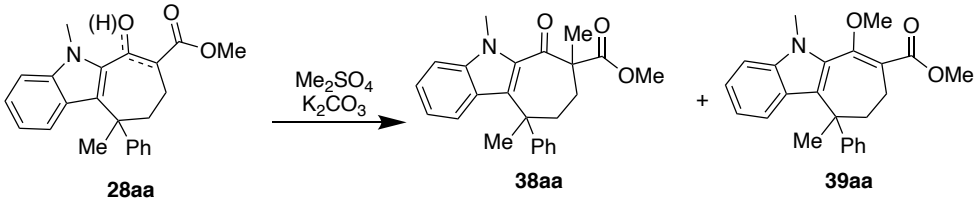

Procedure adapted from Shaw *et al*.[34] To a solution of **28aa** (0.250 g, 0.692 mmol) in 2 mL of acetone was added K_2CO_3 (0.574 g, 4.15 mmol). After the mixture was stirred for 15 minutes, Me_2SO_4 (0.20 mL, 2.08 mmol) was added dropwise. The reaction mixture was heated at 55°C for 12 hours. After the mixture was cooled to room temperature, filtered through a plug of silica gel, and concentrated by rotary evaporation. The resulting oil was partitioned be EtOAc and H_2O (1:1) and the aqueous layer was extracted with EtOAc. The combined organic layers were washed with brine, dried with $MgSO_4$, and concentrated down. The crude product was then purified by flash chromatography (EtOAc/Hexanes) to afford products **38aa** as a white solid (0.134 g, 51% yield) and **39aa** as a yellow solid (0.0713 g, 27% yield).

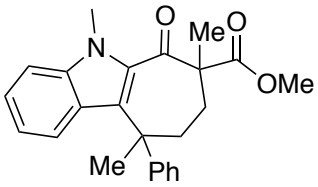

Methyl 5,7,10-trimethyl-6-oxo-10-phenyl-5,6,7,8,9,10-hexahydrocyclohepta[*b*]indole-7-carboxylate (38aa): *Diastereomeric Ratio* (1.2:1) **^{1}H NMR** (300MHz, $CDCl_3$) δ = 7.39

– 7.27 (m, 6H), 7.25 – 7.14 (m, 4H), 7.06 (dt, J = 8.0, 1.0 Hz, 1H), 6.97 – 6.83 (m, 2H), 3.79 (d, J = 2.3 Hz, 4H), 3.72 (d, J = 0.6 Hz, 2H), 3.65 (d, J = 0.6 Hz, 3H), 2.40 – 2.18 (m, 3H), 2.05 – 1.87 (m, 4H), 1.82 (s, 4H), 1.58 (s, 3H), 1.56 – 1.53 (m, 3H). **^{13}C NMR** (500MHz, $CDCl_3$) δ = 197.33, 196.88, 174.02, 148.89, 139.78, 139.75, 134.70, 134.29, 128.16, 128.10, 127.99, 127.87, 127.44, 127.27, 127.05, 126.71, 126.56, 126.10, 126.02, 125.14, 125.08, 124.91, 124.82, 124.00, 123.81, 119.59, 119.44, 110.23, 110.22, 77.30, 77.04, 76.79, 60.86, 60.38, 52.53, 52.48, 45.16, 45.09, 42.16, 41.26, 31.47, 29.73, 29.56, 29.26, 27.20, 22.35, 22.27. **IR** 2945 (w), 1739 (s), 1659 (s), 742 (m), 701 (m) cm^{-1}. **HRMS (ESI)** *m/z:* $[M+Na]^+$ calc. for $C_{24}H_{25}NO_3Na$, 398.1727; Found, 398.1713.

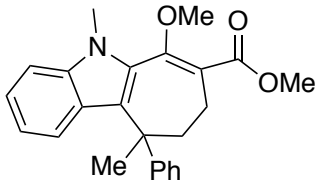

methyl 6-methoxy-5,10-dimethyl-10-phenyl-5,8,9,10-tetrahydrocyclohepta[*b*]indole-7-carboxylate (39aa): ^{1}H NMR 500MHz, $CDCl_3$) δ = 7.34 (dt, J = 8.3, 1.0 Hz, 1H), 7.27 (t, J = 1.8 Hz, 1H), 7.26 – 7.23 (m, 3H), 7.23 – 7.17 (m, 2H), 7.15 – 7.10 (m, 1H), 6.94 (ddd, J = 8.2, 7.0, 1.1 Hz, 1H), 3.83 (d, J = 5.4 Hz, 6H), 3.36 (s, 3H), 2.71 – 2.63 (m, 1H), 2.45 – 2.34 (m, 2H), 2.21 – 2.11 (m, 1H), 1.96 (s, 3H). **^{13}C NMR** (500MHz, $CDCl_3$) δ = 167.90, 154.27, 150.74, 139.19, 130.15, 127.83, 127.13, 126.77, 126.67, 125.60, 123.30, 122.85, 121.72, 119.29, 109.72, 77.30, 77.04, 76.79, 59.09, 51.83, 47.51, 44.99, 32.23, 31.04, 23.62. **IR** 2934 (w), 1713 (s), 744 (s), 701 (s) cm^{-1}. **HRMS (ESI)** *m/z:* $[M+Na]^+$ calc. for $C_{24}H_{25}NO_3Na$, 398.1727; Found, 398.1718.

2.5.2.9 Triflation of cyclohepta[*b*]indole 28aa:

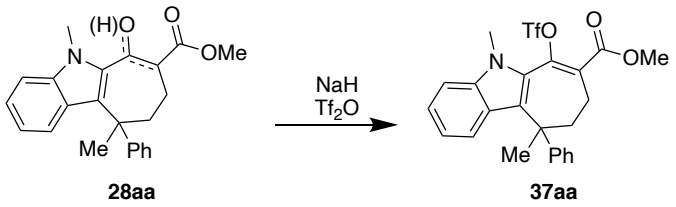

28aa **37aa**

Procedure adapted from Nishii *et al*.[35] A CH_2Cl_2 solution (0.53 mL) of keto enol mixture **28aa** (0.115 g, 0.319 mmol) was added dropwise to a suspension of NaH (0.0255 g, 0.629 mmol) in CH_2Cl_2 (0.53 mL) at 0°C under nitrogen and stirred for 1 hour. Then Tf_2O (0.107 mL, 0.629 mmol) was added to the reaction mixture at 0°C and stirred for 30 minutes. After the consumption of the starting material, the reaction was quenched with $NaHCO_3$ and extracted with EtOAc. The organic layers were combined and washed with brine, dried with Na_2SO_4, and concentrated. The resulting crude product was then purified by flash chromatography (EtOAc/Hexanes) to afford triflated product **37aa** as a yellow solid (0.0780 g, 50 % yield). **^{1}H NMR** (500MHz, $CDCl_3$) δ = 7.34 – 7.27 (m, 3H), 7.25 – 7.22 (m, 2H), 7.16 (ddt, *J* = 19.3, 12.9, 6.2 Hz, 2H), 6.88 (dt, *J* = 14.8, 8.0 Hz, 2H), 3.89 (s, 3H), 3.83 (s, 3H), 2.76 (d, *J* = 8.2 Hz, 1H), 2.68 – 2.58 (m, 1H), 2.19 – 2.14 (m, 2H), 1.92 (s, 3H). **^{13}C NMR** (500MHz, $CDCl_3$) δ = 165.37, 142.60, 140.33, 130.65, 128.26, 128.13, 127.88, 127.85, 127.39, 126.63, 126.58, 126.25, 126.04, 124.70, 123.53, 119.80, 110.02, 77.30, 77.05, 76.80, 52.66, 46.00, 44.95, 42.49, 33.24, 29.31, 23.42. **IR** 2927 (w), 1713 (s), 1632 (m), 744 (m), 699 (m), 600 (m) cm^{-1}. **HRMS (ESI)** *m/z:* $[M+Na]^+$ calc. for $C_{24}H_{22}NO_5F_3SNa$, 516.1063; Found, 516.1048.

2.5.2.10 Cross Coupling of Triflate 37aa:

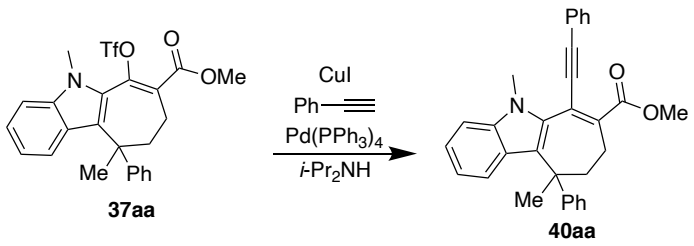

Procedure adapted from Nishii *et al*.[35] A THF solution of $Pd(PPh_3)_4$ (2.93 mg, 2.53 μmol) was added dropwise to a suspension of triflate **37aa** (50.1 mg, 0.102 mmol), and CuI (0.0290 g, 0.152 mmol) in THF (1.02 mL) at 0°C under nitrogen. Phenyl acetylene (0.017 mL, 0.152 mmol) and diisopropylamine (0.043 mL, 0.305 mmol) were successively added dropwise to the mixture and then stirred at 66 °C for 22 h. After an aqueous solution of HCl (1 N) was added to the reaction mixture at 0 °C, then extracted with EtOAc. The organic phase was washed with brine, dried over Na_2SO_4 and concentrated. The resulting crude oil was purified by column chromatography (EtOAc/Hexanes) to give cross coupled product **40aa** as a yellow solid (0.0300 g, 66% yield). **^{1}H NMR** 500MHz, $CDCl_3$) δ = 7.54 – 7.49 (m, 2H), 7.39 – 7.36 (m, 3H), 7.35 – 7.31 (m, 3H), 7.26 – 7.19 (m, 3H), 7.17 – 7.13 (m, 1H), 7.03 (dt, *J* = 8.1, 1.0 Hz, 1H), 6.88 (ddd, *J* = 8.1, 6.9, 1.0 Hz, 1H), 4.02 (s, 3H), 3.90 (s, 3H), 2.82 (ddd, *J* = 14.5, 8.3, 1.5 Hz, 1H), 2.64 (ddd, *J* = 14.4, 9.2, 1.7 Hz, 1H), 2.29 (ddd, *J* = 14.1, 9.3, 1.5 Hz, 1H), 2.19 (ddd, *J* = 14.2, 8.2, 1.7 Hz, 1H), 1.98 (s, 3H). **^{13}C NMR** (500MHz, $CDCl_3$) δ = 168.09, 150.46, 143.23, 139.50, 132.99, 131.54, 128.81, 128.48, 128.04, 127.84, 126.75, 126.63, 126.59, 125.68, 125.29, 124.28, 123.15, 123.12, 123.03, 120.03, 119.94, 119.13, 109.65, 97.87, 88.43, 77.31, 77.06, 76.80, 52.06, 47.13, 45.05, 33.31, 29.89, 25.98. **IR** 3053 (w), 2921 (w), 1698 (s), 740 (s), 688 (s) cm^{-1}. **HRMS (ESI)** *m/z:* $[M+Na]^+$ calc. for $C_{31}H_{27}NO_2Na$, 468.1934; Found, 468.1916.

2.6 References

1) Stempel, E.; Gaich, T. Cyclohepta[*b*]Indoles: A Privileged Structure Motif in Natural Products and Drug Design. *Acc. Chem. Res.* **2016**, *49* (11), 2390–2402.

(2) Carroll, A. R.; Hyde, E.; Smith, J.; Quinn, R. J.; Guymer, G.; Forster, P. I. Actinophyllic Acid, a Potent Indole Alkaloid Inhibitor of the Coupled Enzyme Assay Carboxypeptidase U/Hippuricase from the Leaves of Alatonia Actinophylla (Apocynaceae). *J. Org. Chem.* **2005**, *70* (3), 1096–1099.

(3) Liu, B. Y.; Zhang, C.; Zeng, K. W.; Li, J.; Guo, X. Y.; Zhao, M. B.; Tu, P. F.; Jiang, Y. Exotines A and B, Two Heterodimers of Isopentenyl-Substituted Indole and Coumarin Derivatives from Murraya Exotica. *Org. Lett.* **2015**, *17* (17), 4380–4383.

(4) Andriantsiferana, M.; Besselièvre, R.; Riche, C.; Husson, H. P. Structure de l'ervitsine Alcaloïde α-Acylindolique d'un Type Nouveau. *Tetrahedron Lett.* **1977**, *18* (30), 2587–2590.

(5) Napper, A. D.; Hixon, J.; McDonagh, T.; Keavey, K.; Pons, J. F.; Barker, J.; Yau, W. T.; Amouzegh, P.; Flegg, A.; Hamelin, E.; et al. Discovery of Indoles as Potent and Selective Inhibitors of the Deacetylase SIRT1. *J. Med. Chem.* **2005**, *48* (25), 8045–8054.

(6) Barf, T.; Lehmann, F.; Hammer, K.; Haile, S.; Axen, E.; Medina, C.; Uppenberg, J.; Svensson, S.; Rondahl, L.; Lundbäck, T. N-Benzyl-Indolo Carboxylic Acids: Design and Synthesis of Potent and Selective Adipocyte Fatty-Acid Binding Protein (A-FABP) Inhibitors. *Bioorganic Med. Chem. Lett.* **2009**, *19* (6), 1745–1748.

(7) Kuehm-Caubère, C.; Caubère, P.; Jamart-Grégoire, B.; Pfeiffer, B.; Guardiola-Lemaître, B.; Manechez, D.; Renard, P. Novel Thiopyrano[3,2-b] and Cycloalkeno[1,2-b]Indole Derivatives with High Inhibitory Properties in LTB4 Production. *Eur. J. Med. Chem.* **1999**, *34* (1), 51–61.

(8) For representative examples, see: (a) Tang, W.; Li, X. Preparation of cyclopropyl indoles and cyclohepta[*b*]indoles and therapeutic uses thereof. WO2016090094A1, 2016. (b) Kinnick, M. D.; Mihelich, E. D.; Morin, J. M., Jr.; Sall, D. J.; Sawyer, J. S. Preparation of cyclohepta[*b*]indole derivatives as sPLA2 inhibitors. WO2003016277A1, 2003.

(9) Robinson, B. Recent Studies on the Fischer Indole Synthesis. *Chem. Rev.* **1969**, *69* (2), 227–250.

(10) Inman, M.; Moody, C. J. A Two Step Route to Indoles from Haloarenes-a Versatile Variation on the Fischer Indole Synthesis. *Chem. Commun.* **2011**, *47* (2), 788–790.

(11) For pertinent examples see: (a) Goswami, P.; Borah, A. J.; Phukan, P. Formation of Cyclohepta[*b*]Indole Scaffolds via Heck Cyclization: A Strategy for Structural Analogues of Ervatamine Group of Indole Alkaloid. *J. Org. Chem.* **2015**, *80* (1), 438–446. (b) Liu, C.; Widenhoefer, R. A. Palladium-Catalyzed Cyclization/Carboalkoxylation of Alkenyl Indoles. *J. Am. Chem. Soc.* **2004**, *126* (33), 10250–10251. (c) Ishikura, M.; Kato, H. A Synthetic Use of the Intramolecular Alkyl Migration Process in Indolylborates for Intramolecular Cyclization: A Novel Construction of Carbazole Derivatives. *Tetrahedron* **2002**, *58* (49), 9827–9838.

(12) For representative examples see: (a) Mishra, U. K.; Yadav, S.; Ramasastry, S. S. V. One-Pot Multicatalytic Approaches for the Synthesis of Cyclohepta[*b*]Indoles, Indolotropones, and Tetrahydrocarbazoles. *J. Org. Chem.* **2017**, *82* (13), 6729–6737. (b) Bennasar, M. L.; Zulaica, E.; Solé, D.; Alonso, S. Sequential Ring-Closing Metathesis-Vinyl Halide Heck Cyclization Reactions: Access to the Tetracyclic Ring System of Ervitsine. *Tetrahedron* **2012**, *68* (24), 4641–4648.

(13) Chakraborty, A.; Goswami, K.; Adiyala, A.; Sinha, S. Syntheses of Spiro[Cyclopent[3]Ene-1,3′-Indole]s and Tetrahydrocyclohepta[*b*]Indoles from 2,3-Disubstituted Indoles through Sigmatropic Rearrangement. *European J. Org. Chem.* **2013**, *2013* (31), 7117–7127.

(14) For examples of [4 + 3] cycloadditions toward cyclohepta[b] indoles: (a) Gelis, C.; Levitre, G.; Merad, J.; Retailleau, P.; Neuville, L.; Masson, G. Highly Diastereo- and Enantioselective Synthesis of Cyclohepta[*b*]Indoles by Chiral-Phosphoric-Acid-Catalyzed (4+3) Cycloaddition. *Angew. Chemie - Int. Ed.* **2018**, *57* (37), 12121–12125. (b) Xu, G.; Chen, L.; Sun, J. Rhodium-Catalyzed Asymmetric Dearomative [4 + 3]-Cycloaddition of Vinylindoles with Vinyldiazoacetates: Access to Cyclohepta[b]Indoles. *Org. Lett.* **2018**, *20* (11), 3408–3412. (c) Li, Y.; Zhu, C. Z.; Zhang, J. Gold-Catalyzed [4+3] Cycloaddition/C–H Functionalization Cascade: Regio- and Diastereoselective Route to Cyclohepta[*b*]Indoles. *European J. Org. Chem.* **2017**, *2017* (45), 6609–6613. (d) Zhang, H. H.; Zhu, Z. Q.; Fan, T.; Liang, J.; Shi, F. Intermediate-Dependent Unusual [4+3], [3+2] and Cascade Reactions of 3-Indolylmethanols: Controllable Chemodivergent and Stereoselective Synthesis of Diverse Indole Derivatives. *Adv. Synth. Catal.* **2016**, *358* (8), 1259–1288. (e) Zhang,

J.; Shao, J.; Xue, J.; Wang, Y.; Li, Y. One Pot Hydroamination/[4 + 3] Cycloaddition: Synthesis towards the Cyclohepta[*b*]Indole Core of Silicine and Ervatamine. *RSC Adv.* **2014**, *4* (109), 63850–63854. (f) He, S.; Hsung, R. P.; Presser, W. R.; Ma, Z. X.; Haugen, B. J. An Approach to Cyclohepta[b]Indoles through an Allenamide (4 + 3) Cycloaddition-Grignard Cyclization-Chugaev Elimination Sequence. *Org. Lett.* **2014**, *16* (8), 2180–2183. (g) Shu, D.; Song, W.; Li, X.; Tang, W. Rhodium- and Platinum-Catalyzed [4+3] Cycloaddition with Concomitant Indole Annulation: Synthesis of Cyclohepta[*b*]Indoles. *Angew. Chemie Int. Ed.* **2013**, *52* (11), 3237–3240. (h) Han, X.; Li, H.; Hughes, R. P.; Wu, J. Gallium(III)-Catalyzed Three-Component (4+3) Cycloaddition Reactions. *Angew. Chemie - Int. Ed.* **2012**, *51* (41), 10390–10393.

(15) Mei, G.; Yuan, H.; Gu, Y.; Chen, W.; Chung, L. W.; Li, C. C. Dearomative Indole [5+2] Cycloaddition Reactions: Stereoselective Synthesis of Highly Functionalized Cyclohepta[*b*]Indoles. *Angew. Chemie - Int. Ed.* **2014**, *53* (41), 11051–11055.

(16) Hamada, N.; Yoshida, Y.; Oishi, S.; Ohno, H. Gold-Catalyzed Cascade Reaction of Skipped Diynes for the Construction of a Cyclohepta[b]Pyrrole Scaffold. *Org. Lett.* **2017**, *19* (14), 3875–3878.

(17) Takeda, T.; Harada, S.; Okabe, A.; Nishida, A. Cyclohepta[b]Indole Synthesis through [5 + 2] Cycloaddition: Bifunctional Indium(III)-Catalyzed Stereoselective Construction of 7-Membered Ring Fused Indoles. *J. Org. Chem.* **2018**, *83* (19), 11541–11551.

(18) Kaufmann, J.; Jäckel, E.; Haak, E. Ruthenium-Catalyzed Cascade Annulation of Indole with Propargyl Alcohols. *Angew. Chemie - Int. Ed.* **2018**, *57* (20), 5908–5911.

(19) Jadhav, A. S.; Pankhade, Y. A.; Vijaya Anand, R. Exploring Gold Catalysis in a 1,6-Conjugate Addition/Domino Electrophilic Cyclization Cascade: Synthesis of Cyclohepta[b]Indoles. *J. Org. Chem.* **2018**, *83* (15), 8615–8626.

(20) Shenje, R.; Martin, M. C.; France, S. A Catalytic Diastereoselective Formal [5+2] Cycloaddition Approach to Azepino[1,2- *a*]Indoles: Putative Donor-Acceptor Cyclobutanes as Reactive Intermediates. *Angew. Chemie Int. Ed.* **2014**, *53* (50), 13907–13911.

(21) For seminal contributions see: (a) Begouin, J.-M.; Niggemann, M. Calcium-Based Lewis Acid Catalysts. *Chem. - A Eur. J.* **2013**, *19* (25), 8030–8041. (b) Niggemann, M.; Meel, M. J. Calcium-Catalyzed Friedel–Crafts Alkylation at Room Temperature. *Angew. Chemie Int. Ed.* **2010**, *49* (21), 3684–3687.

(22) (a) Krapcho, A. P.; Ciganek, E. Chapter 1: The Krapcho Dealkoxycarbonylation Reaction of Esters with α-Electron-Withdrawing Substituents. *Org. React.* **2013**, *81* (1), 1–535. (b) Poon, P. S.; Banerjee, A. K.; Laya, M. S. Advances in the Krapcho Decarboxylation. *J. Chem. Res.* **2011***, 35,* 67−73.

(23) (a) Davies, J.; Leonori, D. The First Calcium-Catalysed Nazarov Cyclisation. *Chem. Commun.* **2014**, *50* (96), 15171–15174. (b) Malona, J. A.; Colbourne, J. M.; Frontier, A. J. A General Method for the Catalytic Nazarov Cyclization of Heteroaromatic Compounds. *Org. Lett.* **2006**, *8* (24), 5661–5664.

(24) Sonogashira, K. Development of Pd-Cu Catalyzed Cross-Coupling of Terminal Acetylenes with Sp^2-Carbon Halides. *J. Organomet. Chem.* **2002**, *653* (1–2), 46–49.

(25) Brockway, A. J.; González-López, M.; Fettinger, J. C.; Shaw, J. T. Direct Displacement of Alkoxy Groups of Vinylogous Esters by Grignard Reagents. *J. Org. Chem.* **2011**, *76* (9), 3515–3518.

(26) Mietke, T.; Cruchter, T.; Larionov, V. A.; Faber, T.; Harms, K.; Meggers, E. Asymmetric Nazarov Cyclizations Catalyzed by Chiral-at-Metal Complexes. *Adv. Synth. Catal.* **2018**, *360* (11), 2093–2100.

(27) Vieira, T. O.; Meaney, L. A.; Shi, Y.-L.; Alper, H. Tandem Palladium-Catalyzed N,C-Coupling/Carbonylation Sequence for the Synthesis of 2-Carboxyindoles. *Org. Lett.* **2008**, *10* (21), 4899–4901.

(28) Sechi, M.; Derudas, M.; Dallocchio, R.; Dessì, A.; Bacchi, A.; Sannia, L.; Carta, F.; Palomba, M.; Ragab, O.; Chan, C.; et al. Design and Synthesis of Novel Indole β-Diketo Acid Derivatives as HIV-1 Integrase Inhibitors. *J. Med. Chem.* **2004**, *47* (21), 5298–5310.

(29) Tullberg, E.; Schacher, F.; Peters, D.; Frejd, T. Solvent-Free Heck-Jeffery Reactions under Ball-Milling Conditions Applied to the Synthesis of Unnatural Amino Acids Precursors and Indoles. *Synthesis (Stuttg).* **2006**, *2006* (07), 1183–1189.

(30) Dekhane, M.; Dodd, R. H. A New Efficient Synthesis of Ethyl β-Carboline-3-Carboxylate (β-CCE) and Methyl 4-Methyl-β-Carboline-3-Carboxylate (4-Methyl-β-CCM) Starting Fr. *Tetrahedron* **1994**, *50* (21), 6299–6306.

(31) Flynn, D. L.; Zelle, R. E.; Grieco, P. A. A Mild Two-Step Method for the Hydrolysis of Lactams and Secondary Amides. *J. Org. Chem.* **1983**, *48* (14), 2424–2426.

(32) Malona, J. A.; Colbourne, J. M.; Frontier, A. J. A General Method for the Catalytic Nazarov Cyclization of Heteroaromatic Compounds. *Org. Lett.* **2006**, *8* (24), 5661–5664.

(33) Fryszkowska, A.; Fisher, K.; Gardiner, J. M.; Stephens, G. M. Highly Enantioselective Reduction of β,β-Disubstituted Aromatic Nitroalkenes Catalyzed by *Clostridium Sporogenes*. *J. Org. Chem.* **2008**, *73* (11), 4295–4298.

(34) Brockway, A. J.; González-López, M.; Fettinger, J. C.; Shaw, J. T. Direct Displacement of Alkoxy Groups of Vinylogous Esters by Grignard Reagents. *J. Org. Chem.* **2011**, *76* (9), 3515–3518.

(35) Takada, S.; Takaki, N.; Yamada, K.; Nishii, Y. A Formal Homo-Nazarov Cyclization of Enantioenriched Donor–Acceptor Cyclopropanes and Following Transformations: Asymmetric Synthesis of Multi-Substituted Dihydronaphthalenes. *Org. Biomol. Chem.* **2017**, *15* (11), 2443–2449.

2.6.1 NMR Spectra

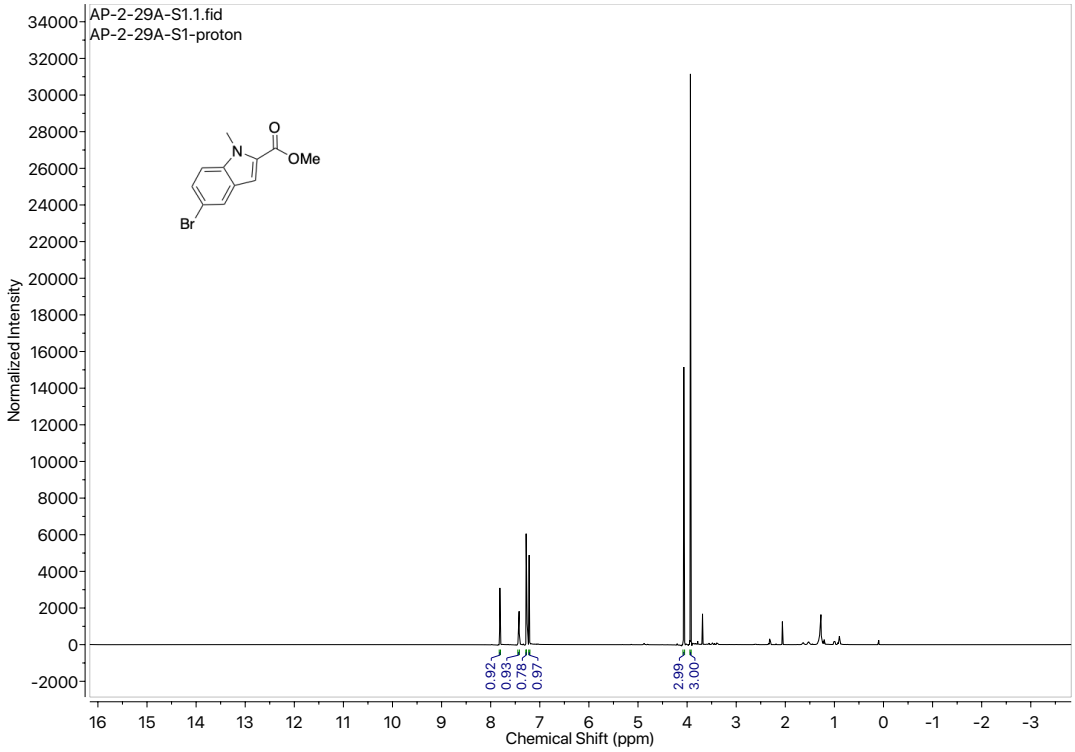

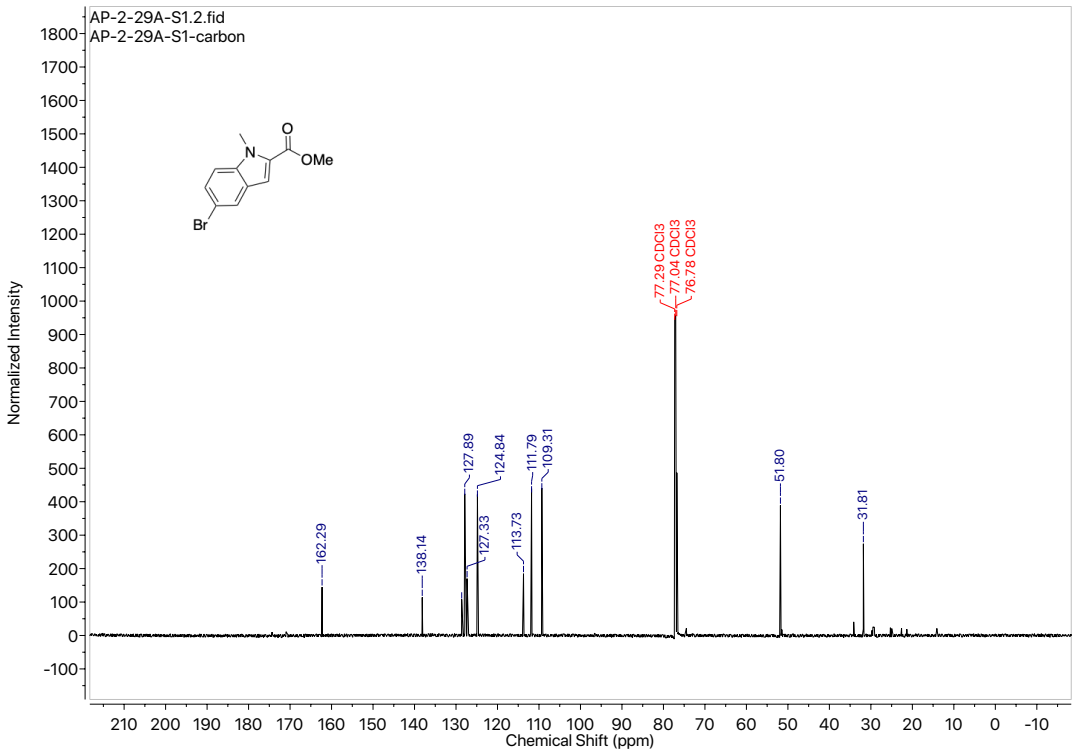
AP-2-29A-S1.2.fid
AP-2-29A-S1-carbon
Normalized Intensity
Chemical Shift (ppm)
162.29
138.14
127.89
127.33
124.84
113.73
111.79
109.31
77.29 CDCl3
77.04 CDCl3
76.78 CDCl3
51.80
31.81
OMe
Br

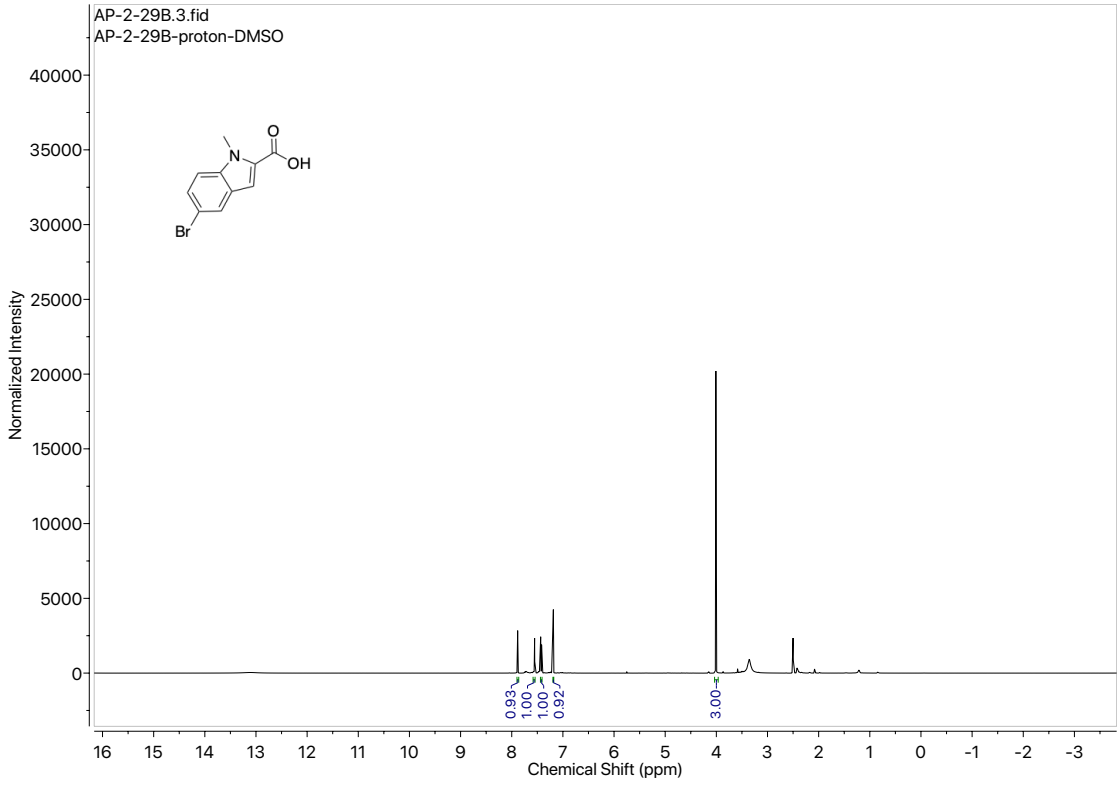
AP-2-29B.3.fid
AP-2-29B-proton-DMSO
Normalized Intensity
Chemical Shift (ppm)
0.93
1.00
1.00
0.92
3.00
OH
Br

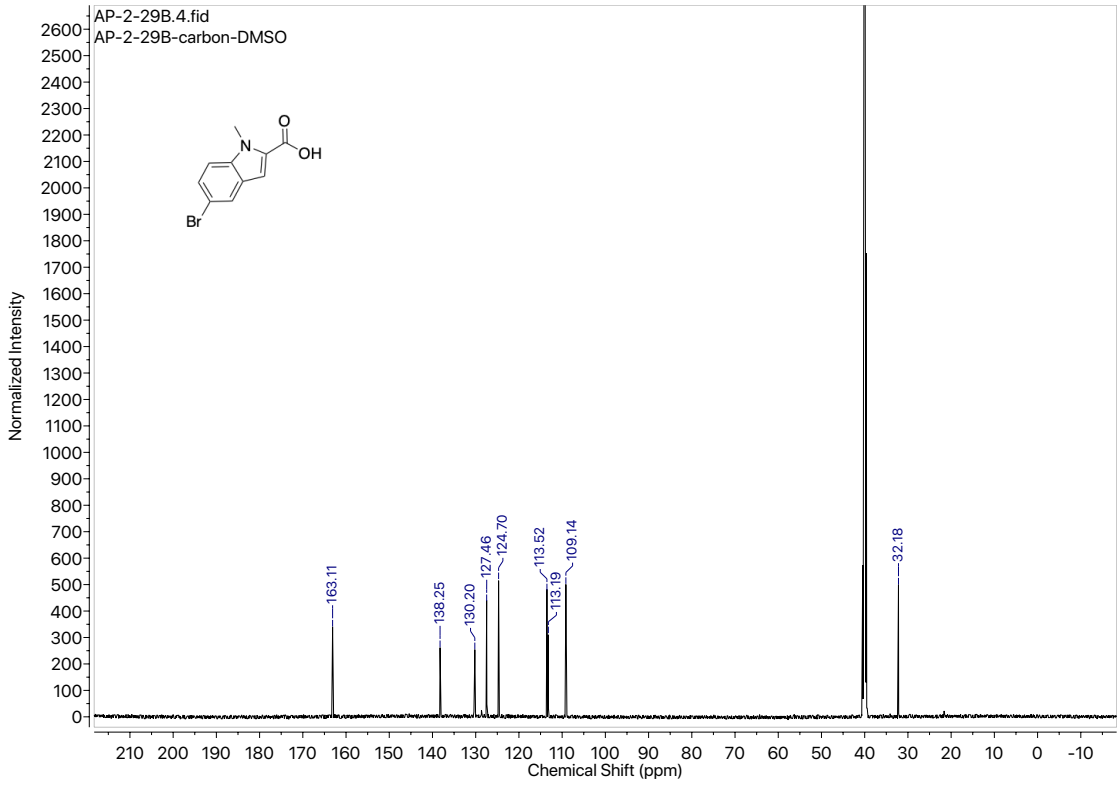
AP-2-29B.4.fid
AP-2-29B-carbon-DMSO
Normalized Intensity
Chemical Shift (ppm)
163.11
138.25
130.20
127.46
124.70
113.52
113.19
109.14
32.18
Br
OH

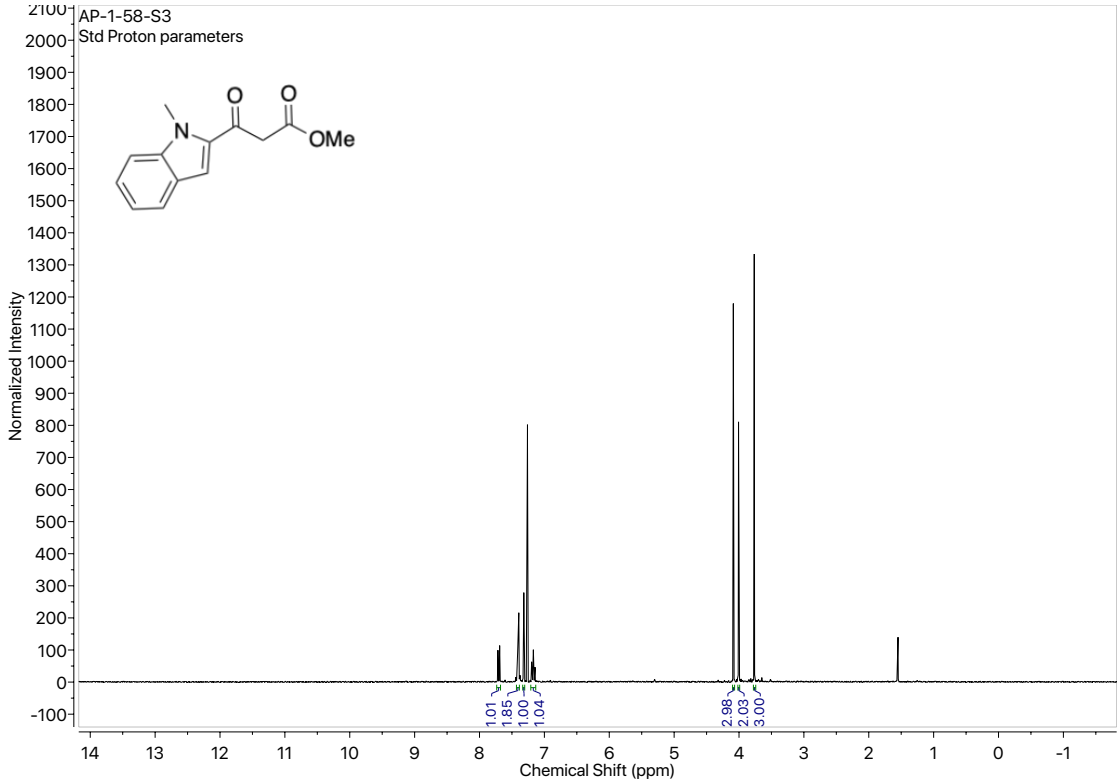
AP-1-58-S3
Std Proton parameters
Normalized Intensity
Chemical Shift (ppm)
OMe
1.01
1.85
1.00
1.04
2.98
2.03
3.00

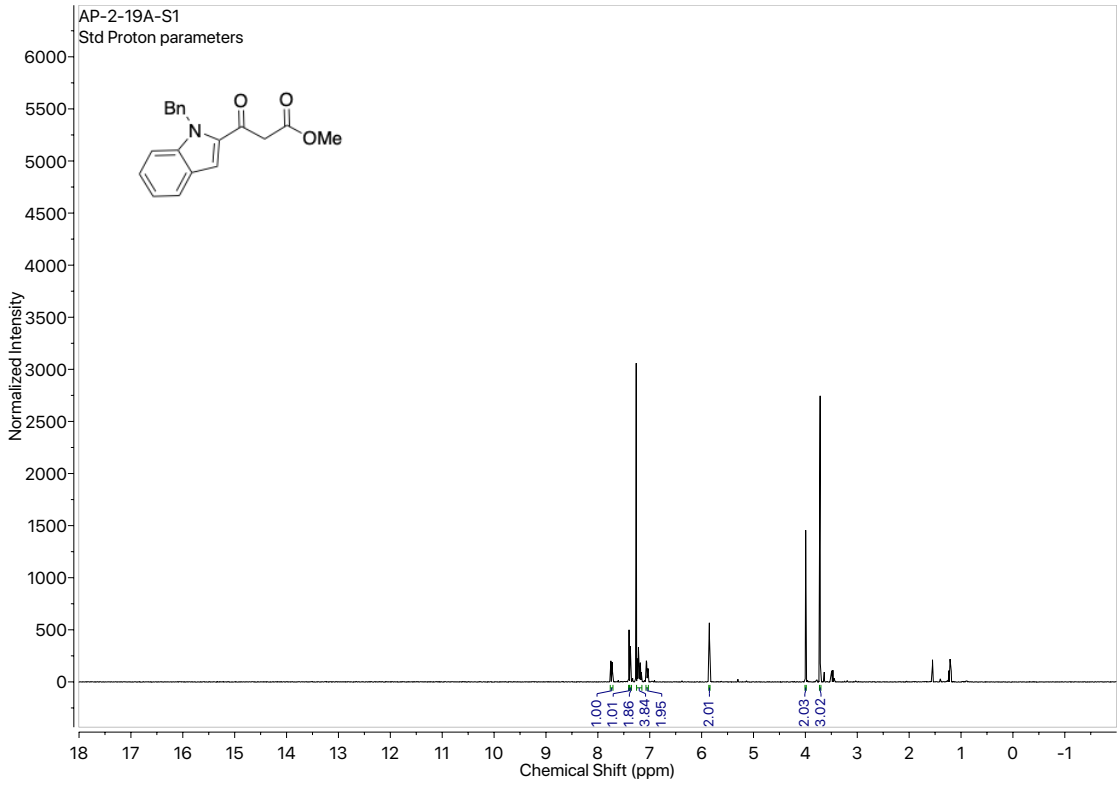
AP-2-19A-S1
Std Proton parameters
Bn
N
O
O
OMe
Normalized Intensity
Chemical Shift (ppm)
1.00
1.01
1.86
3.84
1.95
2.01
2.03
3.02

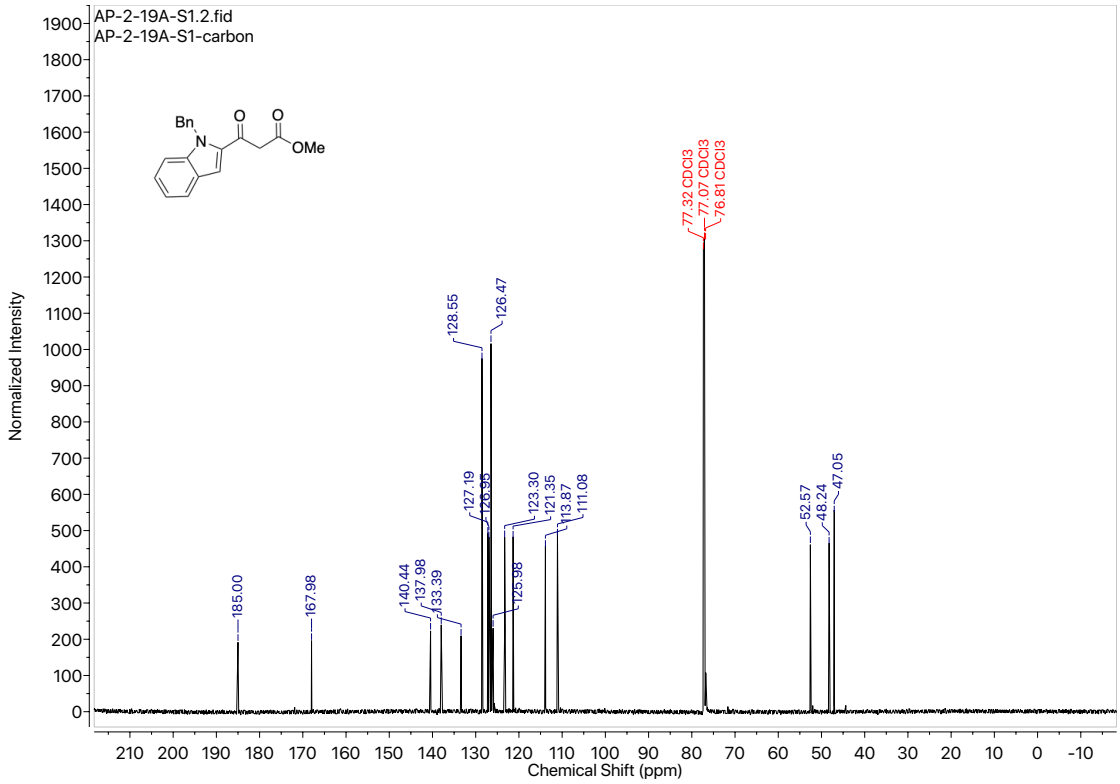
AP-2-19A-S1.2.fid
AP-2-19A-S1-carbon
Bn
N
O
O
OMe
Normalized Intensity
Chemical Shift (ppm)
77.32 CDCl3
77.07 CDCl3
76.81 CDCl3
185.00
167.98
140.44
137.98
133.39
128.55
126.47
127.19
126.95
125.98
123.30
121.35
113.87
111.08
52.57
48.24
47.05

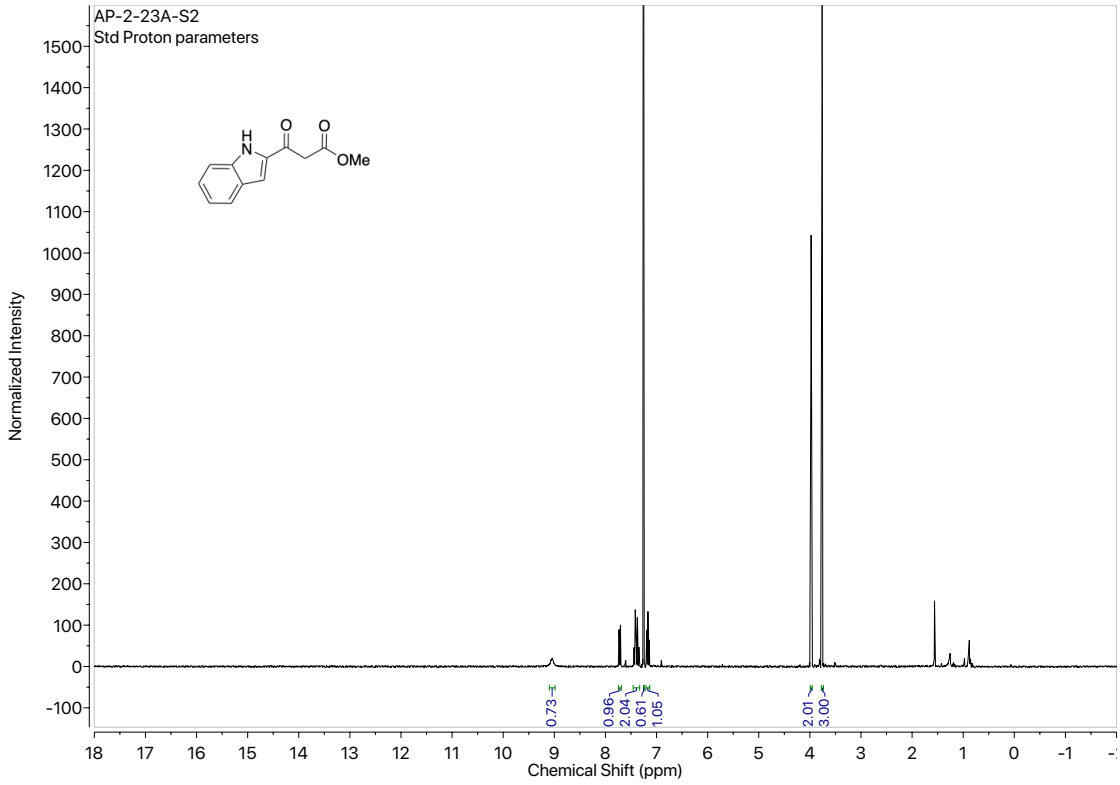
AP-2-23A-S2
Std Proton parameters
Normalized Intensity
Chemical Shift (ppm)
0.73
0.96
2.04
0.61
1.05
2.01
3.00

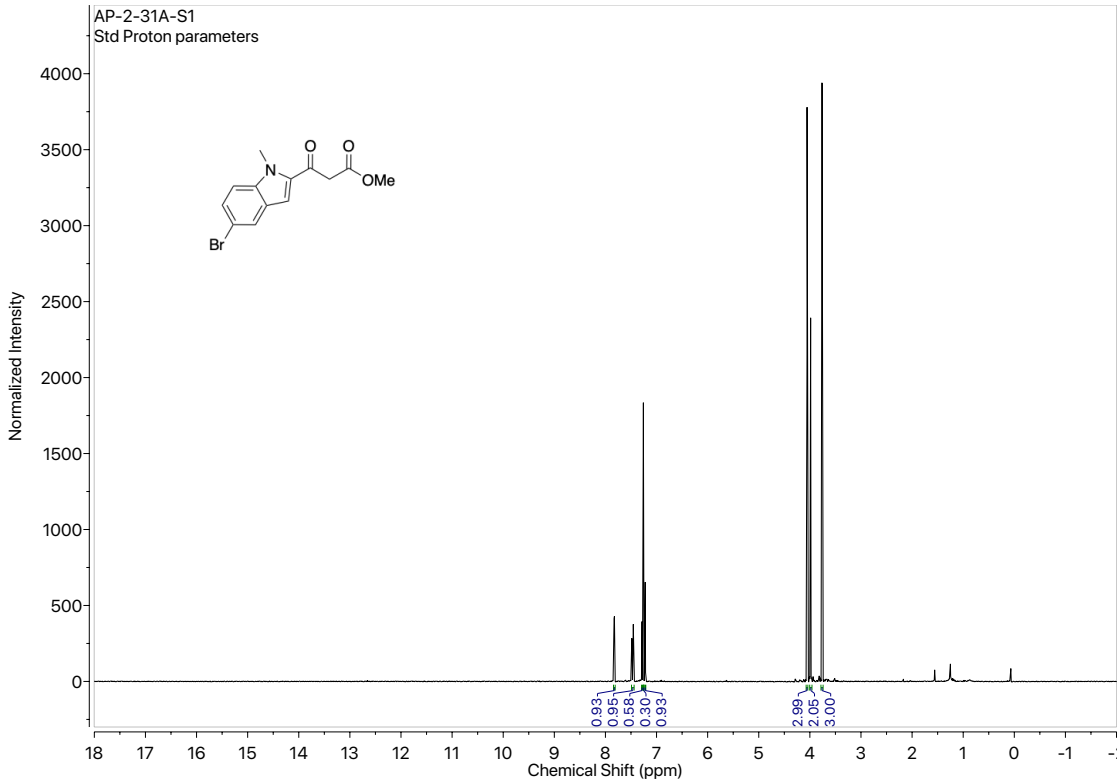
AP-2-31A-S1
Std Proton parameters
Normalized Intensity
Chemical Shift (ppm)
0.93
0.95
0.58
0.30
0.93
2.99
2.05
3.00

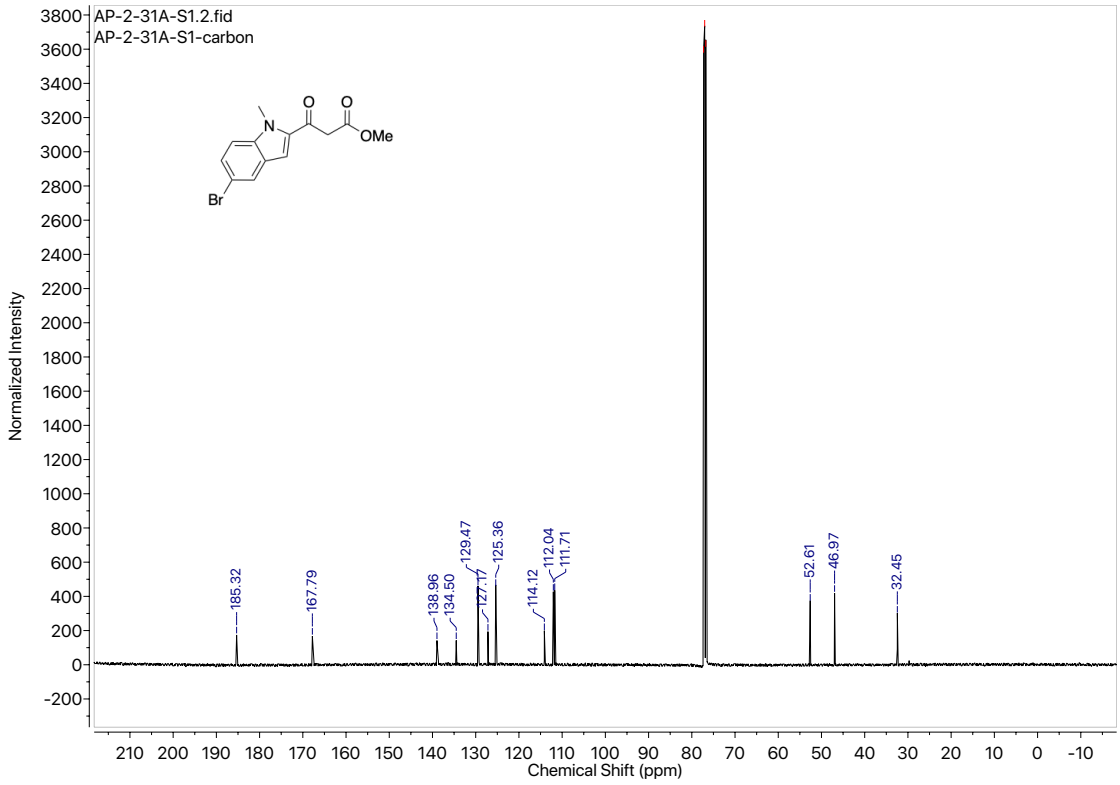
AP-2-31A-S1.2.fid
AP-2-31A-S1-carbon
Br
N
O
O
OMe
Normalized Intensity
Chemical Shift (ppm)
185.32
167.79
138.96
134.50
129.47
127.17
125.36
114.12
112.04
111.71
52.61
46.97
32.45

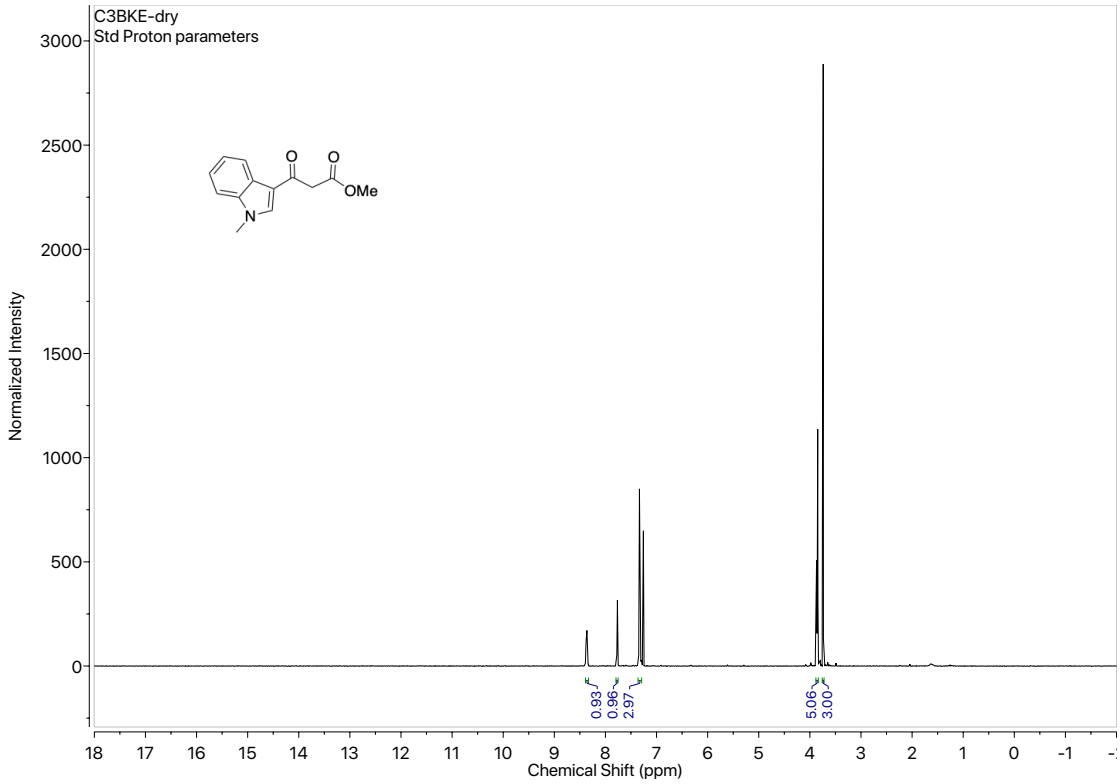
C3BKE-dry
Std Proton parameters
N
O
O
OMe
Normalized Intensity
Chemical Shift (ppm)
0.93
0.96
2.97
5.06
3.00

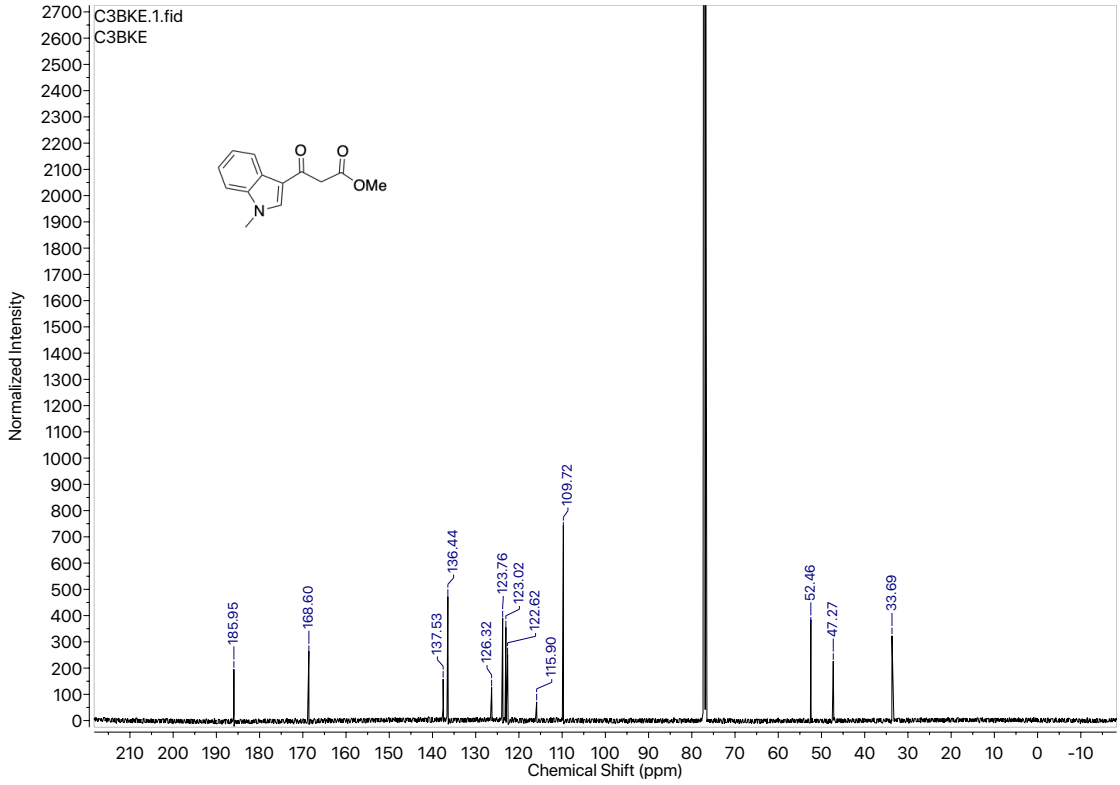
C3BKE.1.fid
C3BKE
O
O
OMe
N
Normalized Intensity
185.95
168.60
137.53
136.44
126.32
123.76
123.02
122.62
115.90
109.72
52.46
47.27
33.69
Chemical Shift (ppm)

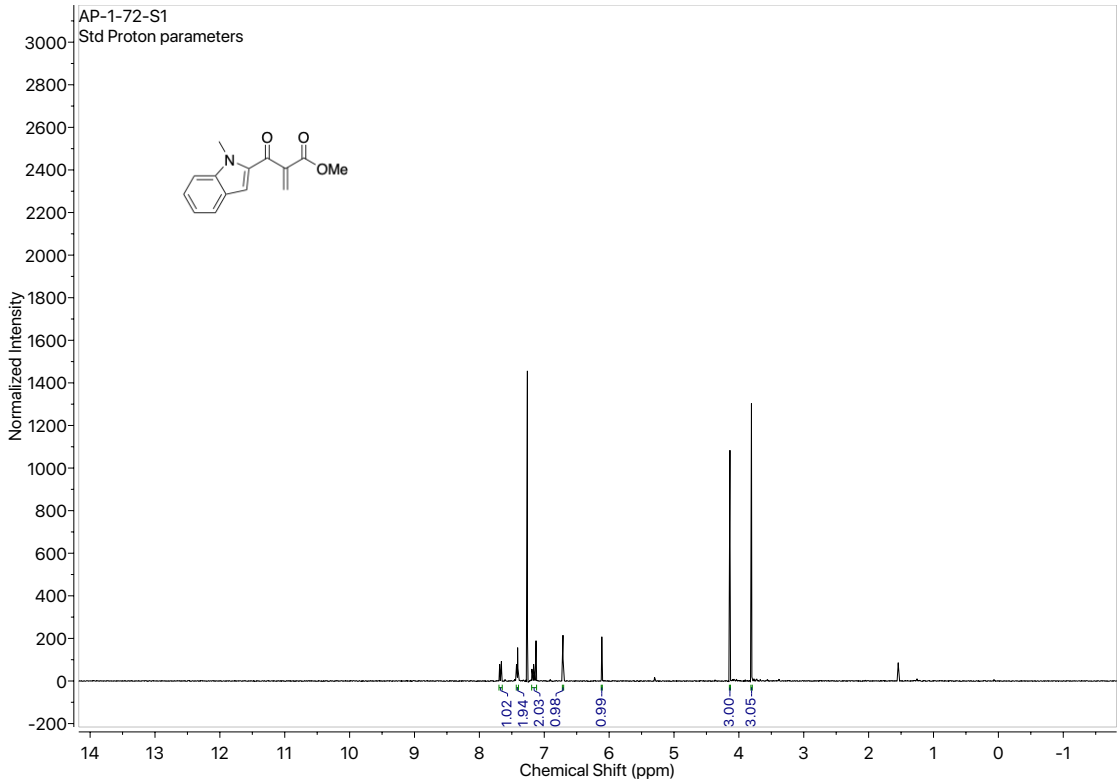
AP-1-72-S1
Std Proton parameters
O
O
OMe
N
Normalized Intensity
1.02
1.94
2.03
0.98
0.99
3.00
3.05
Chemical Shift (ppm)

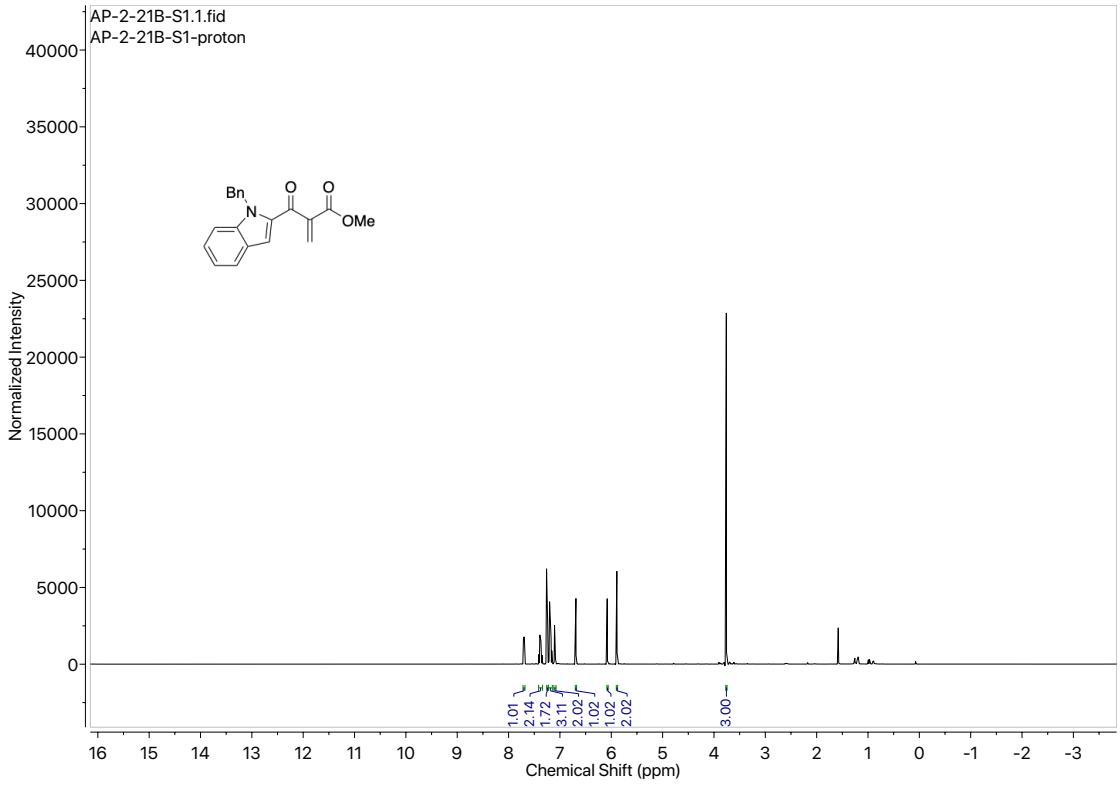
AP-2-21B-S1.1.fid
AP-2-21B-S1-proton
Bn
N
O
O
OMe
Normalized Intensity
Chemical Shift (ppm)
1.01
2.14
1.72
3.11
2.02
1.02
2.02
3.00

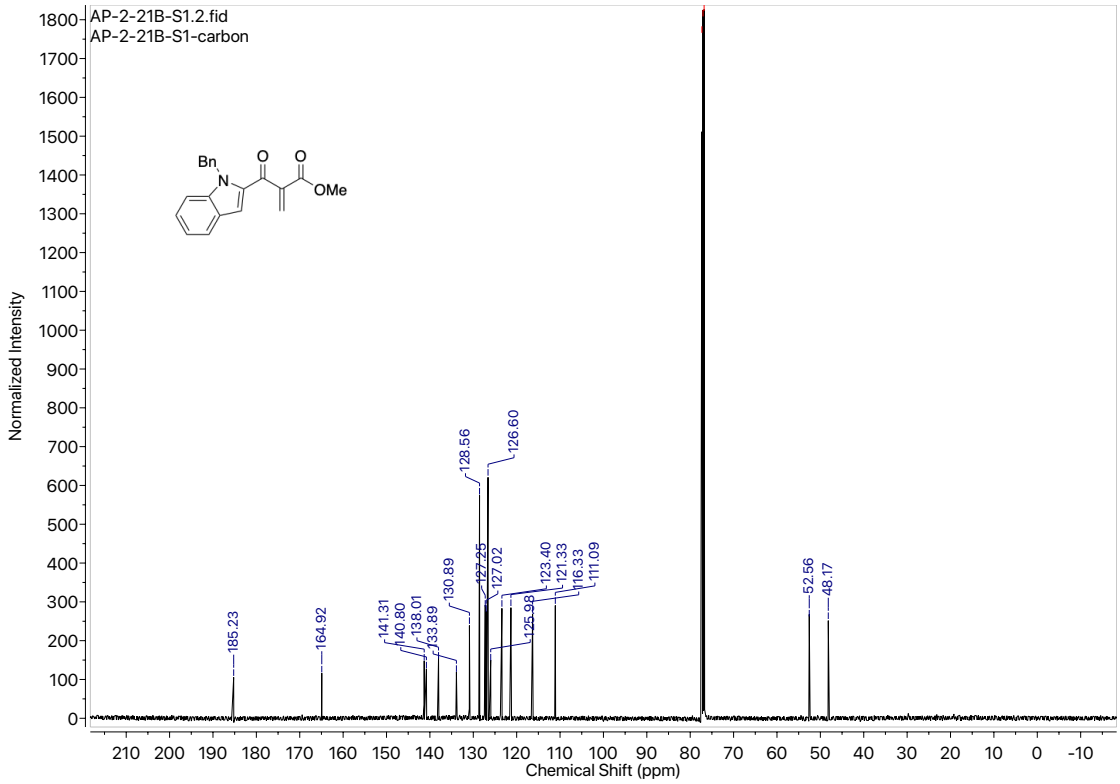
AP-2-21B-S1.2.fid
AP-2-21B-S1-carbon
Bn
N
O
O
OMe
Normalized Intensity
Chemical Shift (ppm)
185.23
164.92
141.31
140.80
138.01
133.89
130.89
128.56
127.25
127.02
126.60
125.98
123.40
121.33
116.33
111.09
52.56
48.17

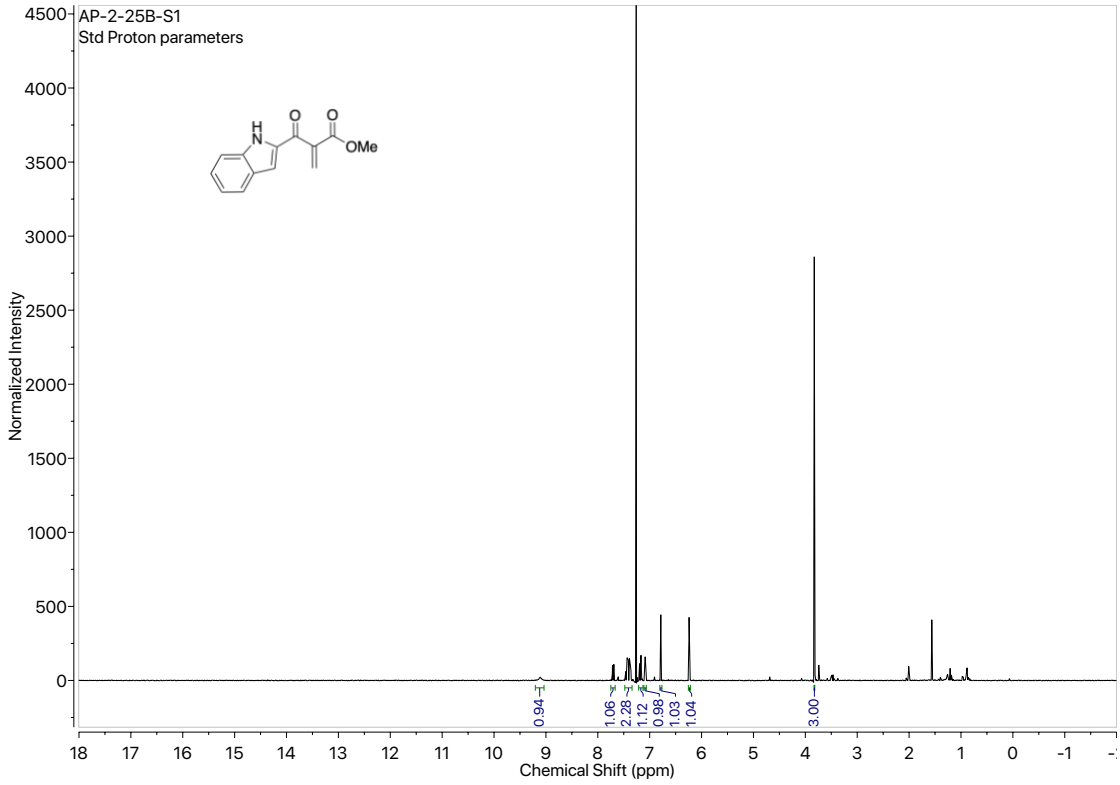
AP-2-25B-S1
Std Proton parameters
Normalized Intensity
Chemical Shift (ppm)
0.94
1.06
2.28
1.12
0.98
1.03
1.04
3.00

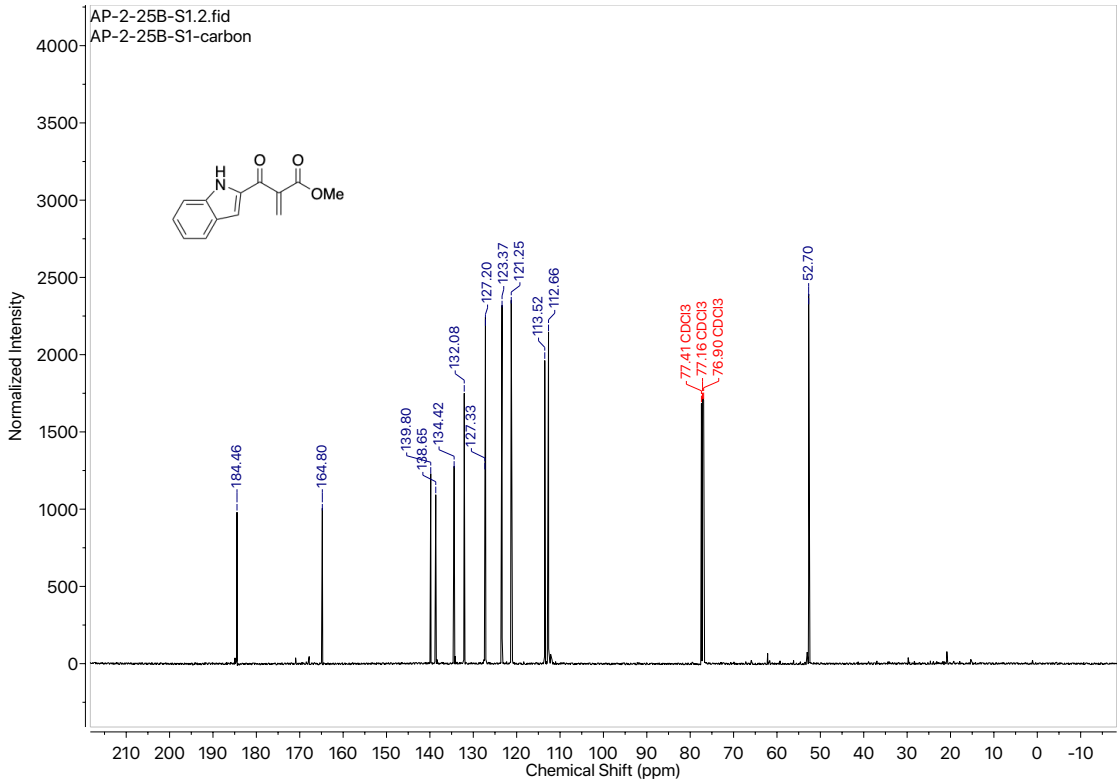
AP-2-25B-S1.2.fid
AP-2-25B-S1-carbon
Normalized Intensity
Chemical Shift (ppm)
184.46
164.80
139.80
138.65
134.42
132.08
127.33
127.20
123.37
121.25
113.52
112.66
77.41 CDCl3
77.16 CDCl3
76.90 CDCl3
52.70

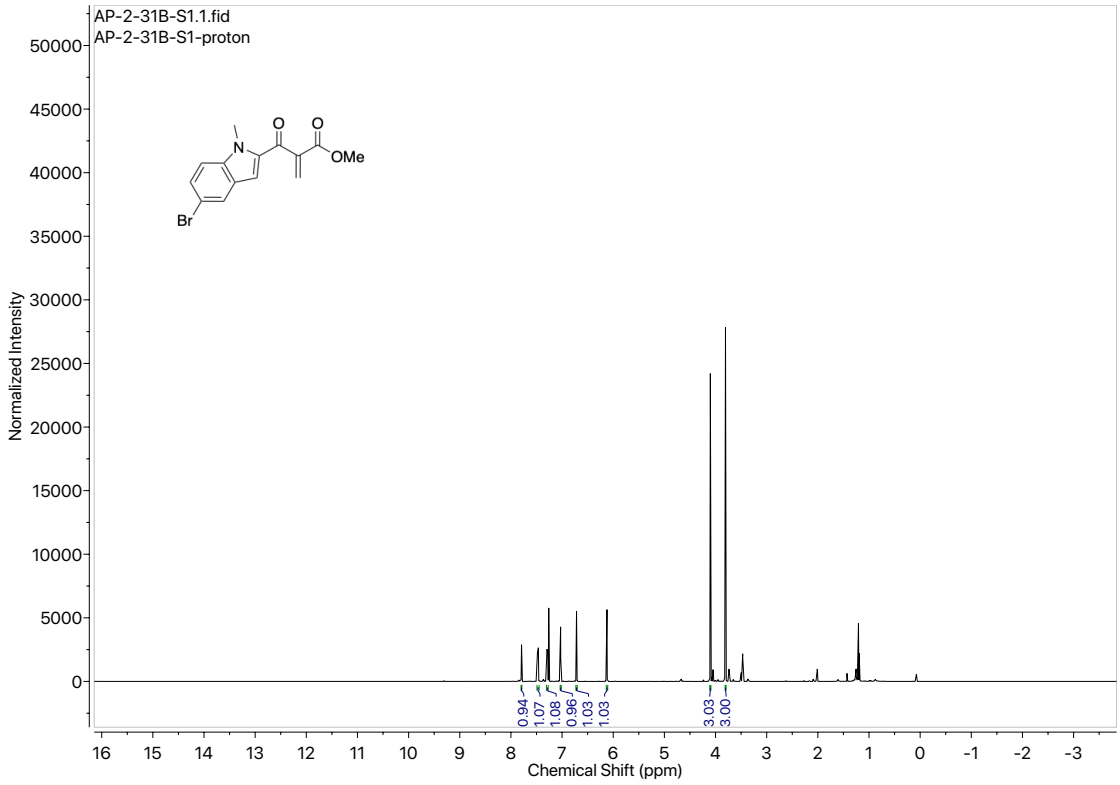
AP-2-31B-S1.1.fid
AP-2-31B-S1-proton
Normalized Intensity
Chemical Shift (ppm)
0.94
1.07
1.08
0.96
1.03
1.03
3.03
3.00
OMe
Br

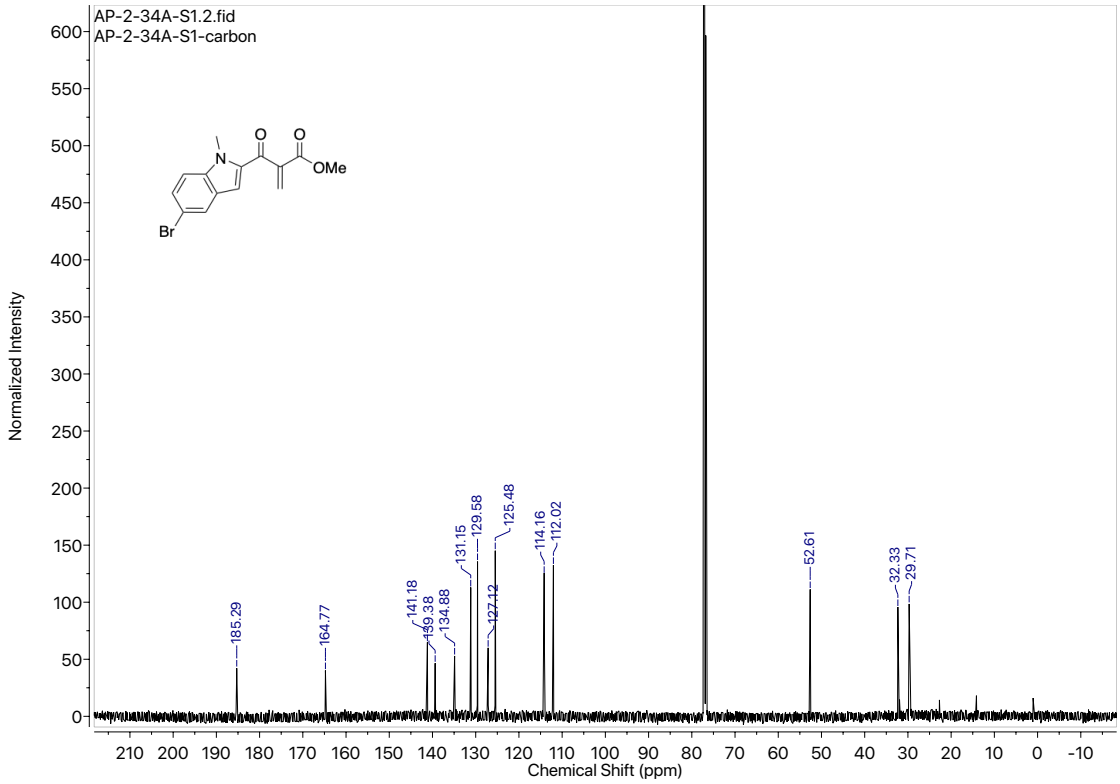
AP-2-34A-S1.2.fid
AP-2-34A-S1-carbon
Normalized Intensity
Chemical Shift (ppm)
185.29
164.77
141.18
139.38
134.88
131.15
129.58
127.12
125.48
114.16
112.02
52.61
32.33
29.71
OMe
Br

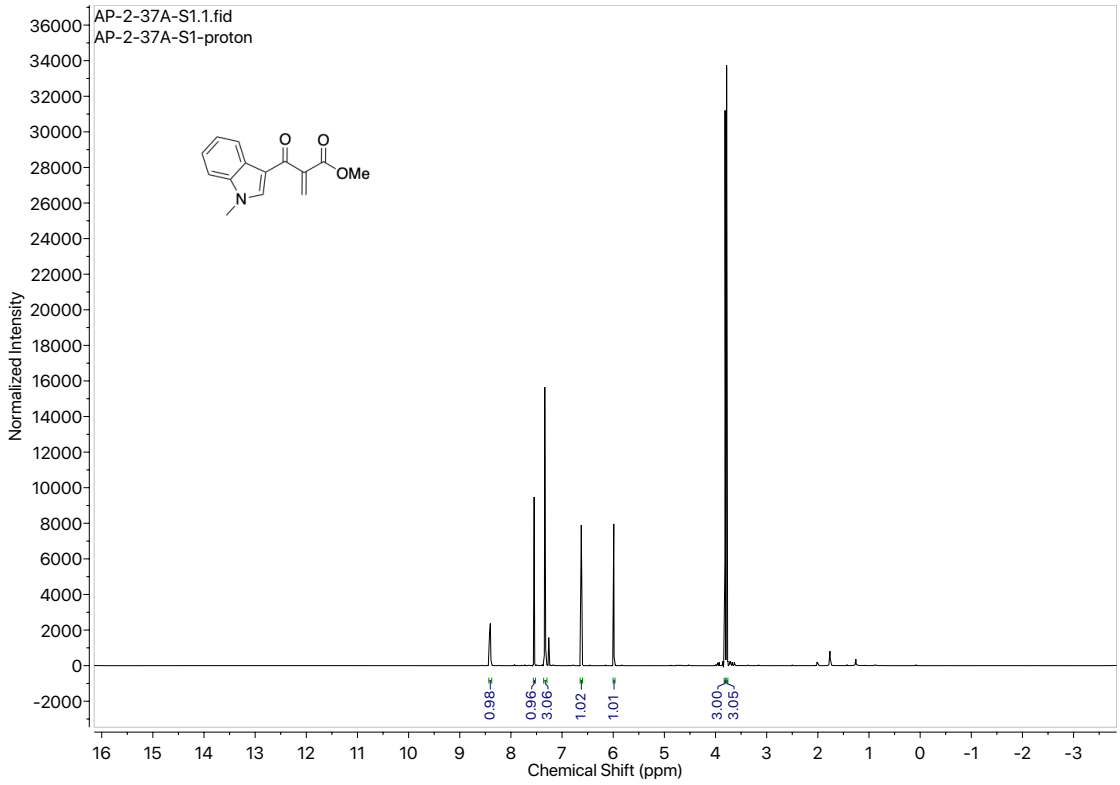
AP-2-37A-S1.1.fid
AP-2-37A-S1-proton
Normalized Intensity
Chemical Shift (ppm)
0.98
0.96
3.06
1.02
1.01
3.00
3.05
OMe

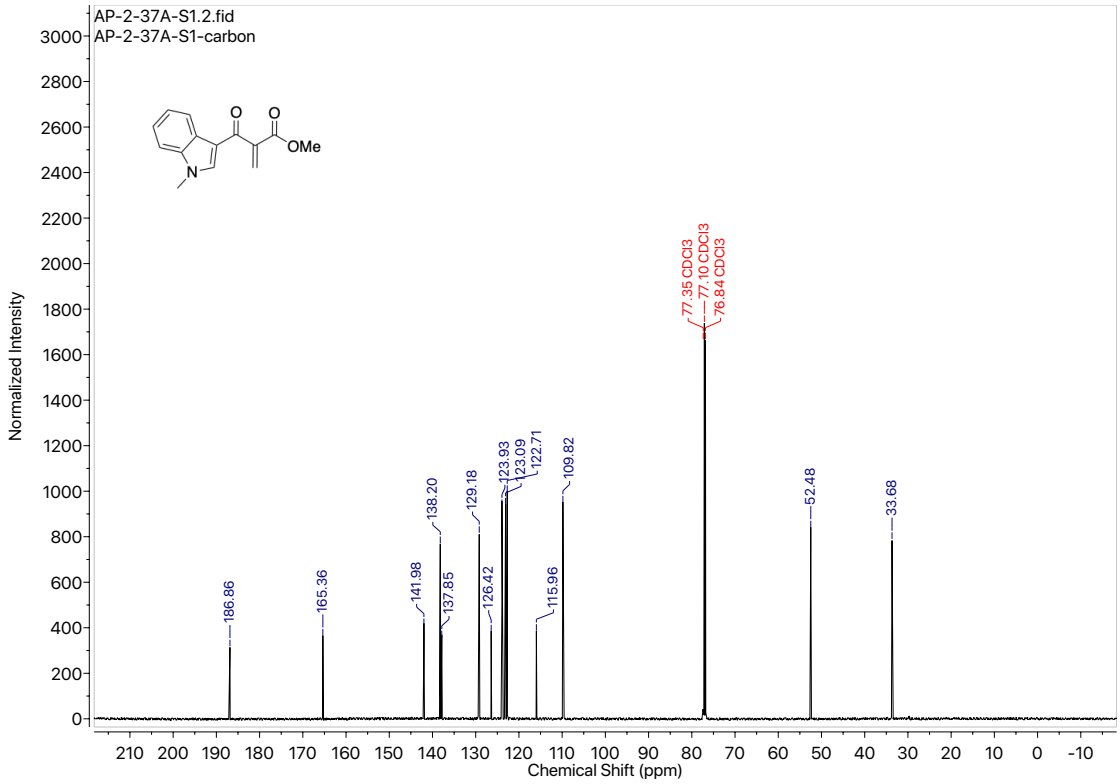
AP-2-37A-S1.2.fid
AP-2-37A-S1-carbon
Normalized Intensity
Chemical Shift (ppm)
77.35 CDCl3
77.10 CDCl3
76.84 CDCl3
186.86
165.36
141.98
138.20
137.85
129.18
126.42
123.93
123.09
122.71
115.96
109.82
52.48
33.68
OMe

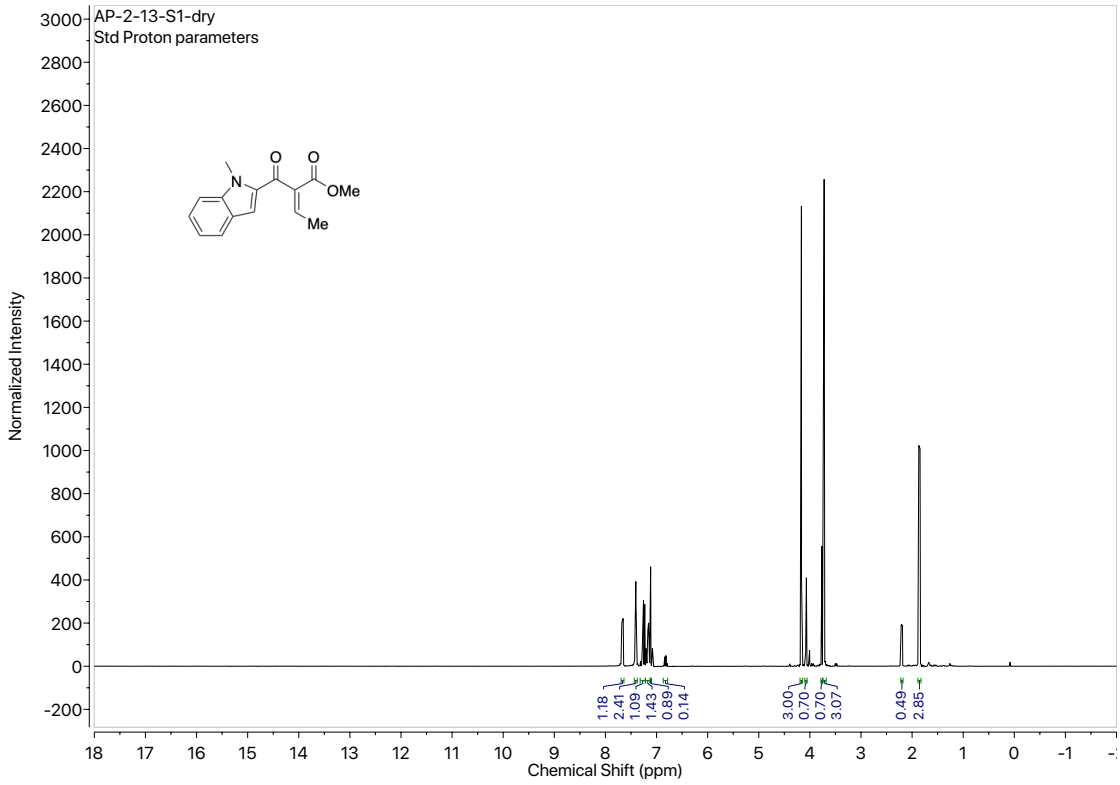
AP-2-13-S1-dry
Std Proton parameters
Normalized Intensity
Chemical Shift (ppm)
1.18
2.41
1.09
1.43
0.89
0.14
3.00
0.70
0.70
3.07
0.49
2.85

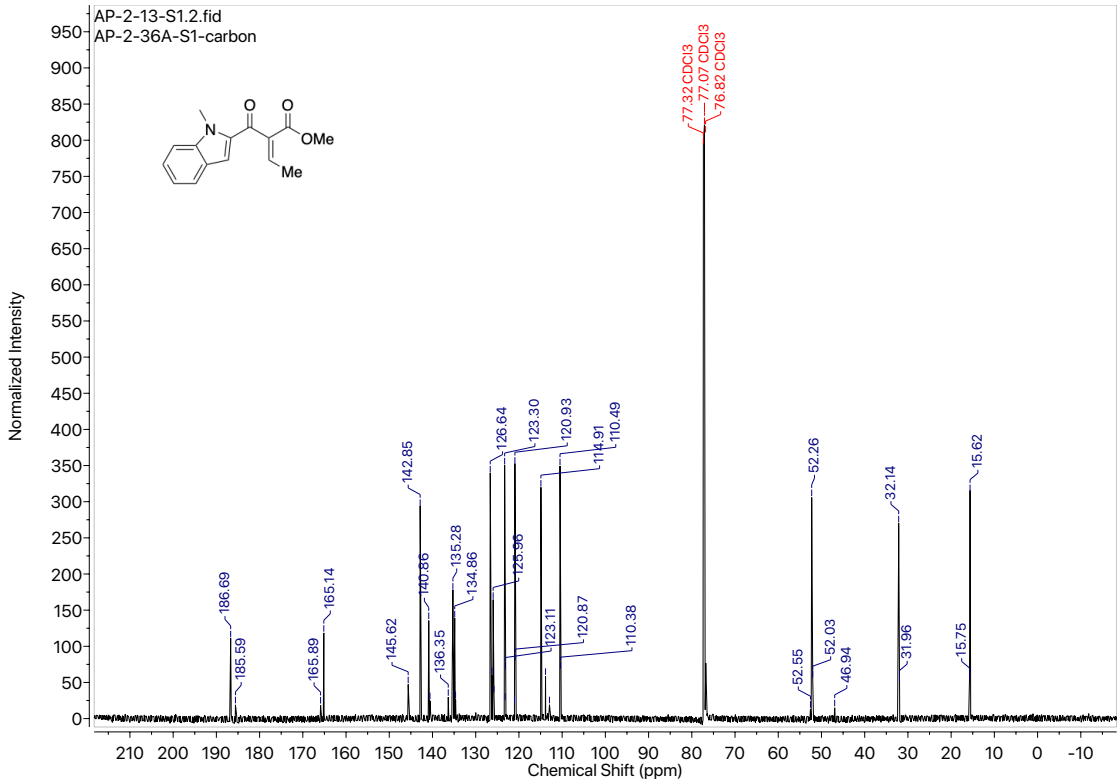
AP-2-13-S1.2.fid
AP-2-36A-S1-carbon
Normalized Intensity
Chemical Shift (ppm)
77.32 CDCl3
77.07 CDCl3
76.82 CDCl3
186.69
185.59
165.89
165.14
145.62
142.85
140.86
136.35
135.28
134.86
126.64
125.96
123.30
123.11
120.93
120.87
114.91
110.49
110.38
52.55
52.26
52.03
46.94
32.14
31.96
15.75
15.62

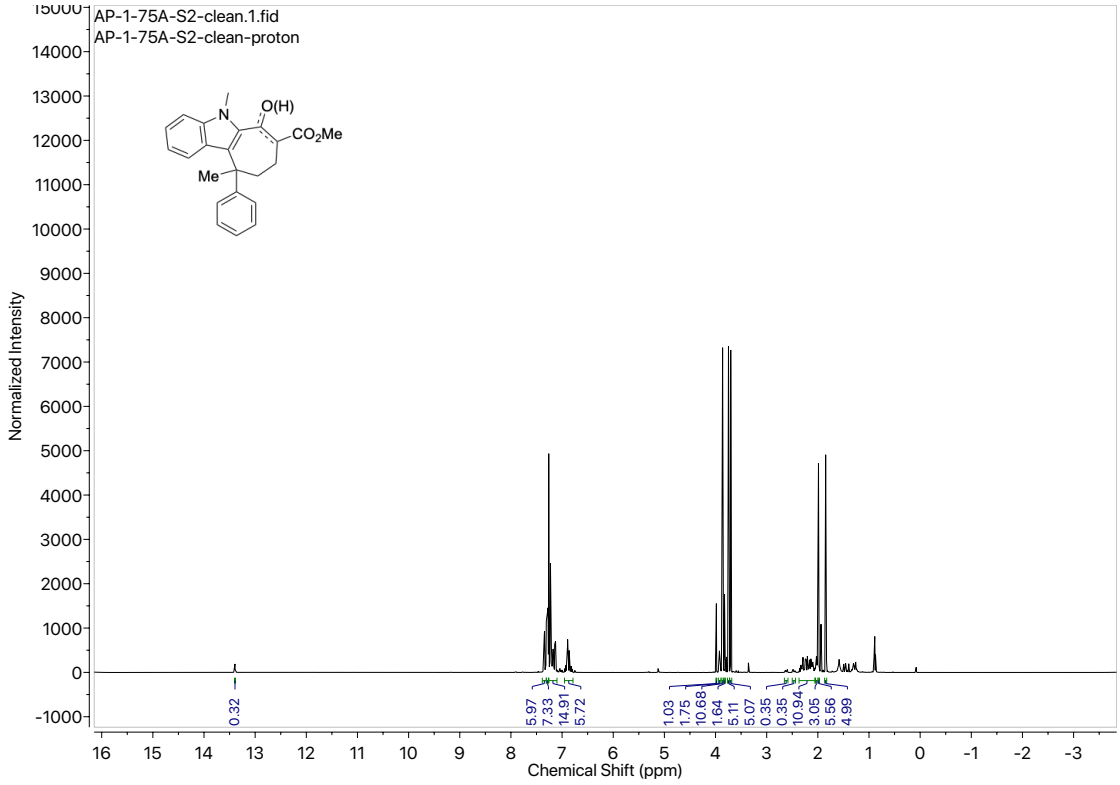
AP-1-75A-S2-clean.1.fid
AP-1-75A-S2-clean-proton
O(H)
CO2Me
Me
Normalized Intensity
Chemical Shift (ppm)
0.32
5.97
7.33
14.91
5.72
1.03
1.75
10.68
1.64
5.11
5.07
0.35
0.35
10.94
3.05
5.56
4.99

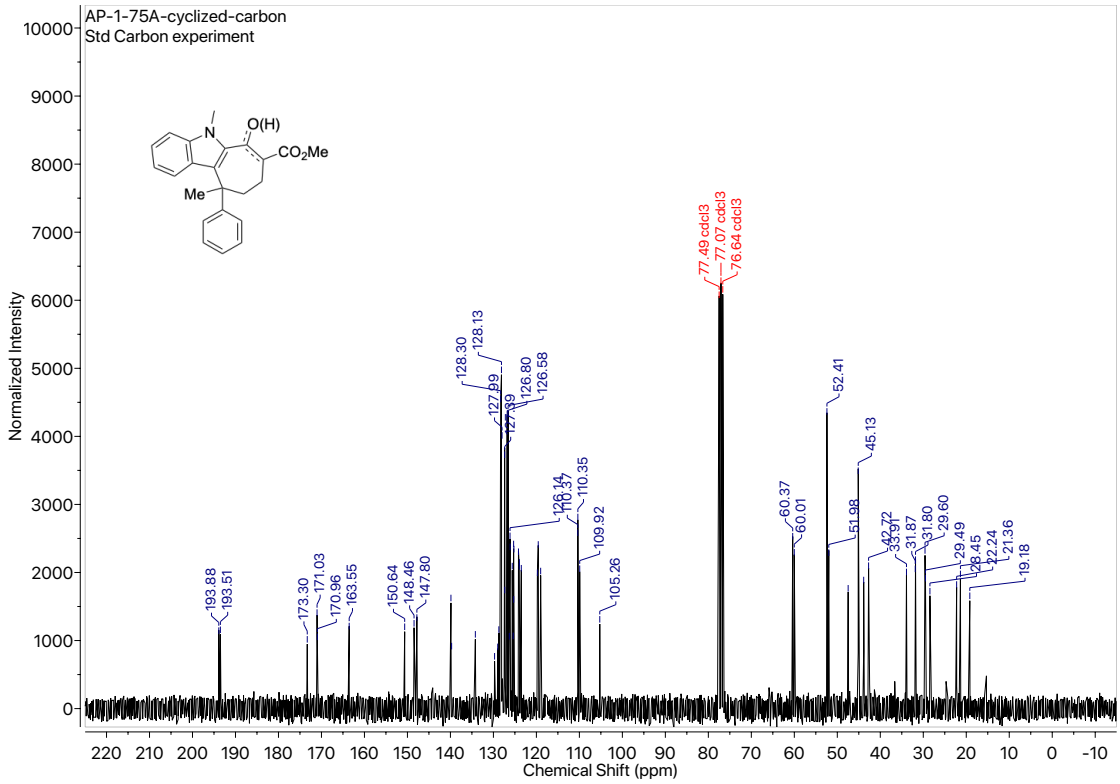
AP-1-75A-cyclized-carbon
Std Carbon experiment
O(H)
CO2Me
Me
Normalized Intensity
Chemical Shift (ppm)
77.49 cdcl3
77.07 cdcl3
76.64 cdcl3
193.88
193.51
173.30
171.03
170.96
163.55
150.64
148.46
147.80
128.30
128.13
127.89
127.39
126.80
126.58
110.35
109.92
105.26
60.37
60.01
52.41
51.98
45.13
42.72
33.91
31.87
31.80
29.60
29.49
28.45
22.24
21.36
19.18

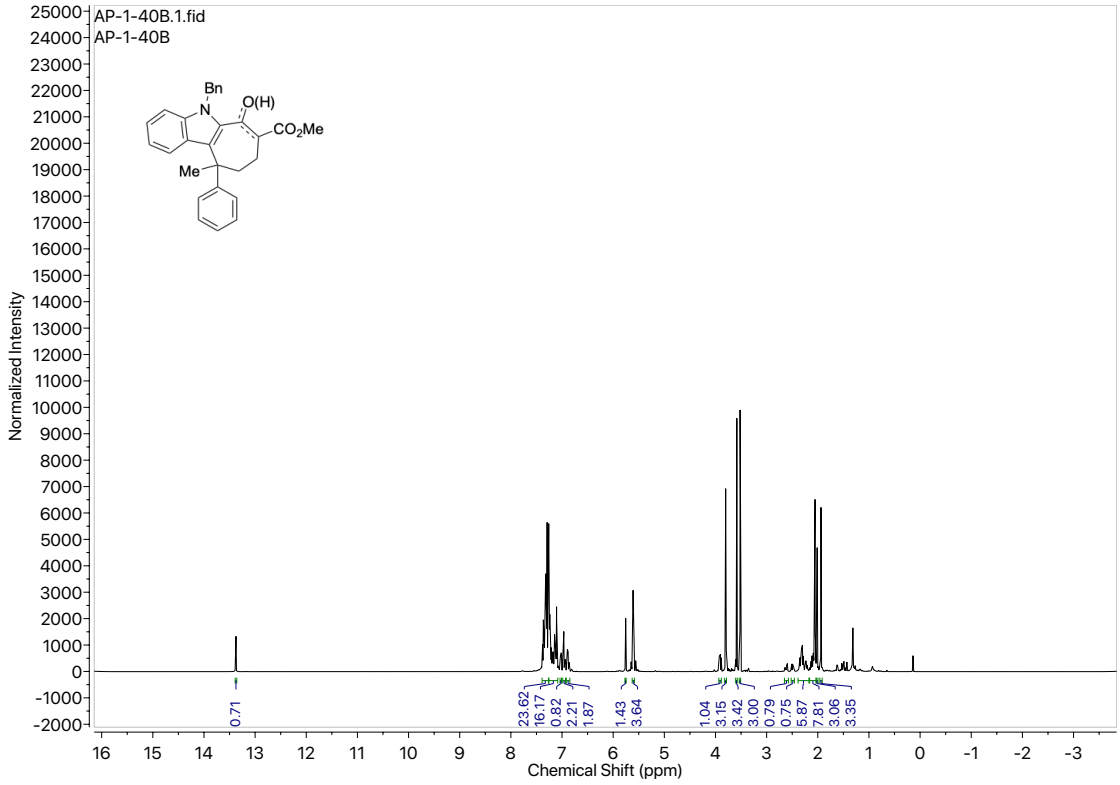
AP-1-40B.1.fid
AP-1-40B
Bn
N
O(H)
CO2Me
Me
Normalized Intensity
Chemical Shift (ppm)
0.71
23.62
16.17
0.82
2.21
1.87
1.43
3.64
1.04
3.15
3.42
3.00
0.79
0.75
5.87
7.81
3.06
3.35

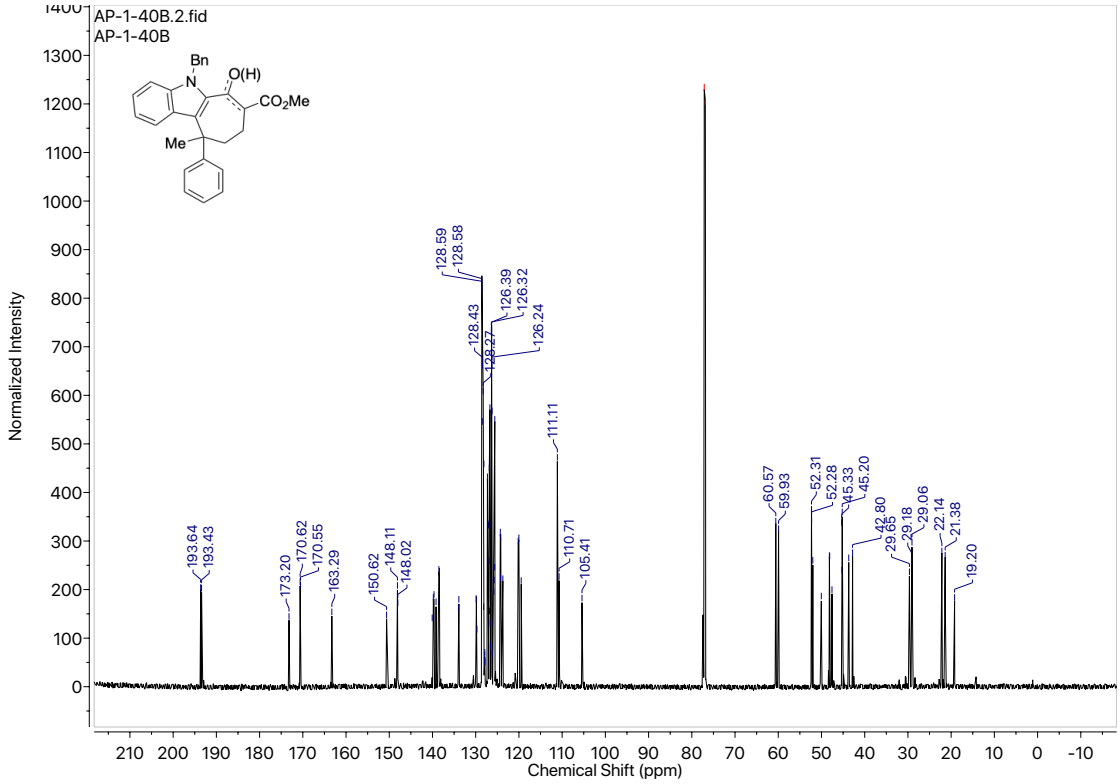
AP-1-40B.2.fid
AP-1-40B
Bn
N
O(H)
CO2Me
Me
Normalized Intensity
Chemical Shift (ppm)
193.64
193.43
173.20
170.62
170.55
163.29
150.62
148.11
148.02
128.59
128.58
128.43
126.39
126.32
126.24
111.11
110.71
105.41
60.57
59.93
52.31
52.28
45.33
45.20
42.80
29.65
29.18
29.06
22.14
21.38
19.20

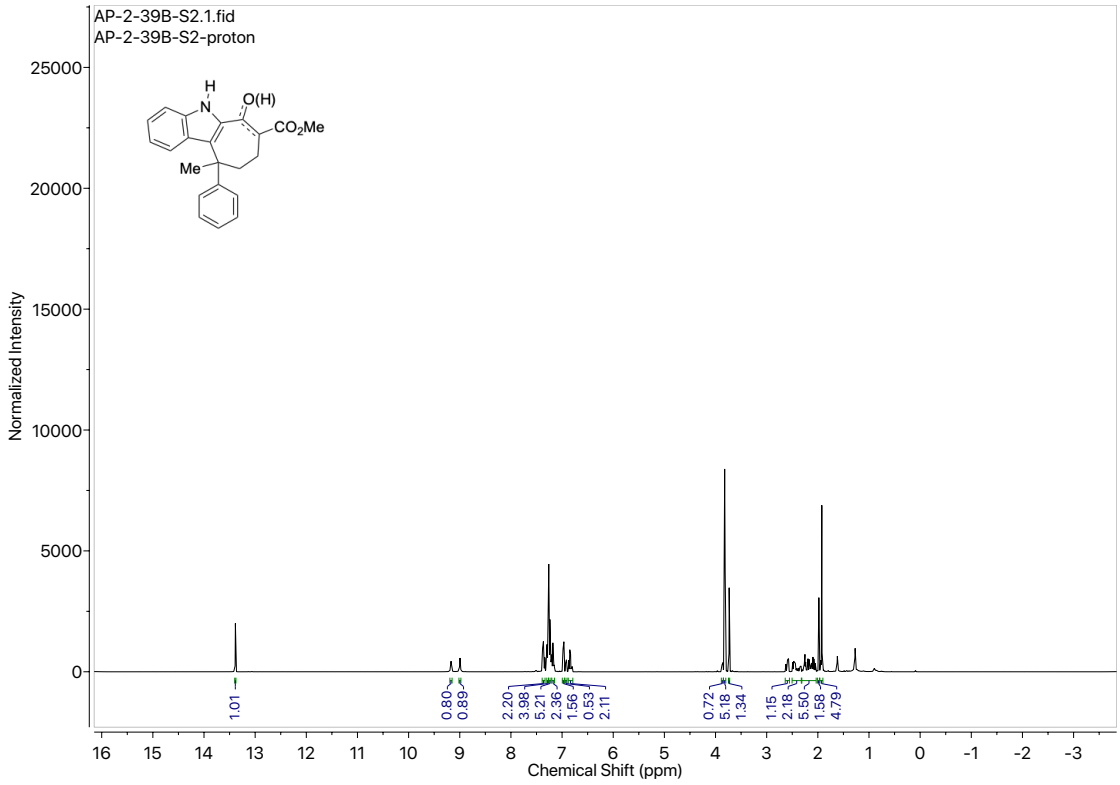
AP-2-39B-S2.1.fid
AP-2-39B-S2-proton
Normalized Intensity
Chemical Shift (ppm)
1.01
0.80
0.89
2.20
3.98
5.21
2.36
1.56
0.53
2.11
0.72
5.18
1.34
1.15
2.18
5.50
1.58
4.79

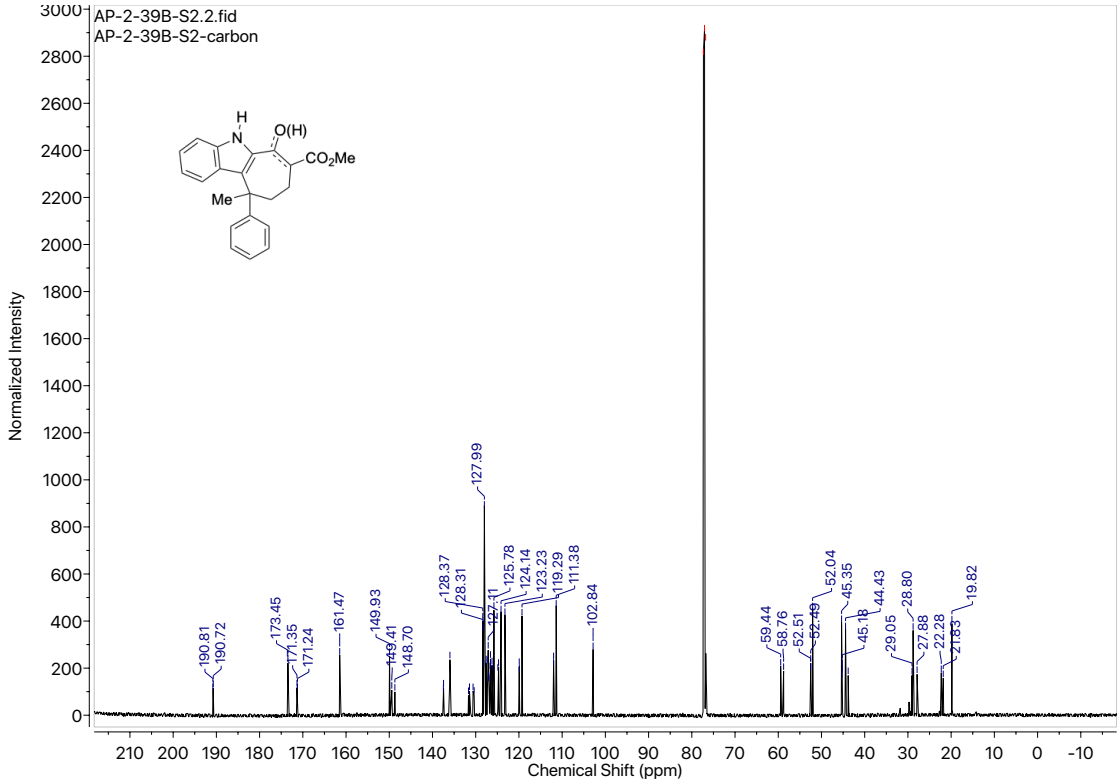
AP-2-39B-S2.2.fid
AP-2-39B-S2-carbon
Normalized Intensity
Chemical Shift (ppm)
190.81
190.72
173.45
171.35
171.24
161.47
149.93
149.41
148.70
128.37
128.31
127.99
127.11
125.78
124.14
123.23
119.29
111.38
102.84
59.44
58.76
52.51
52.49
52.04
45.35
45.18
44.43
29.05
28.80
27.88
22.28
21.33
19.82

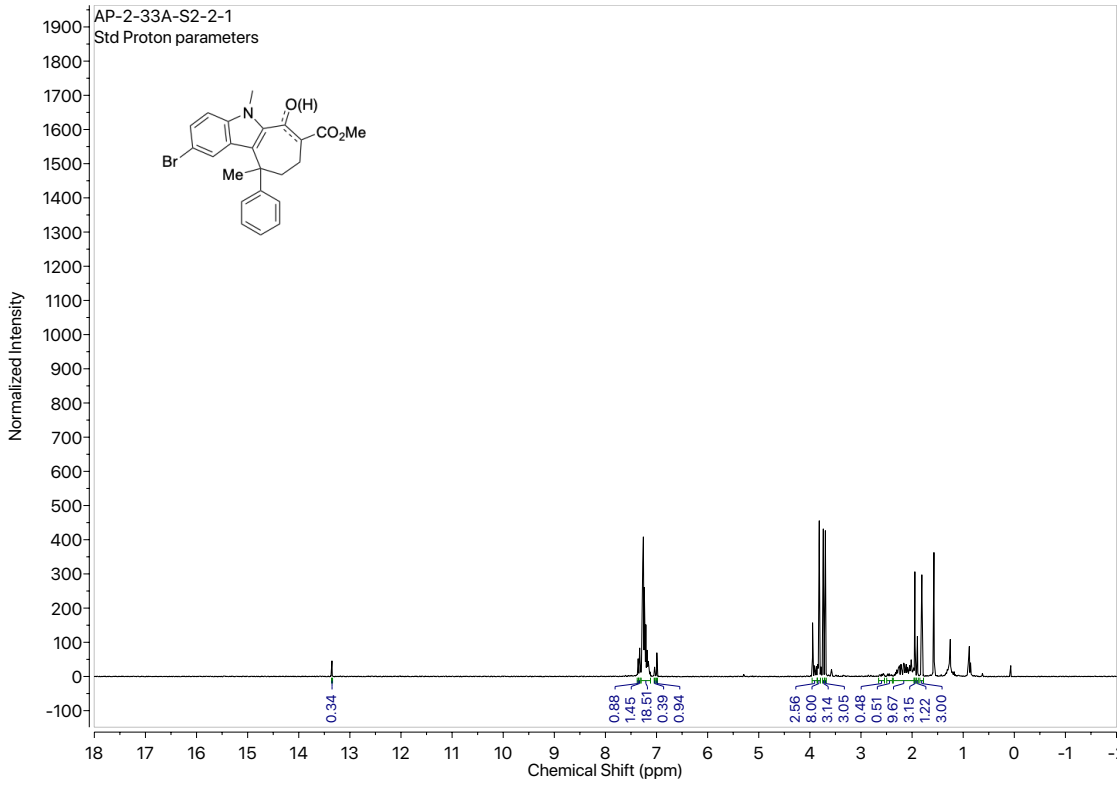
AP-2-33A-S2-2-1
Std Proton parameters
O(H)
N
CO2Me
Br
Me
Normalized Intensity
Chemical Shift (ppm)
0.34
0.88
1.45
18.51
0.39
0.94
2.56
8.00
3.14
3.05
0.48
0.51
9.67
3.15
1.22
3.00

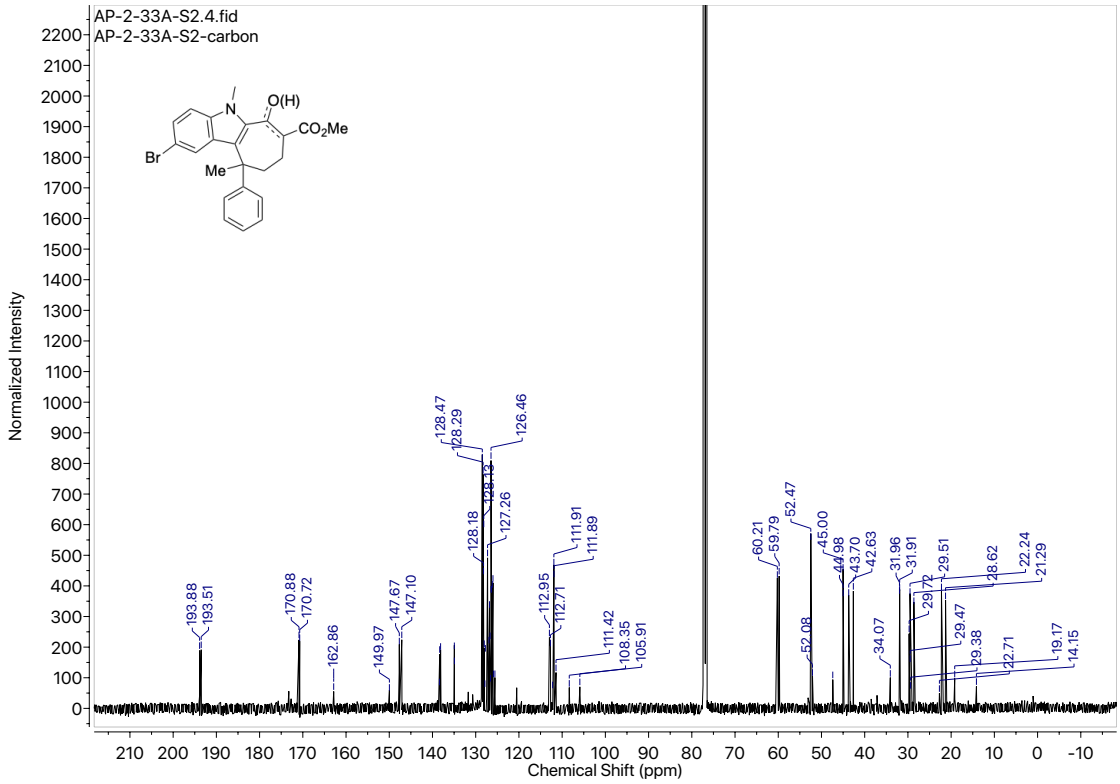
AP-2-33A-S2.4.fid
AP-2-33A-S2-carbon
O(H)
N
CO2Me
Br
Me
Normalized Intensity
Chemical Shift (ppm)
193.88
193.51
170.88
170.72
162.86
149.97
147.67
147.10
128.47
128.29
128.18
128.13
127.26
126.46
112.95
112.71
111.91
111.89
111.42
108.35
105.91
60.21
59.79
52.47
52.08
45.00
44.98
43.70
42.63
34.07
31.96
31.91
29.72
29.51
29.47
29.38
22.71
22.24
21.29
19.17
14.15

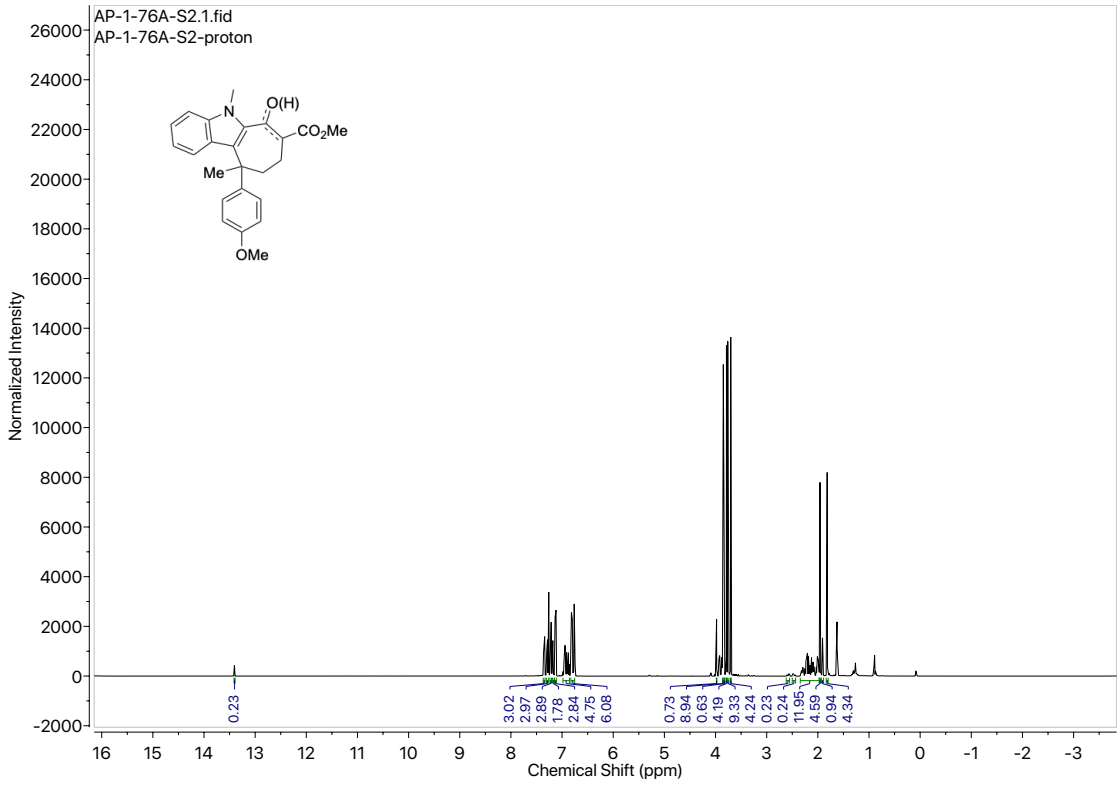
AP-1-76A-S2.1.fid
AP-1-76A-S2-proton
O(H)
CO2Me
Me
OMe
Normalized Intensity
Chemical Shift (ppm)
0.23
3.02
2.97
2.89
1.78
2.84
4.75
6.08
0.73
8.94
0.63
4.19
9.33
4.24
0.23
0.24
11.95
4.59
0.94
4.34

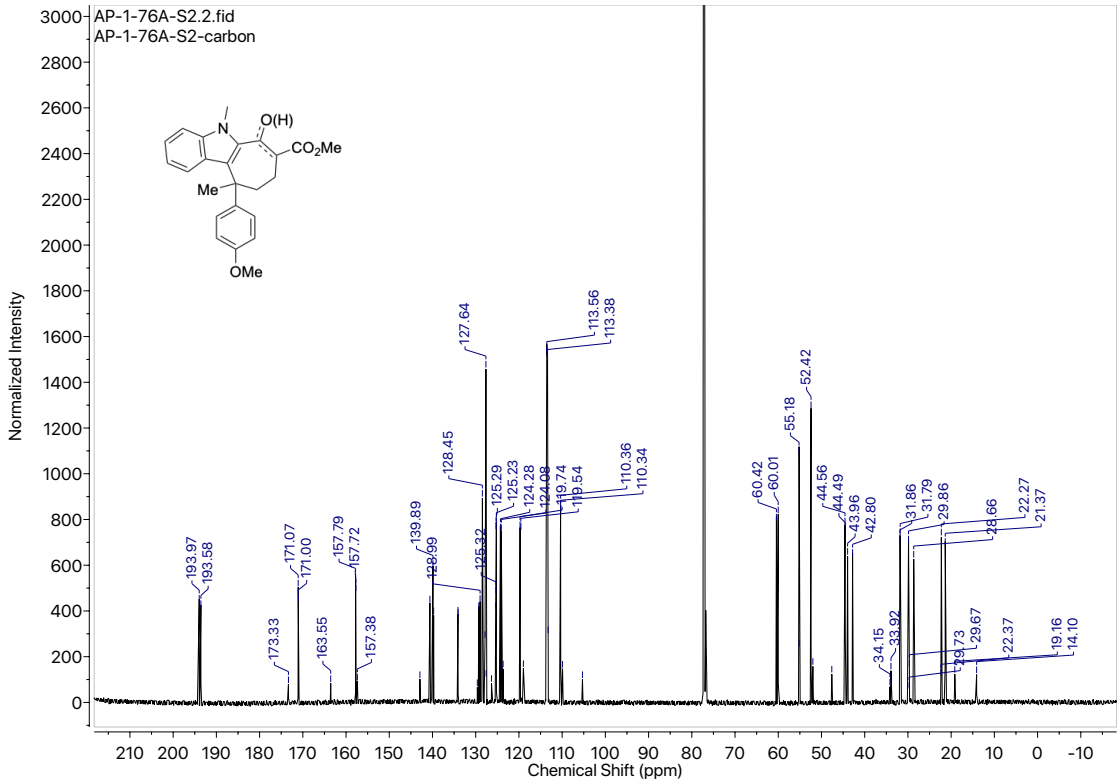
AP-1-76A-S2.2.fid
AP-1-76A-S2-carbon
O(H)
CO2Me
Me
OMe
Normalized Intensity
Chemical Shift (ppm)
193.97
193.58
173.33
171.07
171.00
163.55
157.79
157.72
157.38
139.89
128.99
128.45
127.64
125.32
125.29
125.23
124.28
124.08
119.74
119.54
113.56
113.38
110.36
110.34
60.42
60.01
55.18
52.42
44.56
44.49
43.96
42.80
34.15
33.92
31.86
31.79
29.86
29.73
29.67
28.66
22.37
22.27
21.37
19.16
14.10

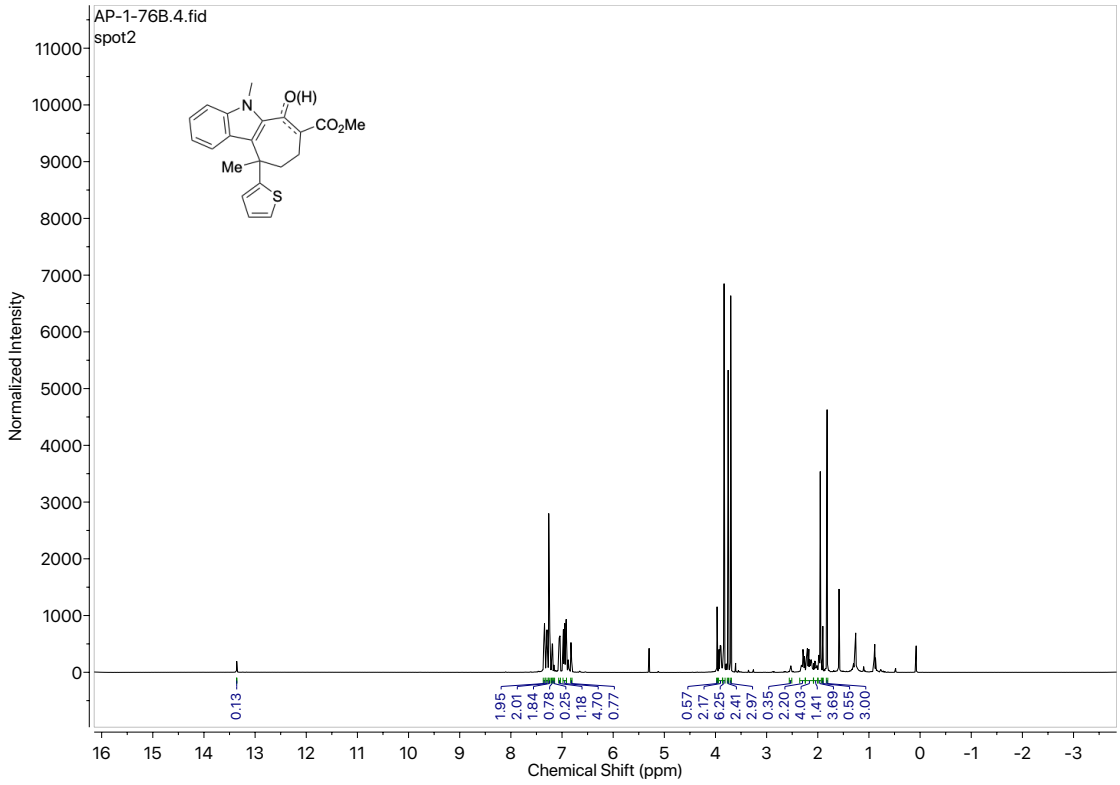
AP-1-76B.4.fid
spot2
O(H)
N
CO2Me
Me
S
Normalized Intensity
Chemical Shift (ppm)
0.13
1.95
2.01
1.84
0.78
0.25
1.18
4.70
0.77
0.57
2.17
6.25
2.41
2.97
0.35
2.20
4.03
1.41
3.69
0.55
3.00

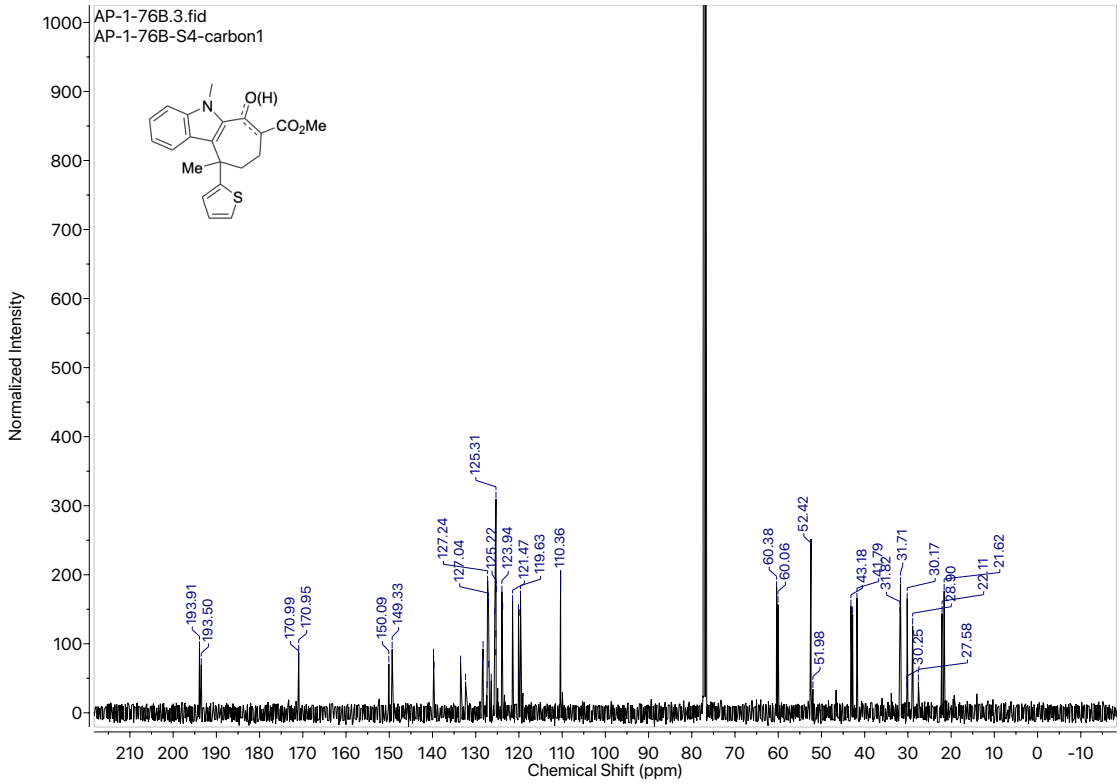
AP-1-76B.3.fid
AP-1-76B-S4-carbon1
O(H)
N
CO2Me
Me
S
Normalized Intensity
Chemical Shift (ppm)
193.91
193.50
170.99
170.95
150.09
149.33
127.24
127.04
125.31
125.22
123.94
121.47
119.63
110.36
60.38
60.06
52.42
51.98
43.18
41.79
31.82
31.71
30.17
28.90
27.58
30.25
23.11
21.62

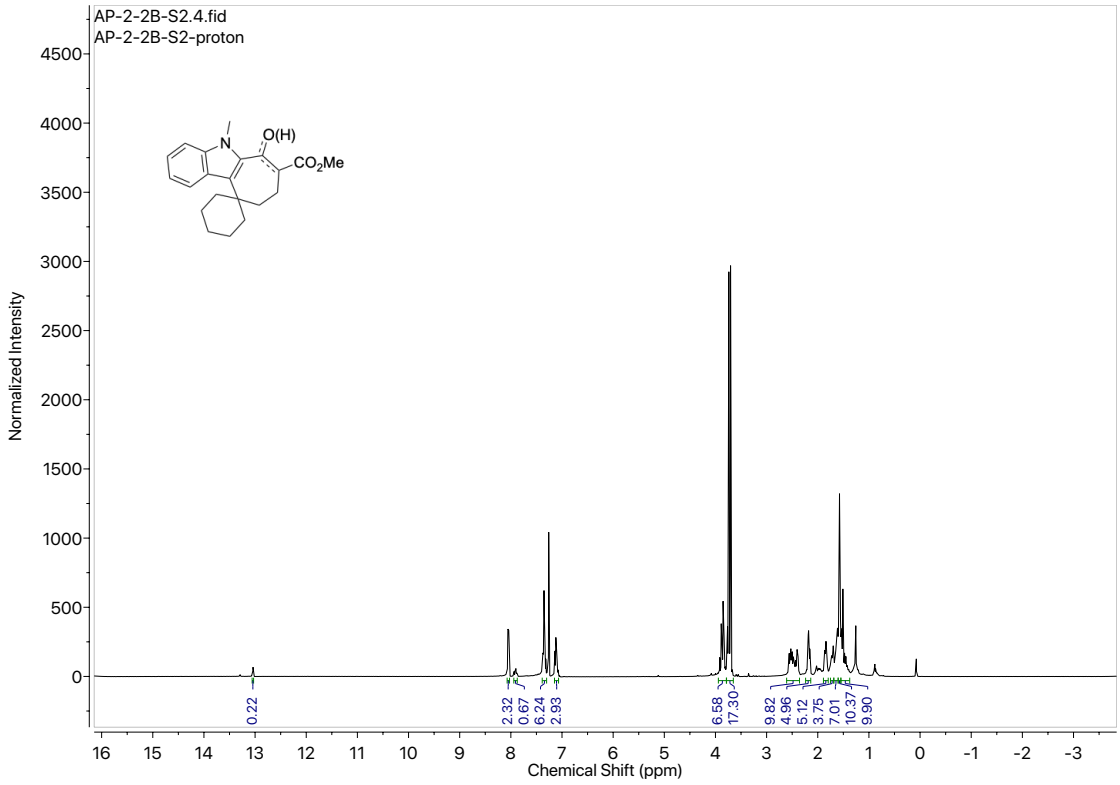
AP-2-2B-S2.4.fid
AP-2-2B-S2-proton
O(H)
CO2Me
Normalized Intensity
Chemical Shift (ppm)
0.22
2.32
0.67
6.24
2.93
6.58
17.30
9.82
4.96
5.12
3.75
7.01
10.37
9.90

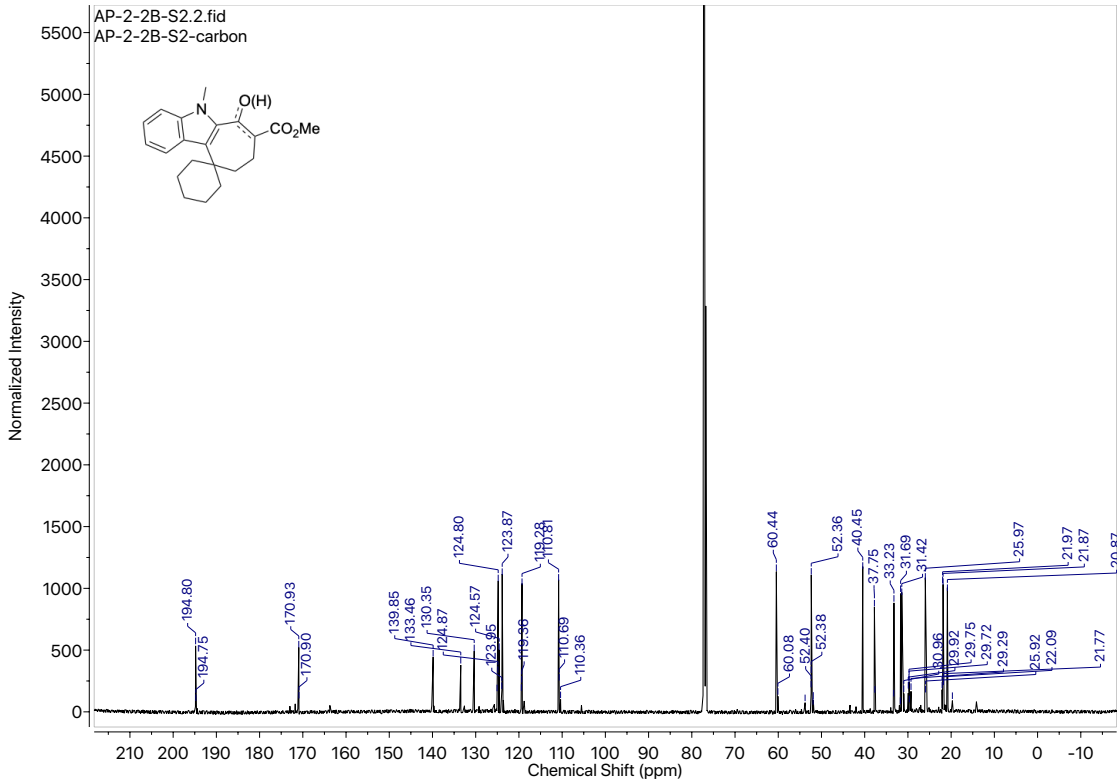
AP-2-2B-S2.2.fid
AP-2-2B-S2-carbon
O(H)
CO2Me
Normalized Intensity
Chemical Shift (ppm)
194.80
194.75
170.93
170.90
139.85
133.46
130.35
124.87
124.80
124.57
123.95
123.87
119.36
110.69
110.36
60.44
60.08
52.40
52.38
52.36
40.45
37.75
33.23
31.69
31.42
25.97
21.97
21.87
29.92
29.75
29.72
29.29
25.92
22.09
21.77

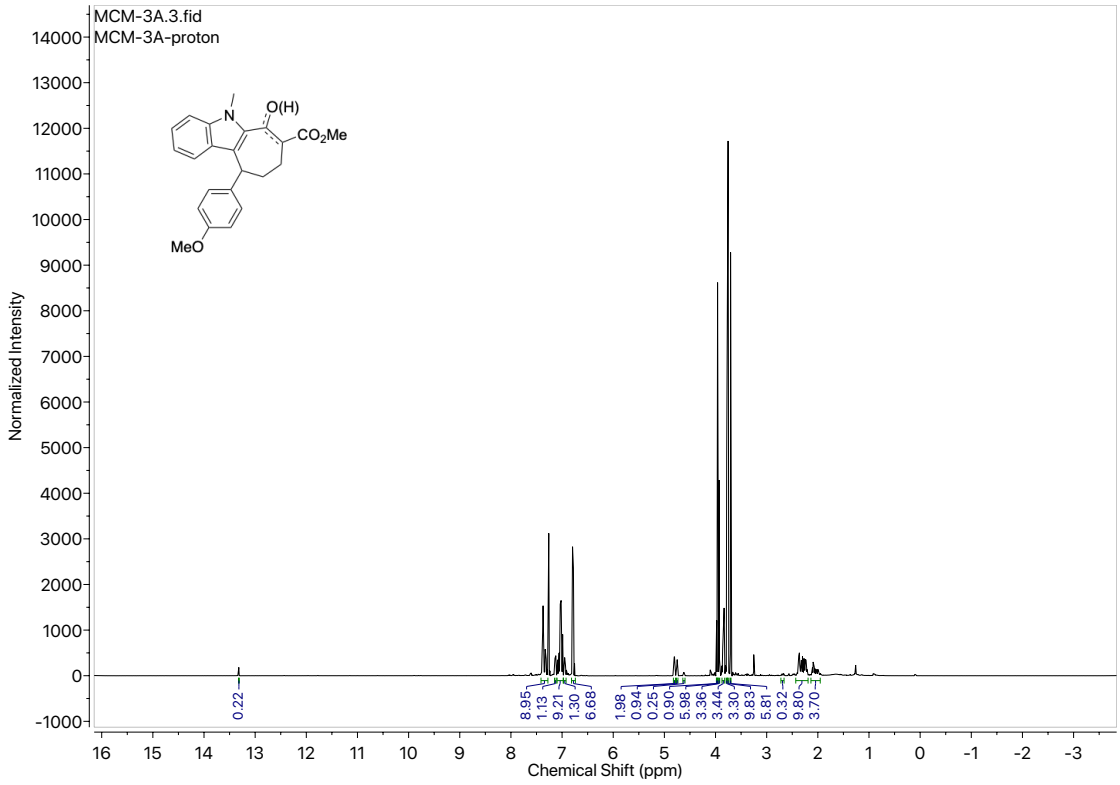
MCM-3A.3.fid
MCM-3A-proton
O(H)
CO2Me
MeO
Normalized Intensity
Chemical Shift (ppm)
0.22
8.95
1.13
9.21
1.30
6.68
1.98
0.94
0.25
0.90
5.98
3.36
3.44
3.30
9.83
5.81
0.32
9.80
3.70

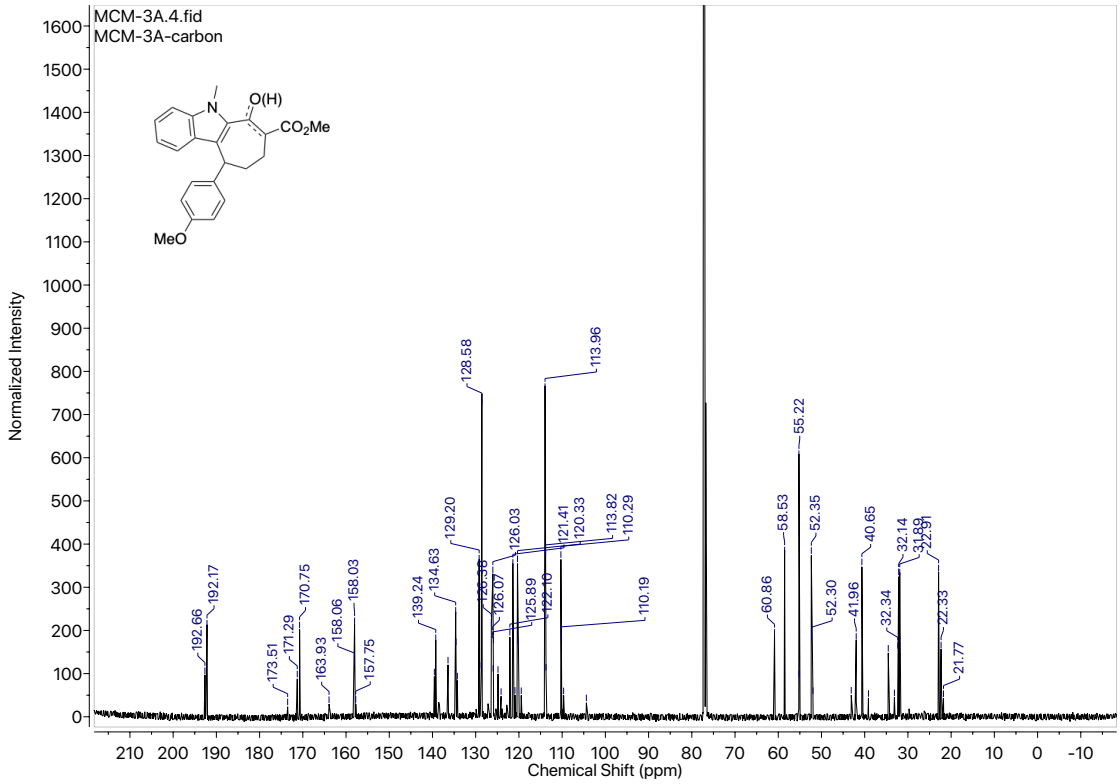
MCM-3A.4.fid
MCM-3A-carbon
O(H)
CO2Me
MeO
Normalized Intensity
Chemical Shift (ppm)
192.66
192.17
173.51
171.29
170.75
163.93
158.06
158.03
157.75
139.24
134.63
129.20
128.58
126.07
126.03
125.89
122.10
121.41
120.33
113.96
113.82
110.29
110.19
60.86
58.53
55.22
52.35
52.30
41.96
40.65
32.34
32.14
31.89
22.91
22.33
21.77

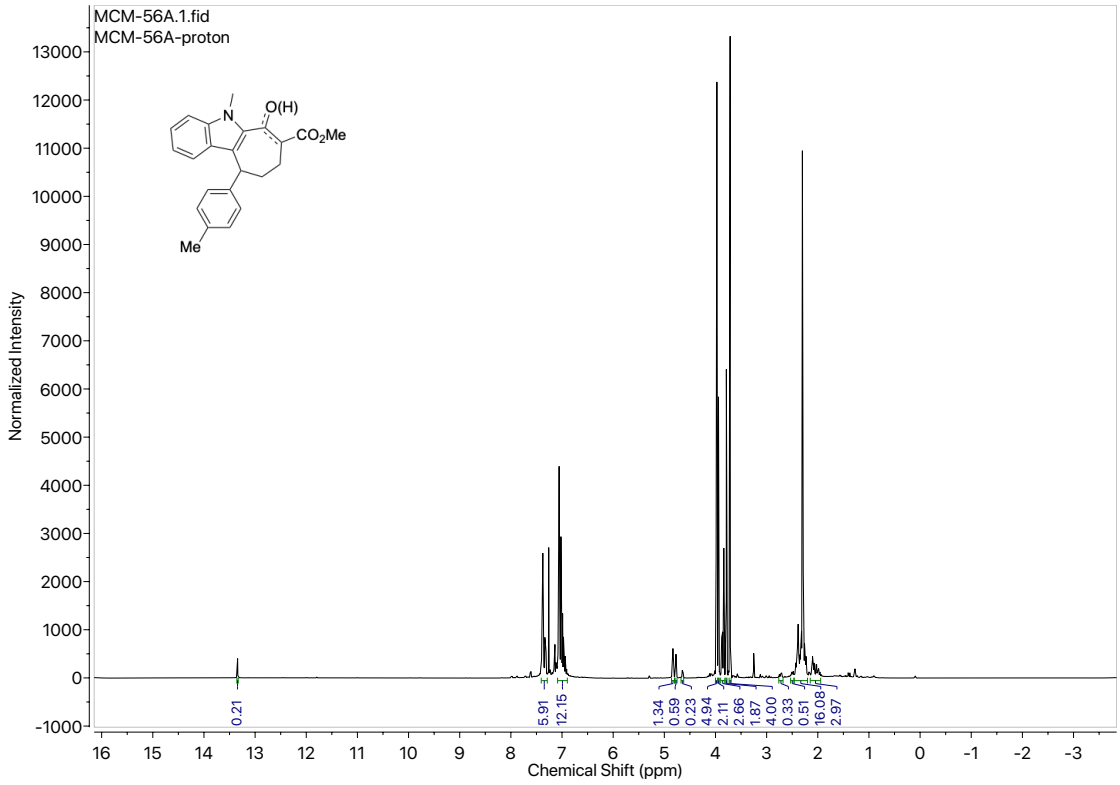
MCM-56A.1.fid
MCM-56A-proton
O(H)
N
CO2Me
Me
Normalized Intensity
Chemical Shift (ppm)
0.21
5.91
12.15
1.34
0.59
0.23
4.94
2.11
2.66
1.87
4.00
0.33
0.51
16.08
2.97

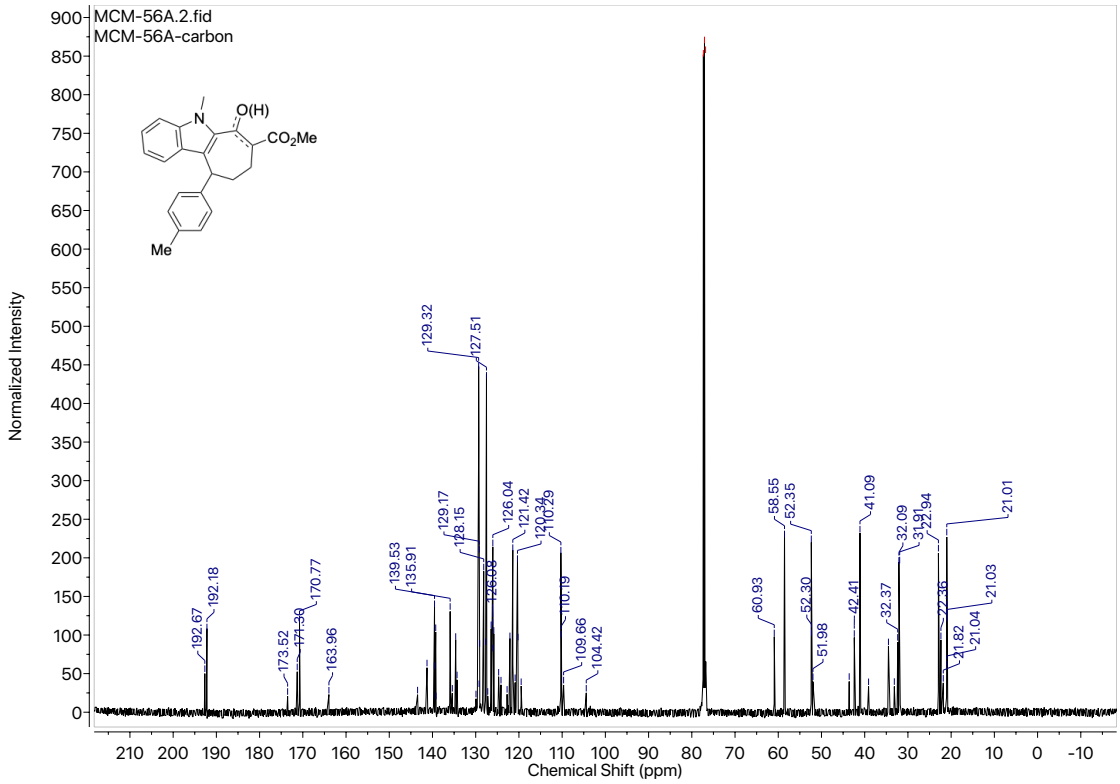
MCM-56A.2.fid
MCM-56A-carbon
O(H)
N
CO2Me
Me
Normalized Intensity
Chemical Shift (ppm)
192.67
192.18
173.52
171.38
170.77
163.96
139.53
135.91
129.32
129.17
128.15
127.51
126.04
121.42
120.34
110.29
110.19
109.66
104.42
60.93
58.55
52.35
52.30
51.98
42.41
41.09
32.37
32.09
31.91
27.94
27.36
21.82
21.04
21.03
21.01

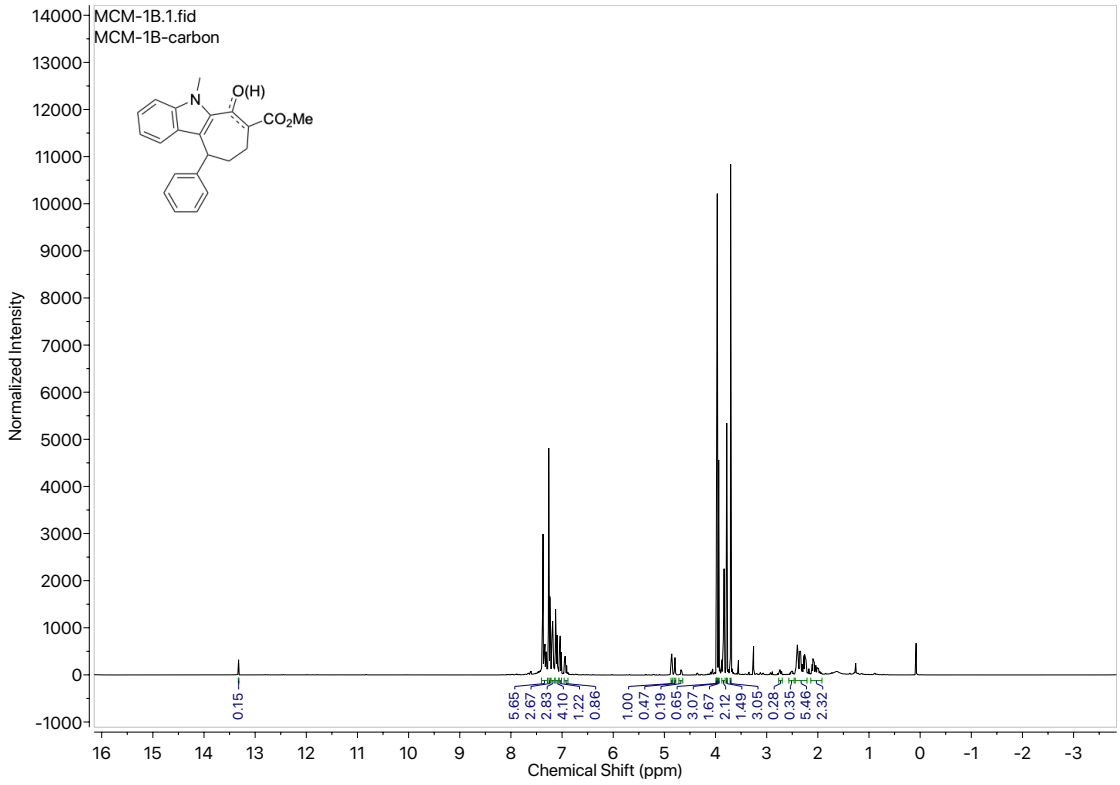
MCM-1B.1.fid
MCM-1B-carbon
O(H)
CO2Me
Normalized Intensity
Chemical Shift (ppm)
0.15
5.65
2.67
2.83
4.10
1.22
0.86
1.00
0.47
0.19
0.65
3.07
1.67
2.12
1.49
3.05
0.28
0.35
5.46
2.32

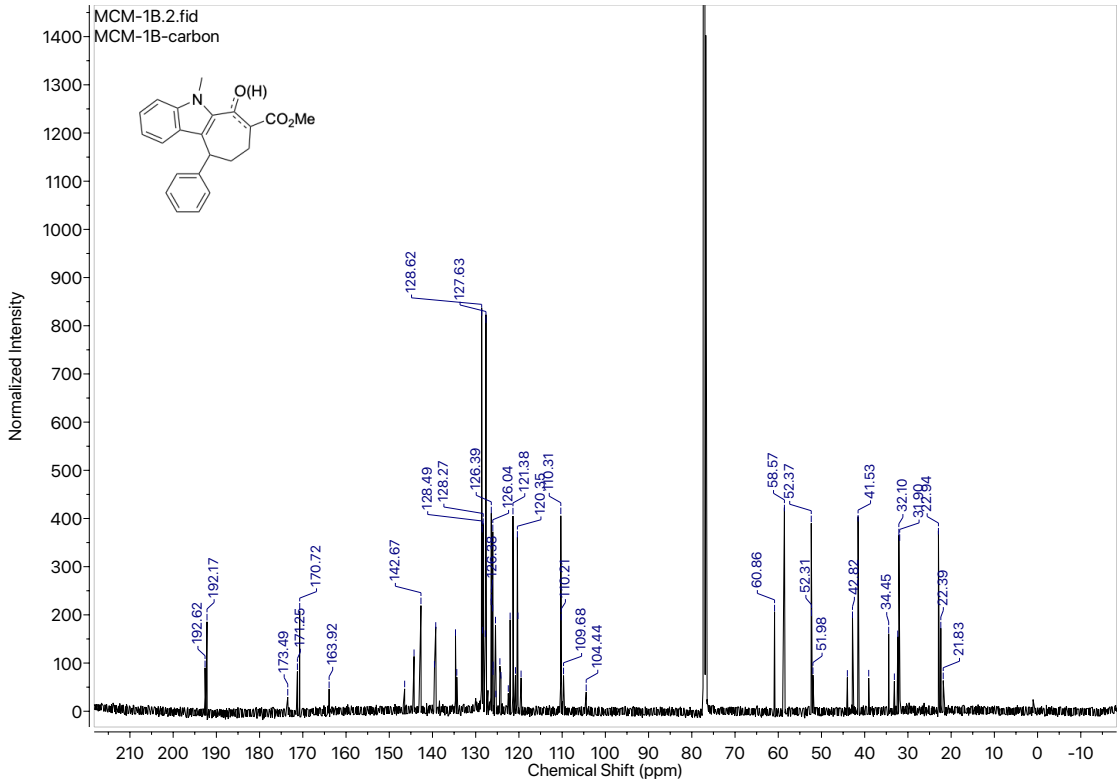
MCM-1B.2.fid
MCM-1B-carbon
O(H)
CO2Me
Normalized Intensity
Chemical Shift (ppm)
192.62
192.17
173.49
171.25
170.72
163.92
142.67
128.62
127.63
128.49
128.27
126.39
126.04
121.38
120.36
110.31
110.21
109.68
104.44
60.86
58.57
52.37
52.31
51.98
42.82
41.53
34.45
32.10
31.98
22.84
22.39
21.83

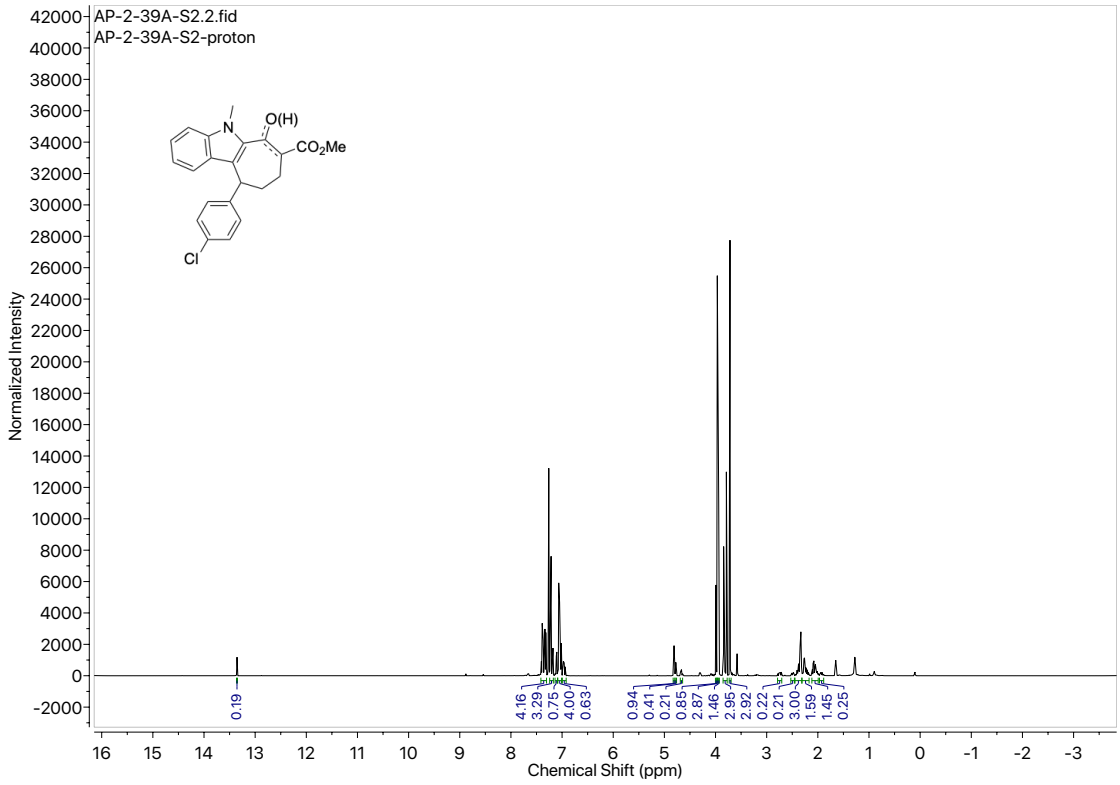
AP-2-39A-S2.2.fid
AP-2-39A-S2-proton
O(H)
CO2Me
Cl
Normalized Intensity
Chemical Shift (ppm)
0.19
4.16
3.29
0.75
4.00
0.63
0.94
0.41
0.21
0.85
2.87
1.46
2.95
2.92
0.22
0.21
3.00
1.59
1.45
0.25

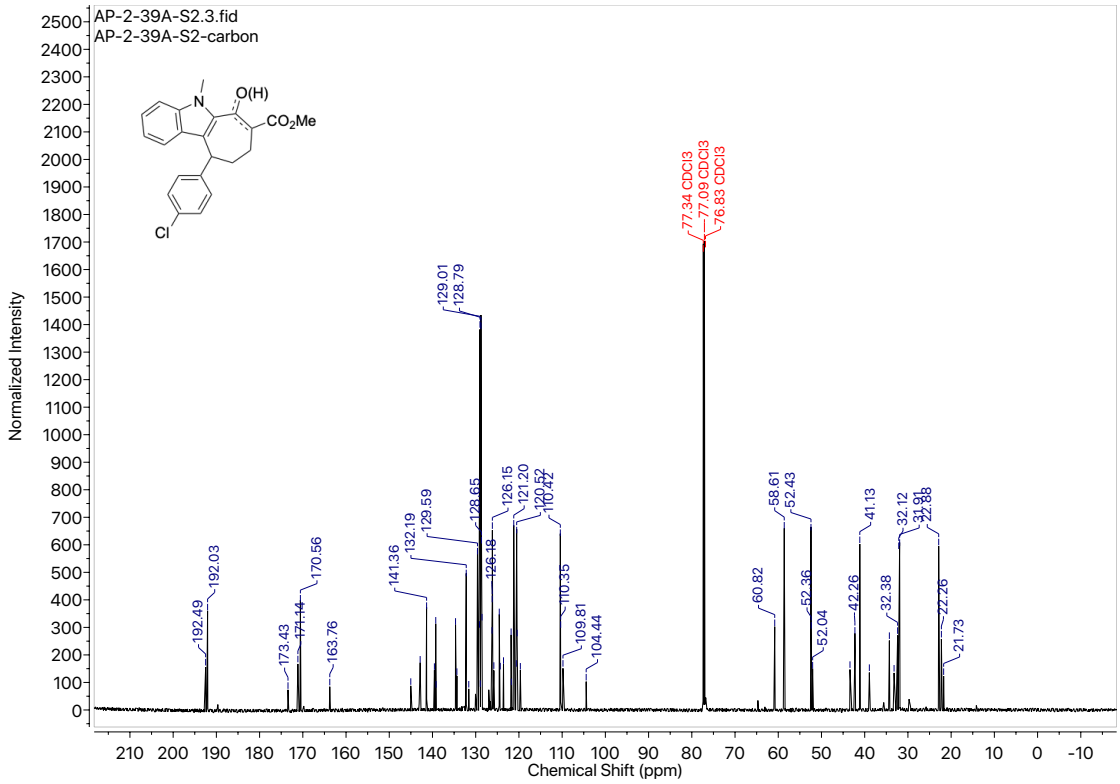
AP-2-39A-S2.3.fid
AP-2-39A-S2-carbon
O(H)
CO2Me
Cl
Normalized Intensity
Chemical Shift (ppm)
77.34 CDCl3
77.09 CDCl3
76.83 CDCl3
129.01
128.79
192.49
192.03
173.43
171.14
170.56
163.76
141.36
132.19
129.59
126.15
121.20
110.42
110.35
109.81
104.44
60.82
58.61
52.43
52.36
52.04
42.26
41.13
32.38
32.12
22.26
21.73

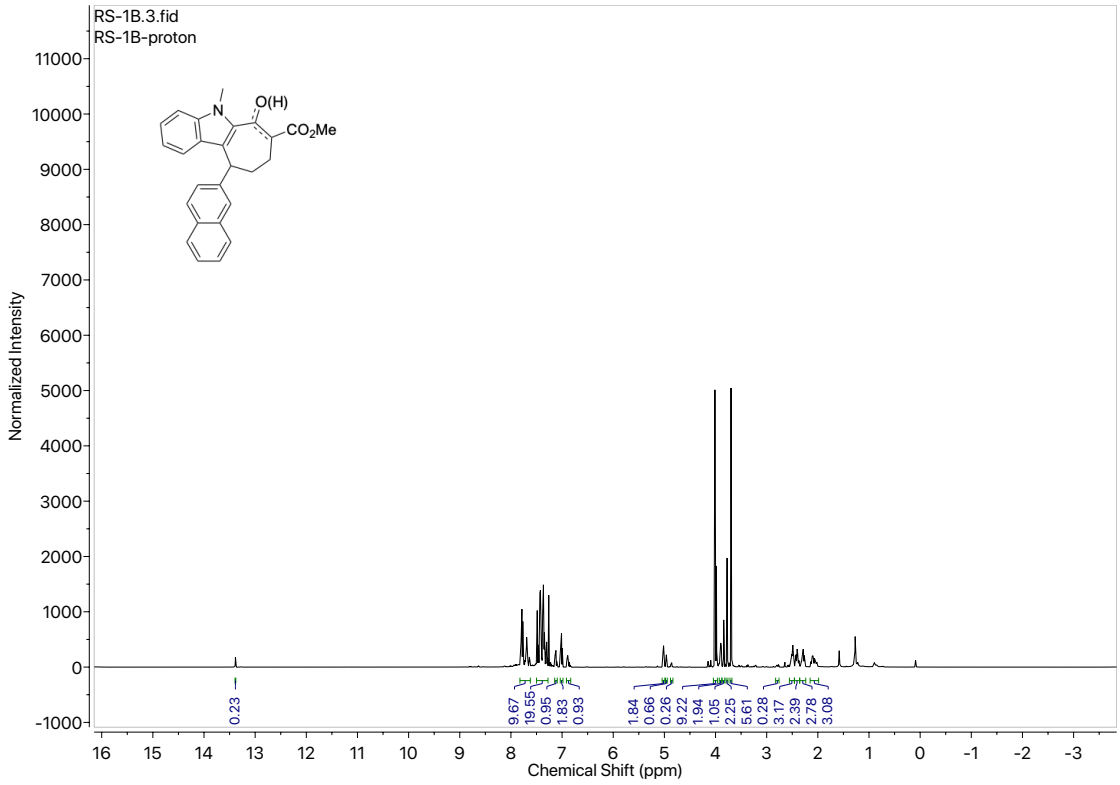
RS-1B.3.fid
RS-1B-proton
O(H)
CO2Me
Normalized Intensity
Chemical Shift (ppm)
0.23
9.67
19.55
0.95
1.83
0.93
1.84
0.66
0.26
9.22
1.94
1.05
2.25
5.61
0.28
3.17
2.39
2.78
3.08

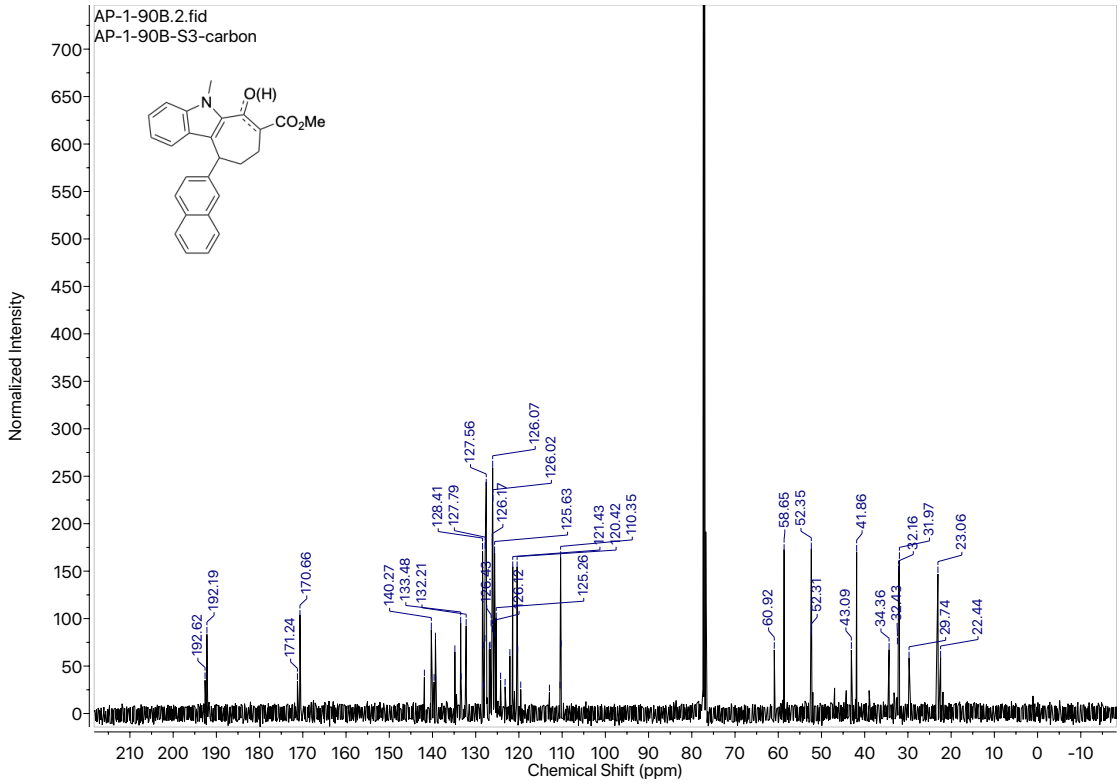
AP-1-90B.2.fid
AP-1-90B-S3-carbon
O(H)
CO2Me
Normalized Intensity
Chemical Shift (ppm)
192.62
192.19
171.24
170.66
140.27
133.48
132.21
128.41
127.79
127.56
126.17
126.07
126.02
125.63
125.26
121.43
120.42
110.35
60.92
58.65
52.35
52.31
43.09
41.86
34.36
32.43
32.16
31.97
29.74
23.06
22.44

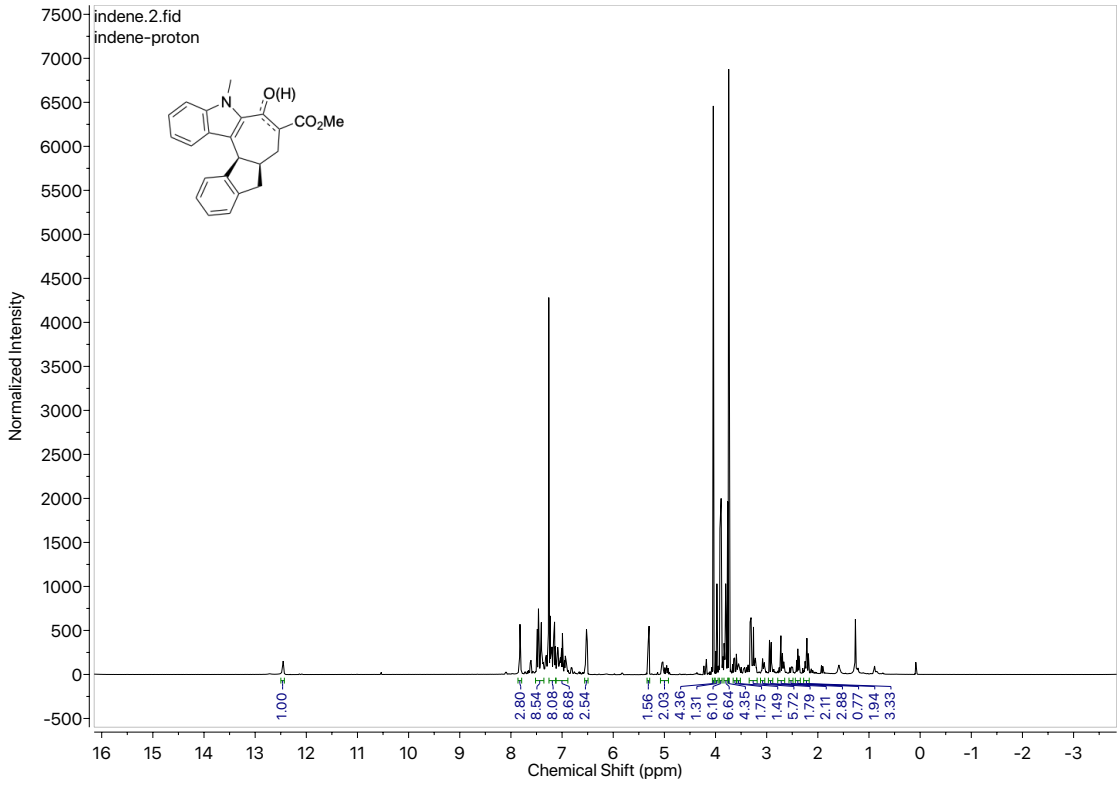
indene.2.fid
indene-proton
O(H)
CO2Me
Normalized Intensity
Chemical Shift (ppm)
1.00
2.80
8.54
8.08
8.68
2.54
1.56
2.03
4.36
1.31
6.10
6.64
4.35
1.75
1.49
5.72
1.79
2.11
2.88
0.77
1.94
3.33

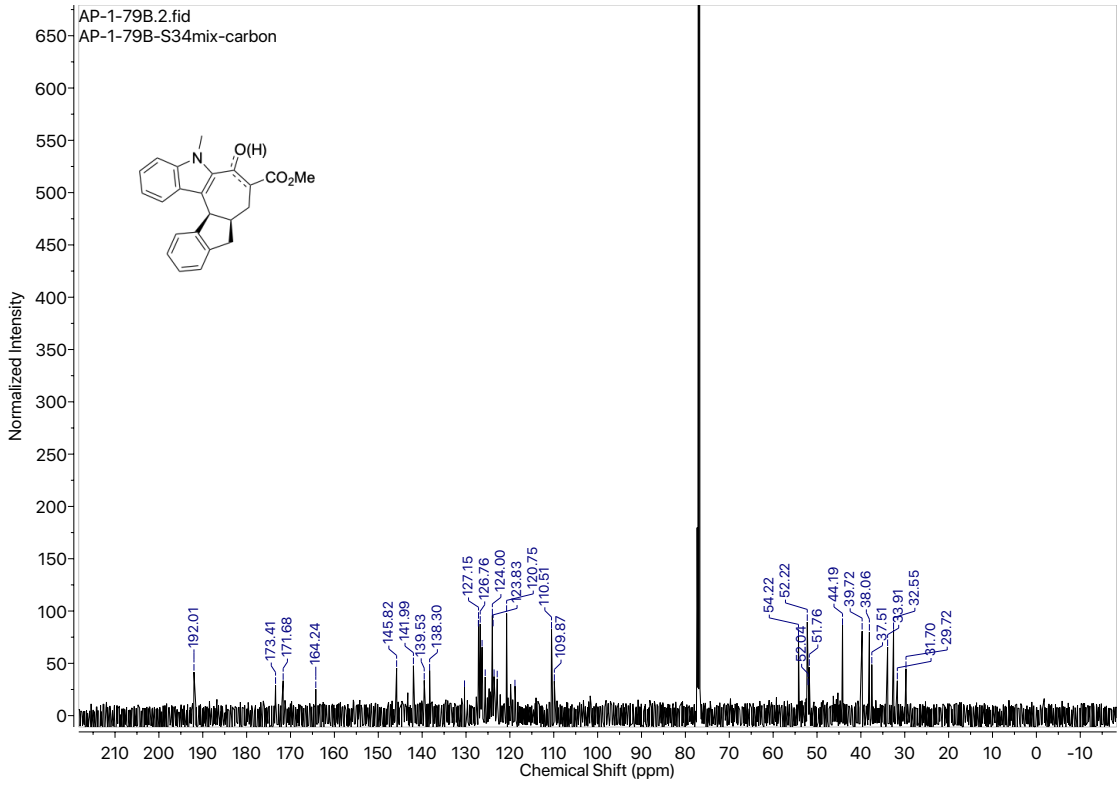
AP-1-79B.2.fid
AP-1-79B-S34mix-carbon
O(H)
CO2Me
Normalized Intensity
Chemical Shift (ppm)
192.01
173.41
171.68
164.24
145.82
141.99
139.53
138.30
127.15
126.76
124.00
123.83
120.75
110.51
109.87
54.22
52.22
52.04
51.76
44.19
39.72
38.06
37.51
33.91
32.55
31.70
29.72

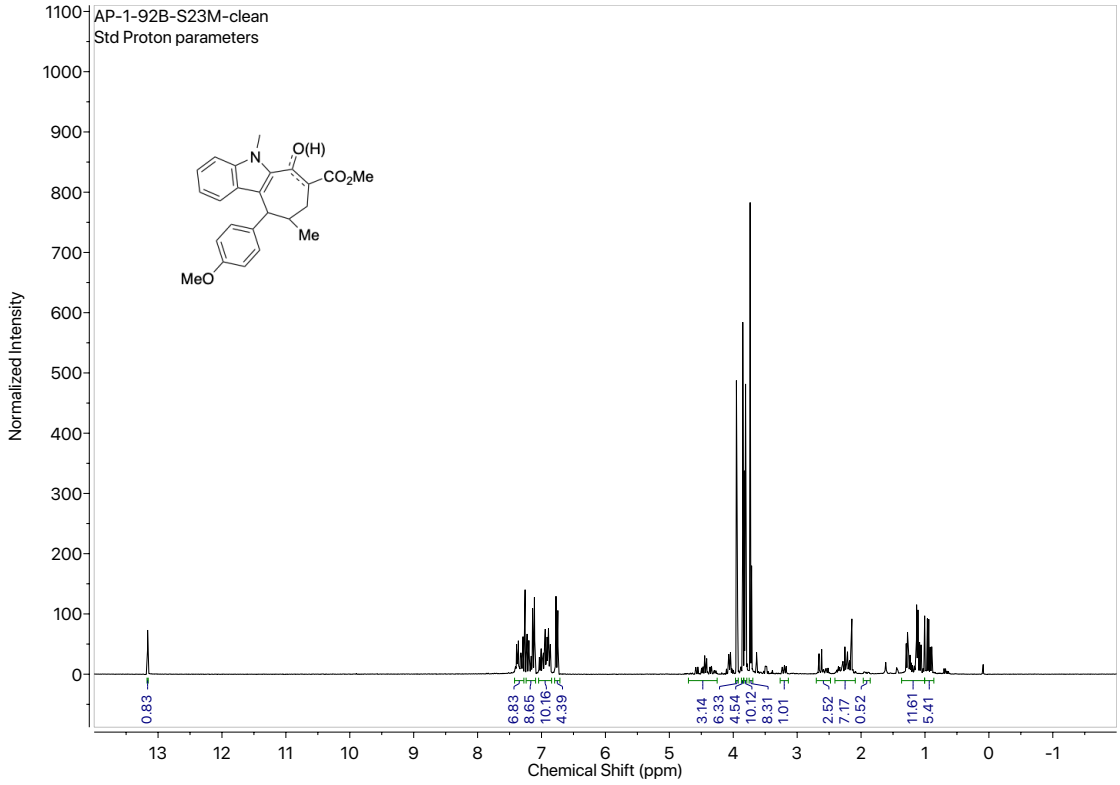
AP-1-92B-S23M-clean
Std Proton parameters
O(H)
CO2Me
Me
MeO
Normalized Intensity
Chemical Shift (ppm)
0.83
6.83
8.65
10.16
4.39
3.14
6.33
4.54
10.12
8.31
1.01
2.52
7.17
0.52
11.61
5.41

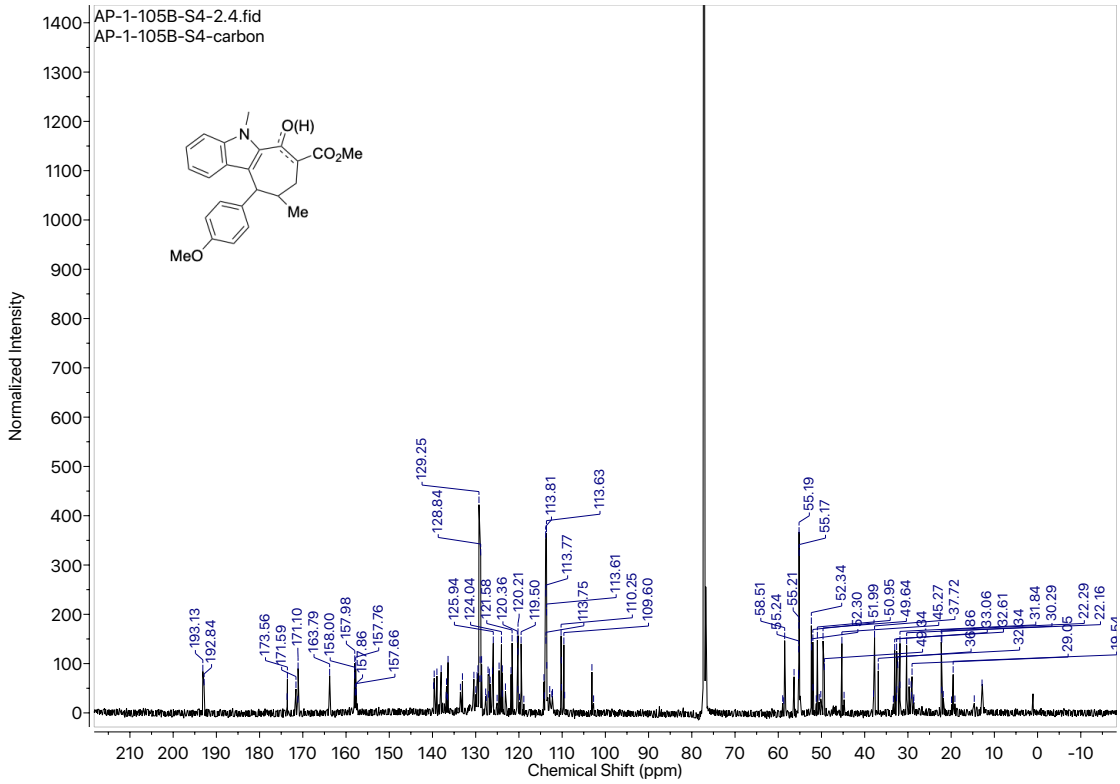
AP-1-105B-S4-2.4.fid
AP-1-105B-S4-carbon
O(H)
CO2Me
Me
MeO
Normalized Intensity
Chemical Shift (ppm)
193.13
192.84
173.56
171.59
171.10
163.79
158.00
157.98
157.86
157.76
157.66
129.25
128.84
125.94
124.04
121.58
120.36
120.21
119.50
113.81
113.63
113.77
113.75
113.61
110.25
109.60
58.51
55.24
55.21
55.19
55.17
52.34
52.30
51.99
50.95
49.64
45.27
37.72
33.06
32.61
31.84
30.29
29.05
22.29
22.16

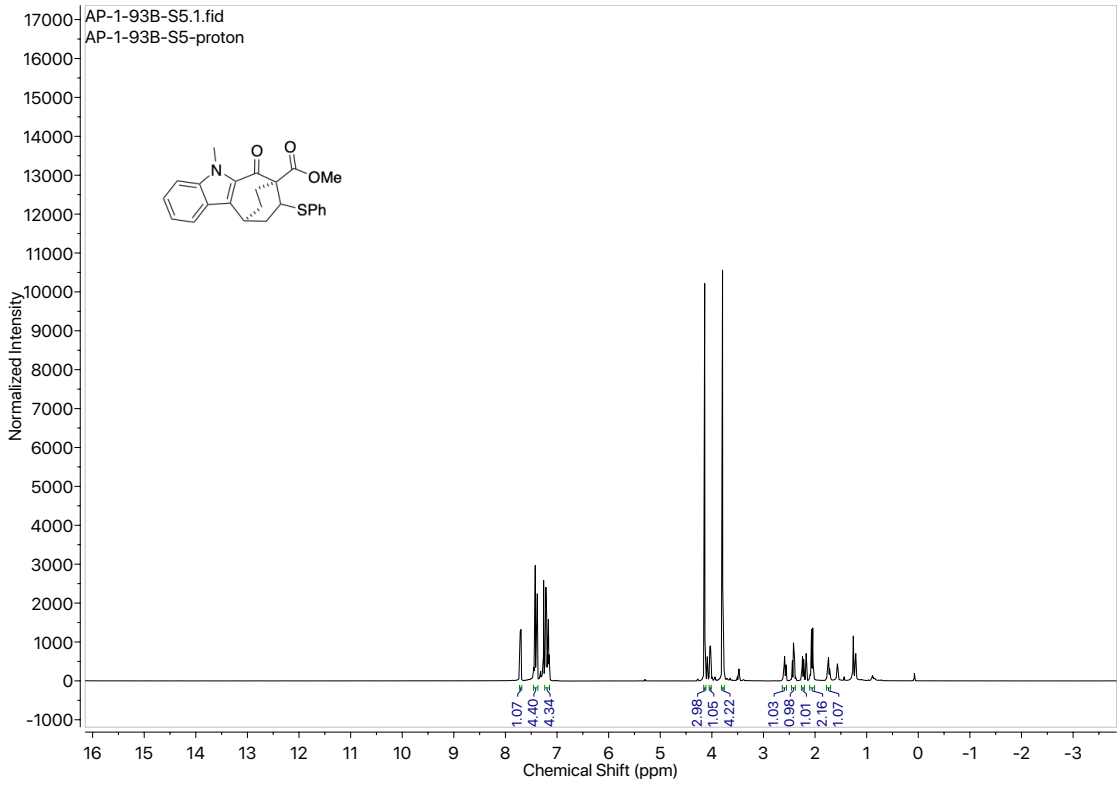
AP-1-93B-S5.1.fid
AP-1-93B-S5-proton
Normalized Intensity
Chemical Shift (ppm)
1.07
4.40
4.34
2.98
1.05
4.22
1.03
0.98
1.01
2.16
1.07
OMe
SPh

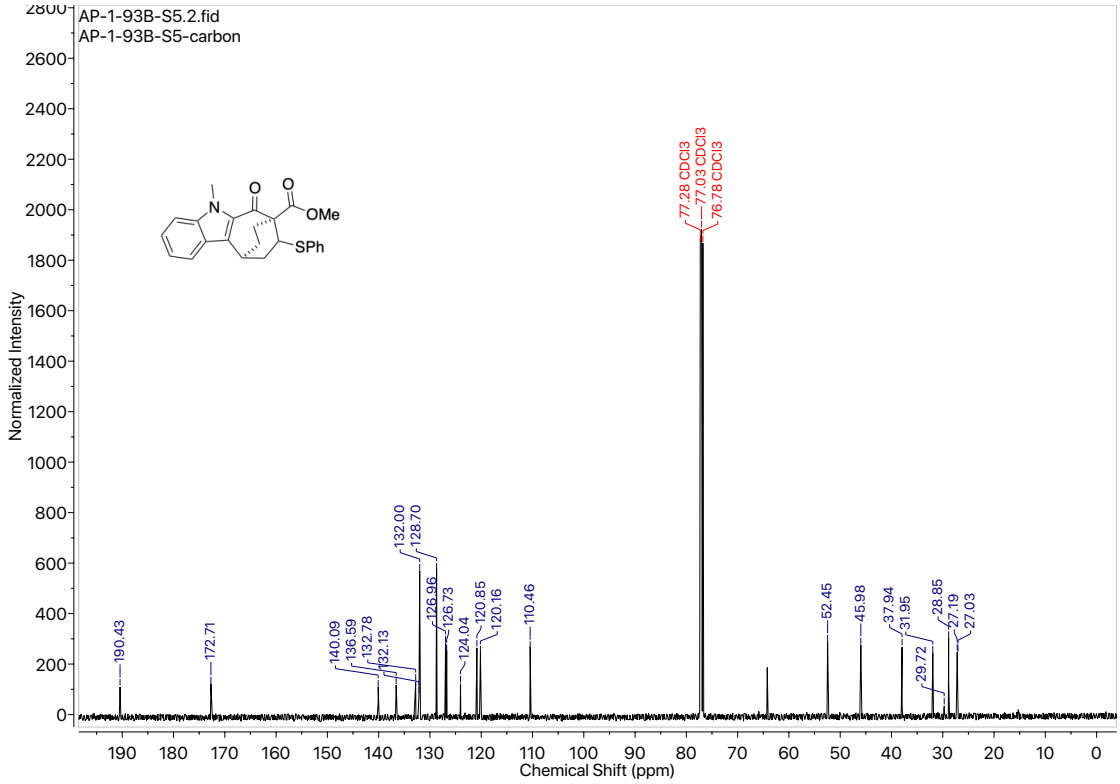
AP-1-93B-S5.2.fid
AP-1-93B-S5-carbon
Normalized Intensity
Chemical Shift (ppm)
77.28 CDCl3
77.03 CDCl3
76.78 CDCl3
190.43
172.71
140.09
136.59
132.78
132.13
132.00
128.70
126.96
126.73
124.04
120.85
120.16
110.46
52.45
45.98
37.94
31.95
29.72
28.85
27.19
27.03
OMe
SPh

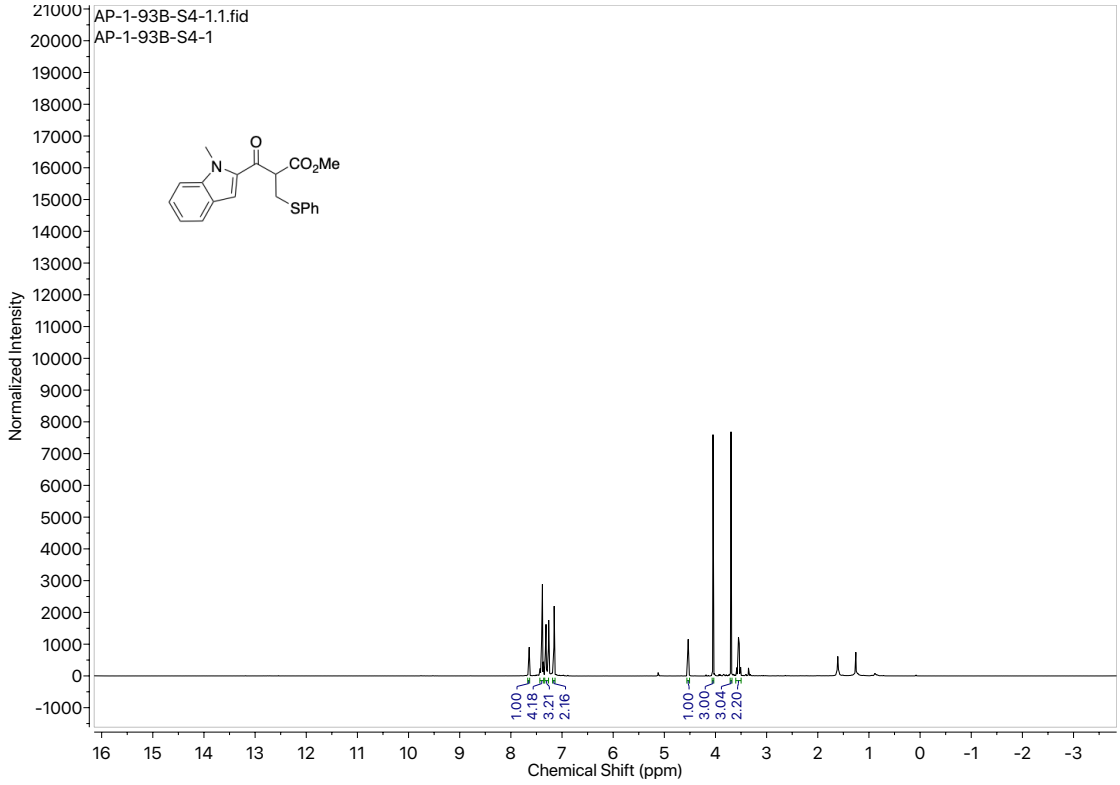
AP-1-93B-S4-1.1.fid
AP-1-93B-S4-1
O
N
CO2Me
SPh
Normalized Intensity
1.00
4.18
3.21
2.16
1.00
3.00
3.04
2.20
Chemical Shift (ppm)

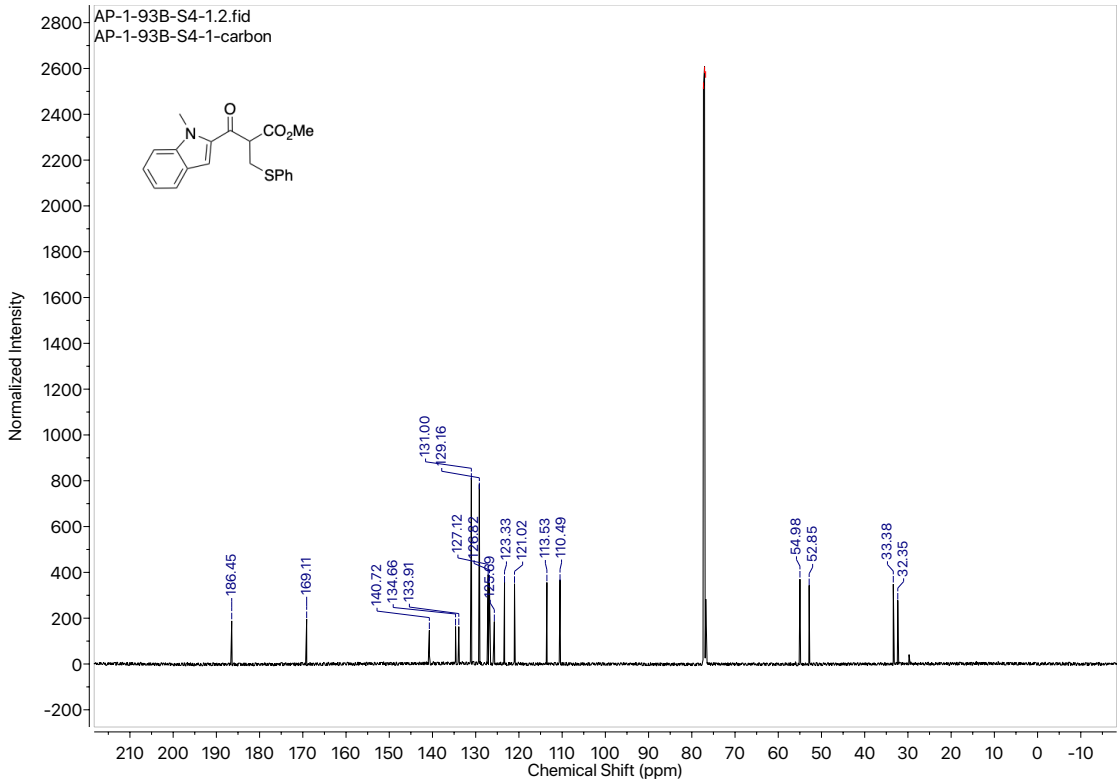
AP-1-93B-S4-1.2.fid
AP-1-93B-S4-1-carbon
O
N
CO2Me
SPh
Normalized Intensity
186.45
169.11
140.72
134.66
133.91
131.00
129.16
127.12
126.82
125.69
123.33
121.02
113.53
110.49
54.98
52.85
33.38
32.35
Chemical Shift (ppm)

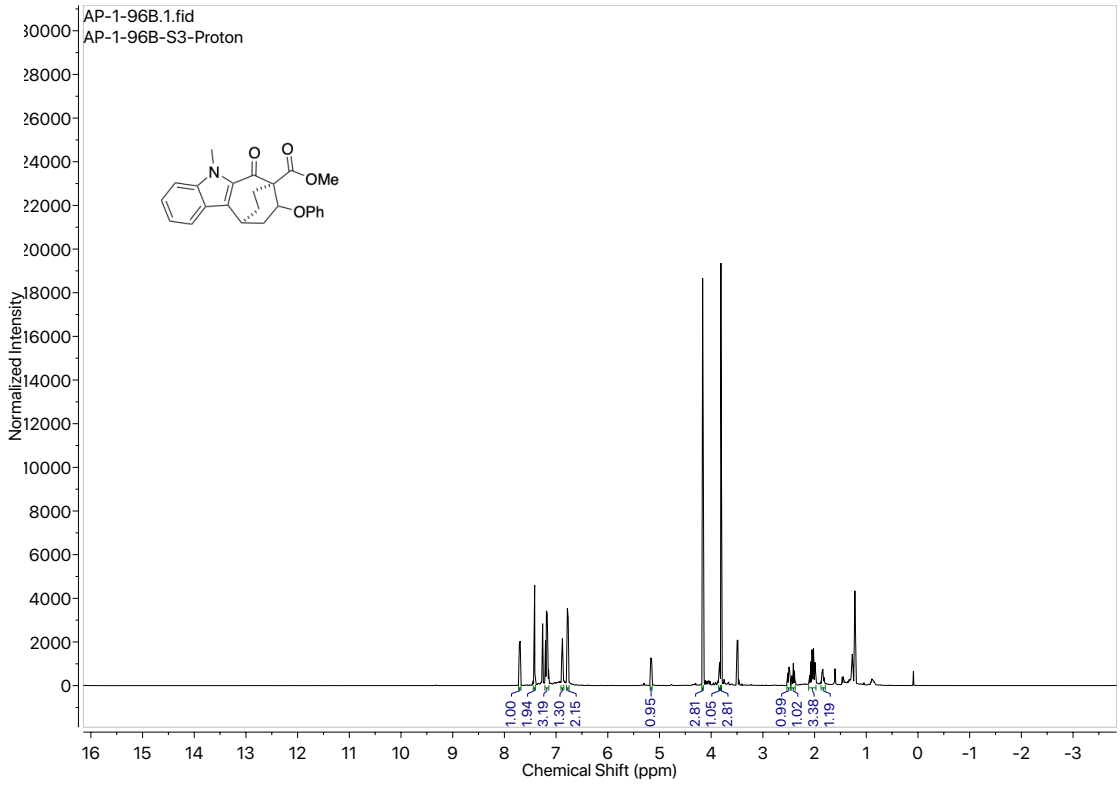
AP-1-96B.1.fid
AP-1-96B-S3-Proton
OMe
OPh
Normalized Intensity
Chemical Shift (ppm)
1.00
1.94
3.19
1.30
2.15
0.95
2.81
1.05
2.81
0.99
1.02
3.38
1.19

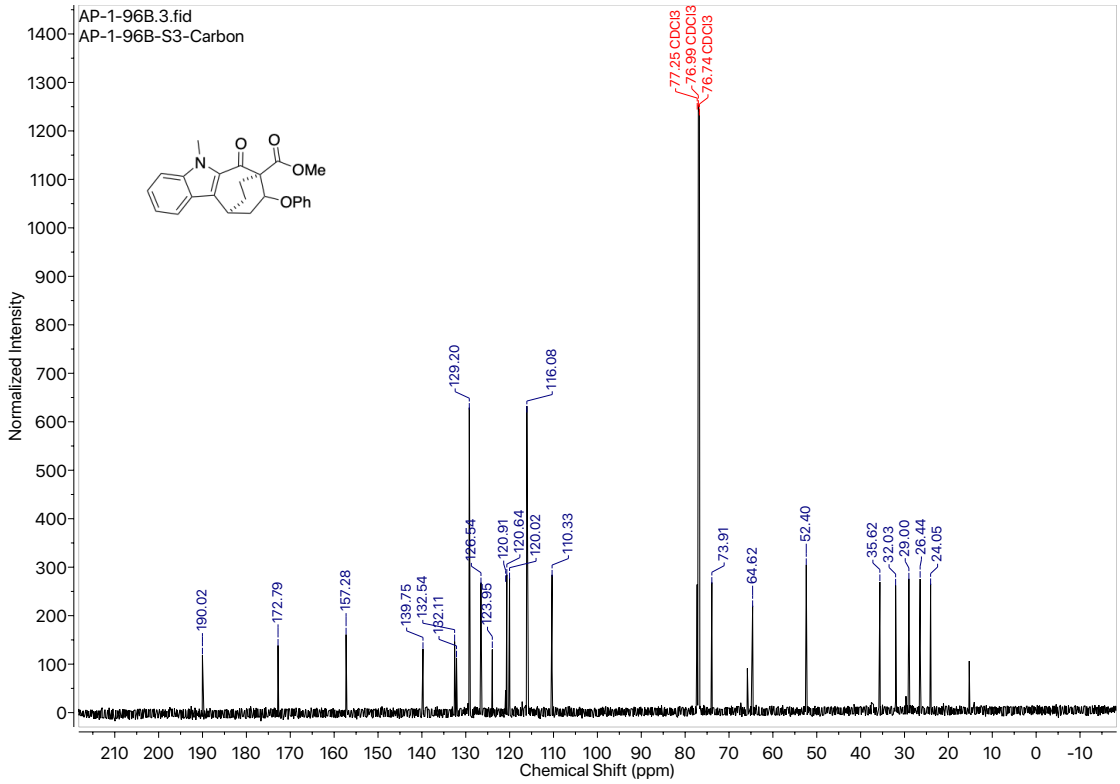
AP-1-96B.3.fid
AP-1-96B-S3-Carbon
OMe
OPh
Normalized Intensity
Chemical Shift (ppm)
77.25 CDCl3
76.99 CDCl3
76.74 CDCl3
190.02
172.79
157.28
139.75
132.54
132.11
129.20
128.54
123.95
120.91
120.64
120.02
116.08
110.33
73.91
64.62
52.40
35.62
32.03
29.00
26.44
24.05

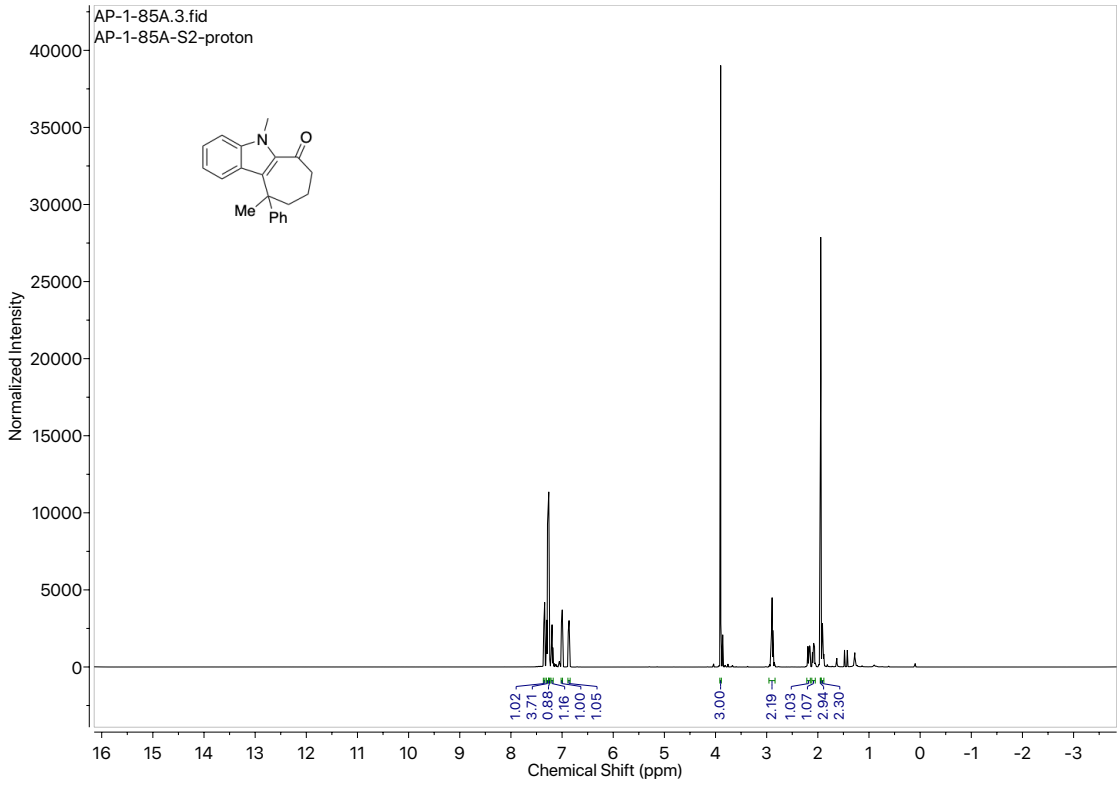
AP-1-85A.3.fid
AP-1-85A-S2-proton
Normalized Intensity
Chemical Shift (ppm)
1.02
3.71
0.88
1.16
1.00
1.05
3.00
2.19
1.03
1.07
2.94
2.30

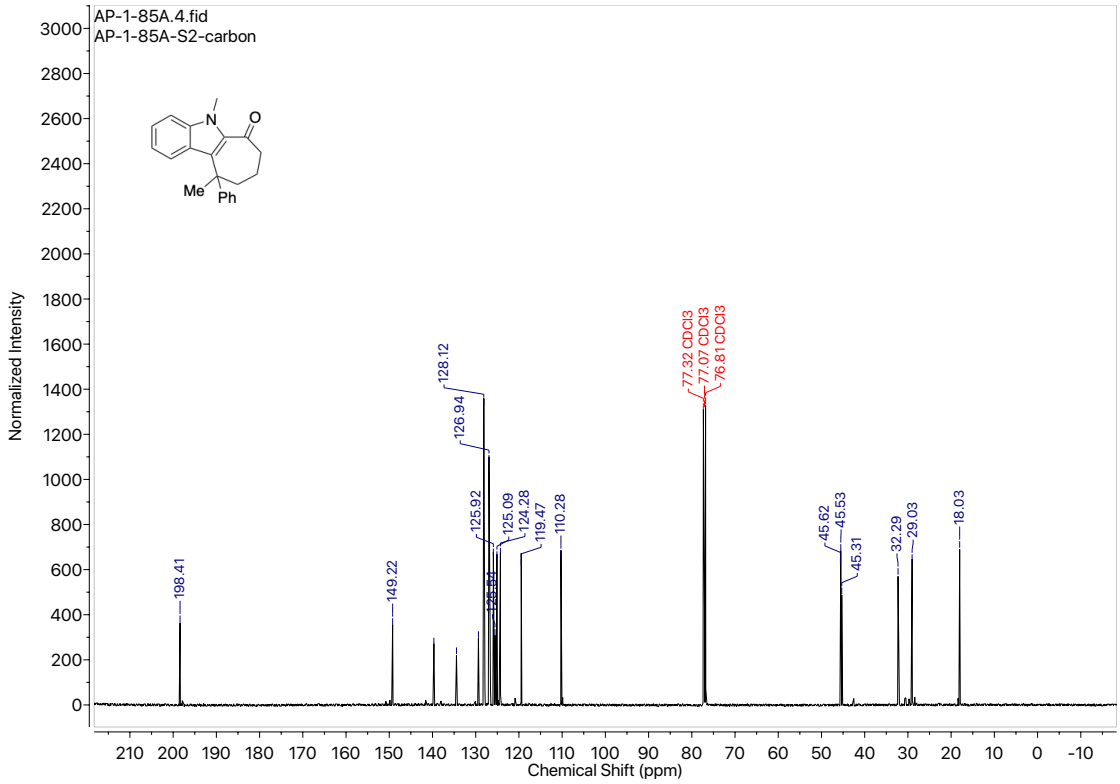
AP-1-85A.4.fid
AP-1-85A-S2-carbon
Normalized Intensity
Chemical Shift (ppm)
198.41
149.22
128.12
126.94
125.92
125.09
124.28
119.47
110.28
77.32 CDCl3
77.07 CDCl3
76.81 CDCl3
45.62
45.53
45.31
32.29
29.03
18.03

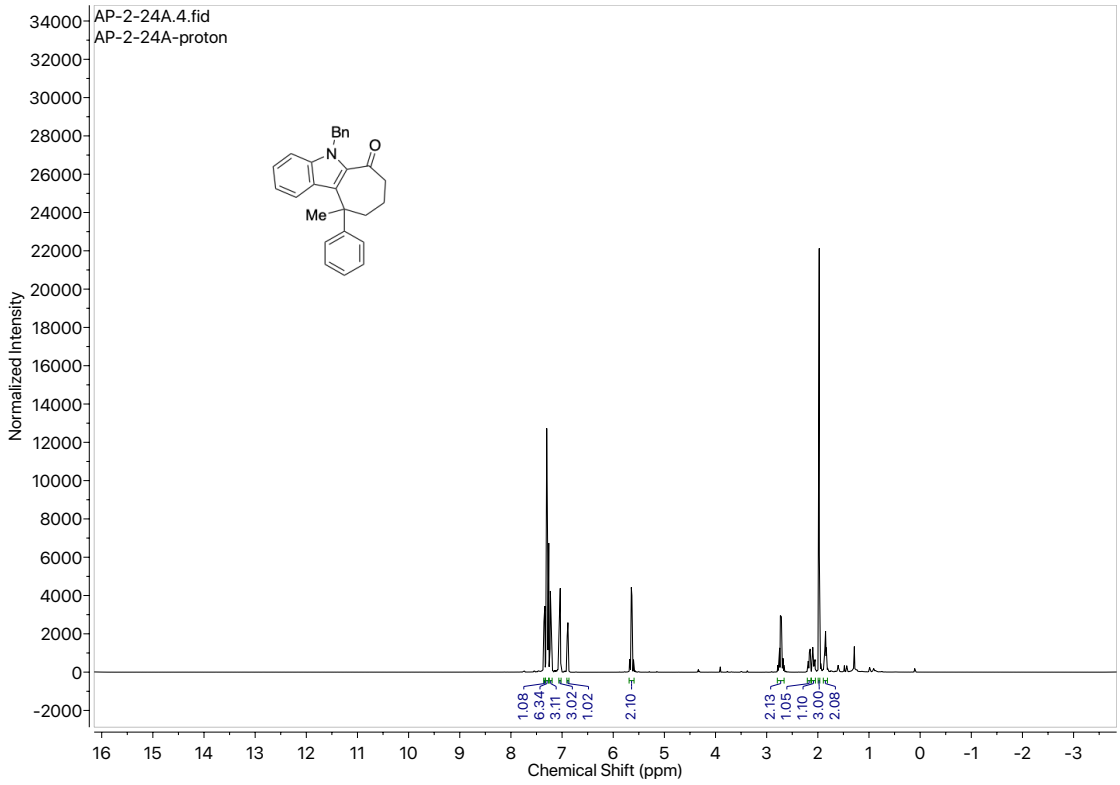
AP-2-24A.4.fid
AP-2-24A-proton
Bn
N
O
Me
Normalized Intensity
1.08
6.34
3.11
3.02
1.02
2.10
2.13
1.05
1.10
3.00
2.08
Chemical Shift (ppm)

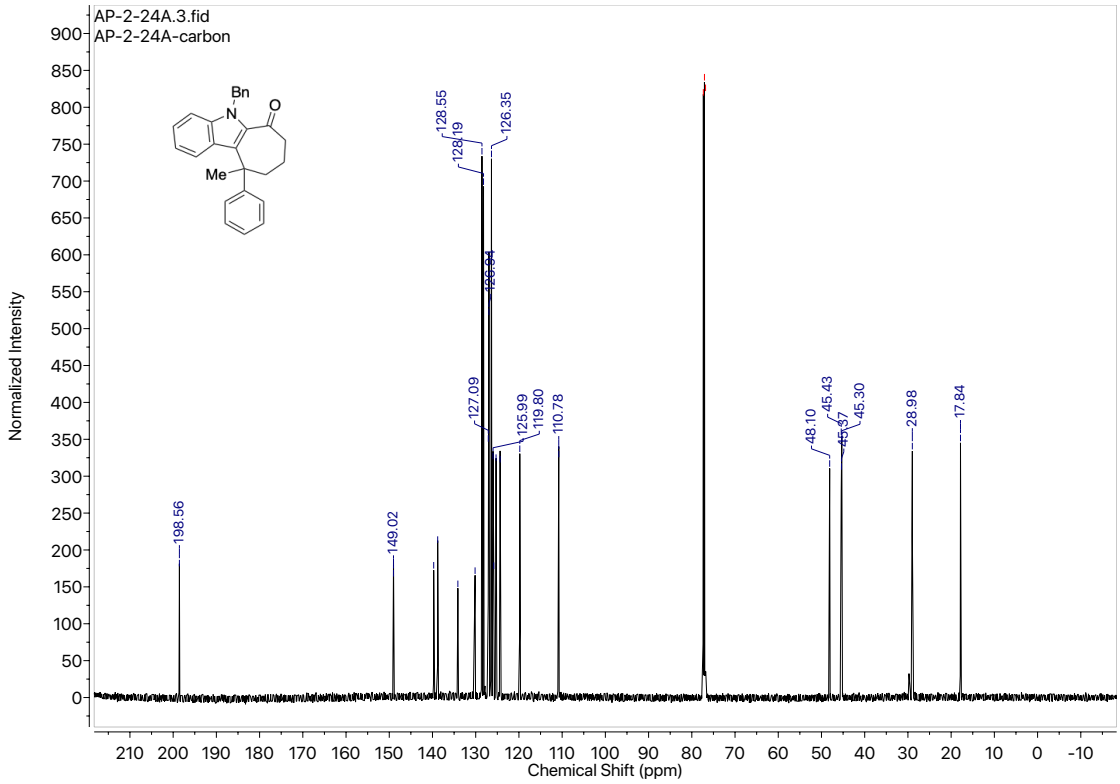
AP-2-24A.3.fid
AP-2-24A-carbon
Bn
N
O
Me
198.56
149.02
128.55
128.19
126.35
127.09
125.99
119.80
110.78
48.10
45.43
45.37
45.30
28.98
17.84
Normalized Intensity
Chemical Shift (ppm)

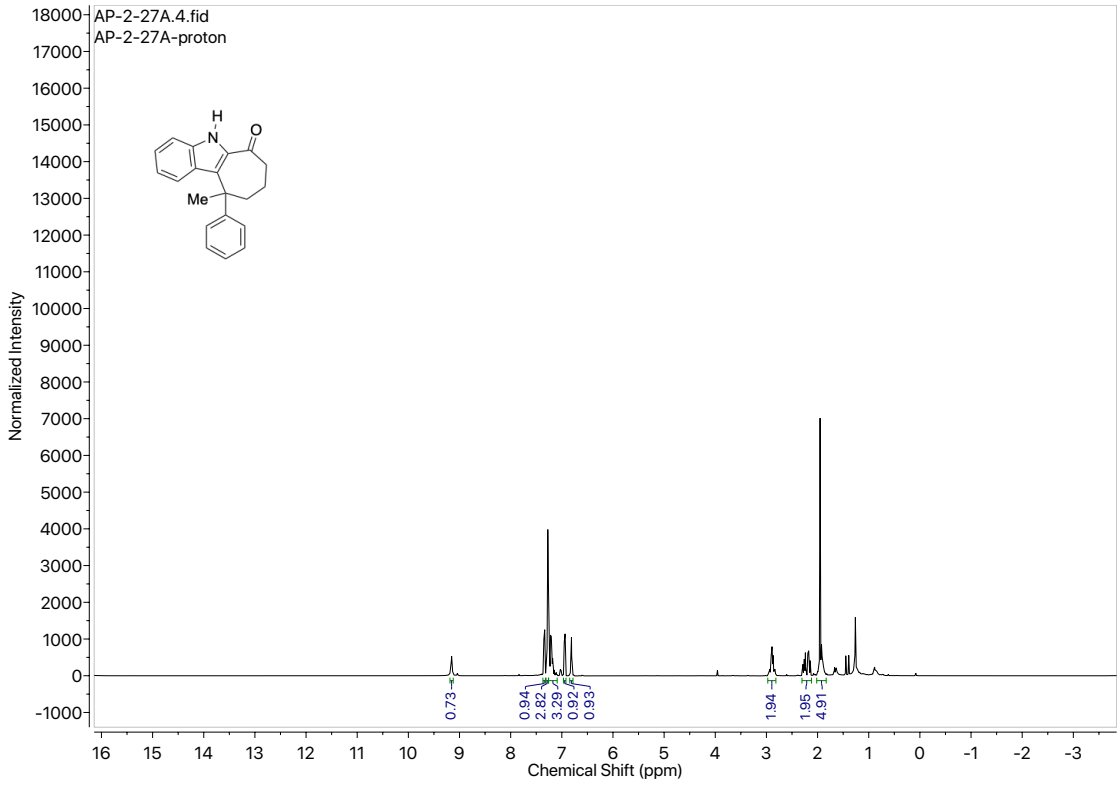
AP-2-27A.4.fid
AP-2-27A-proton
Normalized Intensity
Chemical Shift (ppm)
0.73
0.94
2.82
3.29
0.92
0.93
1.94
1.95
4.91

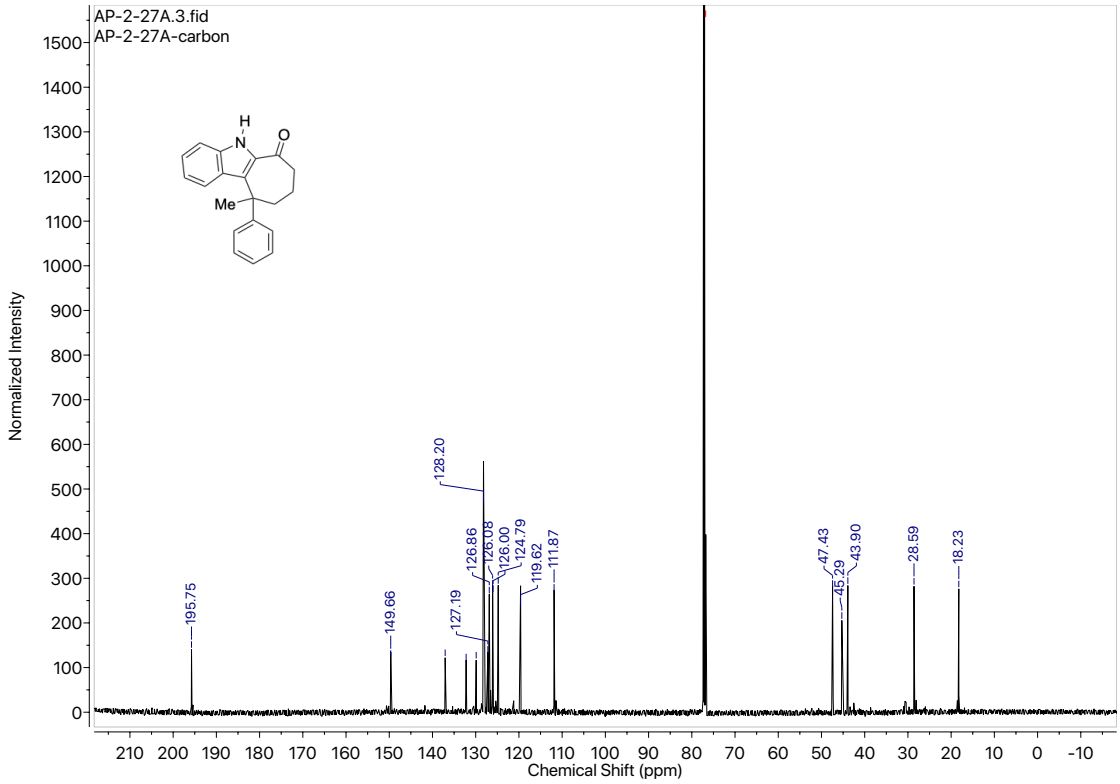
AP-2-27A.3.fid
AP-2-27A-carbon
Normalized Intensity
Chemical Shift (ppm)
195.75
149.66
128.20
127.19
126.86
126.08
126.00
124.79
119.62
111.87
47.43
45.29
43.90
28.59
18.23

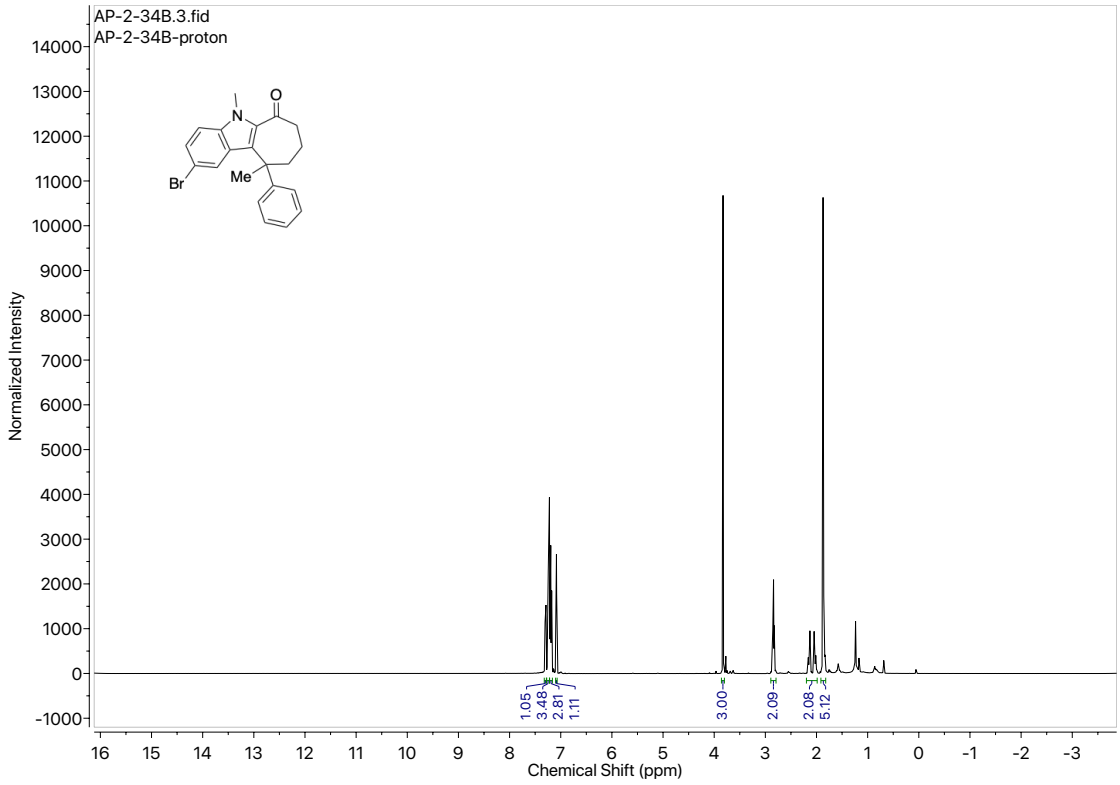
AP-2-34B.3.fid
AP-2-34B-proton
Normalized Intensity
Chemical Shift (ppm)
1.05
3.48
2.81
1.11
3.00
2.09
2.08
5.12

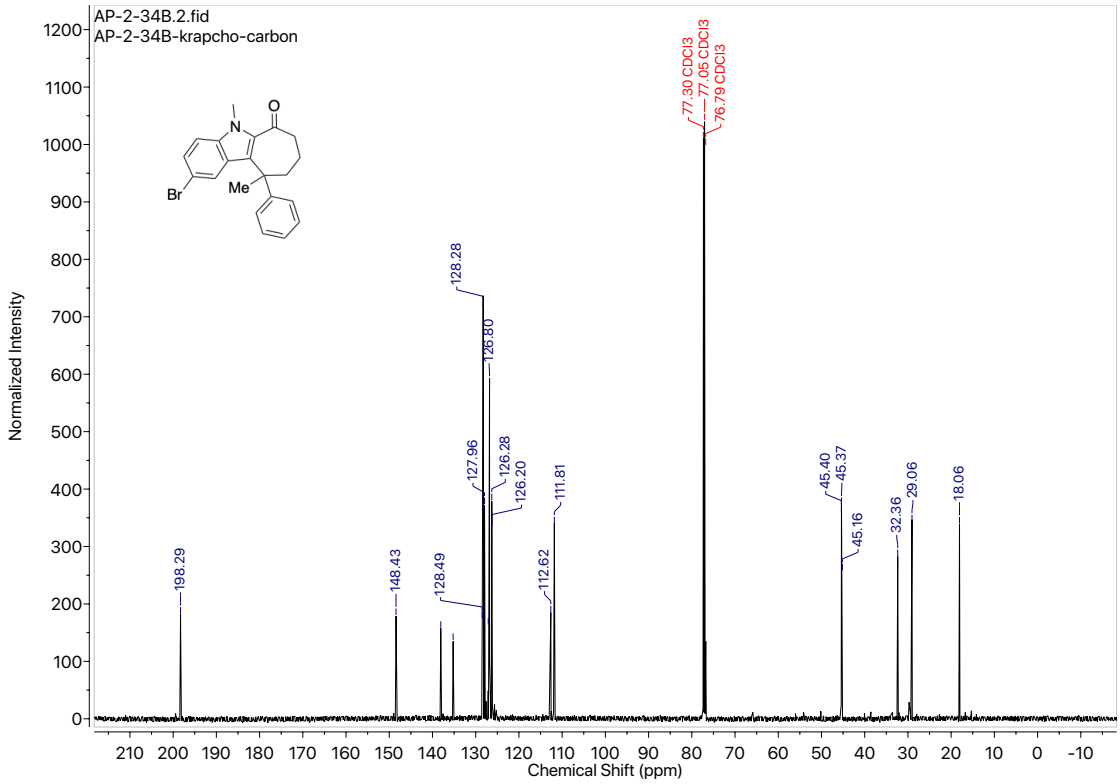
AP-2-34B.2.fid
AP-2-34B-krapcho-carbon
Normalized Intensity
Chemical Shift (ppm)
77.30 CDCl3
77.05 CDCl3
76.79 CDCl3
198.29
148.43
128.49
128.28
126.80
127.96
126.28
126.20
112.62
111.81
45.40
45.37
45.16
32.36
29.06
18.06

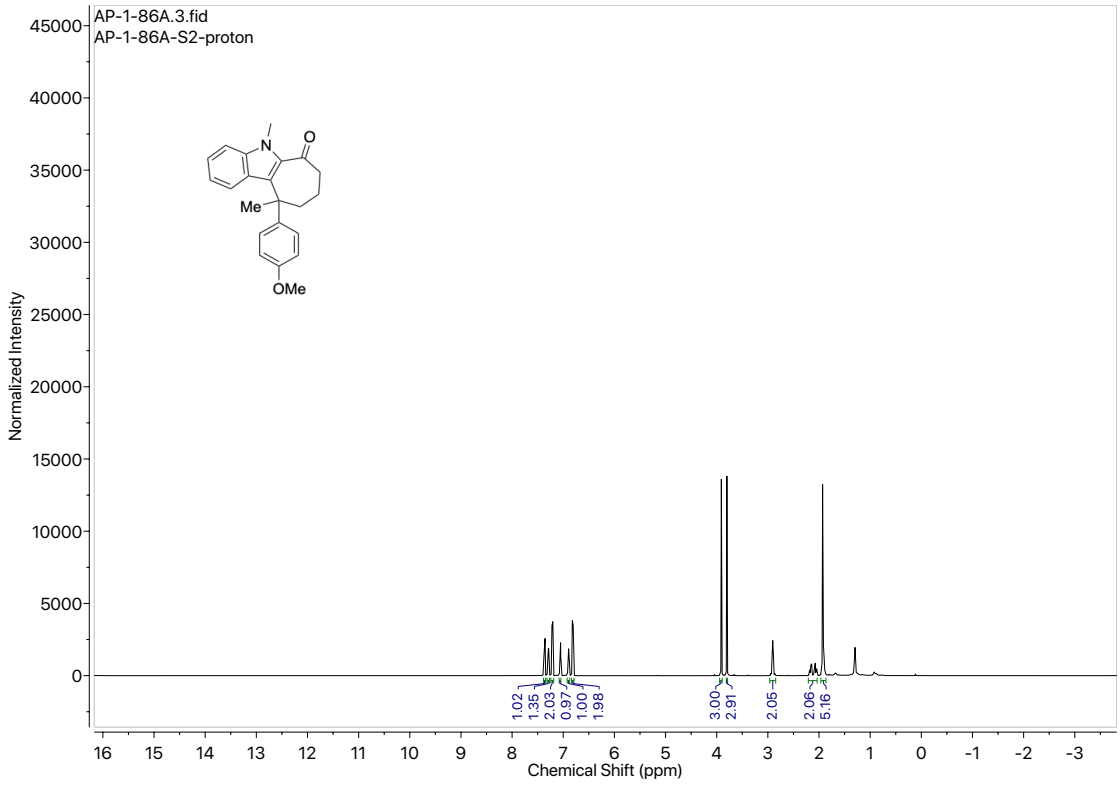
AP-1-86A.3.fid
AP-1-86A-S2-proton
Normalized Intensity
Chemical Shift (ppm)
1.02
1.35
2.03
0.97
1.00
1.98
3.00
2.91
2.05
2.06
5.16

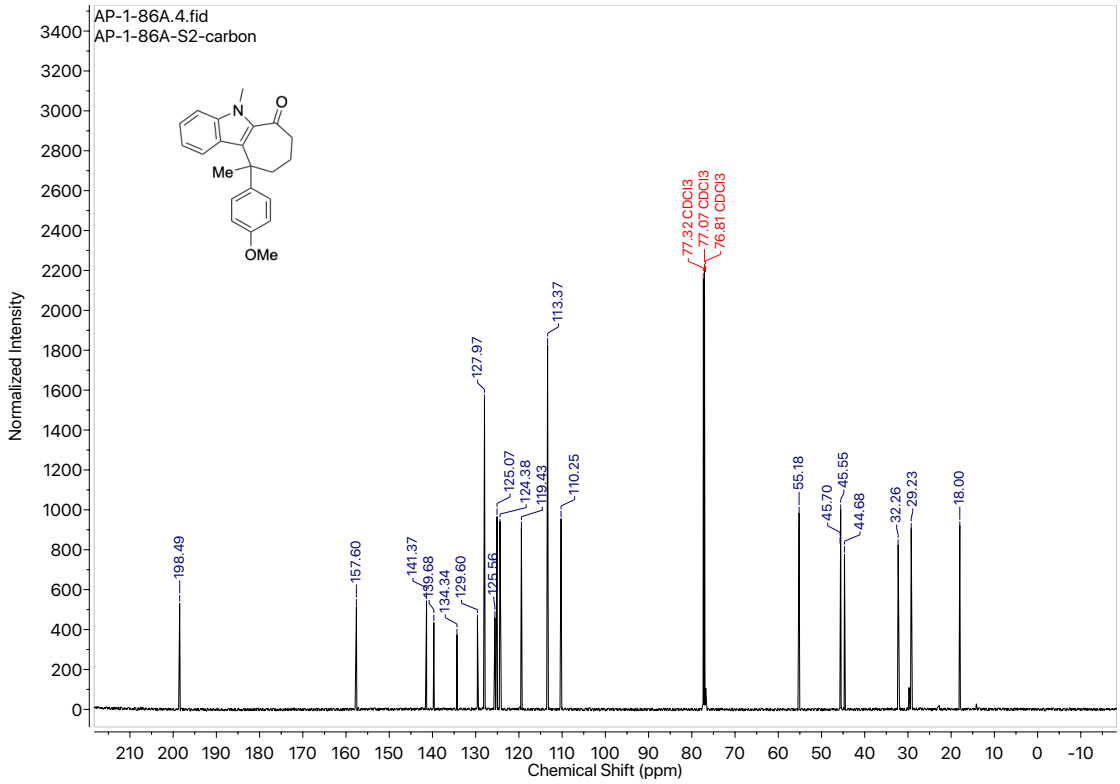
AP-1-86A.4.fid
AP-1-86A-S2-carbon
Normalized Intensity
Chemical Shift (ppm)
77.32 CDCl3
77.07 CDCl3
76.81 CDCl3
198.49
157.60
141.37
139.68
134.34
129.60
125.56
127.97
125.07
124.38
119.43
113.37
110.25
55.18
45.70
45.55
44.68
32.26
29.23
18.00

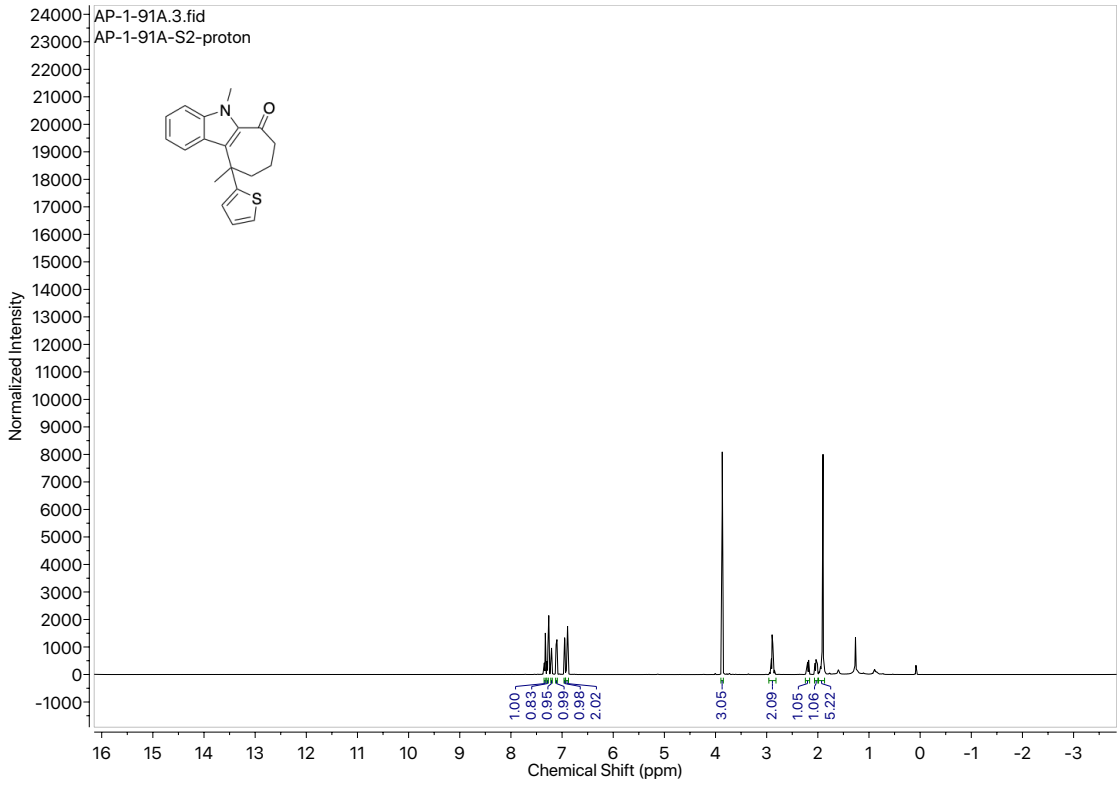
AP-1-91A.3.fid
AP-1-91A-S2-proton
Normalized Intensity
Chemical Shift (ppm)
1.00
0.83
0.95
0.99
0.98
2.02
3.05
2.09
1.05
1.06
5.22

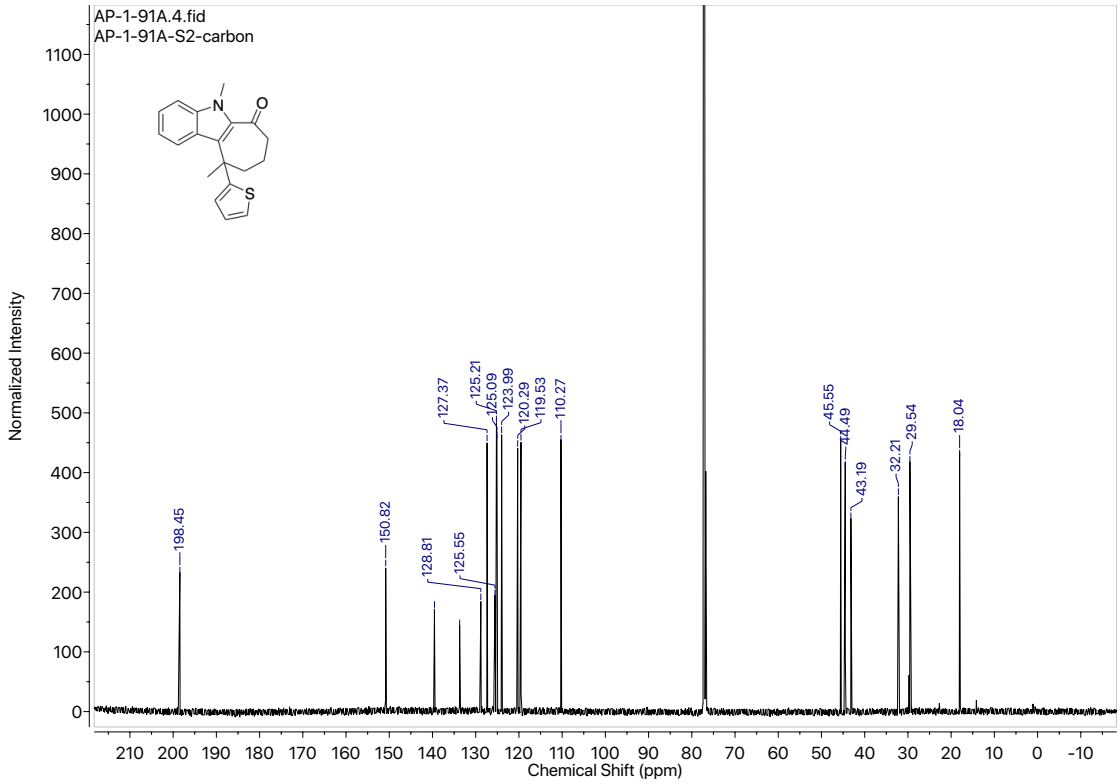
AP-1-91A.4.fid
AP-1-91A-S2-carbon
Normalized Intensity
Chemical Shift (ppm)
198.45
150.82
128.81
125.55
127.37
125.21
125.09
123.99
120.29
119.53
110.27
45.55
44.49
43.19
32.21
29.54
18.04

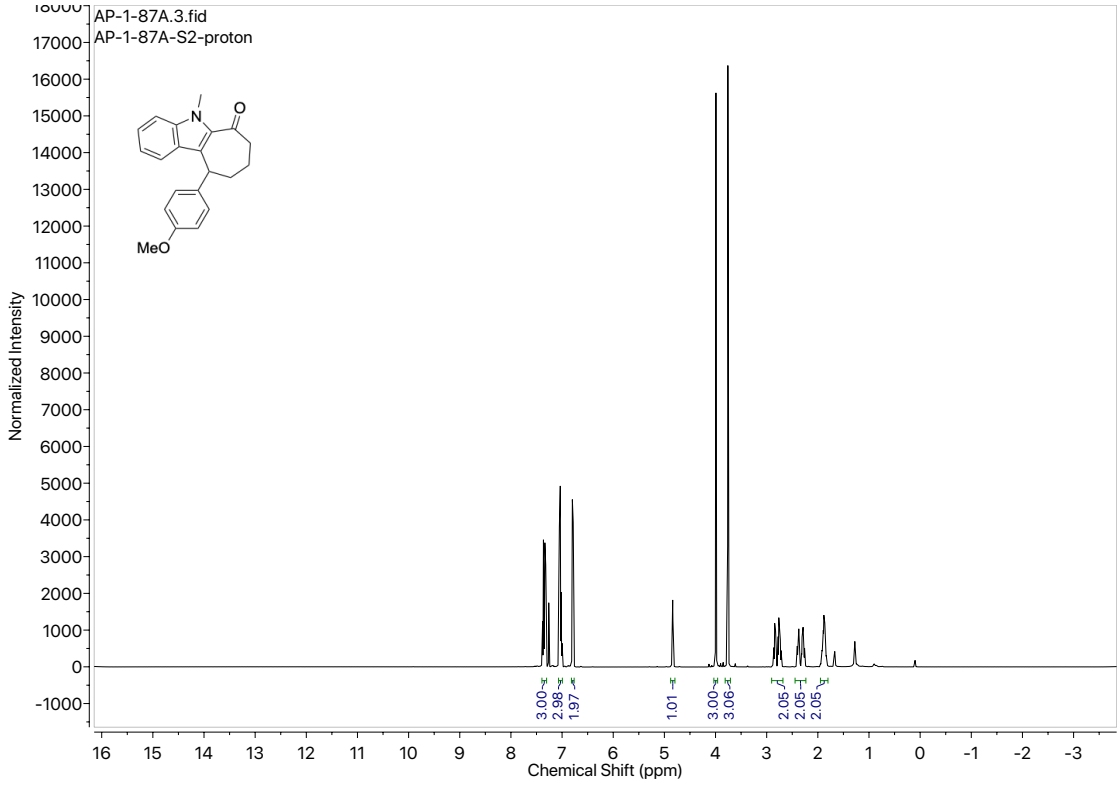
AP-1-87A.3.fid
AP-1-87A-S2-proton
MeO
Normalized Intensity
Chemical Shift (ppm)
3.00
2.98
1.97
1.01
3.00
3.06
2.05
2.05
2.05

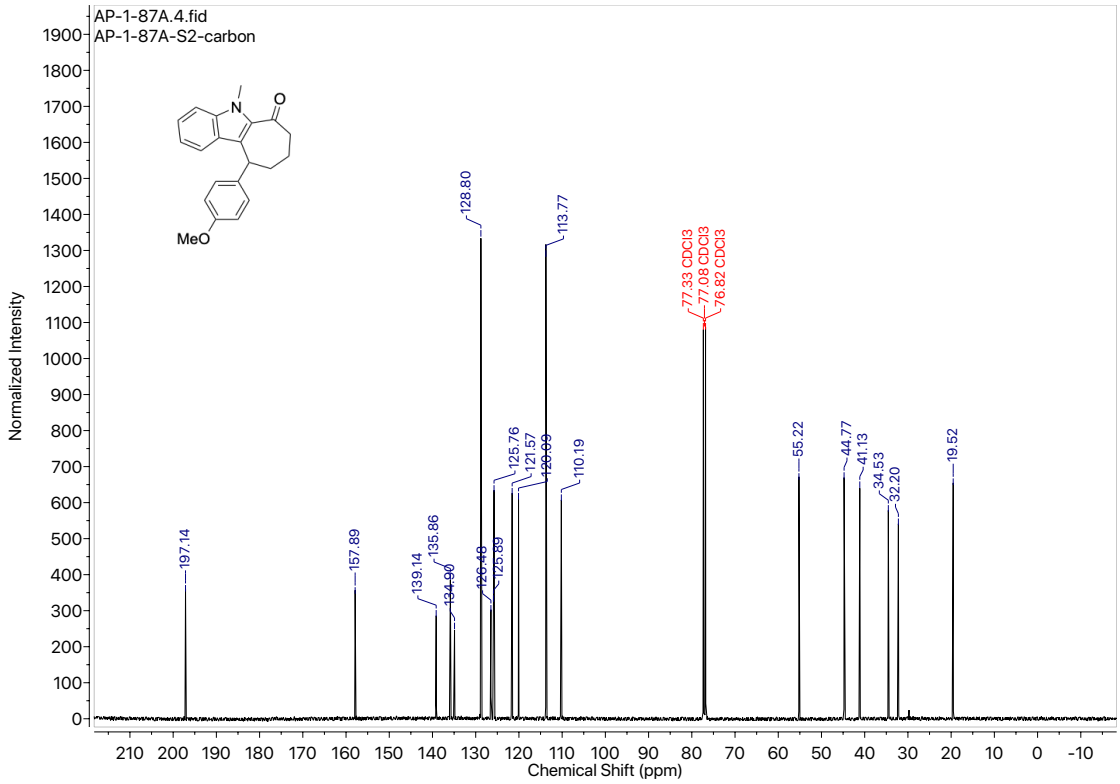
AP-1-87A.4.fid
AP-1-87A-S2-carbon
MeO
Normalized Intensity
Chemical Shift (ppm)
197.14
157.89
139.14
135.86
128.80
126.48
125.89
125.76
121.57
120.99
113.77
110.19
77.33 CDCl3
77.08 CDCl3
76.82 CDCl3
55.22
44.77
41.13
34.53
32.20
19.52

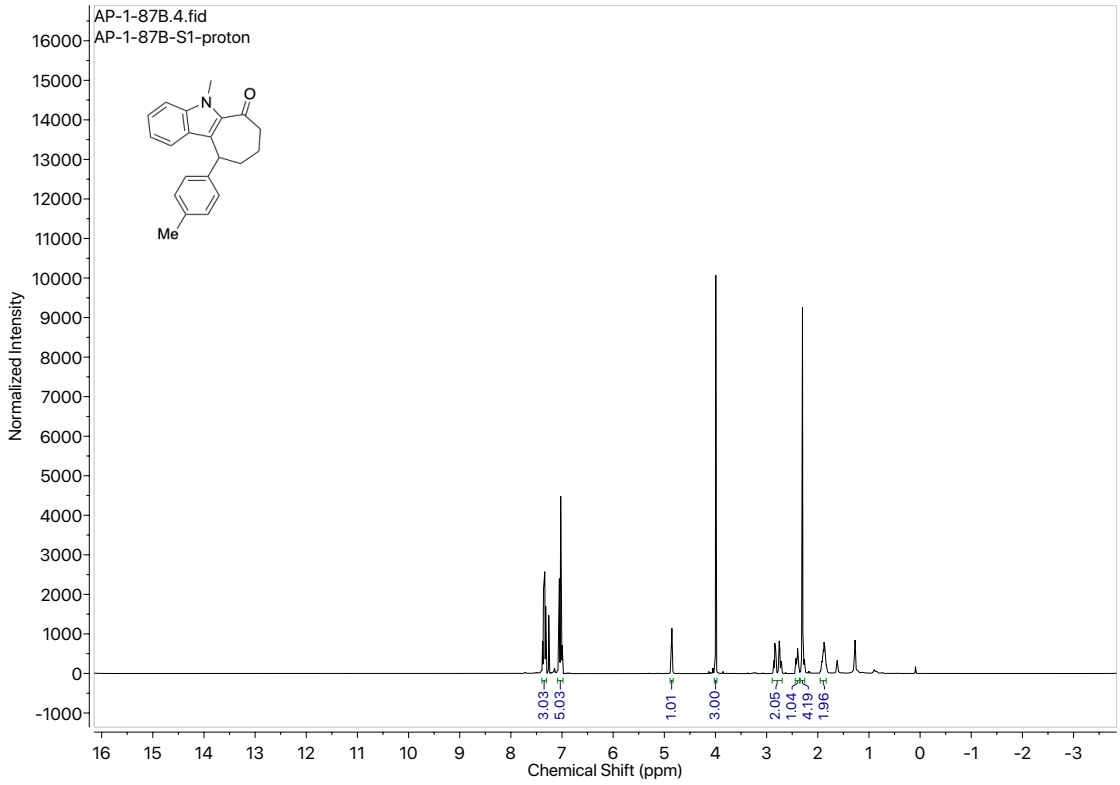
AP-1-87B.4.fid
AP-1-87B-S1-proton
Me
Normalized Intensity
Chemical Shift (ppm)
3.03
5.03
1.01
3.00
2.05
1.04
4.19
1.96

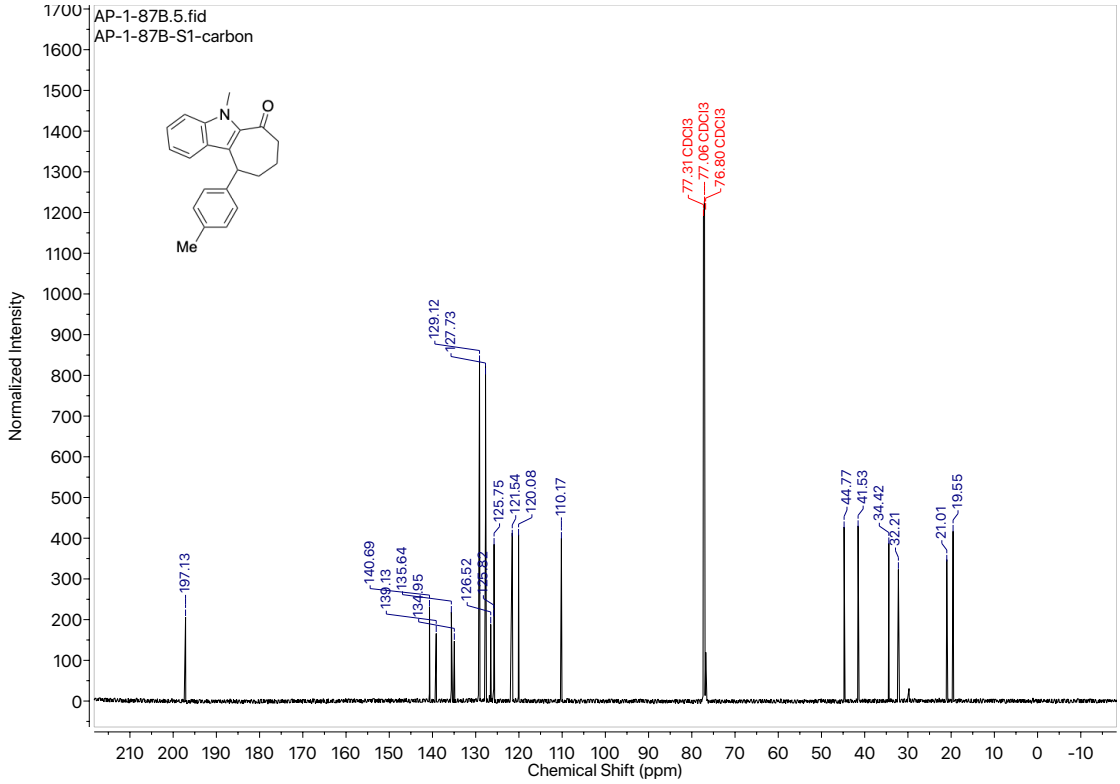
AP-1-87B.5.fid
AP-1-87B-S1-carbon
Me
Normalized Intensity
Chemical Shift (ppm)
77.31 CDCl3
77.06 CDCl3
76.80 CDCl3
197.13
140.69
139.13
135.64
134.95
129.12
127.73
126.52
125.82
125.75
121.54
120.08
110.17
44.77
41.53
34.42
32.21
21.01
19.55

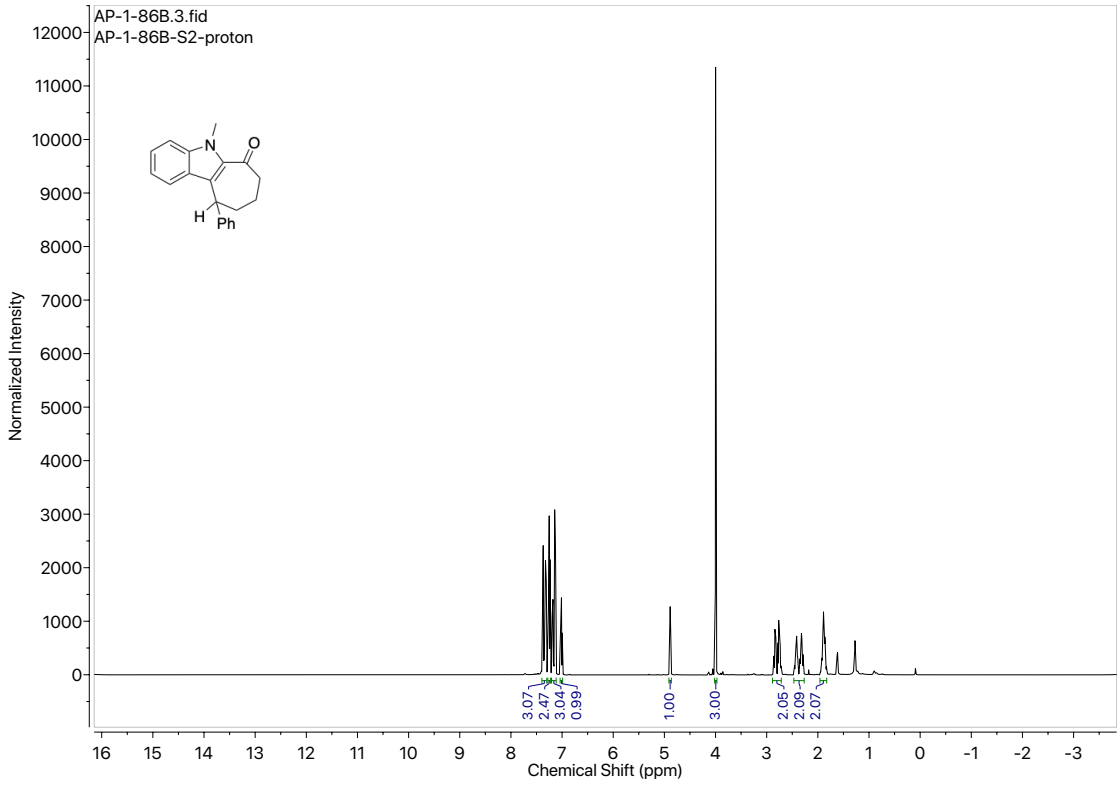
AP-1-86B.3.fid
AP-1-86B-S2-proton
Normalized Intensity
Chemical Shift (ppm)
3.07
2.47
3.04
0.99
1.00
3.00
2.05
2.09
2.07

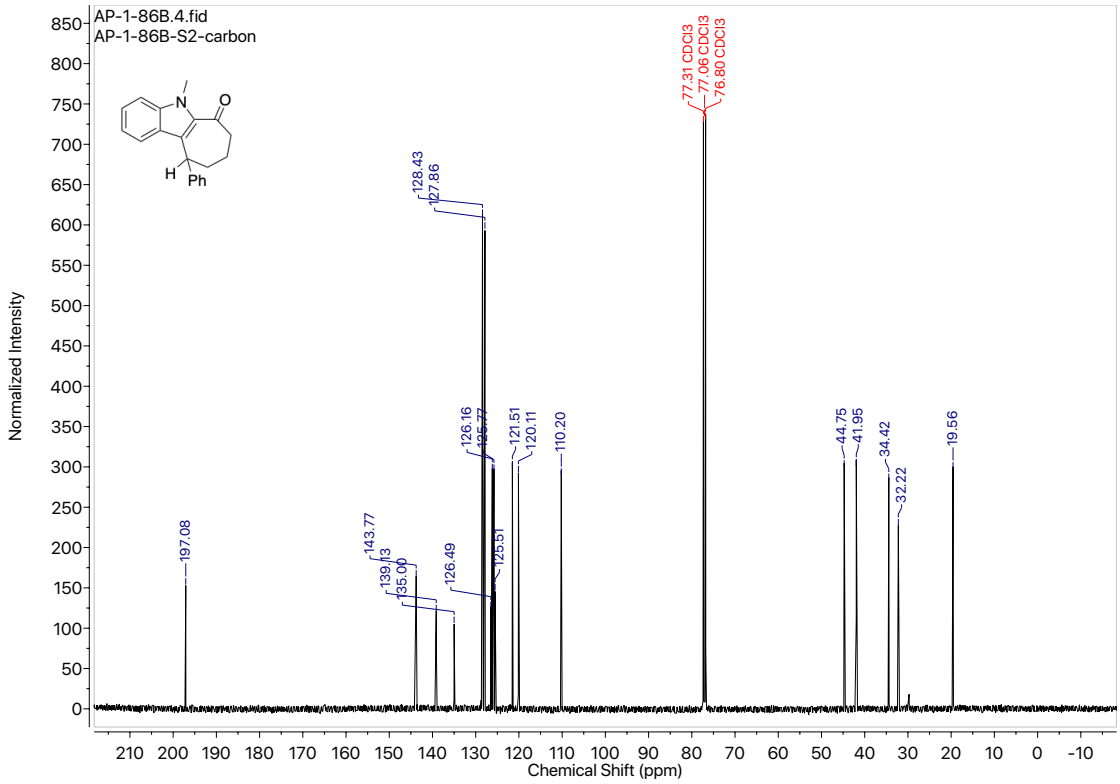
AP-1-86B.4.fid
AP-1-86B-S2-carbon
Normalized Intensity
Chemical Shift (ppm)
77.31 CDCl3
77.06 CDCl3
76.80 CDCl3
128.43
127.86
126.16
121.51
120.11
110.20
44.75
41.95
34.42
32.22
19.56
197.08
143.77
139.13
135.00
126.49
125.51

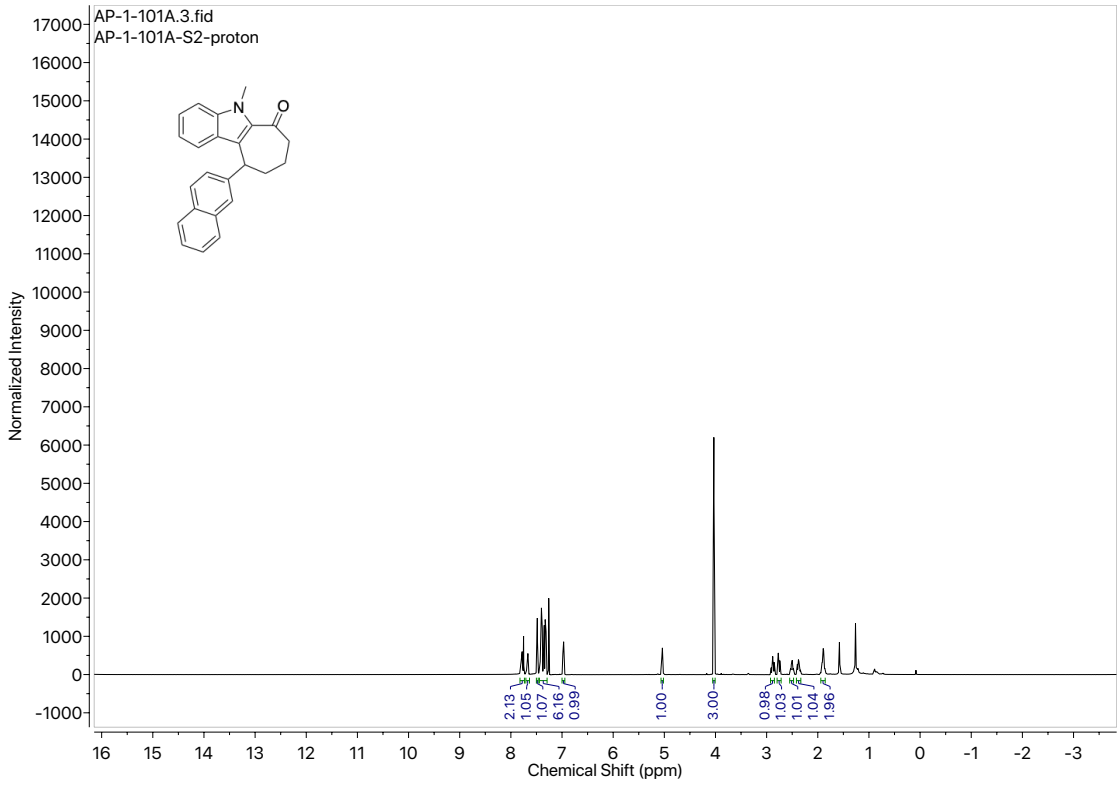
AP-1-101A.3.fid
AP-1-101A-S2-proton
Normalized Intensity
Chemical Shift (ppm)
2.13
1.05
1.07
6.16
0.99
1.00
3.00
0.98
1.03
1.01
1.04
1.96

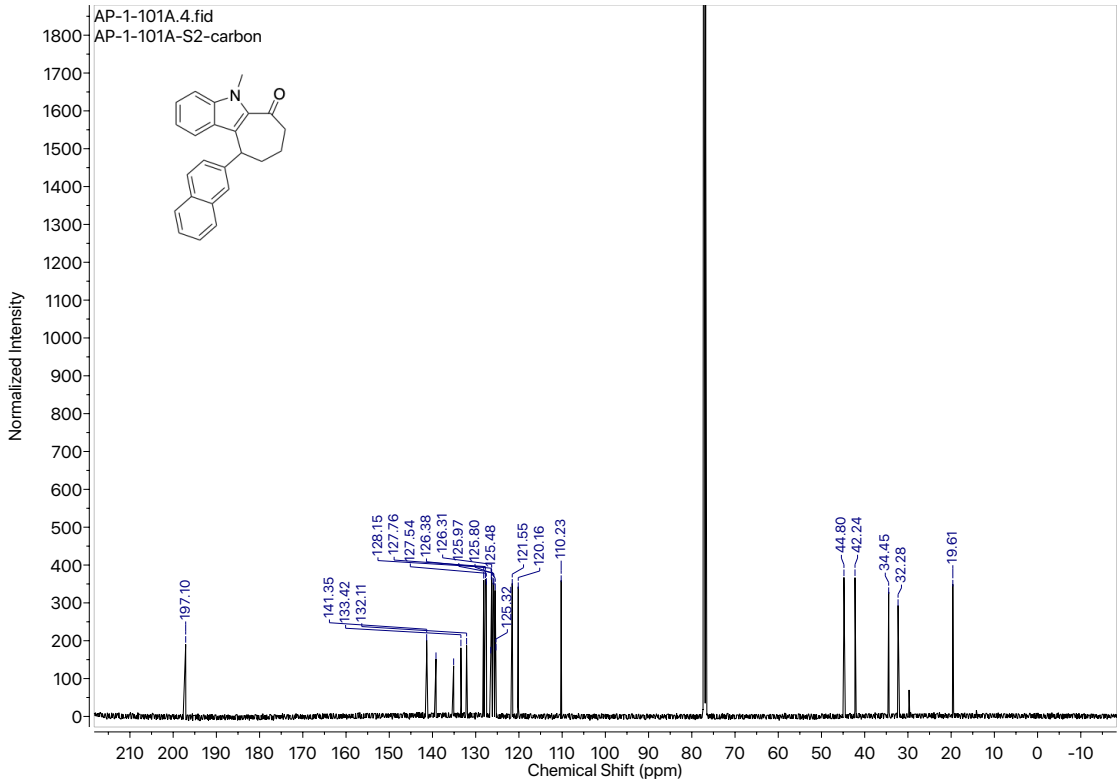
AP-1-101A.4.fid
AP-1-101A-S2-carbon
Normalized Intensity
Chemical Shift (ppm)
197.10
141.35
133.42
132.11
128.15
127.76
127.54
126.38
126.31
125.97
125.80
125.48
125.32
121.55
120.16
110.23
44.80
42.24
34.45
32.28
19.61

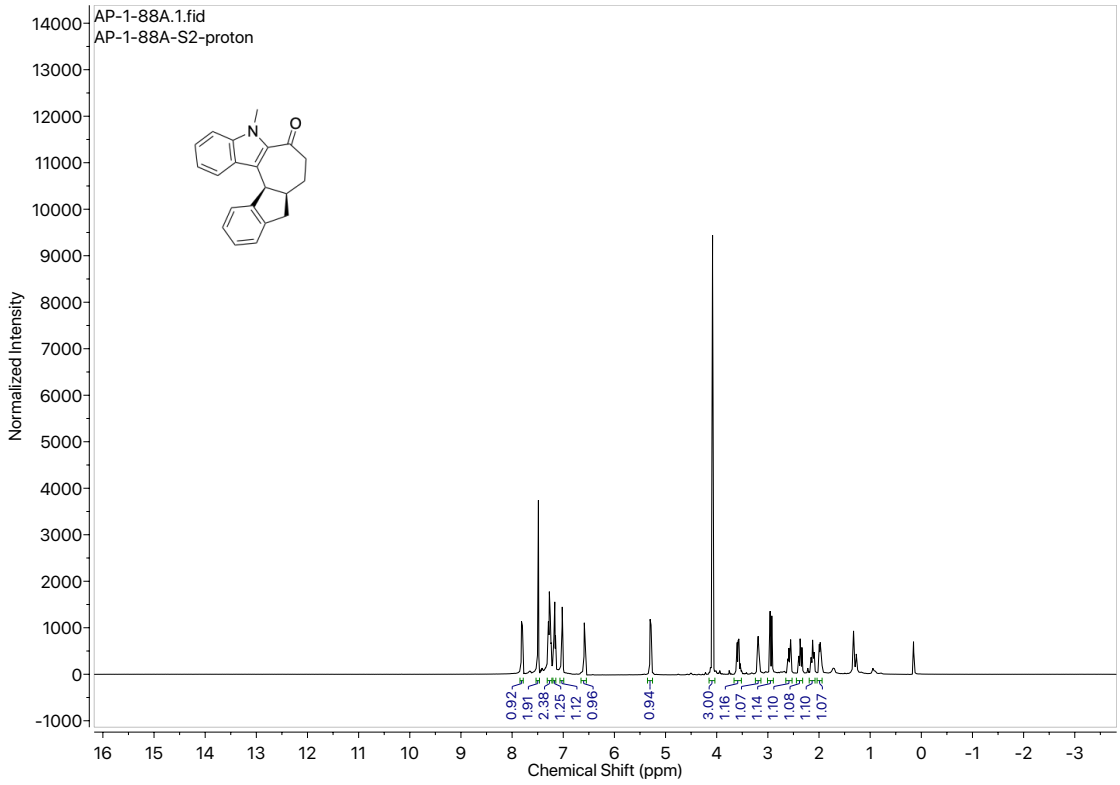
AP-1-88A.1.fid
AP-1-88A-S2-proton
Normalized Intensity
Chemical Shift (ppm)
0.92
1.91
2.38
1.25
1.12
0.96
0.94
3.00
1.16
1.07
1.14
1.10
1.08
1.10
1.07

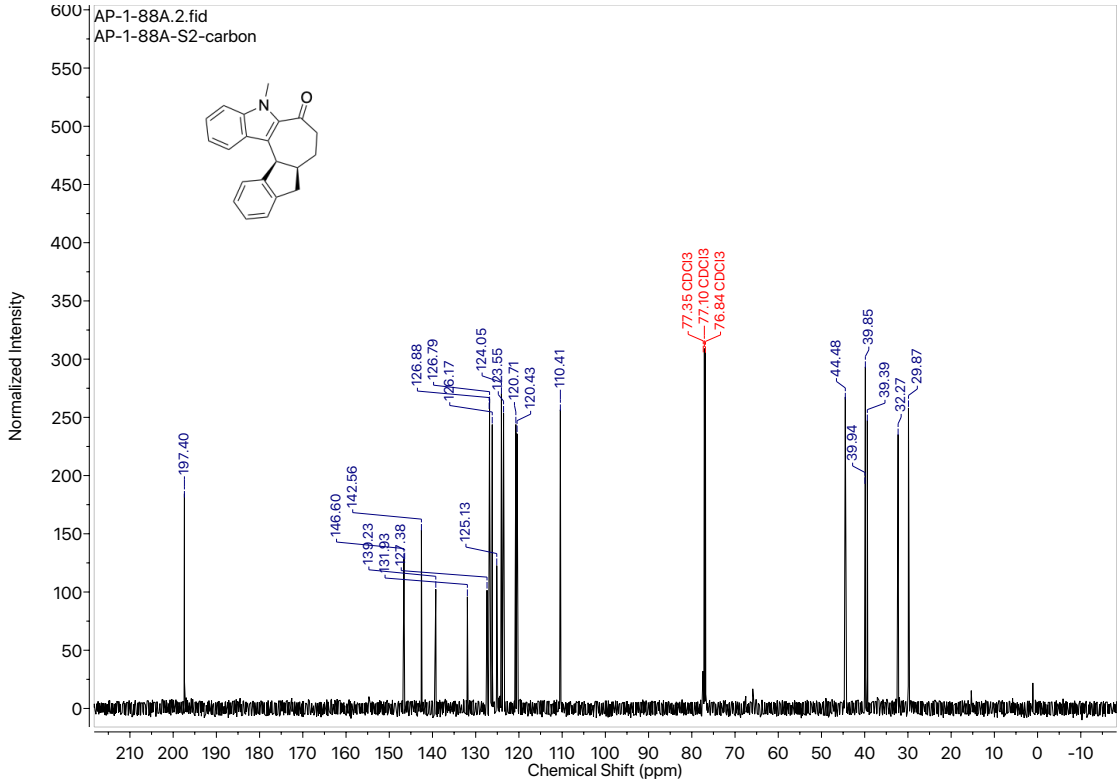
AP-1-88A.2.fid
AP-1-88A-S2-carbon
Normalized Intensity
Chemical Shift (ppm)
197.40
146.60
142.56
139.23
131.93
127.38
126.88
126.79
126.17
125.13
124.05
123.55
120.71
120.43
110.41
77.35 CDCl3
77.10 CDCl3
76.84 CDCl3
44.48
39.94
39.85
39.39
32.27
29.87

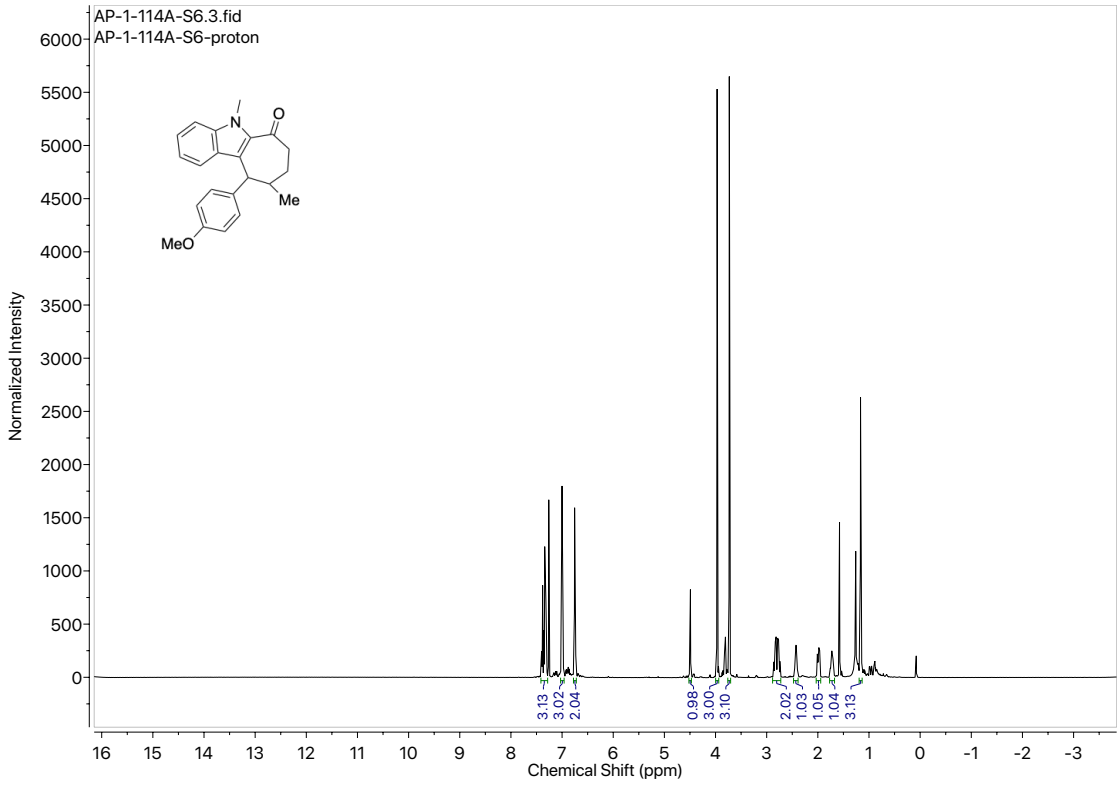
AP-1-114A-S6.3.fid
AP-1-114A-S6-proton
Normalized Intensity
Chemical Shift (ppm)
3.13
3.02
2.04
0.98
3.00
3.10
2.02
1.03
1.05
1.04
3.13
MeO
Me
O
N

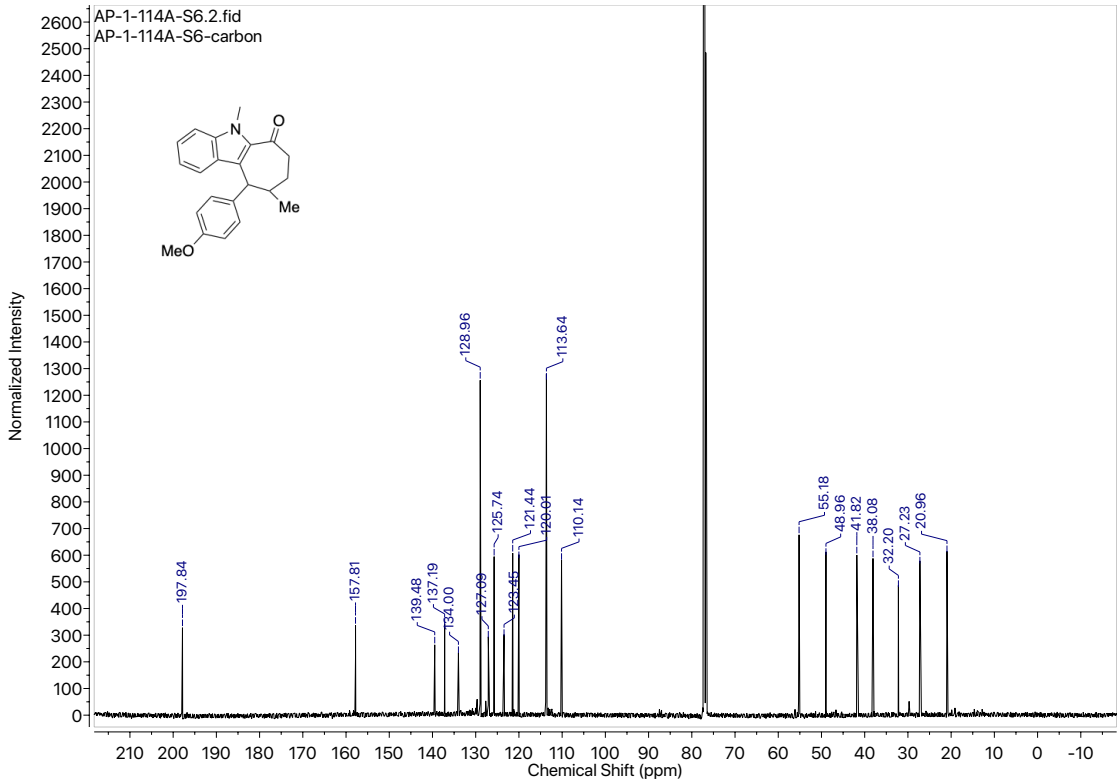
AP-1-114A-S6.2.fid
AP-1-114A-S6-carbon
Normalized Intensity
Chemical Shift (ppm)
197.84
157.81
139.48
137.19
134.00
128.96
127.09
125.74
123.45
121.44
120.01
113.64
110.14
55.18
48.96
41.82
38.08
32.20
27.23
20.96
MeO
Me
O
N

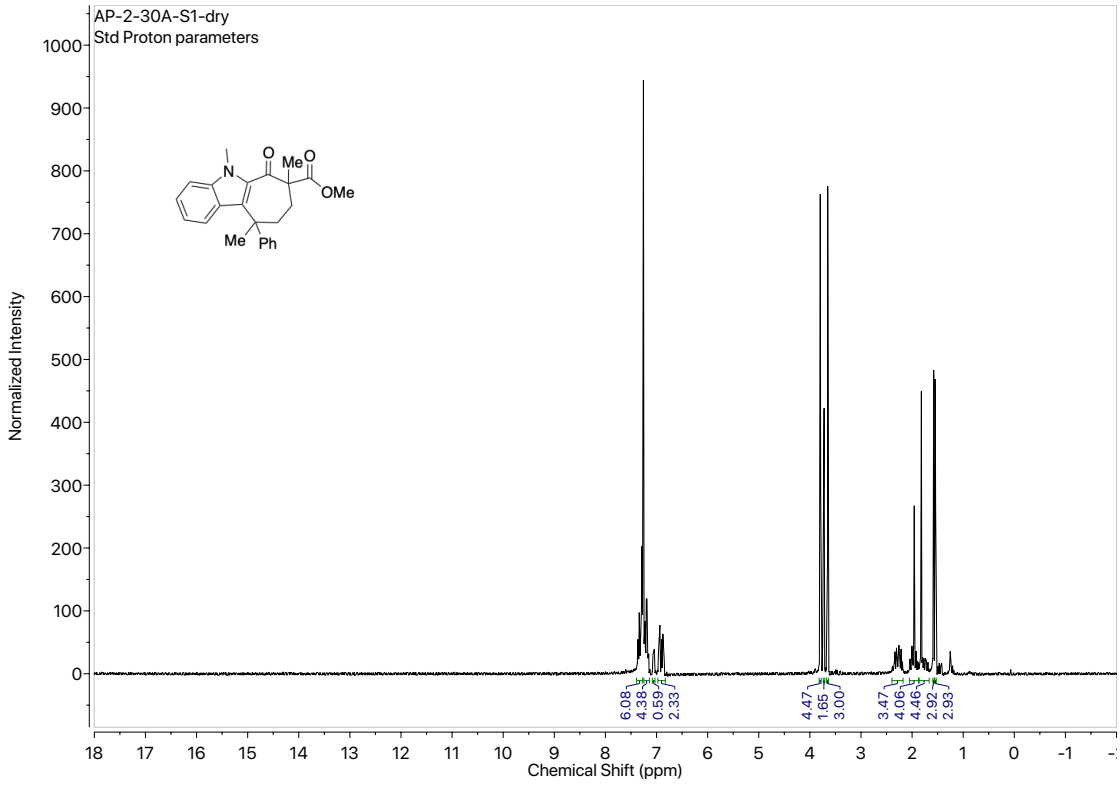
AP-2-30A-S1-dry
Std Proton parameters
Normalized Intensity
Chemical Shift (ppm)
6.08
4.38
0.59
2.33
4.47
1.65
3.00
3.47
4.06
4.46
2.92
2.93

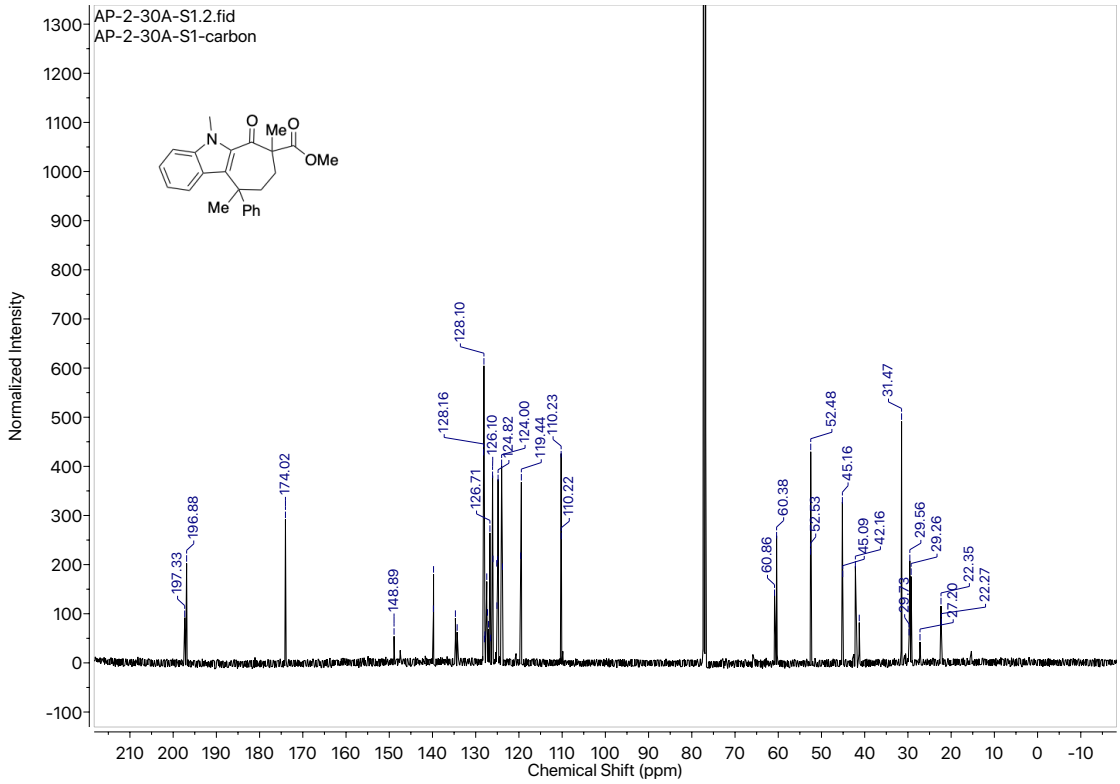
AP-2-30A-S1.2.fid
AP-2-30A-S1-carbon
Normalized Intensity
Chemical Shift (ppm)
197.33
196.88
174.02
148.89
128.16
128.10
126.71
126.10
124.82
124.00
119.44
110.23
110.22
60.86
60.38
52.53
52.48
45.16
45.09
42.16
31.47
29.56
29.26
29.13
22.35
22.27
17.20

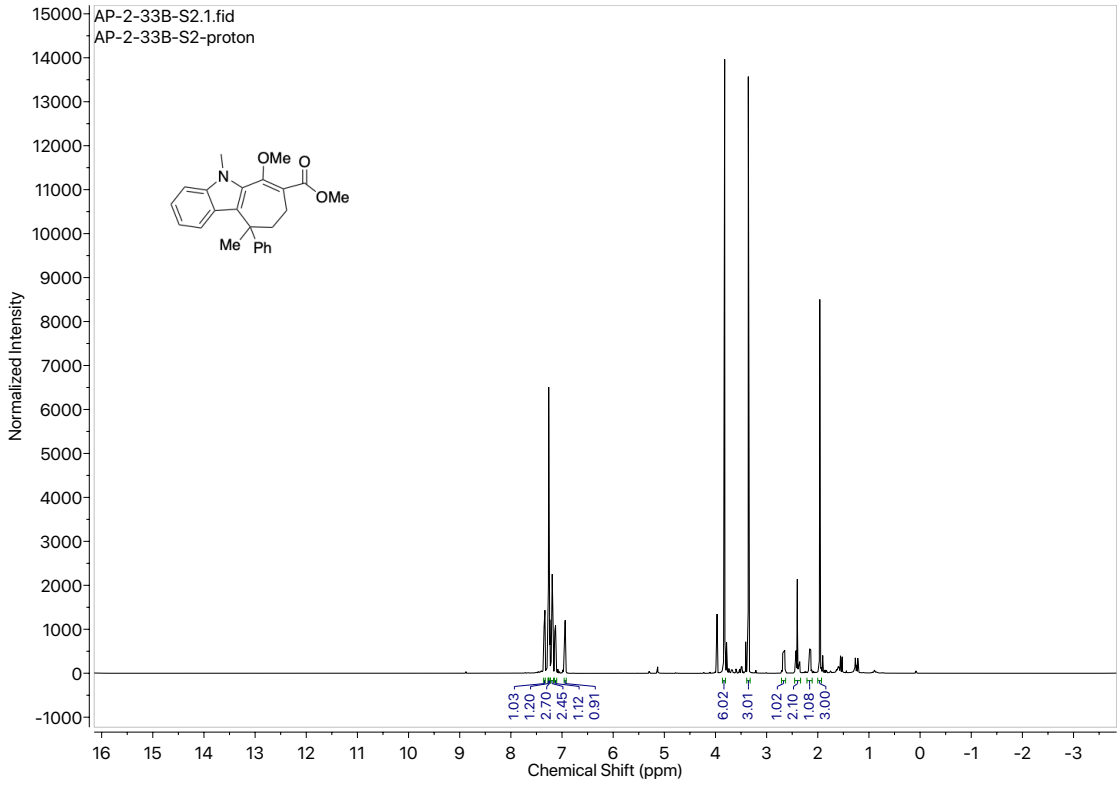
AP-2-33B-S2.1.fid
AP-2-33B-S2-proton
OMe
O
N
OMe
Me
Ph
Normalized Intensity
1.03
1.20
2.70
2.45
1.12
0.91
6.02
3.01
1.02
2.10
1.08
3.00
Chemical Shift (ppm)

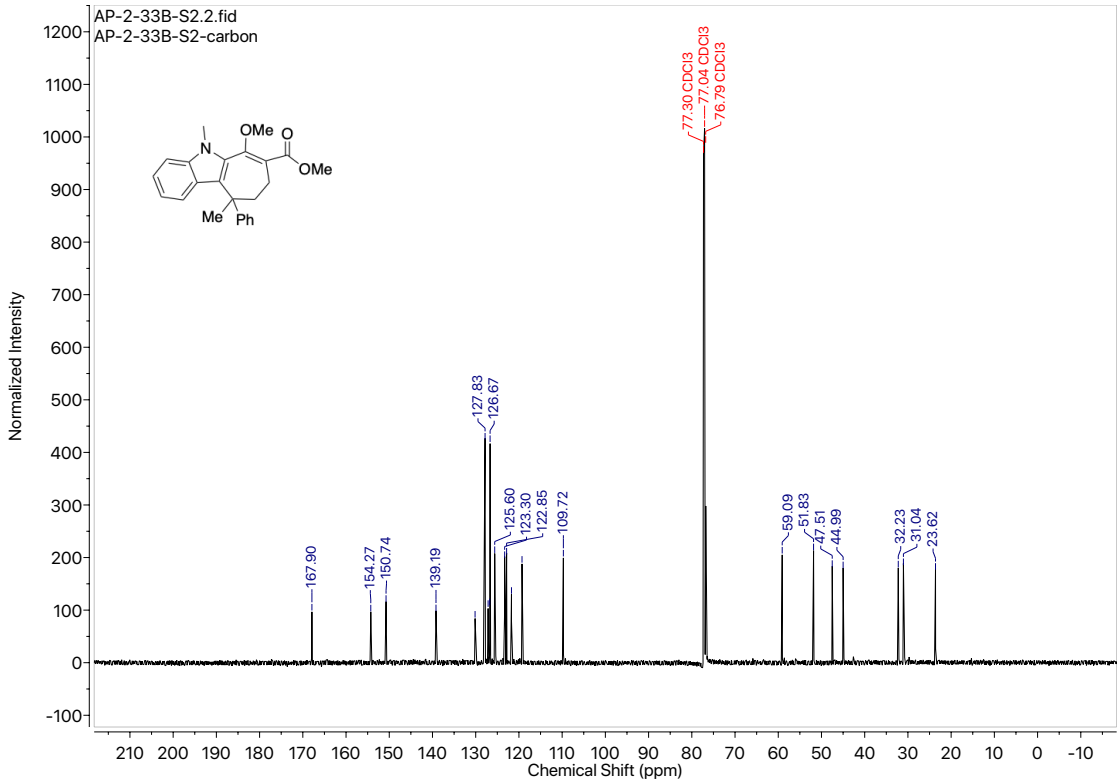
AP-2-33B-S2.2.fid
AP-2-33B-S2-carbon
OMe
O
N
OMe
Me
Ph
Normalized Intensity
77.30 CDCl3
77.04 CDCl3
76.79 CDCl3
167.90
154.27
150.74
139.19
127.83
126.67
125.60
123.30
122.85
109.72
59.09
51.83
47.51
44.99
32.23
31.04
23.62
Chemical Shift (ppm)

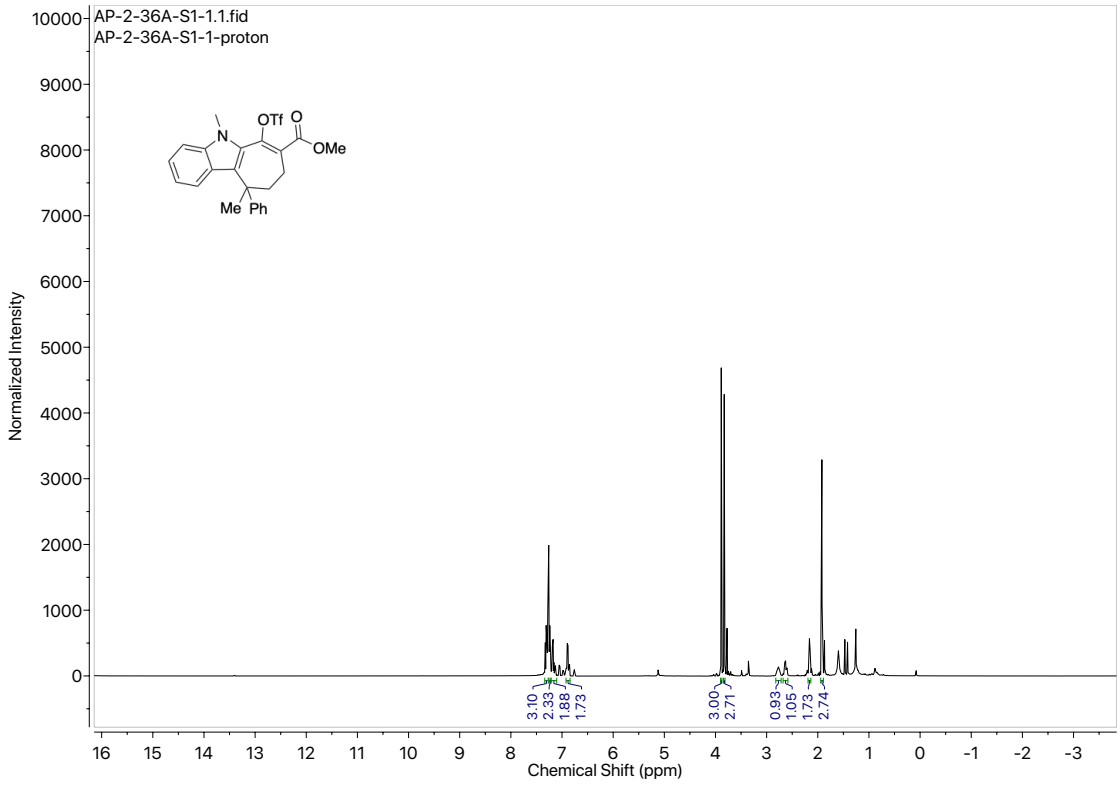
AP-2-36A-S1-1.1.fid
AP-2-36A-S1-1-proton
OTf
O
OMe
N
Me
Ph
Normalized Intensity
Chemical Shift (ppm)
3.10
2.33
1.88
1.73
3.00
2.71
0.93
1.05
1.73
2.74

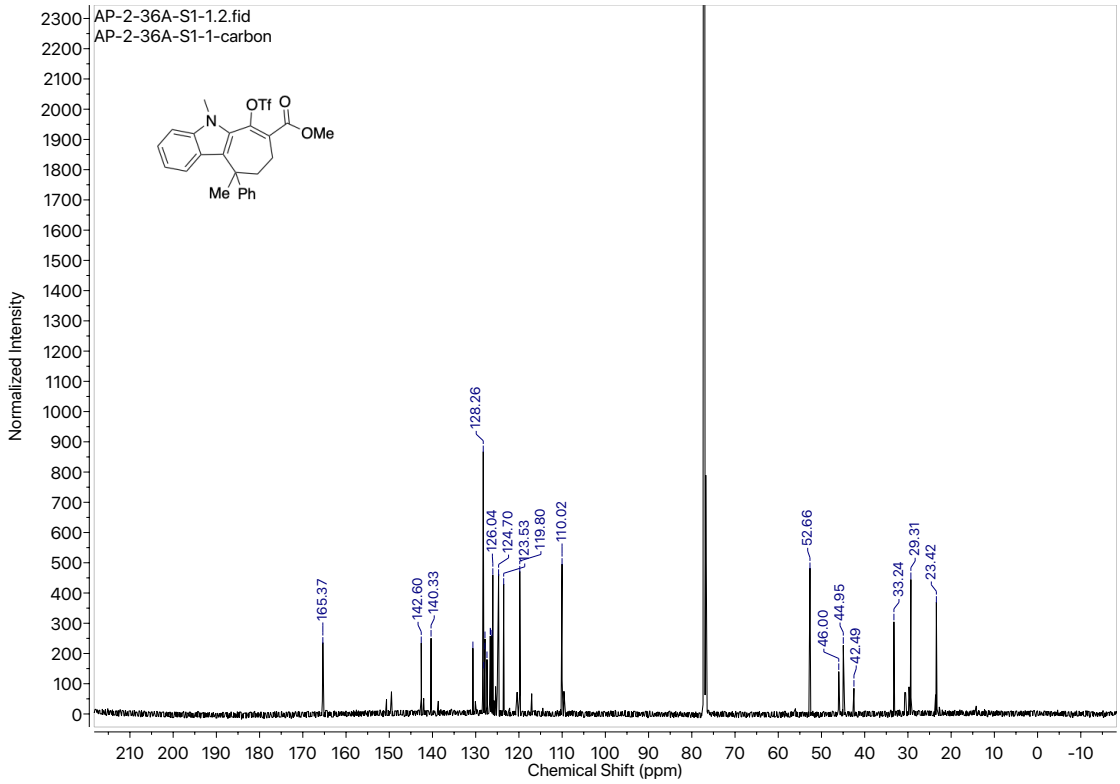
AP-2-36A-S1-1.2.fid
AP-2-36A-S1-1-carbon
OTf
O
OMe
N
Me
Ph
Normalized Intensity
Chemical Shift (ppm)
165.37
142.60
140.33
128.26
126.04
124.70
123.53
119.80
110.02
52.66
46.00
44.95
42.49
33.24
29.31
23.42

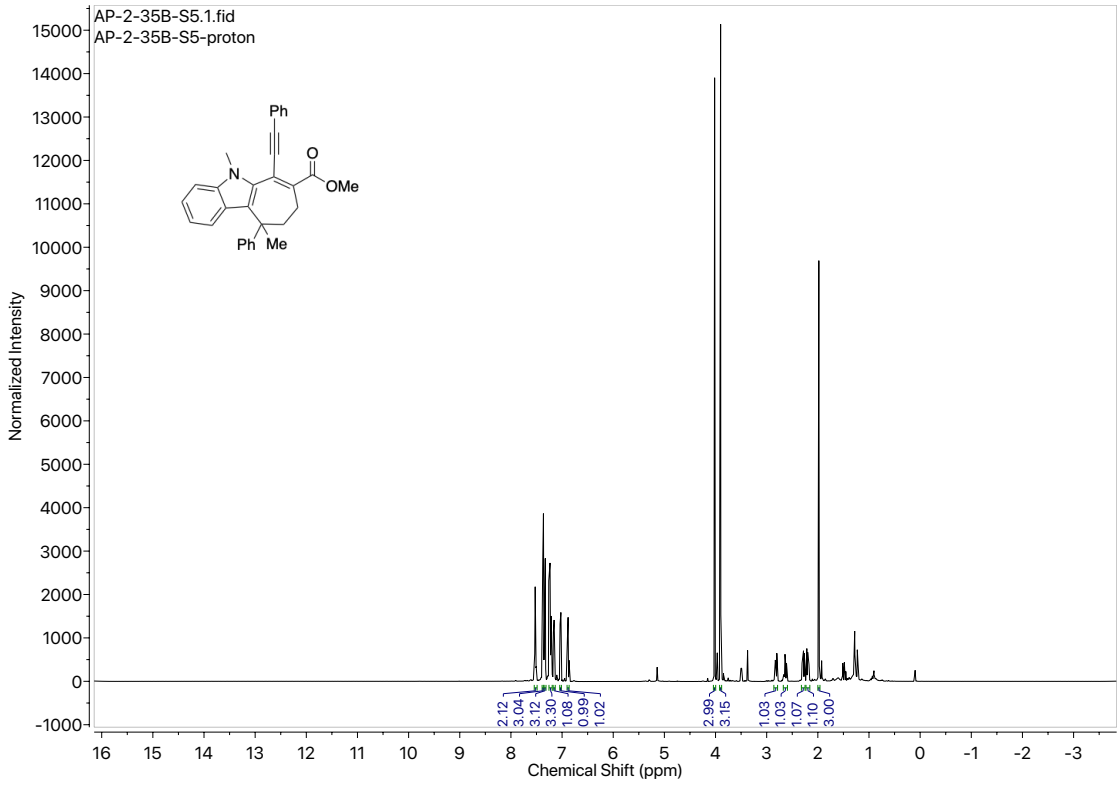
AP-2-35B-S5.1.fid
AP-2-35B-S5-proton
Ph
O
OMe
N
Ph Me
Normalized Intensity
Chemical Shift (ppm)
2.12
3.04
3.12
3.30
1.08
0.99
1.02
2.99
3.15
1.03
1.03
1.07
1.10
3.00

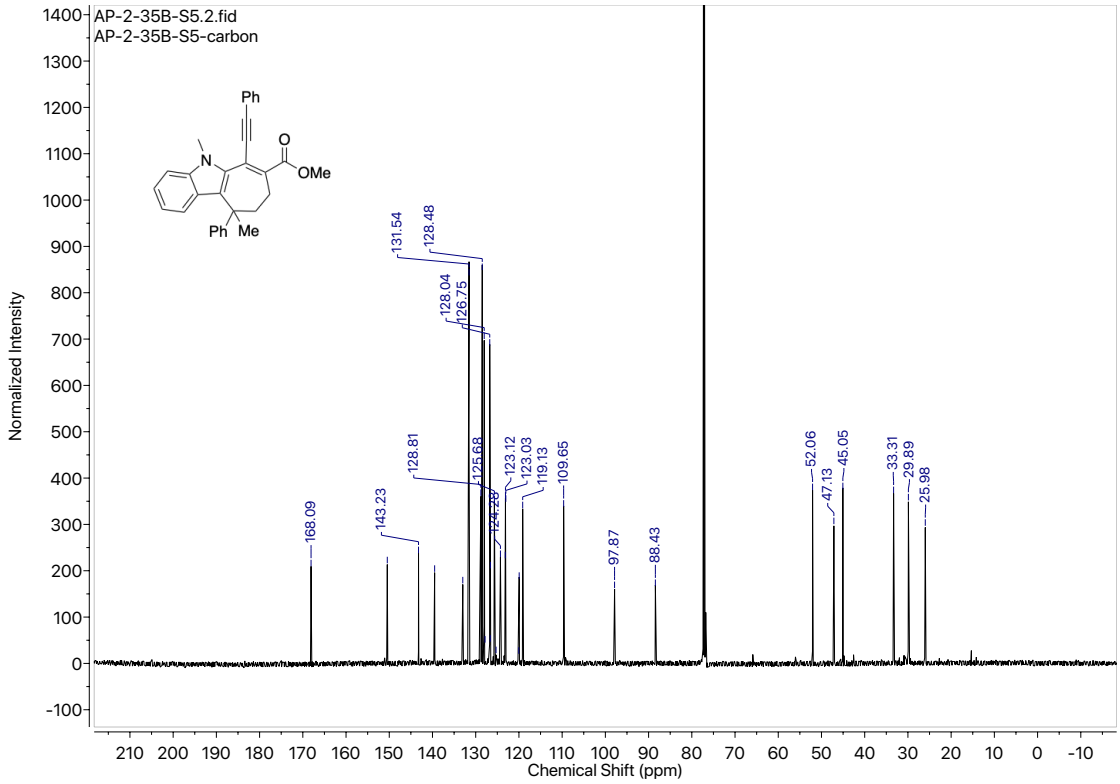
AP-2-35B-S5.2.fid
AP-2-35B-S5-carbon
Ph
O
OMe
N
Ph Me
Normalized Intensity
Chemical Shift (ppm)
168.09
143.23
131.54
128.81
128.48
128.04
126.75
125.68
124.28
123.12
123.03
119.13
109.65
97.87
88.43
52.06
47.13
45.05
33.31
29.89
25.98

CHAPTER 3. SYNTHESIS OF THE THREE (6,X')-FLUBROMAZEPAM POSITIONAL ISOMERS FOR FORENSIC ANAYLSIS

3.1 Designer Benzodiazepines: A Growing Forensic Challenge and Public Health Concern

"Designer drugs," also recognized as Novel Psychoactive Substances (NPS), have rapidly emerged in the illicit drug market becoming a forensic challenge as well as a growing public health issue.[1] NPS are synthetic, lab-engineered, and technically legal drugs created to simulate the effects of well-known illicit drugs.[2] Manufacturers of these drugs develop new chemicals to replace those that get banned, which means that the chemical structures of these drugs are constantly changing to stay ahead of the law.[3] As of January 2020, over 120 countries and territories have reported to the United Nations Office of Drug Control (UNDOC) the emergence of 950 NPS.[4] These NPS can be categorized into one of the following groups: synthetic cannabinoids, phenethylamines, synthetic cathinones, opioids, benzodiazepines, tryptamines, piperazines, and arylalkylamines, to name a few.[5] In recent years, a myriad of NPS belonging to the benzodiazepines class have surfaced and heightened the concern of federal agencies as the quantity, variant, and accessibility continues to increase.[6]

As a class, benzodiazepines are the most widely prescribed central nervous system depressants in the United States.[7] The sedative, depressant, and relaxant properties of these psychoactive drugs are used to treat conditions such as anxiety[8], insomnia[9], and epilepsy.[10]

Clonazepam (**1**), for example, is among the top-ranking most commonly prescribed benzodiazepines and is administered to control a variety of seizures.[11] Though many benzodiazepines are medically prescribed, such as Valium (diazepam, **2**) and Xanax (alprazolam, **3**), their abuse and addiction potential have caused them to be federally controlled under Schedule IV.[12] As a result, designer benzodiazepines have entered the recreational market as technically legal alternatives as they have not been scheduled. In 2017, designer benzodiazepines made their first appearance on the Drug Enforcement Administration (DEA) Emerging Threat Report, with flubromazepam (**4**), a 1,4-benzodiazepine, flubromazolam (**5**), it's triazole derivative, and etizolam (**6**), a triazolothienobenzodiazepine derivative, named among drugs most frequently seized and analyzed in the United States (Figure 3.1).[13] Due to an increase in reporting and identification of designer benzodiazepines, the DEA has since added a section dedicated to benzodiazepines for subsequent years.[14]

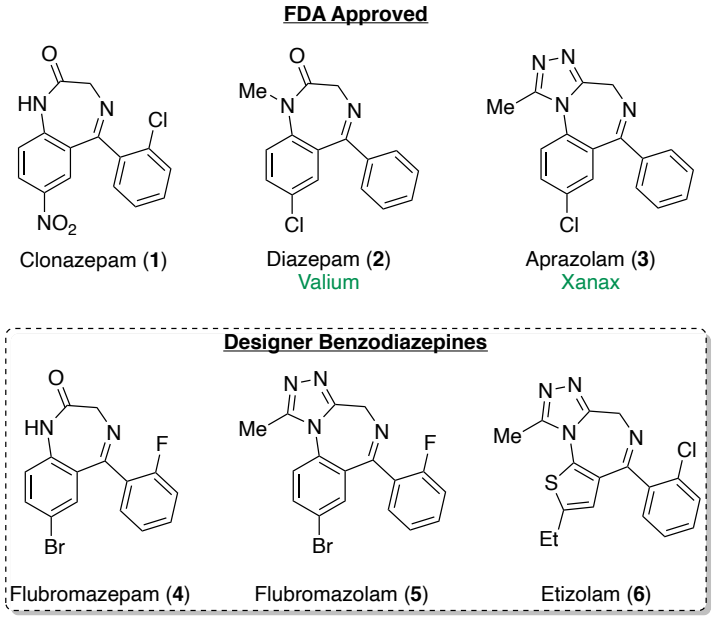

Figure 3.1 Representative Examples of Benzodiazepines

3.1.1 Positional Isomers and the Federal Analogue Act

Since the emergence of designer benzodiazepines in the early 2010s, the pharmacological effects and metabolic pathways of federally controlled parent benzodiazepines have been extensively studied,[15] while their positional isomers or analogs have not. By DEA rules and regulations, positional isomers, by definition, 1) have the same molecular formula and core structure as their parent and 2) have the same functional groups and/or substituents but can be attached at any position on the core structure as long as no new chemical functionalities are created, and no existing functionalities are destroyed.[16] These structural similarities of positional isomers to their parent often translate to similar physiological effects making them more susceptible to being synthesized and legally circulated.

According to the Federal Analogue Act,[17] unless classified as Schedule I or Schedule II substances, designer benzodiazepines and their positional isomers must be processed individually for scheduling. As a result, forensic examiners are concerned that as more parent compounds become federally controlled, distributors may look to positional isomers as technically legal alternatives for distribution.[3] Once new isomers hit the recreational market and begin to surface in toxicology reports, it will be difficult for examiners to interpret results as they must identify the new substances and differentiate them from the parent compounds. Therefore, it is imperative to synthesize analogues as reference standards to help ease this process.

3.1.2 Flubromazepam: A Model for the Synthesis of Positional Isomers as Reference Standards

Flubromazepam (**4**) is an attractive target to address this matter as it currently has no medicinal use and is known to be exclusively manufactured for illicit use. On top of this, flubromazepam is federally uncontrolled, which facilitates unrestricted research. Similar to other benzodiazepines, common physiological effects of flubromazepam include sedation, impaired coordination, respiratory depression, muscle relaxation, and central nervous system (CNS) depression. As a result, recent incidents such as DUI traffic occurrences[18], sexual assault cases[19], and reports of serious and/or fatal intoxications exist for flubromazepam by itself or combined with another drugs[20]. One of the most concerning properties of flubromazepam is its extremely long elimination half-life of 106 h which can lead to accumulation of toxic concentrations after repeated intake.[15a] These instances make flubromazepam a prime candidate for future scheduling.

The chemical isolation, cataloging, and legal scheduling of designer drugs such as flubromazepam is laborious. By the time federal agencies gather data and corresponding legislature is authorized for a given compound, new analogues such as positional isomers are synthesized and dispersed, thus starting the cycle over. To stay on top of the flood of new designer drugs it is important that federal agencies and synthetic chemist join forces to synthesis analogs as reference standards. Synthetically, flubromazepam has twelve positional isomers (including the parent) (Figure 3.2) which maximizes chemical space for synthesis, as well as other biological and analytical studies.

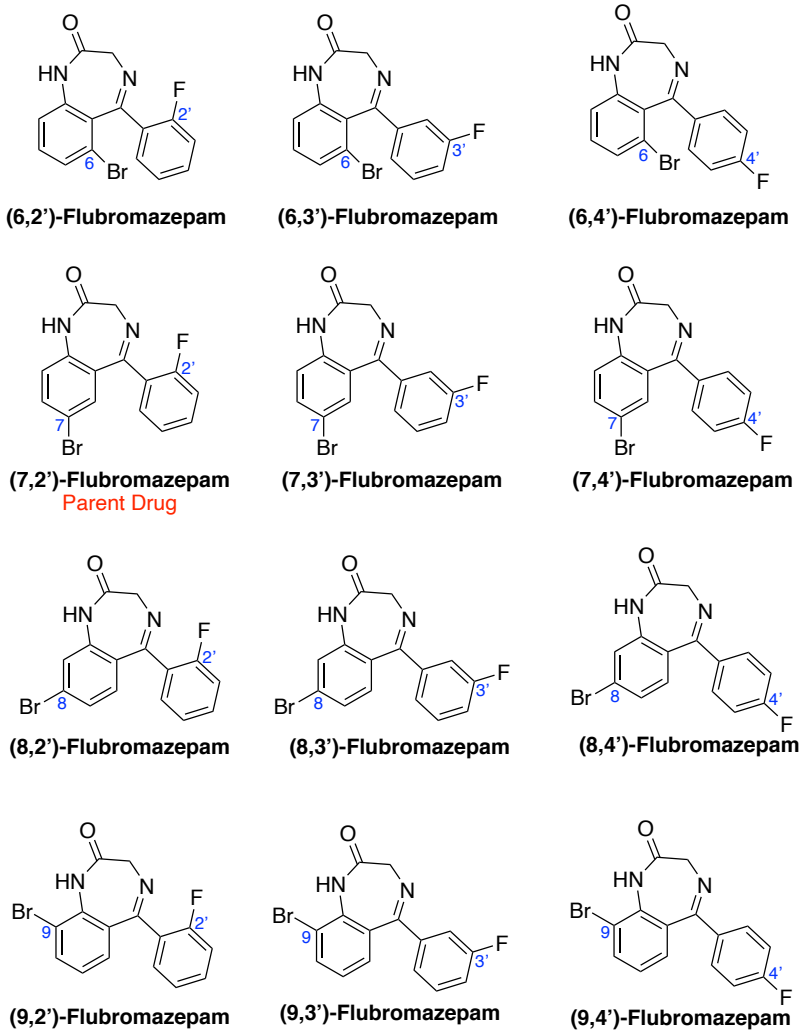

Figure 3.2 Twelve Positional Isomers of Flubromazepam

3.2 Synthetic Journey Toward the Twelve Isomers of Flubromazepam

3.2.1 Previous Synthesis Used to Access Nine of the Twelve Positional Isomers of Flubromazepam

Toward this goal, we previously disclosed a synthetic approach to access nine of the twelve possible positional isomers of flubromazepam (Scheme 3.1).[21] The sequence involved a three-step synthesis to generate the functionalized amino-benzophenones **9**

involving: (1) saponification of bromo-substituted isatins **7** to give 2-amino-X-bromobenzoic acids; (2) amidation of the acids to give the corresponding Weinreb amides **8**; and (3) lithiate addition of the corresponding bromofluorobenzene to the Weinreb amides. Benzophenones **9** were then transformed to the respective (X,X')-flubromazepam by subjecting them to the established Sternbach and co-workers[22] 2-step annulation sequence involving 2-bromoacetyl bromide, to first prepare the 2-bromoacetamidobenzophenone intermediate, then treatment with ammonia to promote ring closure through imine formation. While successful in preparing the **(7,X')**-, **(8,X')**-, and **(9,X')**-flubromazepams, this approach failed to provide the **(6,X')**-isomers.[23]

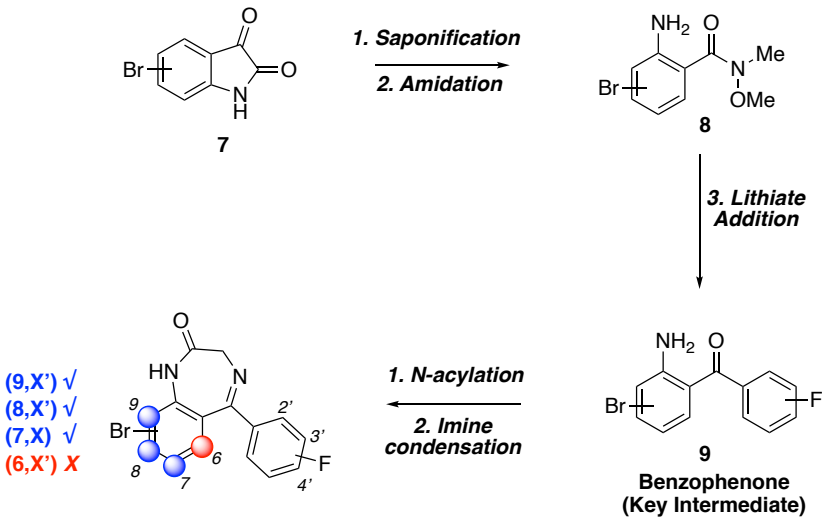

Scheme 3.1 Previous Approach to Flubromazepam Positional Isomers

3.2.2 Shortcomings of the Previous Approach

We hypothesized that the combination of steric hindrance of the bromine at the 6-position (hindering the site of nucleophilic lithiate addition) and potential cross lithium-halogen exchange (due to proximity) may have been the reason for the unsuccessful

reaction. To overcome these limitations, we sought an alternative synthetic approach to access the key amino benzophenone intermediate. In this chapter, we describe our successful efforts in synthesizing the final three (6,X')-isomers in order to complete the full set of flubromazepam positional isomers to provide forensic examiners with proper analytical standards.

3.3 Synthetic Inspiration for the Synthesis of the Elusive (6,X')-Flubromazepam Positional Isomers

Our synthetic design was inspired by seminal work from Huntress and coworkers for the synthesis of 1-bromofluorene **14** from 2-benzoyl-3-bromoaniline **13** (Scheme 3.2).[24] The authors accessed aniline **13** using a 4-step sequence starting with 3-bromophthalic anhydride **10**.[25] Using conditions established by Stephens,[26] benzene undergoes Friedel-Crafts acylation with **10** to form 2-benzoyl-3-bromobenzoic acid **11**. Conversion to the primary amide **12** then set the stage for a Hofmann rearrangement that generates aniline **13**.

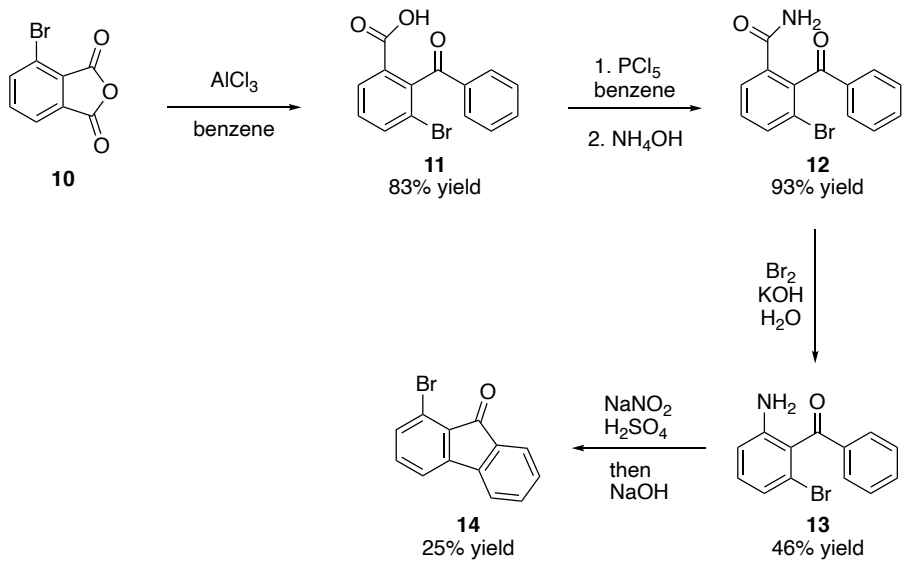

Scheme 3.2 Synthesis of 1-Bromofluorene 14 by Huntress and Coworkers

3.3.1 Retrosynthetic Analysis and Reaction Design for the Synthesis of Elusive (6,X')-Flubromazepam Positional Isomers

We envisioned a similar sequence involving an initial Friedel-Crafts acylation using strategic fluorobenzene derivatives to access the requisite fluorobenzoyl-3-bromobenzoic acids **18**-**20** (Scheme 3.3C). For the *p*-fluoro substituted benzophenone derivative **18**, the reaction would employ fluorobenzene directly. We then envisioned direct conversion of the resulting benzoic acid to the acyl azide followed by thermal Curtius rearrangement[27] to achieve a shorter and milder experimental sequence to the aminobenzophenone (versus acid chloride formation, amidation, and Hofmann rearrangement) (Scheme 3.3A). To ensure Friedel-Crafts site selectivity for the *m*- and *o*-fluoro-substituted derivatives, a thioether group would be used to direct the site of acylation onto the aryl ring. Following acylation, the thioether would be removed before continuing forward (Scheme 3.3B). This strategy was also particularly appealing given the availability

of the thioether starting materials and existing literature examples on the reductive cleavage of the aryl thioether bond. Thioethers have been employed as *ortho*- or *para*-directors for Friedel-Crafts chemistry[28] and as surrogates for sulfonyl groups (formed upon thioether oxidation).[29] Moreover, they have been used as directing groups for C-H functionalization reactions that can be readily removed as needed.[30] However, to the best of our knowledge, examples using the thioether as a removable directing group for Friedel-Crafts reactions have not been reported.

A) Retrosynthetic Analysis for (6,4')-Flubromazepam Isomer

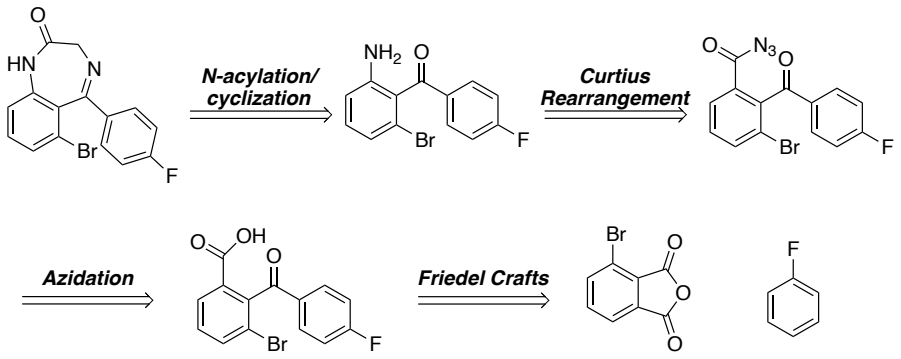

B) Retrosynthetic Analysis for (6,3')- & (6,2')-Flubromazepam Isomers

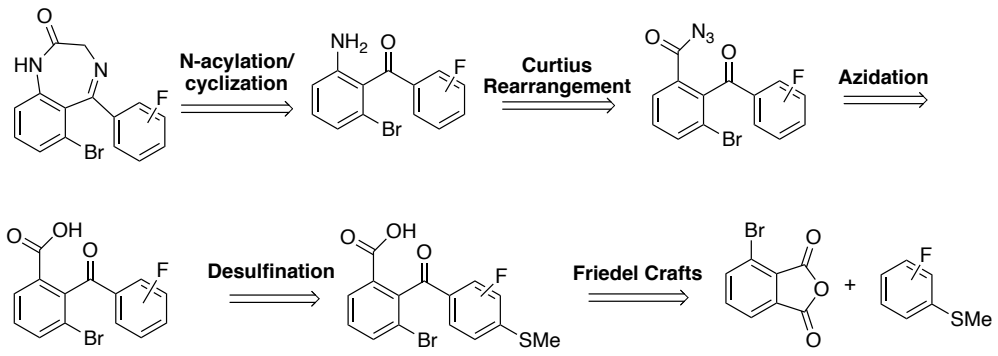

C) Anticipated Reactivity and Outcome of Friedel Crafts Acylation

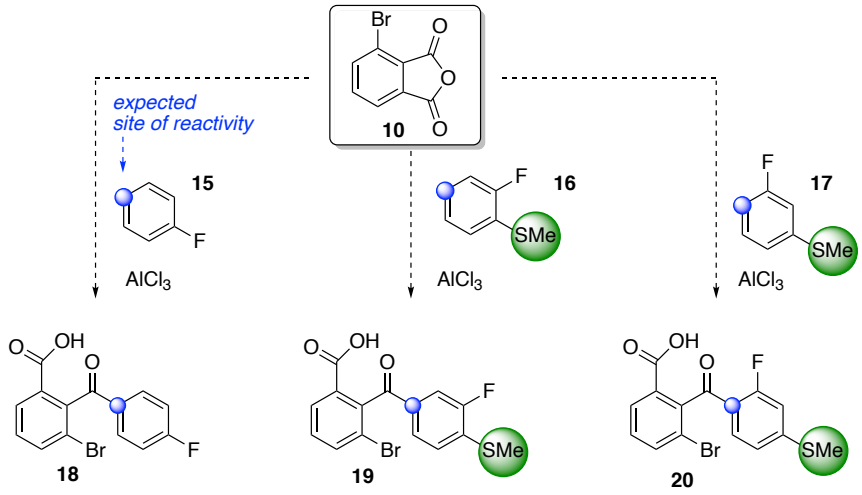

Scheme 3.3 A) Retrosynthesis for (6,4')-flubromazepam B) Retrosynthesis for (6,3')-flubromazepam C) Proposed Friedel-Crafts Approach to Fluoro-Substituted Benzoyl 3-Bromobenzoic Acids 18-20

3.4 Synthesis of (6,4')-Flubromazepam through Friedel Crafts Approach

In route to the **(6,4')**-isomer, 3-bromophthalic anhydride **10**, fluorobenzene **15**, and $AlCl_3$ were first mixed together to affect the Friedel-Crafts acylation (Scheme 3.4). Interestingly, the desired benzoic acid **18** was not observed but, instead, its hemiacetal, 3-hydroxyphthalide **21**, was formed in up to 73% yield. Despite unexpected lactone formation, the material was carried forward in hopes that, under the right azidation reaction conditions, the hemiacetal would ring open to the carboxylic acid *in situ* and subsequently form the desired azide **22**.

Over the years, several methods have been developed using a wide variety of reagents for the formation of acyl azides.[31] These methods generally involve the use of carboxylic acids or activated derivatives such as acyl chlorides and anhydrides. We started our pursuit to acyl azide **22** by treating the masked carboxylic acid **21** with oxalyl chloride to form the acyl chloride followed by sodium azide. Unfortunately, this resulted in no desired product likely due to the lactone starting material failing to ring open *in situ.* With this in mind, we sought to employ a protocol that uses a base to facilitate ring opening. Thus, lactone **21** was subjected to treatment with triethylamine and ethyl chloroformate to form the resultant mixed anhydride then sodium azide in anticipation of the desired acyl azide. However, this reaction resulted in only trace amounts of the desired acyl azide and primarily unreacted mixed anhydride. Since the addition of the azide to the activated intermediate seemed to be problematic for this system, the duel activating-azidating agent diphenylphosphoryl azide was used to directly convert the masked carboxylic acid to the acyl azide in a one pot procedure. This reaction resulted in full conversion (determined by TLC and/or ^{1}H NMR) to the azide. Upon completion, the crude material was heated to

facilitate the Curtius rearrangement to provide the key aminobenzophenone intermediate **23a** in 62% yield over the two steps. With the benzophenone precursor in hand, it was subjected to the known Sternbach procedure to access the **(6,4')**-flubromazepam positional isomer in 51% yield.

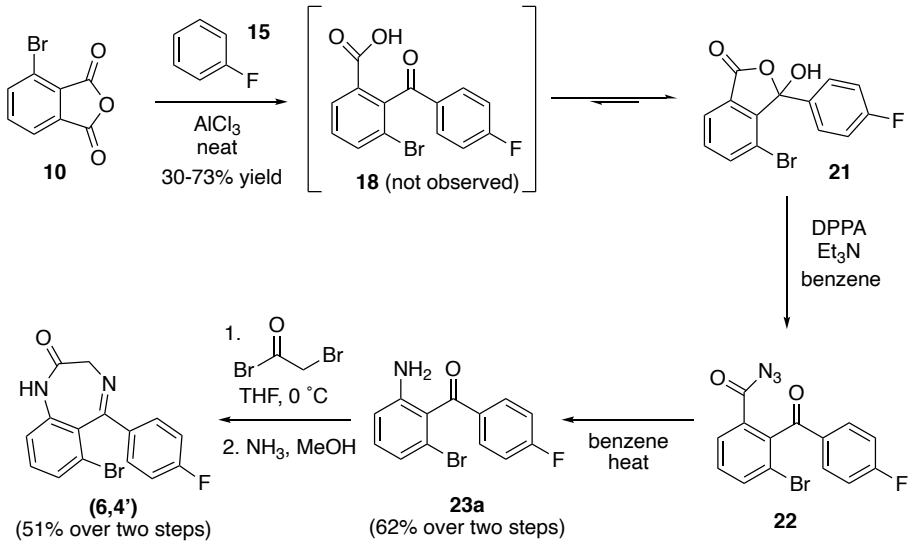

Scheme 3.4 Synthesis of (6,4')-Flubromazepam

3.5 Attempted Synthesis of (6,3')- and (6,2')-Flubromazepams through Friedel Crafts Approach

We next turned our attention to the **(6,3')**-isomer, which we envisioned could be accessed using 2-fluorothioanisole **16** for the Friedel-Crafts acylation with 3-bromophthalic anhydride **10** (Scheme 3.5). We were successful in obtaining the desired carboxylic acid **19** in 40% yield. Unlike previously observed with fluorobenzene, no phthalide product was observed. Phthlide formation in the previous case was likely due to a combination of the electronics of the 4'-fluoro group and the nature of the reaction workup.

We then attempted removal of the thioether group prior to acyl azide formation and Curtius rearrangement. Several approaches for aryl desulfuration, or reductive cleavage of aryl C-S bonds, have been reported with varying degrees of functional group tolerance.[32] We initially attempted a Ni-catalyzed reductive cleavage[32b] of the thioether group but unfortunately only recovered starting material. In another attempt, we tried the reductive cleavage with $PdCl_2$ and Et_3SiH and was able to achieve the desired product **24** in an undesirably low 18% yield as we were plagued by purification issues.[18a] It is likely that the carboxylic acid is the cause of the low yield or poor reactions. Even when the $PdCl_2/Et_3SiH$ reaction was attempted with TMSCl (for *in situ* acid protection), the desired reduced product was not obtained. To circumvent this issue, we sought to change the reaction sequence order by performing the Curtius rearrangement first and then attempting the desulfuration reaction. Treatment of acid **19** with DPPA yielded acyl azide **25** in 40% yield. Unfortunately, multiple attempts at the thermal Curtius rearrangement proved unsuccessful as only starting material was recovered.

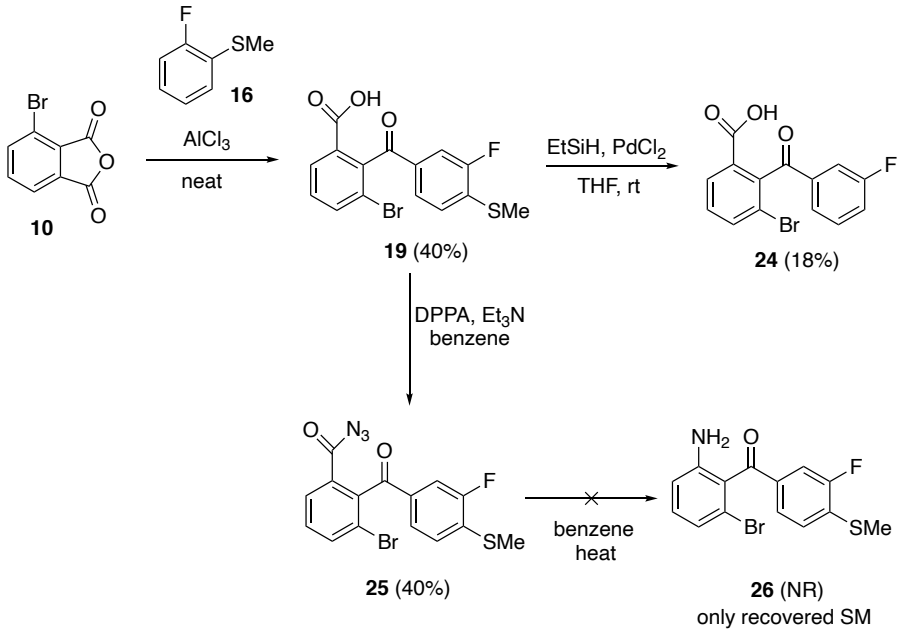

Scheme 3.5 Attempted Synthesis of the (6,3')-Flubromazepam Benzophenone Precursor

While sorting through the issues associated with the 2-fluorothioanisole reaction sequence, we started exploring the reaction of 3-fluorothioanisole **17** with 3-bromophthalic anhydride **10** in parallel (Scheme 3.6). Surprisingly, we were unable to get any conversion to the desired Friedel-Crafts acylation product **20**. In all cases, only starting material was recovered. It is possible that, in this case, having the inductively-withdrawing fluorine atom proximal to the site of attack may be deactivating the ring and reducing its overall nucleophilicity.[33]

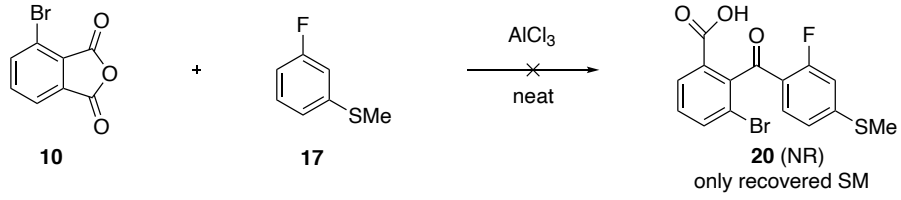

Scheme 3.6 Unsuccessful Friedel-Crafts Acylation of 3-Fluorothioanisole 17

3.6 Completion of the Set: Successful Synthesis of the (6,X')-Flubromazepam Positional Isomers

3.6.1 Redesigned Retrosynthetic Analysis: Grignard Approach

Following the difficulty surrounding the Friedel Crafts approach using thioethers as a removable directing group, an alternate strategy was designed to access the key benzophenone intermediate for the **(6,2')**- and **(6,3')**-isomers (Scheme 3.7). We envisioned the aminobenzophenones arising from the corresponding nitro derivatives, which would be accessible from the corresponding nitro benzhydrols **27**. Finally, benzhydrols **27** would be generated upon the reaction of 2-bromo-3-nitrobenzaldehyde **28** with fluorophenyl Grignard reagents as reaction partners.

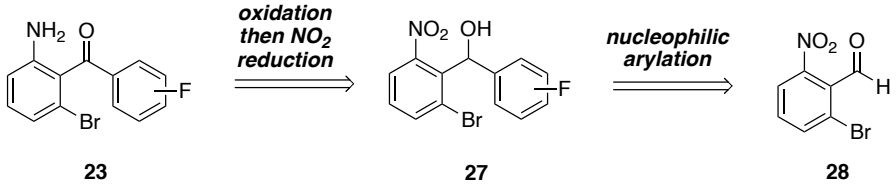

23 **27** **28**

Scheme 3.7 Redesigned Retrosynthetic Analysis

3.6.2 Synthesis of Starting Material for Grignard Coupling

Although commercially available, 2-bromo-6-nitrobenzaldehyde **28** is relatively expensive at >$140/g (Scheme 3.8).[34] To access enough material to perform some screening reactions, we initially sought to synthesize the aldehyde using a two-step sequence from the cheaper 2-bromo-6-toluene **29** (~$7.50/g)[34] established by Carter and coworkers.[35] Treatment of **29** with the dimethyl acetal of DMF (DMF-DMA) afforded a crude enamine that underwent oxidative cleavage to give the aldehyde **28** in up to 56%

yield. However, the results were inconsistent over multiple runs as we primarily observed the homologated aldehyde resulting from the hydrolysis of the enamine intermediate as the major product.[36] Therefore, we explored the oxidation of the corresponding benzyl alcohol **30**. While more expensive than the toluene derivative **29** (~$75/g),[34] the alcohol **30** could be readily and consistently converted to benzaldehyde **28** with PCC in up to 87% yield.

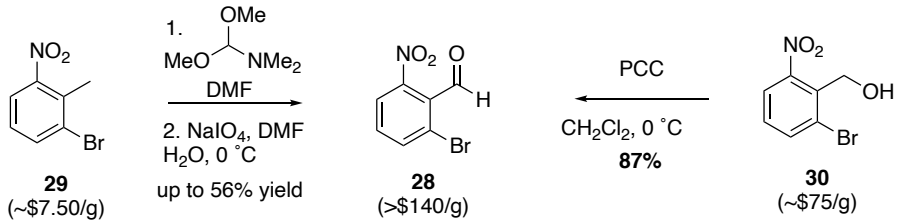

Scheme 3.8 Synthetic Approaches to 2-Bromo-6-nitrobenzaldeyde 23

3.6.3 Forward Synthesis Toward (6,X')-Flubromazepam Positional Isomers Through Grignard Approach

Benzaldehyde **28** was then separately treated with Grignard reagents derived from 1-fluoro-4-iodobenzene (**31a**), 1-fluoro-3-iodobenzene (**31b**), and 1-fluoro-2-iodobenzene (**31c**, Scheme 3.9). Each Grignard reagent was formed *in situ* using iPrMgCl at 0 ˚C and, upon reaction at -100 ˚C with the benzaldehyde **28**, provided the corresponding benzhydrols **27a-c** in 64%, 63%, and 67% yield, respectively. In an effort to optimize the reaction sequence, we attempted to reduce the nitro group in **28** to the amine before Grignard addition as demonstrated by Wang and co-workers.[37] Unfortunately, upon addition of gross excess (6 eq.) of the Grignard reagent, degradation was observed with no detectable benzhydrol formation. Next, copper(II)-catalyzed oxidation of benzhydrols **27a-c** afforded the respective nitro benzophenones **32a**, **32b**, and **32c** in 62%, 64%, and 45%

yield. Subsequent NO_2 reduction with Fe/HCl provided the key amino benzophenones **23a-c** in up to 91% yield.

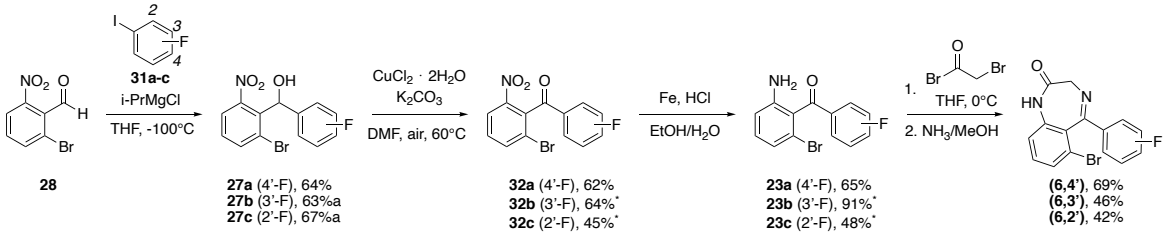

Scheme 3.9 Synthesis of the (6,X')-Flubromazepam Positional Isomers.

With the desired benzophenone intermediates in hand, we next focused on their conversions to the anticipated flubromazepam positional isomers. Benzophenone **23a** was first subjected to the standard protocol by Sternbach to generate the **(6,4')**-isomer in 69% yield. Similarly, the **(6,3')**-isomer was isolated in 46% yield from benzophenone **23b**. Finally, we were able to synthesize the **(6,2')**-isomer in 42% yield from **23c**. Unfortunately, it was found that upon isolation the synthesized **(6,X')**-isomers rapidly degrade (within about 4 hours-overnight), according to NMR. Although not ideal synthetically, this information is useful for forensic analysis as it eliminates the (6,X')-flubromazepam isomers from likely being readily prepared and abused compared to the other nine.

3.7 Summary

In conclusion, we have completed the synthesis of all twelve positional isomers of flubromazepam after devising a modular approach to the **(6,X')**-isomers. Although an initial approach involving the use of a thioether as a removable directing group for Friedel-Crafts acylation proved unsuccessful for the synthesis of respective **(6,X')**-isomers, proof of concept for the strategy was established. Ultimately, the successful approach involves

aryl Grignard attack on a *o*-nitrobenzaldehyde followed by an oxidation-reduction sequence to access the key aminobenzophenone precursors, which are readily converted to the benzodiazepines. This modular strategy offers a straightforward means to access other halogen-containing designer benzodiazepines (e.g., phenazepam and diclazepam) and their isomers for analysis.

3.8 Experimental

3.8.1 General Methods

Chromatographic purification was performed as flash chromatography with Silicycle SiliaFlash P60 silica gel (40-63μm) or preparative thin-layer chromatography (prep-TLC) using silica gel F254 (1000 μm) plates and solvents indicated as eluent with 0.1-0.5 bar pressure. For quantitative flash chromatography, technical grades solvents were utilized. Analytical thin-layer chromatography (TLC) was performed on Silicycle SiliaPlate TLC silica gel F254 (250 μm) TLC glass plates. Visualization was accomplished with UV light. Infrared (IR) spectra were obtained via attenuated total reflection (ATR) with a diamond plate using a Bruker ALPHA Fourier-transform infrared spectrophotometer. The IR bands are characterized as broad (br), weak (w), medium (m), and strong (s). Proton and carbon nuclear magnetic resonance spectra (^{1}H NMR and ^{13}C NMR) were recorded on a Varian Mercury Vx 300 MHz spectrometer or a Bruker 500 MHz spectrometer with solvent resonances as the internal standard (^{1}H NMR: $CDCl_3$ at 7.26 ppm or DMSO-d_6 at 2.50; ^{13}C NMR: $CDCl_3$ at 77.0 ppm or DMSO-d_6 at 39.5; ^{19}F NMR: locked to $CDCl_3$ or DMSO-d_6). ^{1}H NMR data are reported as follows: chemical shift (ppm), multiplicity (s = singlet, d = doublet, dd = doublet of doublets, dt = doublet of triplets, ddd = doublet of doublet of

doublets, t = triplet, m = multiplet, br = broad), coupling constants (Hz), and integration. Mass spectra were obtained through EI on a Micromass AutoSpec machine or through ESI on a Thermo Orbitrap XL. The accurate mass analyses run in EI mode were at a mass resolution of 10,000 and were calibrated using PFK (perfluorokerosene) as an internal standard. The accurate mass analyses run in EI mode were at a mass resolution of 30,000 using the calibration mixture supplied by Thermo. Uncorrected melting points were measured with a digital melting point apparatus (DigiMelt MPA 160).

3.8.2 Experimental Procedures

3-Bromo-2-(3-fluoro-4-(methylthio)benzoyl)benzoic acid (19): To a dry flask under nitrogen charged with a stir bar was added anhydrous $AlCl_3$ (1.17 g, 8.81 mmol), 3-bromophthalic anhydride (1.00 g, 4.41 mmol), and 2-fluorothioanisole (0.782 g, 5.51 mmol). The mixture was then stirred at 0°C and monitored by TLC until all starting material was consumed. Upon completion, the reaction was poured onto ice and extracted with CH_2Cl_2, washed with 10% sulfuric acid, and dried with $MgSO_4$. After work-up, the residue was purified by flash chromatography on silica gel (Hex/EtOAc) to afford compound **14** as an off-white solid (0.639 g, 39% yield). **^{1}H NMR** (500 MHz, $CDCl_3$) δ 8.13 (dd, *J* = 7.9, 1.1 Hz, 1H), 7.89 (dd, *J* = 8.0, 1.1 Hz, 1H), 7.48 – 7.43 (m, 3H), 7.26 – 7.19 (m, 1H), 2.53 (s, 3H). **13C{1H} NMR (126 MHz, $CDCl_3$)** 193.3, 169.4, 159.1 (d, *J* = 245.6 Hz), 142.4, 140.7, 138.2, 136.9, 134.2 (d, *J* = 6.0 Hz), 130.4 (d, *J* = 16.2 Hz), 129.3, 125.8 (d, *J* = 2.8 Hz), 125.4, 124.7, 120.4, 114.6 (d, *J* = 22.5 Hz), 14.2 (d, *J* = 2.1 Hz). **^{19}F NMR** (471 MHz, $CDCl_3$) δ -111.59 (dd, *J* = 10.6, 7.4 Hz). **HMRS (ESI)** *m/z:* [M+H] calc. for $C_{15}H_{11}O_3BrFS$, 368.9591; Found: 368.9590.

4-Bromo-3-(4-fluorophenyl)-3-hydroxyisobenzofuran-1(3*H*)-one (21): To a dry flask under nitrogen charged with a stir bar was added anhydrous $AlCl_3$ (1.17 g, 8.81 mmol), 3-bromophthalic anhydride **10** (1.00 g, 4.41 mmol), and fluorobenzene **15** (0.52 mL, 5.51 mmol). The mixture was then stirred at 0°C and monitored by TLC until all starting material was consumed. Upon completion, the reaction was poured onto ice and extracted with CH_2Cl_2, washed with 10% sulfuric acid, extracted with aqueous Na_2CO_3. The aqueous layer was then acidified with 10% sulfuric acid and extracted with CH_2Cl_2. The organic layer was then dried with $MgSO_4$ and concentrated under reduced pressure. After work-up, the crude material (1.13 g, 73% yield) was carried forwarded without any further purification. **^{1}H NMR** (500 MHz, $CDCl_3$) δ 8.12 (dd, *J* = 7.9, 1.1 Hz, 1H), 7.89 (dd, *J* = 8.1, 1.0 Hz, 1H), 7.78 (dd, *J* = 8.5, 5.4 Hz, 2H), 7.46 (t, *J* = 8.0 Hz, 1H), 7.13 (t, *J* = 8.7 Hz, 2H). **13C{1H} NMR (126 MHz, $CDCl_3$)** δ 169.0, 165.9 (d, *J* = 255.6 Hz), 142.7, 138.2, 132.7 (d, *J* = 2.9 Hz), 131.6 (d, *J* = 9.4 Hz), 130.3 (d, *J* = 20.1 Hz), 129.3, 120.4, 115.9 (d, *J* = 22.1 Hz), 29.7. **^{19}F NMR** (471 MHz, $CDCl_3$) δ -104.36. **HMRS (ESI)** *m/z:* [M+Na^+] calc. for $C_{14}H_8O_3BrFNa$, 344.9533; Found: 344.9530.

3-Bromo-2-(3-fluorobenzoyl)benzoic acid (24): Prepared according to the literature procedure established by Nakada et al.[18a] To a solution of aryl alkyl sulfide **19** (0.100 g, 0.271 mmol) and $PdCl_2$ (14.4 mg, 0.008 mmol, 3 mol %) in 2.36 mL of THF was added triethylsilane (0.091 mL, 0.569 mmol) under nitrogen. The resulting mixture was stirred at room temperature. After the reaction was complete, it was quenched with water, the aqueous layer was extracted with CH_2Cl_2, and the combined organic layers were dried over Na_2SO_4 and evaporated. The residue was purified by silica gel column chromatography using hexane/ethyl acetate as eluent to afford the title compound **24** as an off white solid

(0.016 g, 18% yield) **^{1}H NMR** (500 MHz, $CDCl_3$) δ 8.10 (ddd, *J* = 7.8, 1.4, 0.5 Hz, 1H), 7.69 (td, *J* = 7.5, 1.4 Hz, 1H), 7.60 (td, *J* = 7.6, 1.4 Hz, 1H), 7.48 – 7.34 (m, 4H). **13C{1H} NMR (126 MHz, $CDCl_3$)**δ 195.7, 169.8, 162.7 (d, *J* = 248.1 Hz), 142.1, 139.2 (d, *J* = 6.4 Hz), 133.4, 131.0, 130.2 (d, *J* = 7.7 Hz), 129.8, 127.7 (d, *J* = 6.5 Hz), 125.2 (d, *J* = 2.9 Hz), 120.2 (d, *J* = 21.6 Hz), 115.8 (d, *J* = 22.3 Hz). **^{19}F NMR** (471 MHz, $CDCl_3$) δ -111.91 (td, *J* = 8.7, 5.0 Hz). **HMRS (ESI)** *m/z:* [M+Na] calc. for $C_{14}H_8O_3BrFNa$, 344.9533; Found: 344.9531.

3-Bromo-2-(3-fluoro-4-(methylthio)benzoyl)benzoyl azide (25): Azide **25** was prepared according to the literature procedure adopted from Brouet et al.[24] To a dry flask charged with a stir bar and carboxylic acid **19** (0.100 g, 0.271 mmol) under nitrogen was added benzene (1.35 mL) to make a 0.2 M solution. Triethylamine (0.038 mL, 0.271 mmol) was then added, and the reaction was stirred for 30 min. Diphenylphosphorazidate (DPPA) (0.058 mL, 0.271 mmol) was then added dropwise, and the resulting reaction mixture was stirred for 40 min. The solvent was removed *in vacuo* and the resulting oil was carried forward crude.

General Grignard Coupling Procedure: (2-Bromo-6-nitrophenyl)(X-fluorophenyl)methanol **27** was prepared according to a modified literature procedure adapted from Wang et al.[23] Isopropyl magnesium chloride (1.1 eq., 2M in THF) was added dropwise to a solution of X-fluoroiodobenzene **31** (1.1 eq.) in THF (1.1M) at 0°C. The mixture was allowed to stir for 1 h at 0°C, then cooled to -100 ˚C. Once cooled, 2-bromo-6-nitrobenzaldehyde **23** (1 eq.) was dissolved in THF (1M) and added dropwise over 30 min. After 1 h, the reaction was warmed to room temperature and stirred overnight. Upon

completion, the reaction was quenched with NH_4Cl and extracted with EtOAc (x3). The organic phase was separated and washed with water and brine and dried over Na_2SO_4. The combined organic layers were concentrated under reduced pressure and the crude material was carried forward or purified by prep TLC using EtOAc/Hexanes.

(2-Bromo-6-nitrophenyl)(4-fluorophenyl)methanol (27a): Prepared following general coupling procedure. Isopropyl magnesium chloride (2.39 mL, 2 M in THF, 4.78 mmol) and 4-fluoroiodobenzene **31a** (0.553 mL, 4.78 mmol) in THF (4.78 mL) were stirred for 1 hour at 0˚C before cooling to -100°C. 2-bromo-6-nitrobenzaldehyde (1.00 g, 4.34 mmol) in THF (4.78 mL) was added to the mixture over 30 min and stirred at -100°C for 1 h then warmed to room temperature and allowed to stir overnight. After work up, the crude material (1.46 g) was carried forward or purified by silica preparatory TLC (EtOAc/Hexanes) for analysis to afford compound **27a** as a dark green solid (0.868 g, 64% yield). Quantitative NMR yield calculated using dimethyl terephthalate (6.7 mg) as internal standard and a portion of the crude pdt (0.0238 g). Total crude mass = 1.45 g. **^{1}H NMR** (500 MHz, $CDCl_3$) δ 7.87 (dd, *J* = 8.0, 1.3 Hz, 1H), 7.69 (dd, *J* = 8.1, 1.2 Hz, 1H), 7.37 (t, *J* = 8.1 Hz, 1H), 7.27 – 7.24 (m, 2H), 7.05 – 6.99 (m, 2H), 6.42 (s, 1H), 3.37 (s, 1H). **13C{1H} NMR (126 MHz, $CDCl_3$)** 162.3 (d, *J* = 247.0 Hz), 151.4, 137.5, 136.0 (d, *J* = 3.2 Hz), 135.8, 129.9, 127.9 (d, *J* = 8.2 Hz), 125.9, 124.3, 115.4 (d, *J* = 21.7 Hz), 73.9. **^{19}F NMR** (471 MHz, Chloroform-*d*) δ -114.26 – -114.47 (m). **IR** 3530 (br), 3410 (s), 3082 (w), 2358 (w), 1600 (m), 1535 (s), 1508 (s) 1368 (m), 1224 (m), 841 (s), 682 (m**)** cm^{-1}. **HMRS (ESI)** *m/z:* $[M+Cl]^-$ calc. for $C_{13}H_9BrFNO_3Cl$, 359.9443; Found, 359.9442.

(2-Bromo-6-nitrophenyl)(3-fluorophenyl)methanol (27b): Prepared following general coupling procedure. Isopropyl magnesium chloride (0.478 mL, 2 M in THF, 0.956 mmol) and 3-fluoroiodobenzene **31b** (0.111 mL, 0.956 mmol) in THF (0.87 mL) were stirred for 1 h at 0 ˚C before cooling to -100 ˚C. 2-bromo-6-nitrobenzaldehyde (0.208 g, 0.869 mmol) in THF (0.87 mL) was added to the mixture over 30 min and stirred at -100˚C for 1 h then warmed to room temperature and allowed to stir overnight. After work up, the crude material (0.2761 g) was carried forward or purified by silica preparatory TLC (EtOAc/Hexanes) for analysis to afford compound **27b** as a brown solid (0.172 g, 58% yield). Quantitative NMR yield calculated using dimethyl terephthalate (5.2mg) as internal standard and a portion of the crude pdt (0.0267 g). Total crude mass = 0.2761 g. **^{1}H NMR** (500 MHz, $CDCl_3$) δ 7.90 (dd, *J* = 8.0, 1.2 Hz, 1H), 7.72 (dd, *J* = 8.1, 1.3 Hz, 1H), 7.40 (t, *J* = 8.1 Hz, 1H), 7.30 (ddd, *J* = 8.2, 6.4, 1.8 Hz, 1H), 7.06 – 6.97 (m, 3H), 6.47 (d, *J* = 9.3 Hz, 1H), 3.65 (d, *J* = 9.6 Hz, 1H). **13C{1H} NMR (126 MHz, $CDCl_3$)** δ 162.9 (d, *J* = 246.3 Hz), 151.3, 143.01 (d, *J* = 6.9 Hz), 137.6, 135.5, 130.0 (d, *J* = 9.1 Hz), 126.1, 124.4, 121.5 (d, *J* = 3.0 Hz), 114.7 (d, *J* = 21.3 Hz), 113.2 (d, *J* = 23.0 Hz), 73.6 (d, *J* = 1.9 Hz). **^{19}F NMR** (471 MHz, Chloroform-*d*) δ -112.35 – -112.43 (m). **IR** 3500 (br), 1533 (s), 1403 (m), 1370 (m), 1250 (m), 1040 (m), 712 (m), 690 (s), 540 (m) cm^{-1}. **HMRS (ESI)** *m/z:* $[M+Cl]^-$ calc. for $C_{13}H_9BrFNO_3Cl$, 359.9443; Found, 359.9443.

(2-Bromo-6-nitrophenyl)(2-fluorophenyl)methanol (27c): Prepared following general coupling procedure. Isopropyl magnesium chloride (1.09 mL, 2 M in THF, 2.17 mmol) and 2-fluoroiodobenzene **26c** (0.254 mL, 2.17 mmol) in THF (0.870 mL) were stirred for 1 hour at 0˚C before cooling to -100 ˚C. 2-bromo-6-nitrobenzaldehyde (0.200 g, 0.869 mmol) in THF (0.870 mL) was added to the mixture over 30 min and stirred at -100˚C for

1 h then warmed to room temperature and allowed to stir overnight. After work up, the crude material was carried forward or purified by silica preparatory TLC (EtOAc/Hexanes) for analysis to afford compound **31c** as a yellow solid (0.195 g, 67% yield). **^{1}H NMR** (500 MHz, $CDCl_3$) δ = 7.85 (dd, *J* = 8.1, 1.3 Hz, 1H), 7.61 (dd, *J* = 8.1, 1.3 Hz, 1H), 7.41 (td, *J* = 7.8, 1.8 Hz, 1H), 7.38 – 7.30 (m, 2H), 7.16 (td, *J* = 7.6, 1.2 Hz, 1H), 7.02 (ddd, *J* = 10.7, 8.2, 1.2 Hz, 1H), 6.63 (d, *J* = 8.4 Hz, 1H), 3.41 (d, *J* = 8.8 Hz, 1H). **13C{1H} NMR (126 MHz, $CDCl_3$)** δ 160.1 (d, *J* = 247.4 Hz), 151.5, 137.1, 134.8, 130.1 (d, *J* = 8.2 Hz), 129.7, 128.8 (d, *J* = 3.3 Hz), 126.9 (d, *J* = 13.0 Hz), 125.8, 124.0 (d, *J* = 3.4 Hz), 123.9, 115.4 (d, *J* = 21.3 Hz), 70.2 (d, *J* = 2.7 Hz). **^{19}F NMR** δ = -116.45 – -116.53 (m). **IR** 3530 (br), 3400 (s), 1531 (s), 1409 (s), 1360 (s), 1230 (s), 1150 (s), 1030 (s), 815 (s), 631 (m) cm^{-1}. **HMRS (ESI)** *m/z:* $[M+Na]^+$ calc. for $C_{13}H_9BrFNO_3Na$, 347.9642; Found, 347.9644.

General Benzhydrol Oxidation Procedure: (2-Bromo-6-nitrophenyl)(X-fluorophenyl)methanone **32** was prepared according to a modified literature procedure adapted from Wang et al.[23] (2-bromo-6-nitrophenyl)(X-fluorophenyl)methanol **27** (1 eq.) was dissolved in DMF (0.13M) with $CuCl_2 \cdot 2H_2O$ (0.1 eq.) and K_2CO_3 (2 eq.). The mixture was then stirred at 60˚C (in an oil bath) in air for 24 h. Upon completion the reaction mixture was diluted with water, extracted with EtOAc (3x), washed with water (x3) and brine (x1), and dried over Na_2SO_4. The combined organic layers were concentrated under reduced pressure and the crude material was carried forward or purified by prep TLC using EtOAc/Hexanes.

(2-Bromo-6-nitrophenyl)(4-fluorophenyl)methanone (32a): Prepared following general oxidation procedure. (2-bromo-6-nitrophenyl)(4-fluorophenyl)methanol **27a** (0.867 g,

2.66 mmol) was dissolved in DMF (20.0 mL) with $CuCl_2 \cdot 2H_2O$ (0.0454 g, 0.266 mmol) and K_2CO_3 (0.735 g, 5.32 mmol). The mixture was then stirred at 60°C (in an oil bath) in air for 24 h. After work up, the crude material (1.67 g) was carried forward or purified by silica preparatory TLC (EtOAc/Hexanes) for analysis to afford compound **32a** as a brown solid (0.537 g, 62% yield). Quantitative NMR yield calculated using dimethyl terephthalate (7.5 mg) as internal standard and a portion of the crude pdt (0.0644 g). Total crude mass = 1.67 g. **^{1}H NMR** (500 MHz, $CDCl_3$) δ 8.30 (dq, *J* = 8.4, 1.0 Hz, 1H), 8.00 (dt, *J* = 8.0, 1.1 Hz, 1H), 7.87 – 7.82 (m, 2H), 7.58 (td, *J* = 8.2, 0.8 Hz, 1H), 7.18 (tt, *J* = 8.2, 1.0 Hz, 2H). **13C{1H} NMR (126 MHz, $CDCl_3$)** δ 190.1, 166.3 (d, *J* = 256.9 Hz), 147.2, 139.0, 136.5, 131.8, 131.7, 130.9, 123.9, 121.3, 116.4 (d, *J* = 22.2 Hz). **^{19}F NMR** (471 MHz, $CDCl_3$) δ -102.91 – -103.09 (m). **IR** 1710 (s), 1680 (s), 1594 (s), 1519 (s), 1343 (s), 1260 (s), 1223 (s), 1096 (s) ,925 (s), 719 (s), 625 (s), 531 (w) cm^{-1}. **HMRS (APCI)** *m/z:* $[M+H]^+$ calc. for $C_{13}H_8BrFNO_3$**,** 323.9666; Found, 323.9666.

(2-Bromo-6-nitrophenyl)(3-fluorophenyl)methanone (32b): Prepared following general oxidation procedure. (2-bromo-6-nitrophenyl)(3-fluorophenyl)methanol **27b** (1.45 g, 4.46 mmol) was dissolved in DMF (32.7 mL) with $CuCl_2 \cdot 2H_2O$ (0.0760 g, 0.446 mmol) and K_2CO_3 (1.23 g, 8.92 mmol). The mixture was then stirred at 60˚C (in an oil bath) in air for 24 h. After work up, the crude material (1.09 g) was carried forward or purified by silica preparatory TLC (EtOAc/Hexanes) for analysis to afford compound **32b** as a brown solid (0.9280 g, 64% yield). Quantitative NMR yield calculated using dimethyl terephthalate (7.3 mg) as internal standard and a portion of the crude pdt (0.0234 g). Total crude mass = 1.09 g. **^{1}H NMR** (500 MHz, $CDCl_3$) δ 8.31 (dd, *J* = 8.4, 1.0 Hz, 1H), 8.02 (dd, *J* = 8.0, 1.0 Hz, 1H), 7.62 – 7.52 (m, 3H), 7.48 (td, *J* = 8.1, 5.4 Hz, 1H), 7.34 (tdd, *J* =

8.2, 2.5, 1.2 Hz, 1H). **13C{1H} NMR (126 MHz, $CDCl_3$)** δ 190.4 (d, *J* = 2.7 Hz), 163.0 (d, *J* = 248.9 Hz), 147.2, 139.0, 137.3 (d, *J* = 6.4 Hz), 136.3, 131.1, 130.8 (d, *J* = 7.7 Hz), 124.9 (d, *J* = 3.1 Hz), 123.9, 121.3, 121.1, 115.6 (d, *J* = 22.7 Hz). **^{19}F NMR** (500 MHz, $CDCl_3$) δ -111.14 – -111.24 (m). **IR** 1620 (s), 1589 (m), 1532 (s), 1459 (s), 1348 (s), 1269 (s), 1129 (s), 965 (s), 673 (m), 522 (w) cm^{-1}. **HMRS (APCI)** *m/z:* $[M+H]^+$ calc. for $C_{13}H_8BrFNO_3$, 322.9587; Found, 322.9594.

(2-Bromo-6-nitrophenyl)(2-fluorophenyl)methanone (32c): Prepared following general oxidation procedure. (2-bromo-6-nitrophenyl)(2-fluorophenyl)methanol **27c** (1.00 g, 3.07 mmol) was dissolved in DMF (23.1 mL) with $CuCl_2{\cdot}2H_2O$ (0.0523 g, 0.307 mmol) and K_2CO_3 (0.848 g, 6.13 mmol). The mixture was then stirred at 60˚C (in an oil bath) in air for 24 h. After work up, the crude material (0.8268 g) was carried forward or purified by silica preparatory TLC (EtOAc/Hexanes) for analysis to afford compound **32c** as a brown solid (0.372 g, 41% yield). **^{1}H NMR** (500 MHz, $CDCl_3$) δ 8.27 (dd, *J* = 8.4, 1.1 Hz, 1H), 8.15 (td, *J* = 7.7, 1.9 Hz, 1H), 7.96 (dd, *J* = 8.0, 1.0 Hz, 1H), 7.62 (dddd, *J* = 8.4, 7.1, 5.0, 1.9 Hz, 1H), 7.51 (t, *J* = 8.2 Hz, 1H), 7.36 (td, *J* = 7.6, 1.1 Hz, 1H), 7.09 (ddd, *J* = 11.3, 8.4, 1.1 Hz, 1H). **13C{1H} NMR (126 MHz, $CDCl_3$)** δ 187.7, 162.1 (d, *J* = 257.5 Hz), 146.4, 138.9, 138.8, 136.1 (d, *J* = 9.2 Hz), 131.1, 130.4, 124.9 (d, *J* = 3.5 Hz), 123.8, 123.7, 119.9 (d, *J* = 2.4 Hz), 116.8 (d, *J* = 22.7 Hz). **^{19}F NMR** (471 MHz, $CDCl_3$) δ -111.36 (dt, *J* = 11.7, 6.1 Hz). **IR** 1670 (s), 1607 (s), 1526 (s), 1350 (s), 1210 (s), 1100 (s), 720 (s), 928 (s), 636 (s), 542 (s) cm^{-1}. **HMRS (ESI)** *m/z:* $[M+Na]^+$ calc. for $C_{13}H_7BrFNO_3Na$, 345.9485; Found, 345.9492.

General NO_2 Reduction Procedure: (2-Amino-6-bromophenyl)(X-fluorophenyl)methanone **23** was prepared according to a modified literature procedure

adapted from Wang et al.[23] (2-Bromo-6-nitrophenyl)(X-fluorophenyl)methanone **32** (1 eq.) was dissolved in EtOH (0.33M) and H_2O (1.3M). Once dissolved, iron powder (2.5 eq.) was added along with 3 drops of concentrated HCl. The reaction was then heated in an oil bath at reflux for 1h. After consumption of the starting material detected my TLC, the reaction was filter through a pad of celite using EtOAc. The filtrate was washed with water and brine then dried over Na_2SO_4. The combined organic layers were concentrated under reduced pressure and the crude material was purified by column chromatography using EtOAc/Hexanes.

(2-Amino-6-bromophenyl)(4-fluorophenyl)methanone (23a): Prepared following the general reduction procedure. (2-Bromo-6-nitrophenyl)(4-fluorophenyl)methanone **32a** (0.537 g, 1.66 mmol) was dissolved in EtOH (5.02 mL) and H_2O (1.27 mL) Once dissolved, iron powder (0.231 g, 4.14 mmol) was added along with 3 drops of concentrated HCl. The reaction was then heated in an oil bath at reflux for 1 h. After work-up, the crude material was purified by column chromatography (EtOAc/Hexanes) to afford compound **23a** as a yellow solid (0.316 g, 65% yield). **^{1}H NMR** (500 MHz, Chloroform-*d*) δ 7.93 – 7.87 (m, 2H), 7.18 – 7.09 (m, 3H), 7.00 (dd, *J* = 7.9, 0.9 Hz, 1H), 6.73 (dd, *J* = 8.1, 1.0 Hz, 1H), 4.03 (s, 2H). **13C{1H} NMR (126 MHz, $CDCl_3$)** δ 195.5, 166.3 (d, *J* = 256.2 Hz), 146.1, 133.2 (d, *J* = 3.0 Hz), 132.5 (d, *J* = 9.6 Hz), 131.5, 125.2, 122.4, 120.4, 116.1 (d, *J* = 22.1 Hz), 115.4. **^{19}F NMR** (471 MHz, Chloroform-*d*) δ -103.57 (ddd, *J* = 13.9, 9.0, 5.3 Hz). **IR** 3466 (s), 3372 (s), 1661 (m), 1590 (s), 1460 (s), 1271(s), 927 (s), 616 (s), 579 (s) cm^{-1} **HMRS (ESI)** *m/z:* $[M+H]^+$ calc. for $C_{13}H_{10}ONBrF$, 293.9924; Found, 293.9920.

(2-Amino-6-bromophenyl)(3-fluorophenyl)methanone (23b): Prepared following the general reduction procedure. (2-Bromo-6-nitrophenyl)(3-fluorophenyl)methanone **32b**

(0.828 g, 2.55 mmol) was dissolved in EtOH (13.2 mL) and H_2O (3.34 mL). Once dissolved, iron powder (0.357 g, 6.39 mmol) was added along with 3 drops of concentrated HCl. The reaction was then heated in an oil bath at reflux for 1h. After work-up, the crude material was purified by preparative TLC (EtOAc/Hexanes) to afford compound **23b** as a yellow solid (0.680 g, 91% yield). **^{1}H NMR** (500 MHz, $CDCl_3$) δ 7.62 (dt, *J* = 7.7, 1.3 Hz, 1H), 7.57 (ddd, *J* = 9.2, 2.7, 1.5 Hz, 1H), 7.45 (td, *J* = 8.0, 5.4 Hz, 1H), 7.31 (tdd, *J* = 8.2, 2.6, 1.0 Hz, 1H), 7.11 (t, *J* = 8.0 Hz, 1H), 7.00 (dd, *J* = 7.9, 0.9 Hz, 1H), 6.74 (dd, *J* = 8.1, 1.0 Hz, 1H), 3.90 (s, 2H). **13C{1H} NMR (126 MHz, $CDCl_3$)** δ 195.9 (d, *J* = 2.4 Hz), 162.9 (d, *J* = 248.2 Hz), 146.4, 139.1 (d, *J* = 6.4 Hz), 131.8, 130.5 (d, *J* = 7.7 Hz), 125.6 (d, *J* = 3.1 Hz), 124.8, 122.4, 120.8 (d, *J* = 21.4 Hz), 120.5, 116.1 (d, *J* = 22.6 Hz), 115.4. **^{19}F NMR** (471 MHz, $CDCl_3$) δ -111.74 (td, *J* = 8.6, 5.2 Hz). **IR** 3480 (s), 3378 (s), 1665 (s), 1620 (m), 1590 (s), 1440 (s), 1270 (s), 964 (m), 658 (m), 525 (w) cm^{-1} **HMRS (APCI)** *m/z:* $[M+H]^+$ calc. for $C_{13}H_{10}BrFNO$, 293.9924; Found, 293.9924.

(2-Amino-6-bromophenyl)(2-fluorophenyl)methanone (23c): Prepared following general procedure. (2-bromo-6-nitrophenyl)(2-fluorophenyl)methanone **32c** (0.717 g, 2.21 mmol) was dissolved in EtOH (6.71 mL) and H_2O (1.70 mL). Once dissolved, iron powder (0.309 g, 5.53 mmol) was added along with 3 drops of concentrated HCl. The reaction was then heated in an oil bath at reflux for 1h. After work-up, the crude material was purified by column chromatography (EtOAc/Hexanes) to afford compound **23c** as a yellow solid (0.313 g, 48% yield). **^{1}H NMR** (500 MHz, $CDCl_3$) δ 7.69 (td, *J* = 7.6, 1.8 Hz, 1H), 7.58 – 7.53 (m, 1H), 7.24 (td, *J* = 7.6, 1.1 Hz, 1H), 7.16 – 7.06 (m, 2H), 6.95 (dd, *J* = 7.9, 1.0 Hz, 1H), 6.73 (dd, *J* = 8.1, 1.0 Hz, 1H), 4.41 (s, 2H). **13C{1H} NMR (126 MHz, $CDCl_3$)** δ 194.3, 161.5 (d, *J* = 258.2 Hz), 147.1, 134.7 (d, *J* = 9.0 Hz), 132.1, 131.4, 127.2 (d, *J* =

10.0 Hz), 125.4, 124.5 (d, J = 3.7 Hz), 122.5, 121.1 (d, J = 1.8 Hz), 116.7 (d, J = 21.9 Hz), 115.7. **^{19}F NMR** (471 MHz, $CDCl_3$) δ -112.20 (dt, J = 11.6, 6.3 Hz). **IR** 3473 (m), 3381 (s), 1656 (s), 1605 (s), 1460 (s), 1270 (s), 928 (s), 773 (s) 652 (s), 541(w) cm^{-1} **HMRS (ESI)** *m/z:* $[M+Na]^+$ calc. for $C_{13}H_9BrFNONa$, 315.9743; Found, 315.9749.

General Procedure for Benzodiazepine Formation: 6-bromo-5-(X-fluorophenyl)-1,3-dihydro-2*H*-benzo[*e*][1,4]diazepin-2-ones were prepared according to the literature procedure adapted by France et al.[7] (2-Amino-6-bromophenyl)(X-fluorophenyl)methanone (1 eq.) was dissolved in anhydrous THF (0.2M) and cooled to 0˚C. Bromoacetyl bromide (1.3 eq.) was slowly added to the mixture dropwise. The reaction mixture was allowed to stir for 1h then quenched with water. The aqueous layer was extracted with EtOAc (x3) and the combined organic layers were washed with aqueous NaOH (0.5M in water), dried over Na_2SO_4, filtered through celite, and concentrated by rotary evaporation. The crude N-acylated product was dissolved in a solution of ammonia in methanol (0.08M, 7N NH_3/MeOH) and stirred for 18 h. The mixture was then concentrated by rotary evaporation then partitioned between Et_2O and H_2O. The aqueous layer was extracted with Et_2O (3x) and the combined organic layers were dried over Na_2SO_4, filtered through celite, and concentrated by rotary evaporation. The crude product was purified by silica preparatory thin-layer chromatography (1% MeOH/CH_2Cl_2).

(6,4')-Flubromazepam [6-Bromo-5-(4-fluorophenyl)-1,3-dihydro-2*H*-benzo[*e*][1,4]diazepin-2-one]: Prepared following general procedure using (2-amino-6-bromophenyl)(4-fluorophenyl)methanone **23a** (0.143 g, 0.485 mmol) and bromoacetyl bromide (0.055 mL, 0.631 mmol) in THF (2.43 mL). The reaction mixture was allowed to stir for 1 h then worked up. The crude N-acylated product was dissolved in a solution of

ammonia in methanol (6.06 mL, 0.08M, 7N NH_3/MeOH) and stirred for 18h. The crude product was purified by silica preparatory thin-layer chromatography (1% MeOH/CH_2Cl_2) to afford the **(6,4)-isomer** as a yellow solid (0.111 g, 69% yield). **^{1}H NMR** (300 MHz, $CDCl_3$) δ 9.78 (s, 1H), 8.29 (dt, *J* = 6.5, 1.7 Hz, 1H), 7.85 (ddd, *J* = 10.5, 5.5, 2.7 Hz, 2H), 7.43 – 7.32 (m, 2H), 7.12 (td, *J* = 8.1, 7.5, 1.8 Hz, 2H), 3.31 (d, *J* = 2.2 Hz, 2H). **13C{1H} NMR (126 MHz, $CDCl_3$)** δ 194.2, 171.3, 166.5(d, *J* = 257.1 Hz), 136.4, 132.6 (d, *J* = 9.7 Hz), 131.4, 130.7, 128.4, 128.2, 121.1, 120.8, 119.3, 116.2 (d, *J* = 22.2 Hz), 44.9. **^{19}F NMR** (471 MHz, $CDCl_3$) δ -102.56 (td, *J* = 8.9, 8.5, 4.6 Hz). **IR** 3479 (w), 3387 (w), 2921 (m), 2851 (m), 2362 (m), 1666 (s), 1567 (m), 1552 (m), 1209 (m) 829 (w), 675 (m) cm^{-1} **HMRS (ESI)** *m/z:* $[M+H]^+$ calc. for $C_{15}H_{11}ON_2BrF$, 333.0033; Found, 333.0030.

(6,3')-Flubromazepam [6-Bromo-5-(3-fluorophenyl)-1,3-dihydro-2*H*-benzo[*e*][1,4]diazepin-2-one]: Prepared following general procedure using (2-amino-6-bromophenyl)(3-fluorophenyl)methanone **23b** (0.141 g, 0.478 mmol) and bromoacetyl bromide (0.0540 mL, 0.621 mmol) in THF (2.39 mL). The reaction mixture was allowed to stir for 1 h then worked up. The crude *N*-acylated product was dissolved in a solution of ammonia in methanol (5.98 mL, 0.08M, 7N NH_3/MeOH) and stirred for 18h. The crude product was purified by silica preparatory thin-layer chromatography (1% MeOH/CH_2Cl_2) to afford the **(6,3)-isomer** as a yellow solid (0.052 g, 46% yield). **^{1}H NMR** (500 MHz, $CDCl_3$) δ 9.83 (s, 1H), 8.31 (dt, *J* = 8.4, 2.6 Hz, 1H), 7.61 – 7.52 (m, 2H), 7.47 – 7.30 (m, 4H), 3.34 (s, 2H). **13C{1H} NMR (126 MHz, $CDCl_3$)** δ 194.7, 171.4, 162.9 (d, *J* = 248.9 Hz), 138.3 (d, *J* = 6.4 Hz), 136.6, 131.7, 130.6 (d, *J* = 7.7 Hz), 130.4, 128.4, 125.9 (d, *J* = 3.0 Hz), 121.3 (d, *J* = 21.7 Hz), 121.0, 119.4, 116.0 (d, *J* = 22.6 Hz), 44.9. **^{19}F NMR** (471 MHz, $CDCl_3$) δ -111.21 (q, *J* = 8.0 Hz). **IR** 3255 (br), 2921 (w), 2360 (w), 1704 (s), 1672

(s), 1267 (s), 962 (m), 836 (s) cm^{-1}. **HMRS (APCI)** *m/z:* $[M+H]^+$ calc. for $C_{15}H_{11}BrFN_2O$, 333.0033; Found, 333.0039.

(6,2')-Flubromazepam [6-Bromo-5-(2-fluorophenyl)-1,3-dihydro-2*H*-benzo[*e*][1,4]diazepin-2-one]: Prepared following general procedure using (2-amino-6-bromophenyl)(2-fluorophenyl)methanone **23c** (0.103 g, 0.340 mmol) and bromoacetyl bromide (0.0390 mL, 0.442 mmol) in THF (1.70 mL). The reaction mixture was allowed to stir for 1h then worked up. The crude *N*-acylated product was dissolved in a solution of ammonia in methanol (4.25 mL, 0.08M, 7N NH_3/MeOH) and stirred for 18h. The crude product was purified by silica preparatory thin-layer chromatography (1% MeOH/CH_2Cl_2) to afford the **(6,2)-isomer** as a yellow solid (0.0471 g, 40% yield). **^{1}H NMR** (500 MHz, Chloroform-*d*) δ 10.08 (s, 1H), 8.32 (dd, *J* = 7.8, 1.6 Hz, 1H), 7.74 (td, *J* = 7.6, 1.9 Hz, 1H), 7.59 (dddd, *J* = 8.5, 7.0, 4.9, 1.8 Hz, 1H), 7.39 – 7.32 (m, 2H), 7.25 (td, *J* = 7.6, 1.1 Hz, 1H), 7.14 (ddd, *J* = 10.9, 8.3, 1.1 Hz, 1H), 3.40 (s, 2H). **13C{1H} NMR (126 MHz, $CDCl_3$)** δ 192.9, 171.4, 161.8 (d, *J* = 260.2 Hz), 136.5, 135.6 (d, *J* = 9.1 Hz), 131.7, 131.7, 131.7, 128.5, 125.9 (d, *J* = 9.3 Hz), 124.5 (d, *J* = 3.9 Hz), 121.1, 119.4 (d, *J* = 2.0 Hz), 116.9 (d, *J* = 22.0 Hz), 45.0. **^{19}F NMR** (471 MHz, Chloroform-*d*) δ -110.56 (dt, *J* = 11.4, 5.9 Hz).). **IR** 3255 (br), 3080 (w), 2922 (w), 2360 (w), 1670 (s), 1606 (s), 1563 (s), 1446 (s), 1290 (s), 927 (s), 757 (s) cm^{-1}. **HMRS (ESI)** *m/z:* $[M+H]^+$ calc. for $C_{15}H_{11}BrFN_2O$, 333.0033; Found, 333.0041.

3.8.3 NMR Spectra

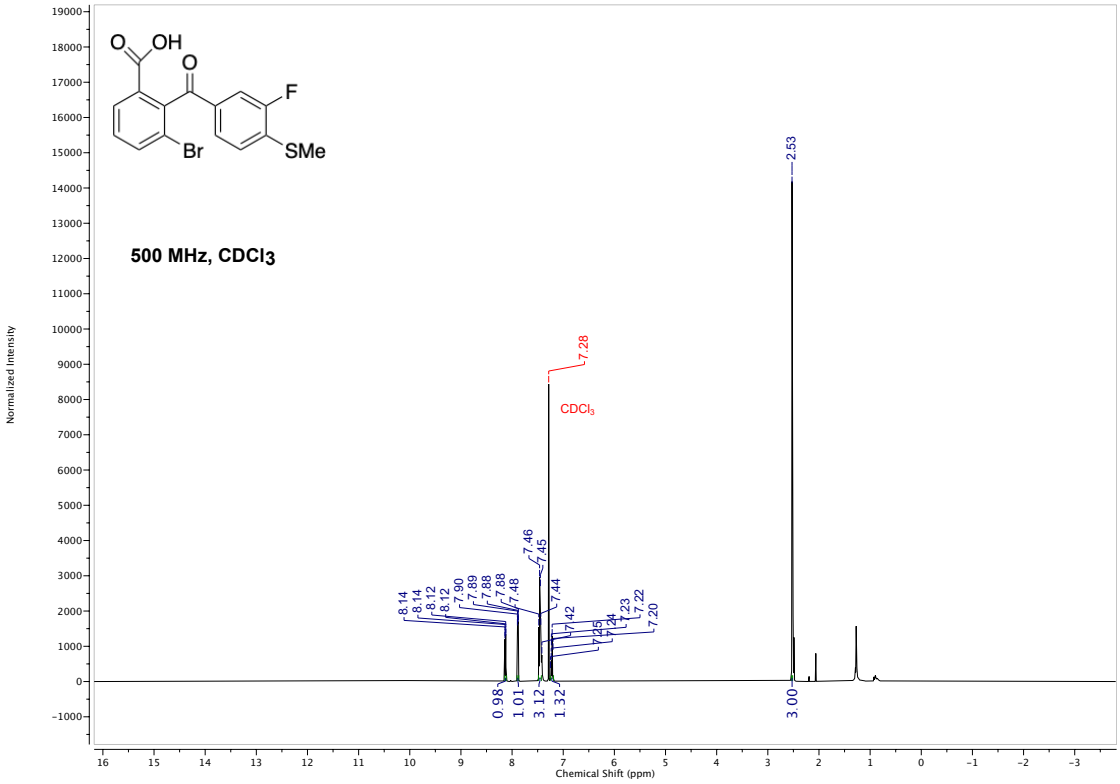

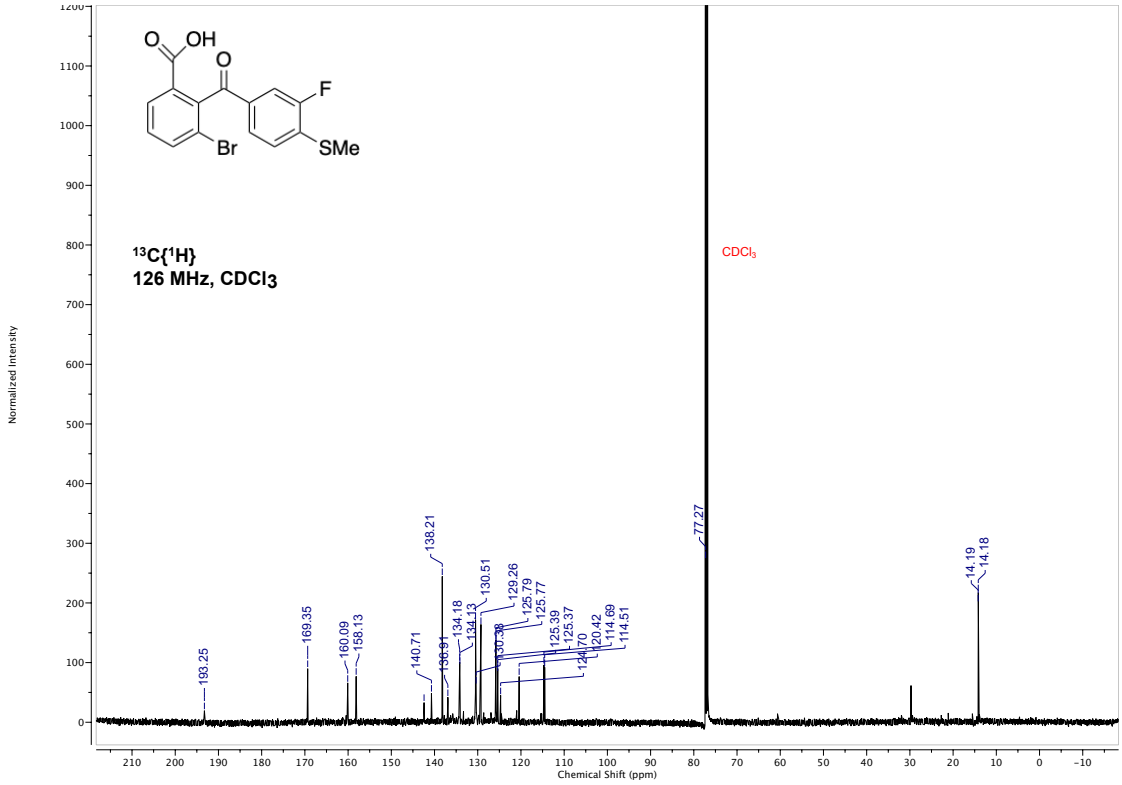
O
OH
O
F
Br
SMe
$^{13}C\{^{1}H\}$
126 MHz, $CDCl_3$
$CDCl_3$
Normalized Intensity
Chemical Shift (ppm)
193.25
169.35
160.09
158.13
140.71
138.21
136.91
134.18
134.13
130.51
129.26
125.79
125.77
125.39
125.37
124.70
120.42
114.69
114.51
77.27
14.19
14.18

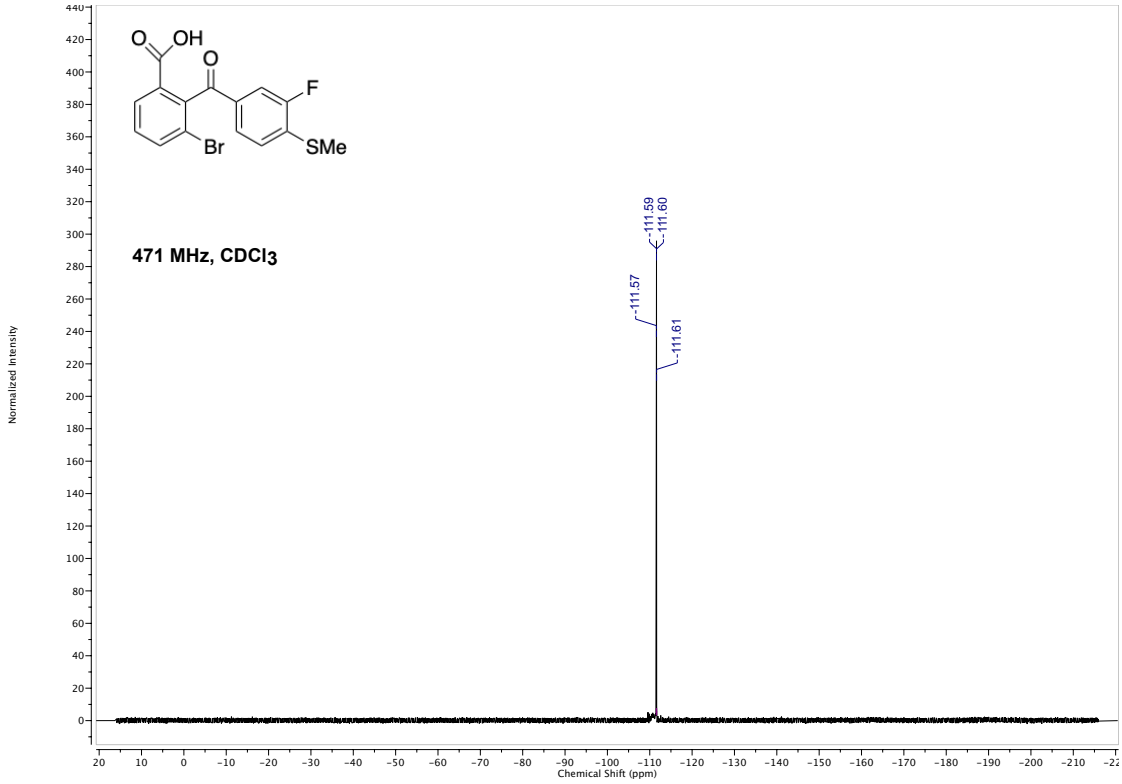
O
OH
O
F
Br
SMe
471 MHz, $CDCl_3$
Normalized Intensity
Chemical Shift (ppm)
111.59
111.60
111.57
111.61

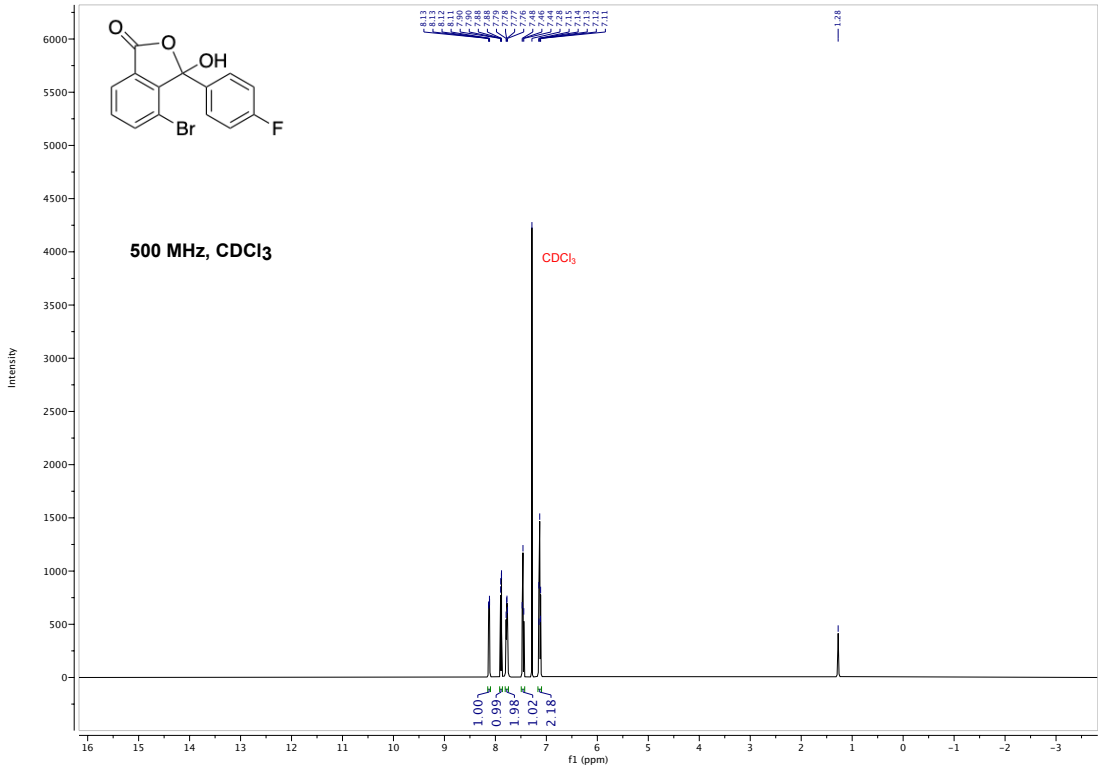
500 MHz, CDCl3
CDCl3
Intensity
f1 (ppm)
1.00
0.99
1.98
1.02
2.18
Br
F
OH

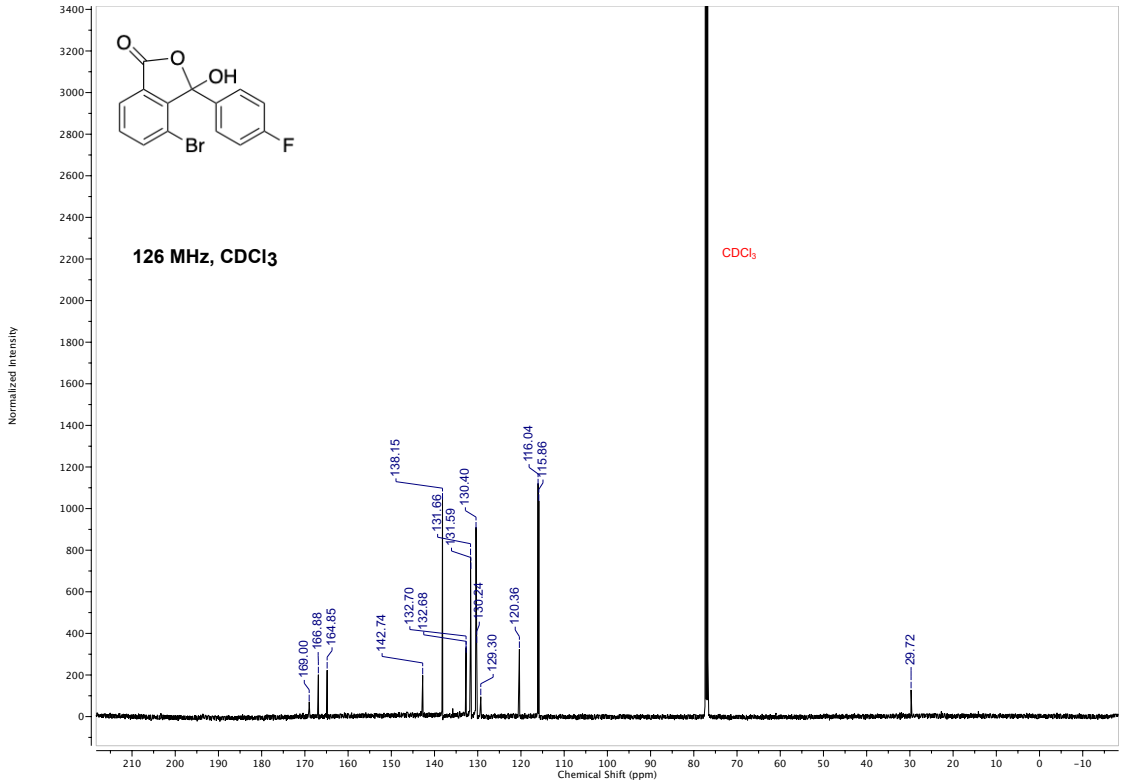
126 MHz, CDCl3
CDCl3
Normalized Intensity
Chemical Shift (ppm)
169.00
166.88
164.85
142.74
138.15
132.70
132.68
131.66
131.59
130.40
130.24
129.30
120.36
116.04
115.86
29.72
Br
F
OH

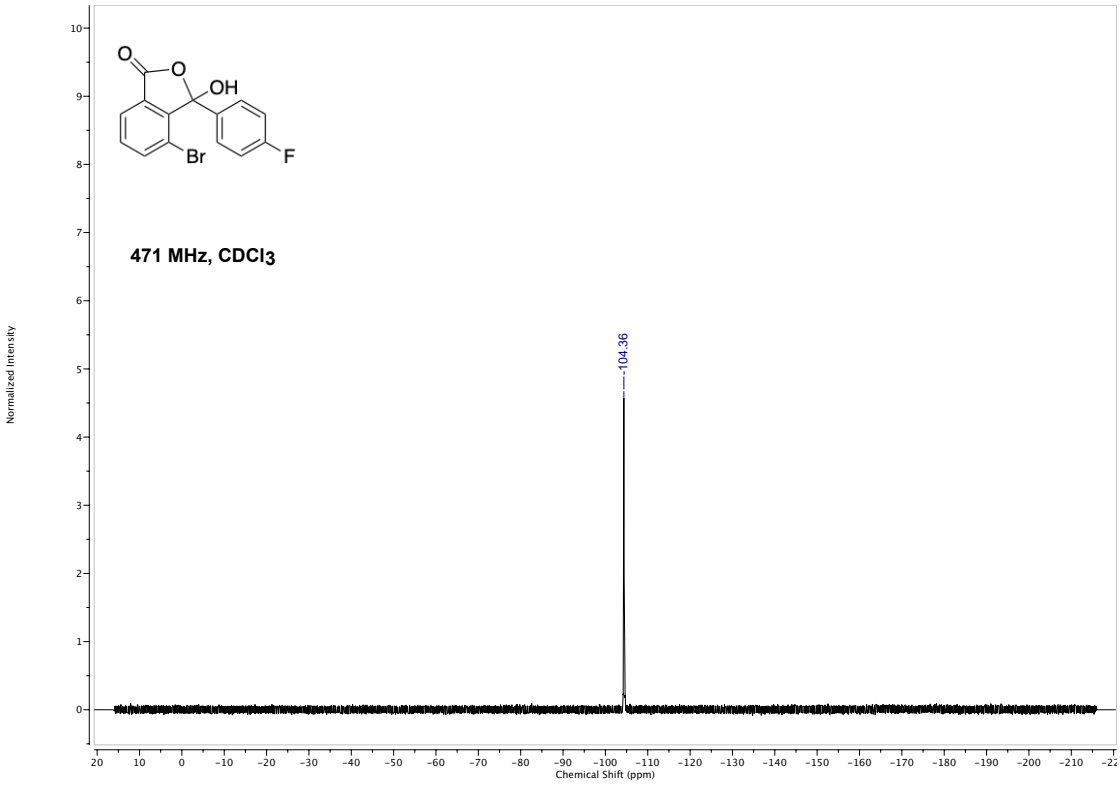
O
O
OH
Br
F
471 MHz, CDCl3
-104.36
Normalized Intensity
Chemical Shift (ppm)

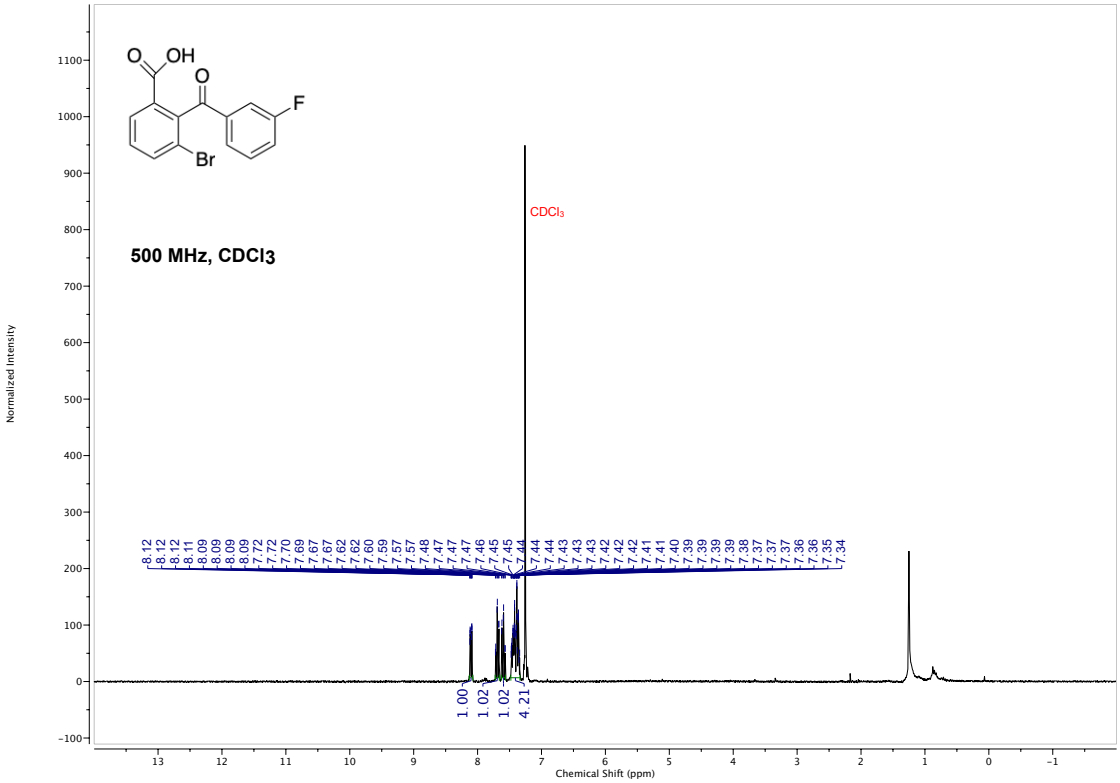
O
OH
O
F
Br
500 MHz, CDCl3
CDCl3
8.12
8.12
8.12
8.11
8.09
8.09
8.09
8.09
8.09
7.72
7.72
7.70
7.69
7.67
7.67
7.62
7.62
7.60
7.59
7.57
7.57
7.48
7.47
7.47
7.47
7.46
7.45
7.45
7.44
7.44
7.44
7.43
7.43
7.43
7.42
7.42
7.42
7.41
7.41
7.40
7.39
7.39
7.39
7.38
7.37
7.37
7.37
7.36
7.36
7.35
7.34
1.00
1.02
1.02
4.21
Normalized Intensity
Chemical Shift (ppm)

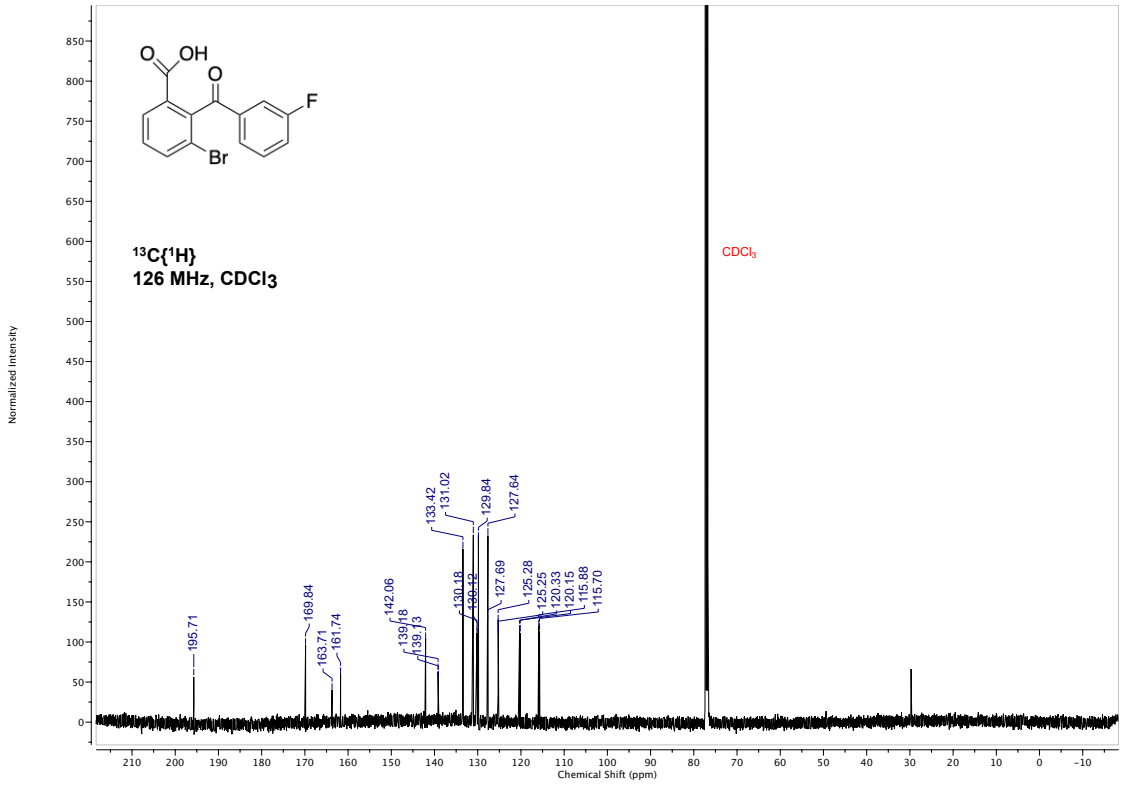
O
OH
O
F
Br
$^{13}C\{^{1}H\}$
126 MHz, $CDCl_3$
$CDCl_3$
Normalized Intensity
195.71
169.84
163.71
161.74
142.06
139.18
139.13
133.42
131.02
130.18
129.84
129.12
127.64
127.69
125.28
125.25
120.33
120.15
115.88
115.70
Chemical Shift (ppm)

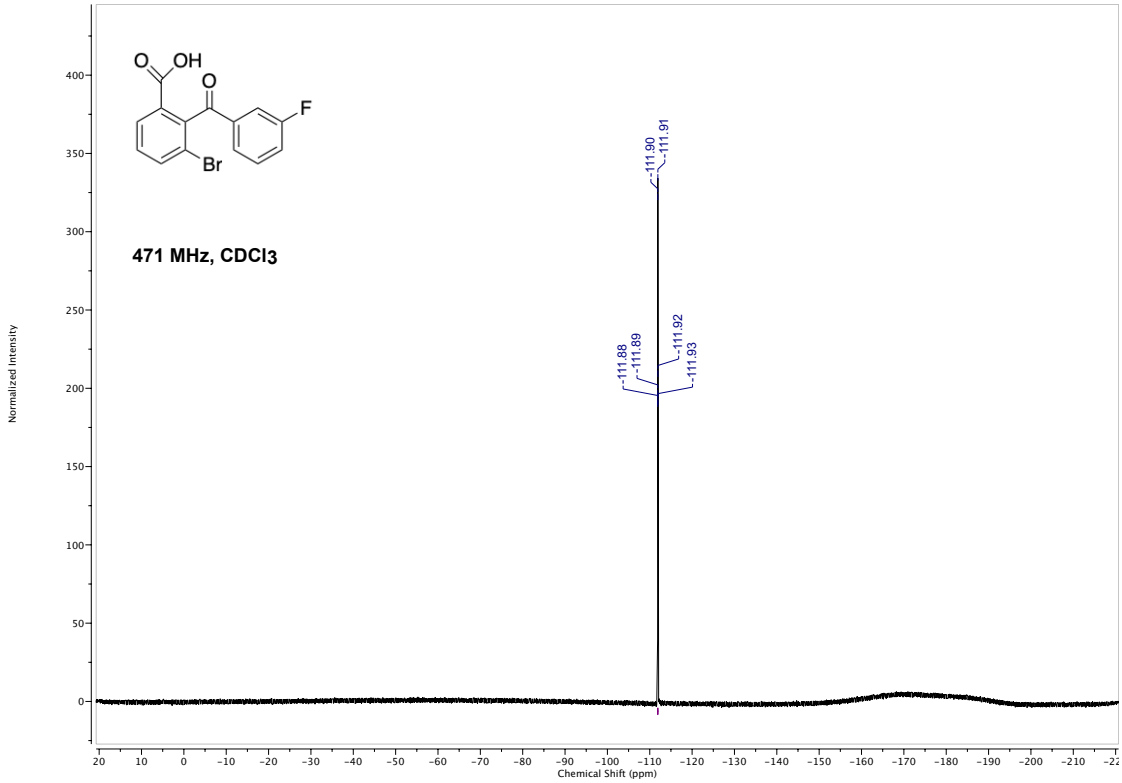
O
OH
O
F
Br
471 MHz, $CDCl_3$
Normalized Intensity
111.90
111.91
111.88
111.89
111.92
111.93
Chemical Shift (ppm)

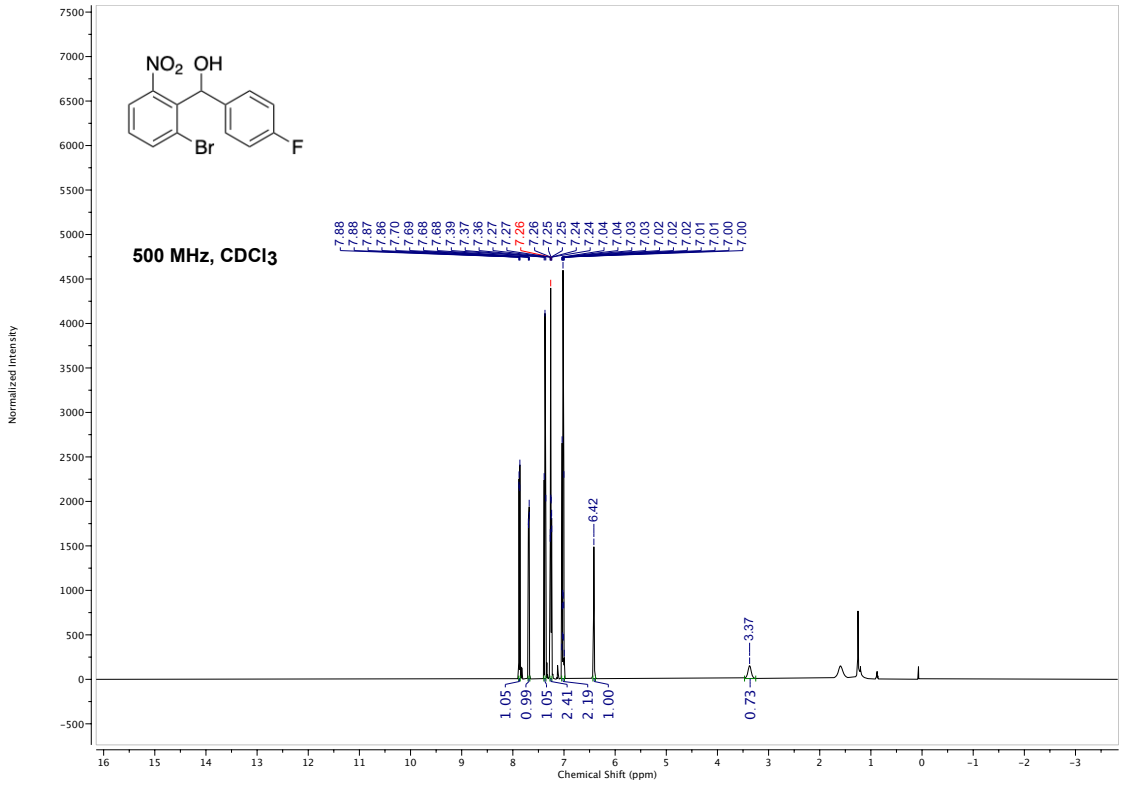
NO2 OH
Br
F
500 MHz, CDCl3
7.88
7.88
7.87
7.86
7.70
7.69
7.68
7.68
7.39
7.37
7.36
7.27
7.27
7.26
7.26
7.25
7.25
7.24
7.24
7.04
7.04
7.03
7.03
7.02
7.02
7.02
7.01
7.01
7.00
7.00
6.42
3.37
1.05
0.99
1.05
2.41
2.19
1.00
0.73
Normalized Intensity
Chemical Shift (ppm)

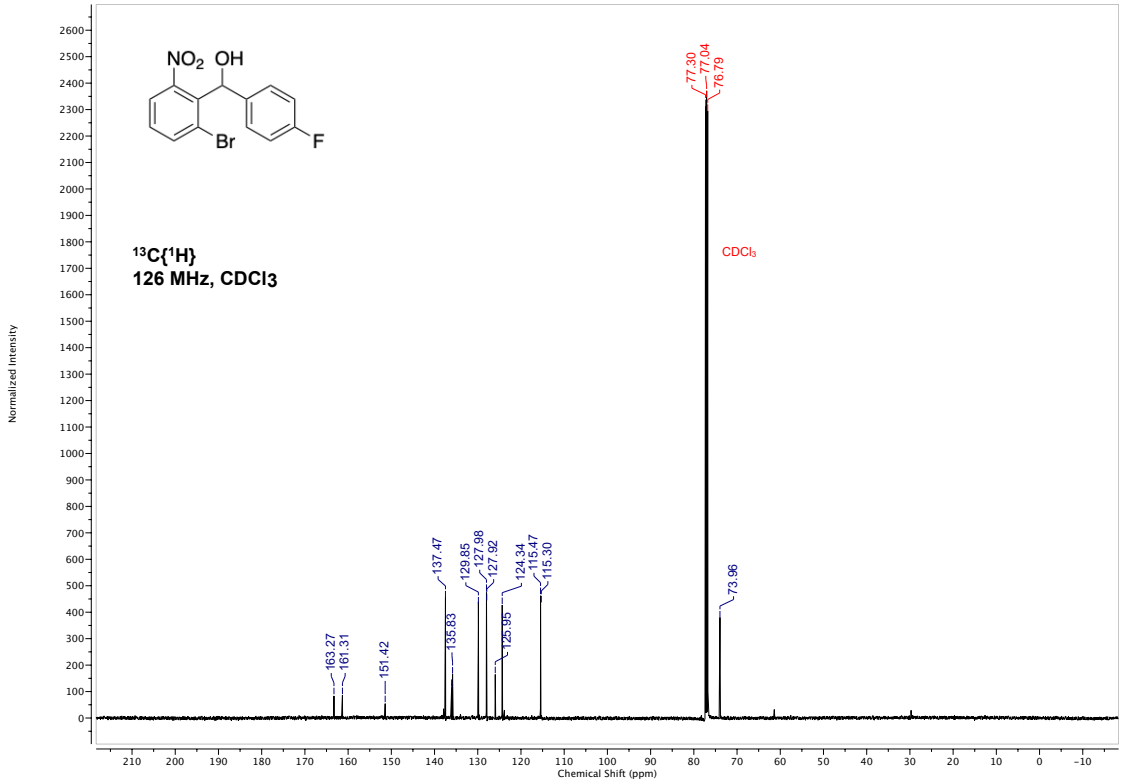
NO2 OH
Br
F
13C{1H}
126 MHz, CDCl3
77.30
77.04
76.79
CDCl3
73.96
163.27
161.31
151.42
137.47
135.83
129.85
127.98
127.92
125.95
124.34
115.47
115.30
Normalized Intensity
Chemical Shift (ppm)

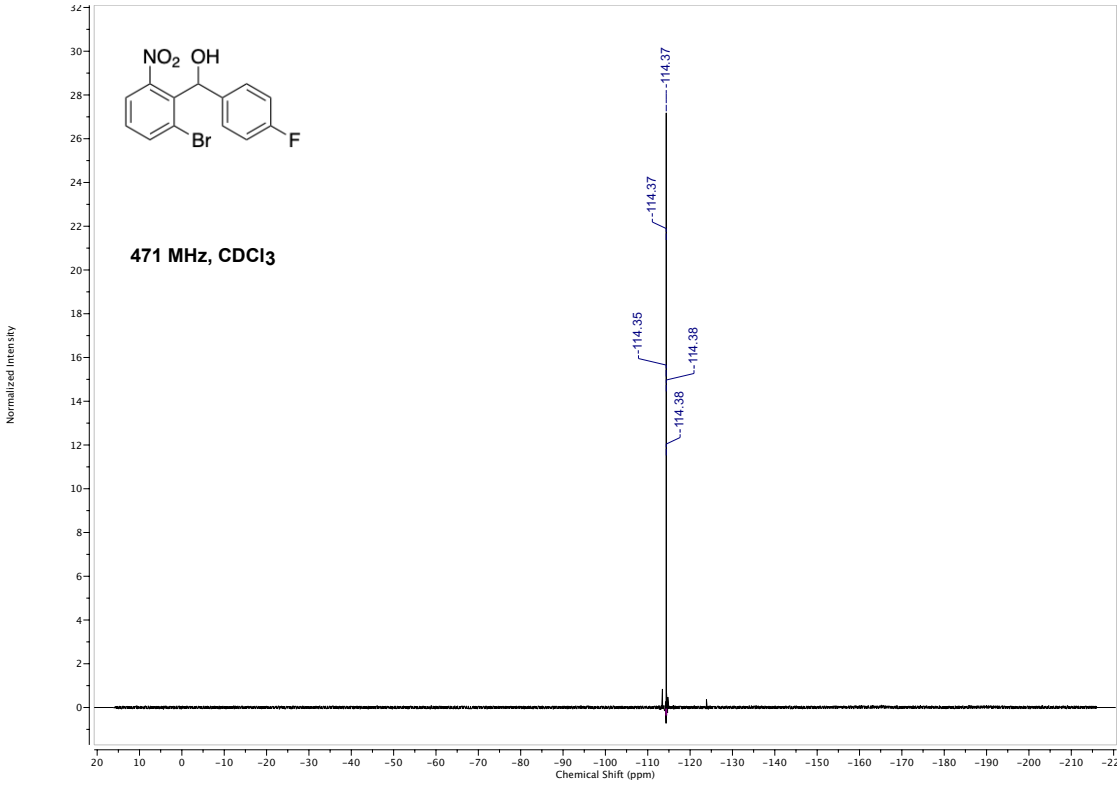
NO2 OH
Br
F
471 MHz, CDCl3
-114.37
-114.37
-114.35
-114.38
-114.38
Normalized Intensity
Chemical Shift (ppm)

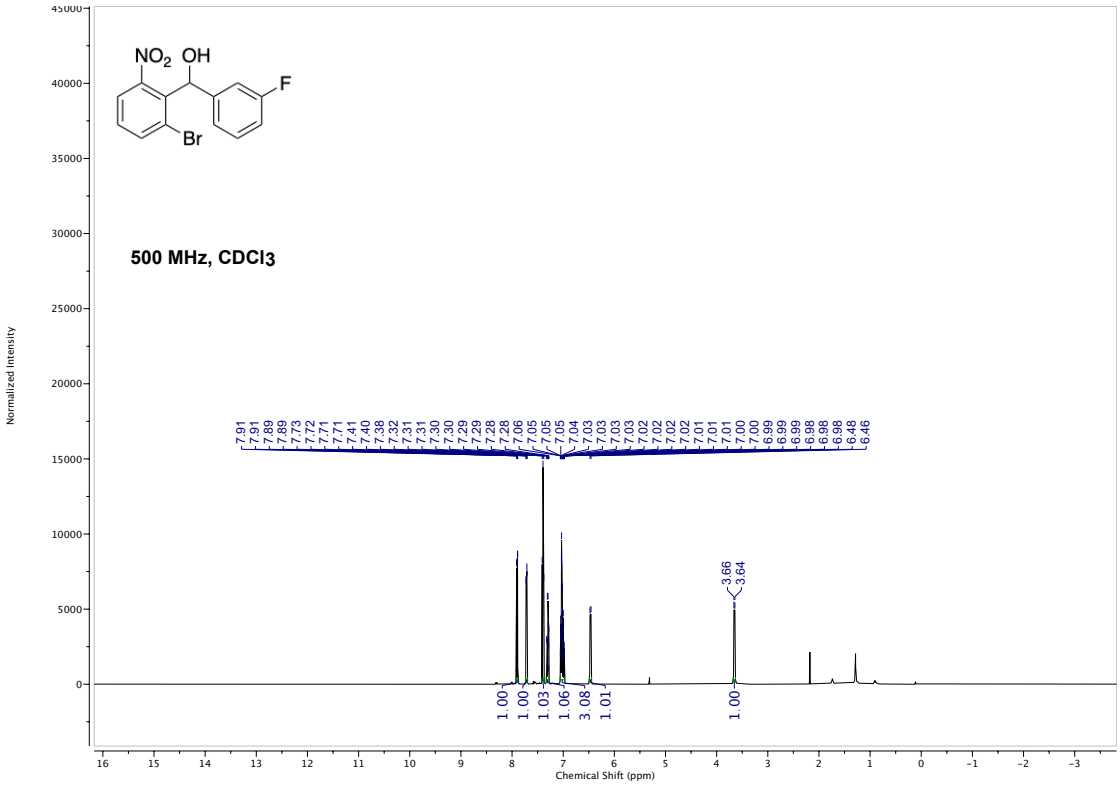
NO2 OH
Br
F
500 MHz, CDCl3
7.91
7.91
7.89
7.89
7.73
7.72
7.71
7.71
7.41
7.40
7.38
7.32
7.31
7.31
7.30
7.30
7.29
7.29
7.28
7.28
7.06
7.05
7.05
7.05
7.04
7.03
7.03
7.03
7.02
7.02
7.02
7.02
7.01
7.01
7.01
7.00
7.00
6.99
6.99
6.99
6.98
6.98
6.98
6.48
6.46
3.66
3.64
1.00
1.00
1.03
1.06
3.08
1.01
1.00
Normalized Intensity
Chemical Shift (ppm)

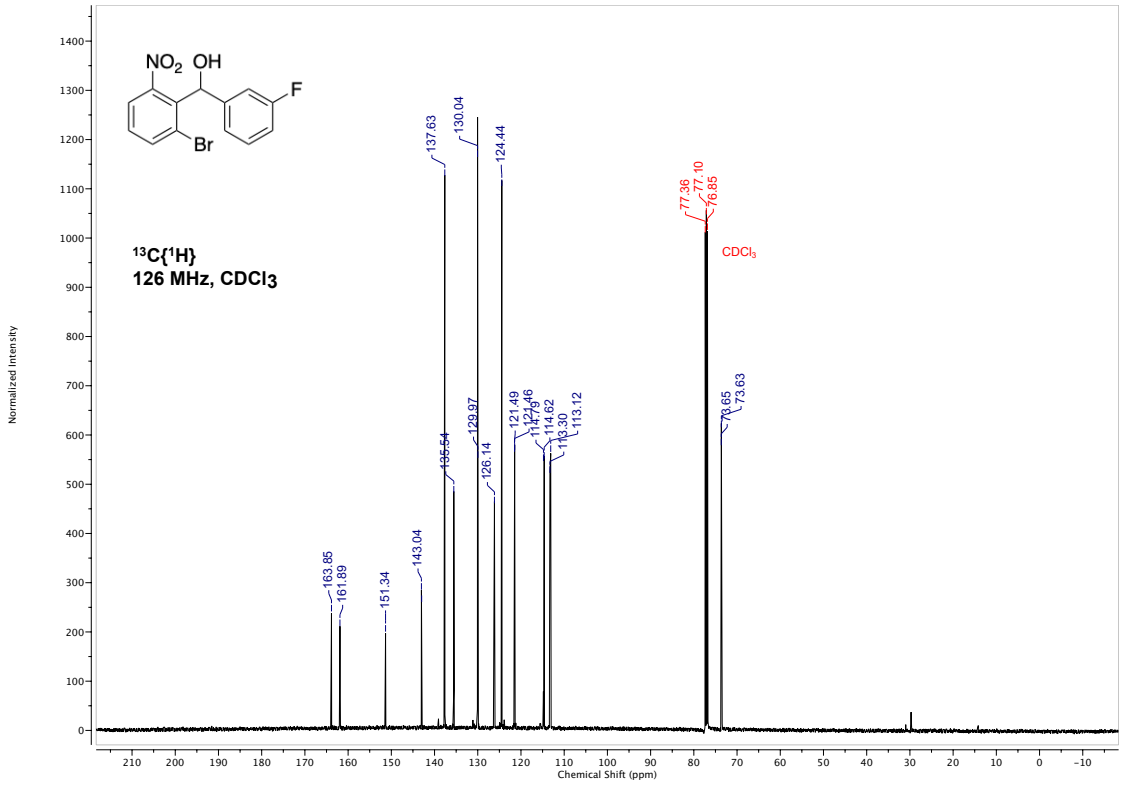
NO2 OH
F
Br
13C{1H}
126 MHz, CDCl3
137.63
130.04
124.44
77.36
77.10
76.85
CDCl3
73.65
73.63
121.49
114.62
113.30
113.12
126.14
129.97
135.54
143.04
151.34
163.85
161.89
Normalized Intensity
Chemical Shift (ppm)

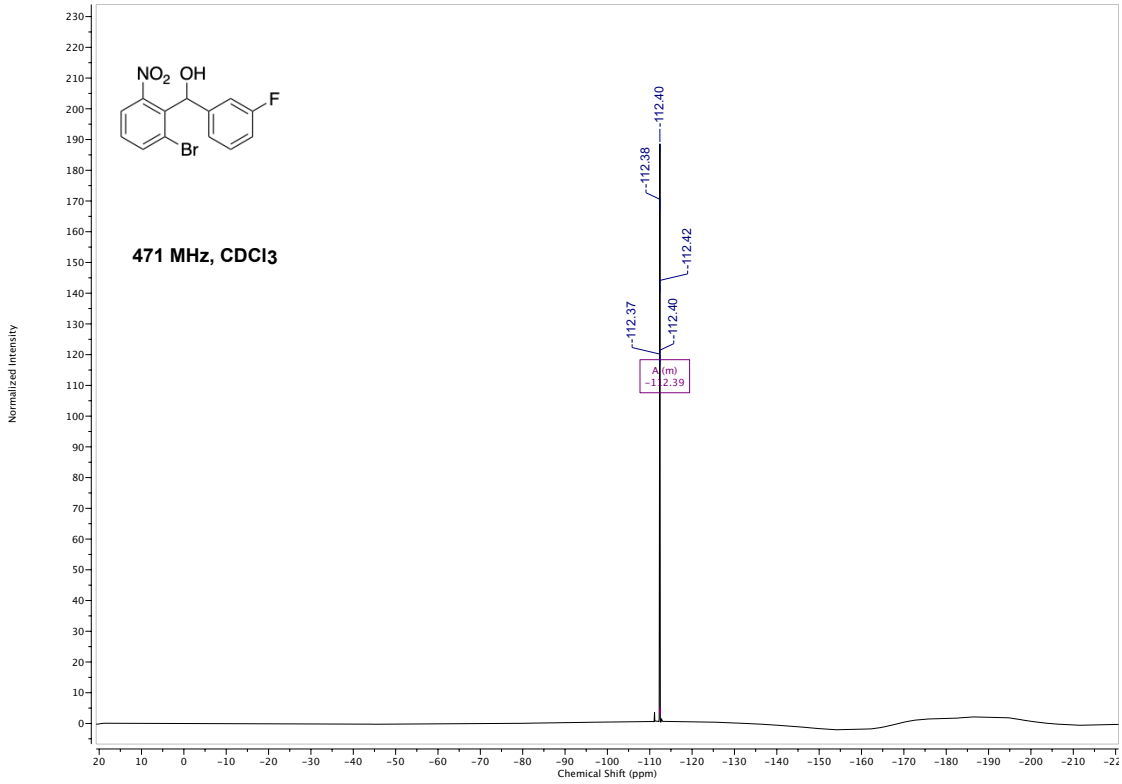
NO2 OH
F
Br
471 MHz, CDCl3
112.40
112.38
112.42
112.37
112.40
A(m)
-112.39
Normalized Intensity
Chemical Shift (ppm)

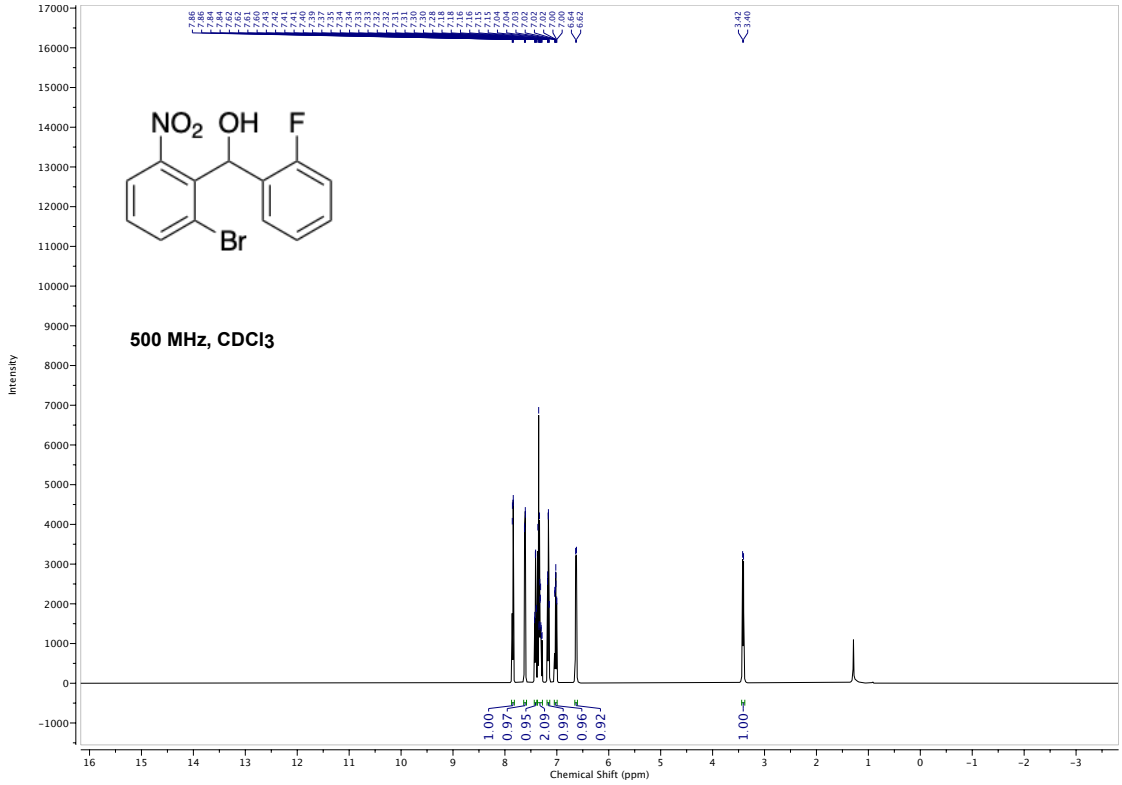
NO2 OH F
Br
500 MHz, CDCl3
Intensity
Chemical Shift (ppm)

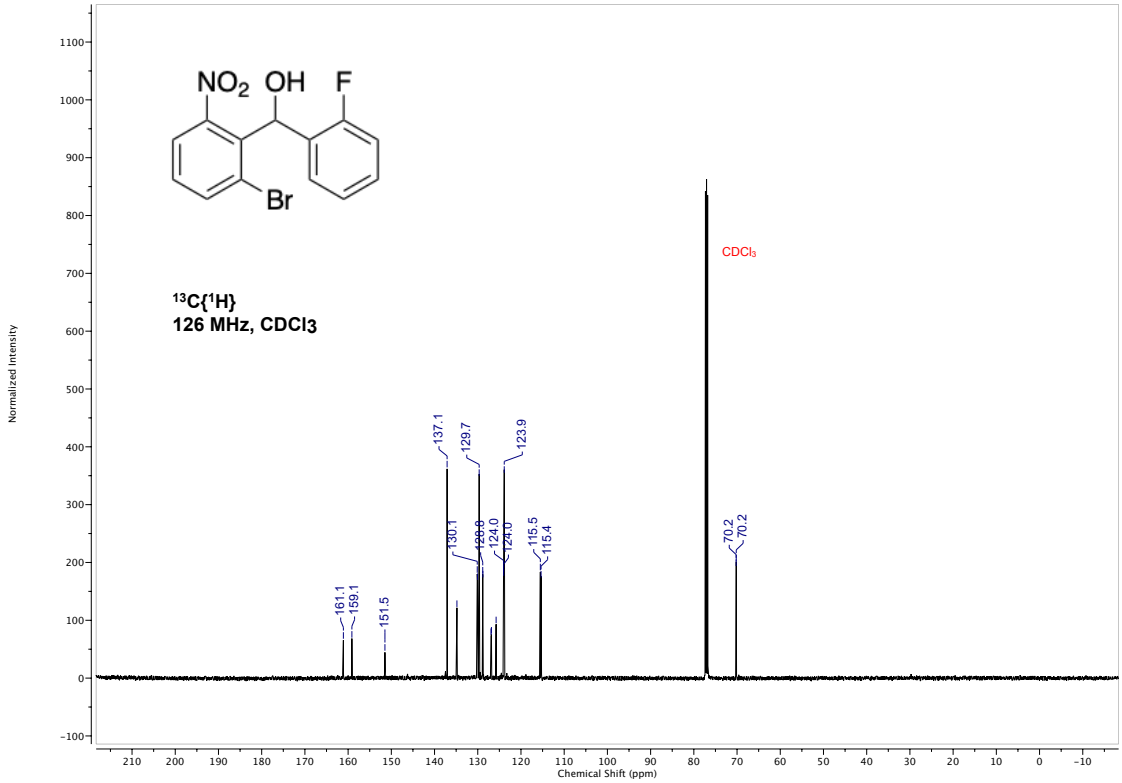
NO2 OH F
Br
13C{1H}
126 MHz, CDCl3
CDCl3
Normalized Intensity
Chemical Shift (ppm)

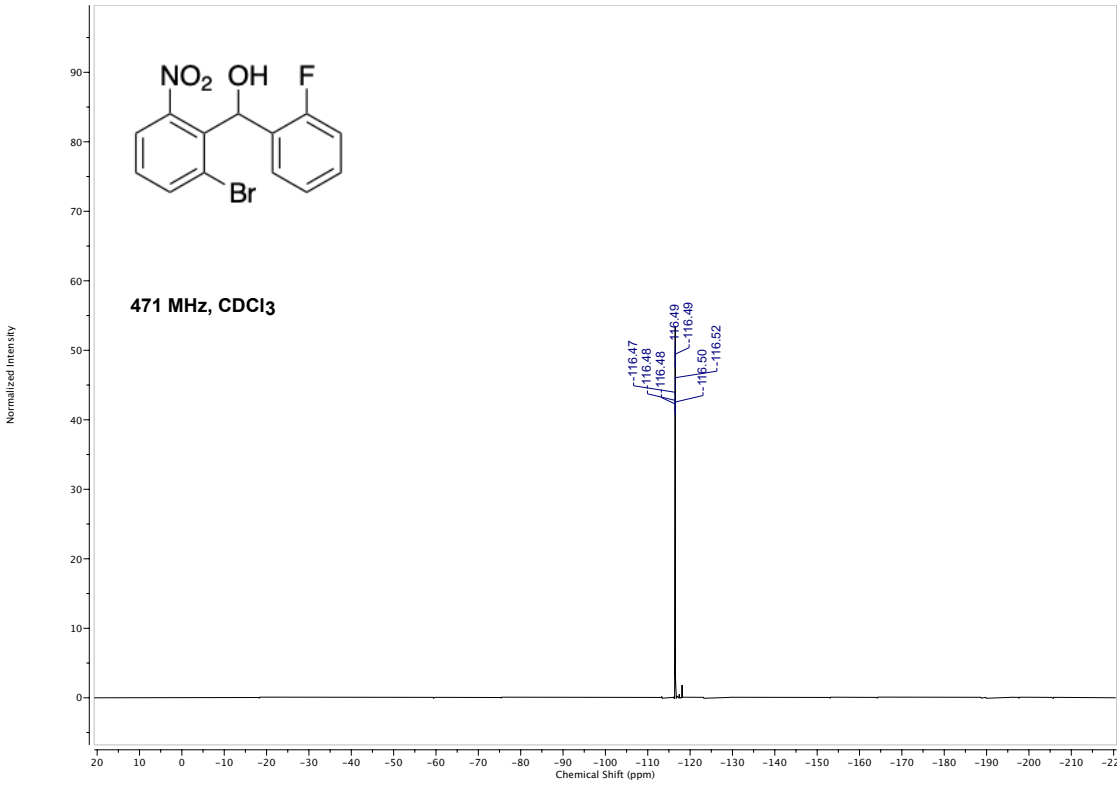
NO2 OH F
Br
471 MHz, CDCl3
Normalized Intensity
Chemical Shift (ppm)
-116.47
-116.48
-116.48
-116.49
-116.49
-116.50
-116.52

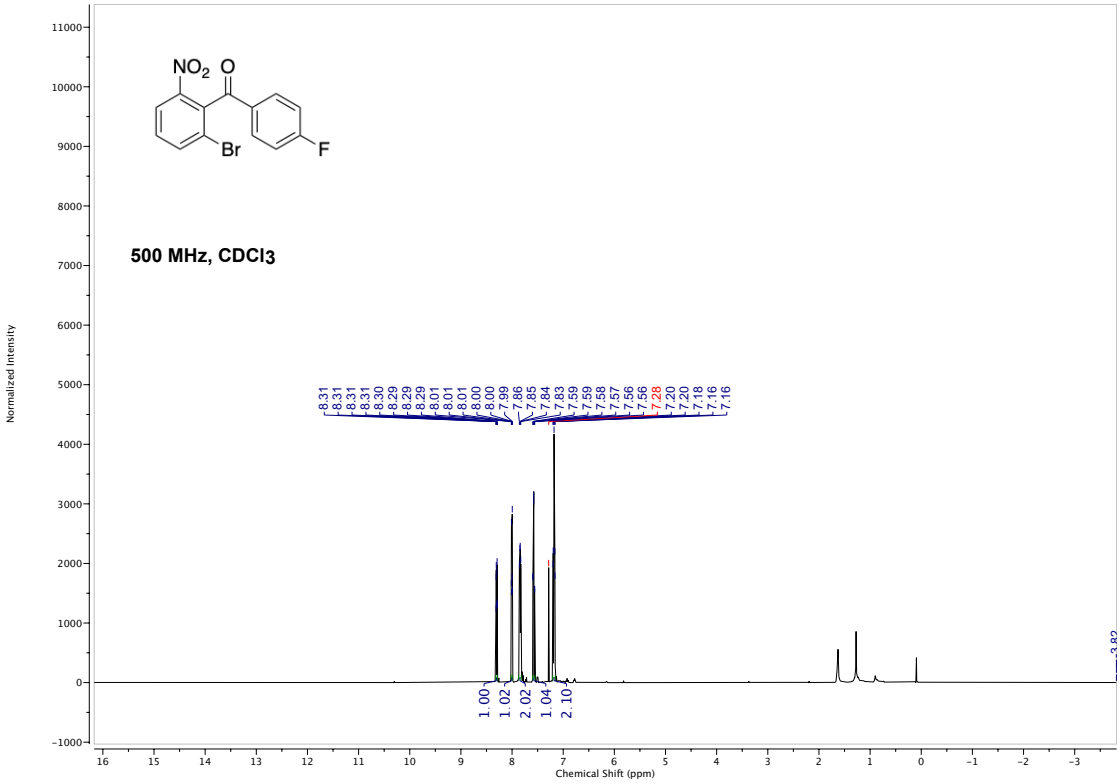
NO2 O
Br
F
500 MHz, CDCl3
Normalized Intensity
Chemical Shift (ppm)
8.31
8.31
8.31
8.31
8.30
8.29
8.29
8.29
8.01
8.01
8.01
8.00
8.00
7.99
7.86
7.85
7.84
7.83
7.59
7.59
7.58
7.57
7.56
7.56
7.28
7.20
7.20
7.18
7.16
7.16
1.00
1.02
2.02
1.04
2.10

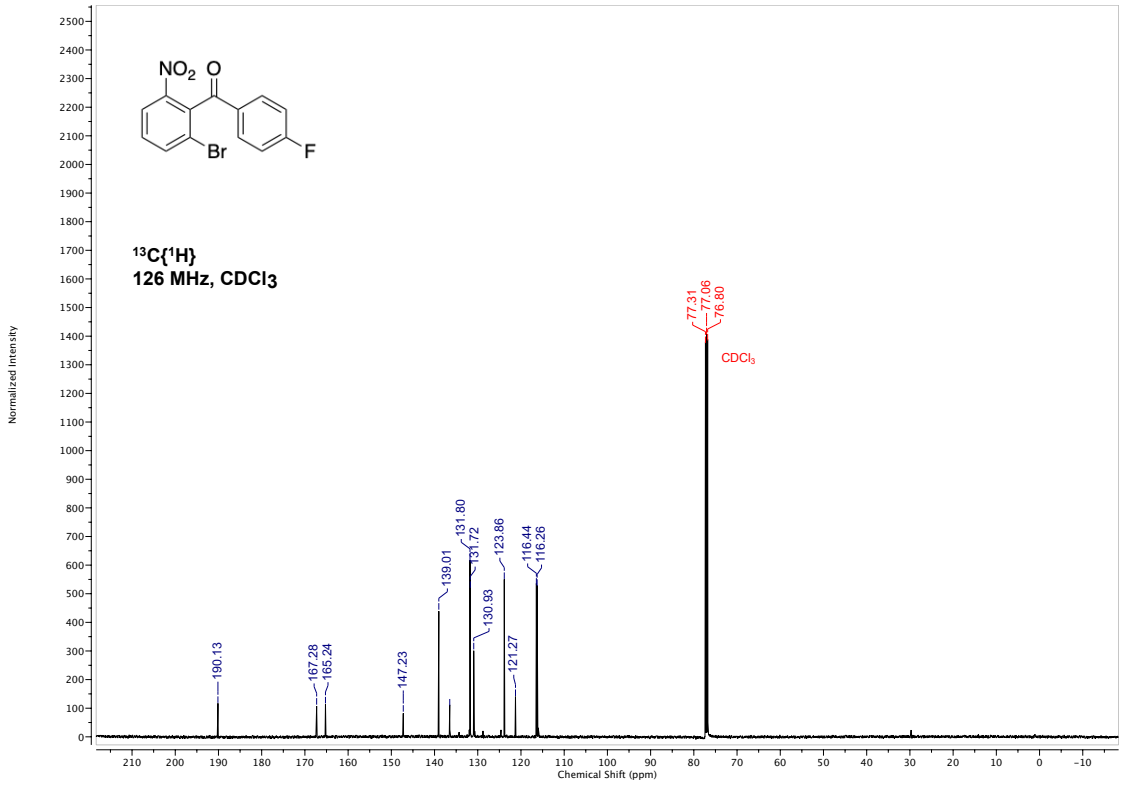
NO2 O
Br
F
13C{1H}
126 MHz, CDCl3
Normalized Intensity
77.31
77.06
76.80
CDCl3
190.13
167.28
165.24
147.23
139.01
131.80
131.72
130.93
123.86
121.27
116.44
116.26
Chemical Shift (ppm)

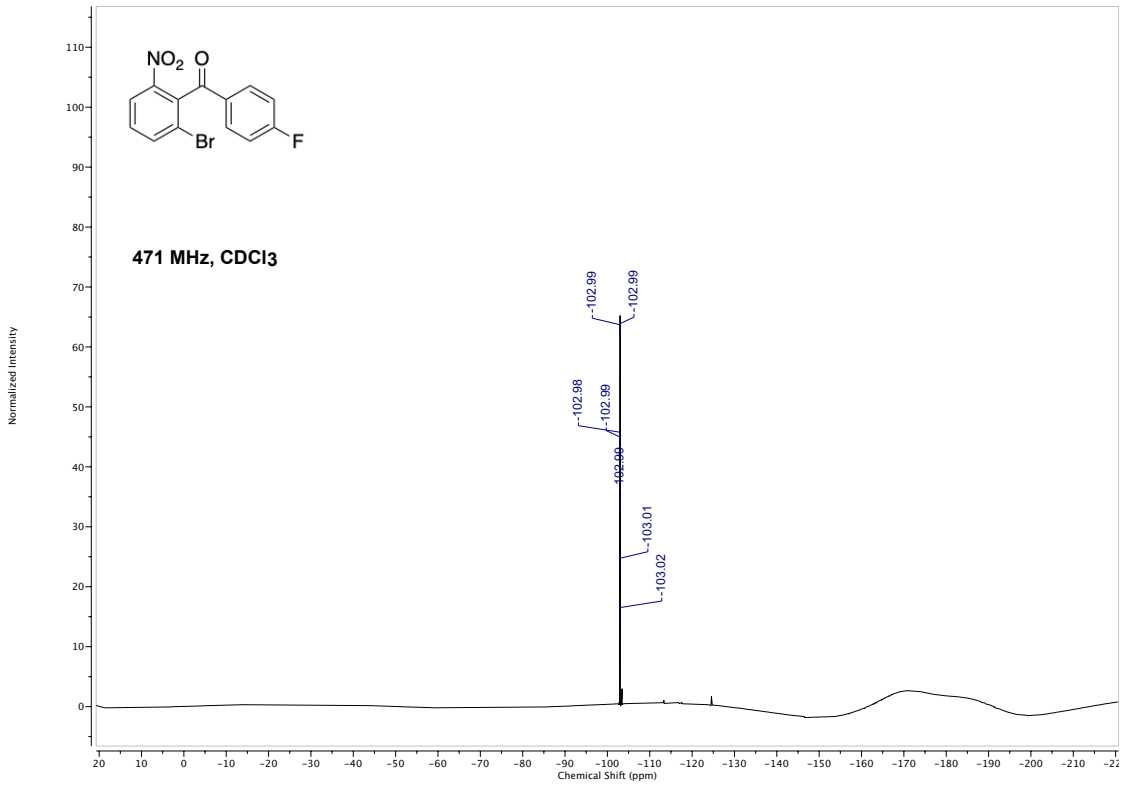
NO2 O
Br
F
471 MHz, CDCl3
Normalized Intensity
102.99
102.99
102.98
102.99
103.01
103.02
Chemical Shift (ppm)

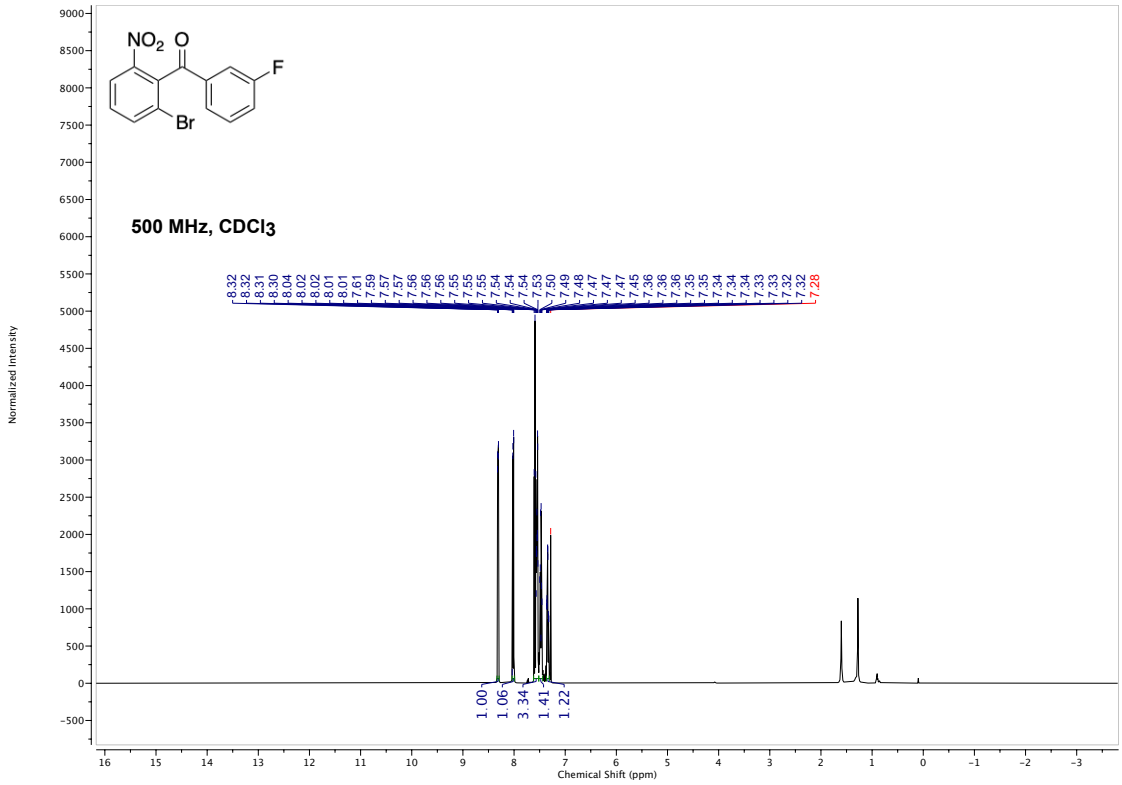
NO2 O
F
Br
500 MHz, CDCl3
Normalized Intensity
Chemical Shift (ppm)
1.00
1.06
3.34
1.41
1.22

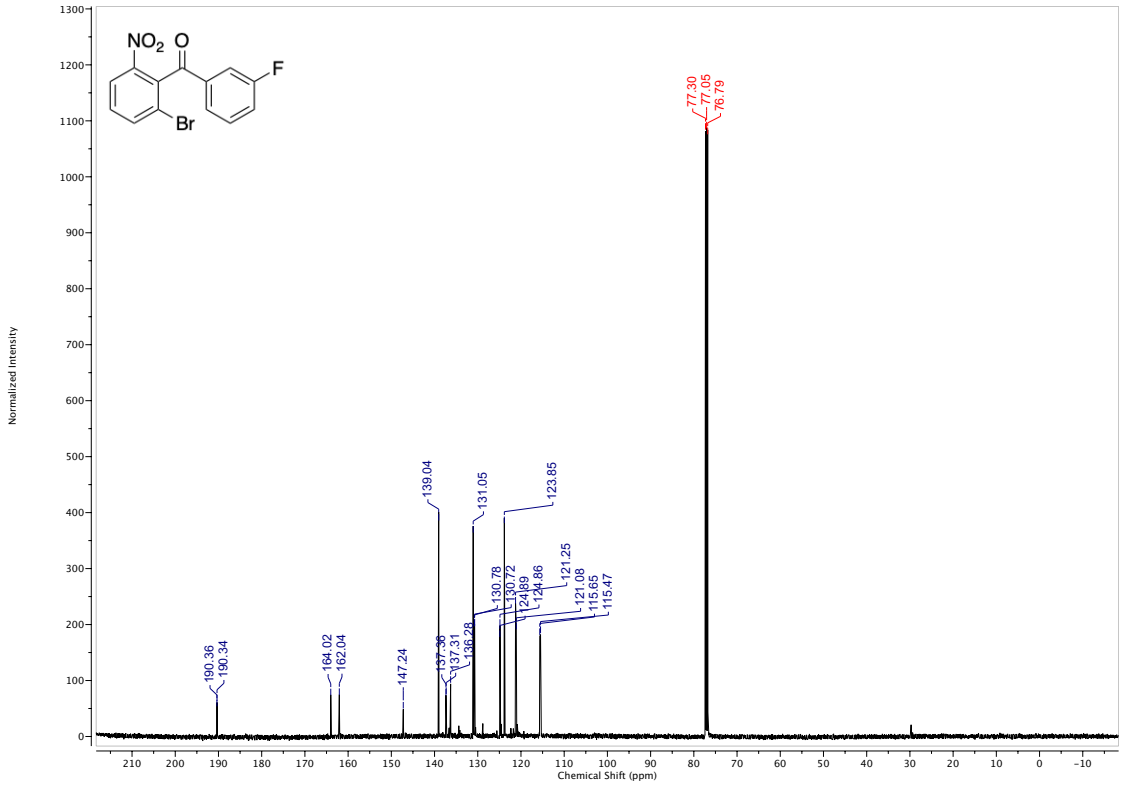
NO2 O
F
Br
Normalized Intensity
Chemical Shift (ppm)
77.30
77.05
76.79
139.04
131.05
123.85
121.25
121.08
115.65
115.47
130.78
130.72
124.89
124.86
190.36
190.34
164.02
162.04
147.24
137.36
137.31
136.28

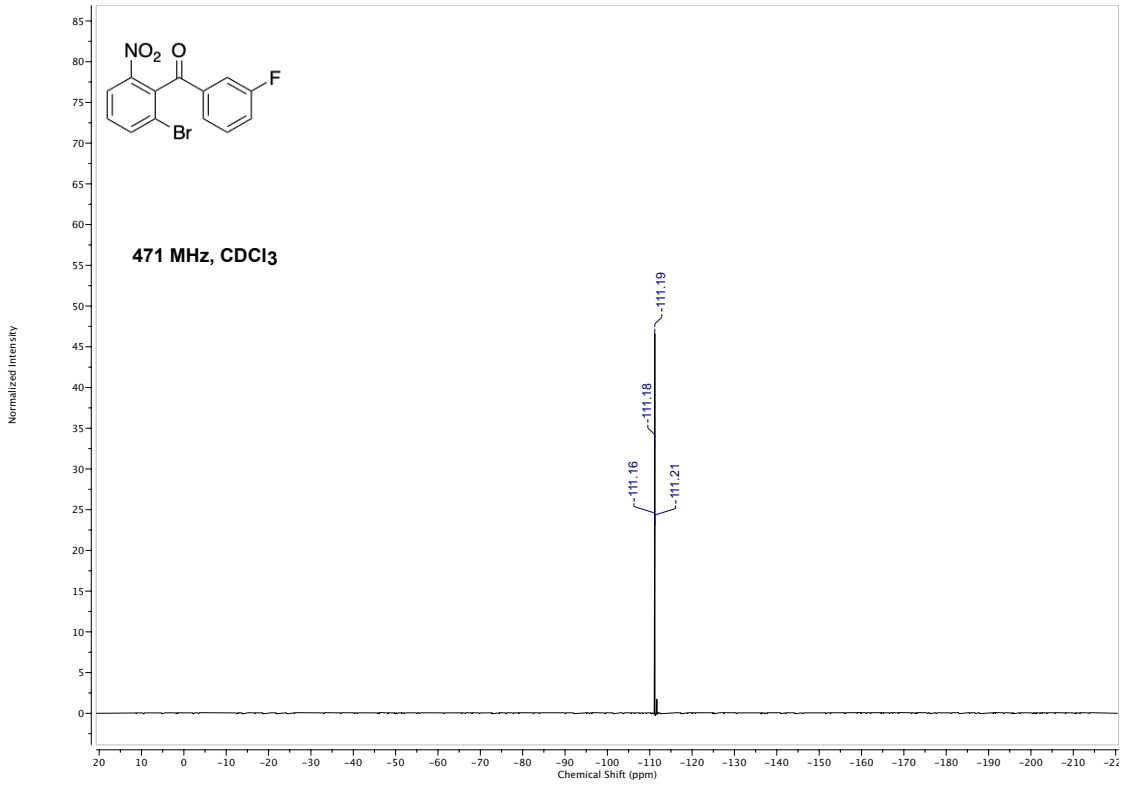
NO2 O
F
Br
471 MHz, CDCl3
111.19
111.18
111.16
111.21
Normalized Intensity
Chemical Shift (ppm)

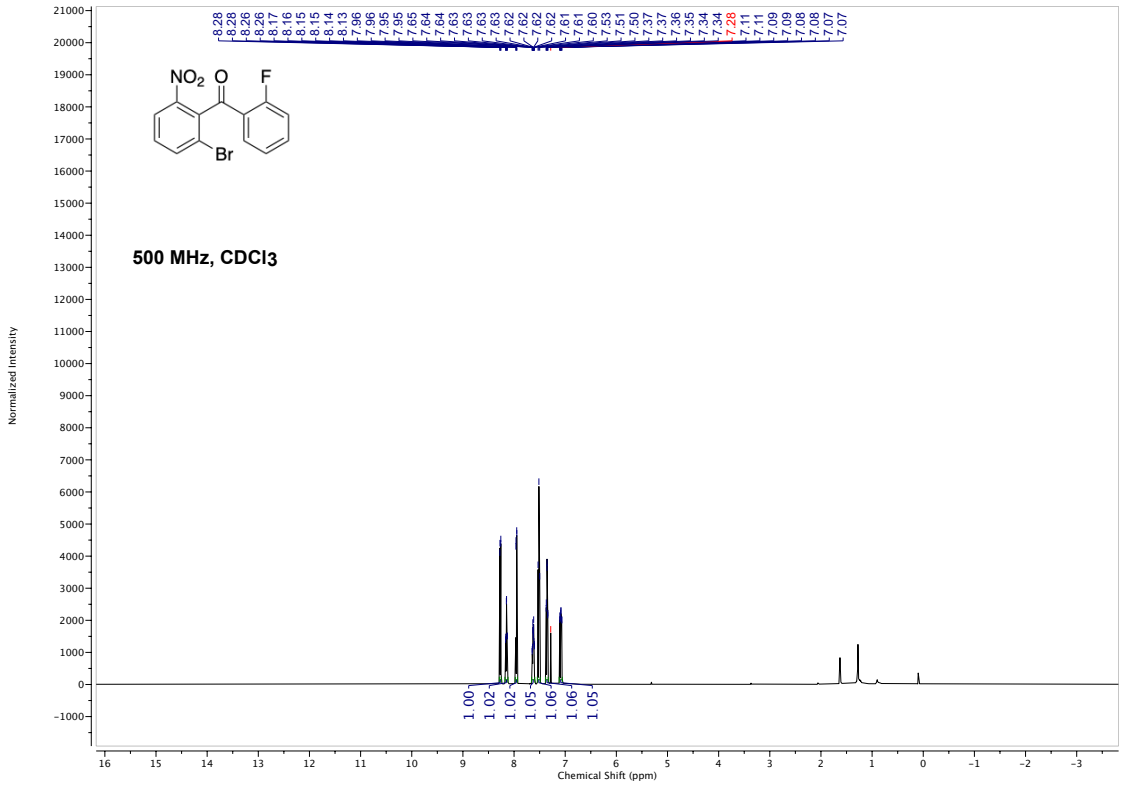
NO2 O
F
Br
500 MHz, CDCl3
8.28 8.28 8.26 8.26 8.17 8.16 8.15 8.15 8.14 8.13 7.96 7.96 7.95 7.95 7.65 7.64 7.64 7.63 7.63 7.63 7.62 7.62 7.62 7.62 7.61 7.61 7.60 7.53 7.51 7.50 7.37 7.36 7.35 7.34 7.34 7.28 7.11 7.09 7.09 7.08 7.08 7.07 7.07
1.00 1.02 1.02 1.05 1.06 1.06 1.05
Normalized Intensity
Chemical Shift (ppm)

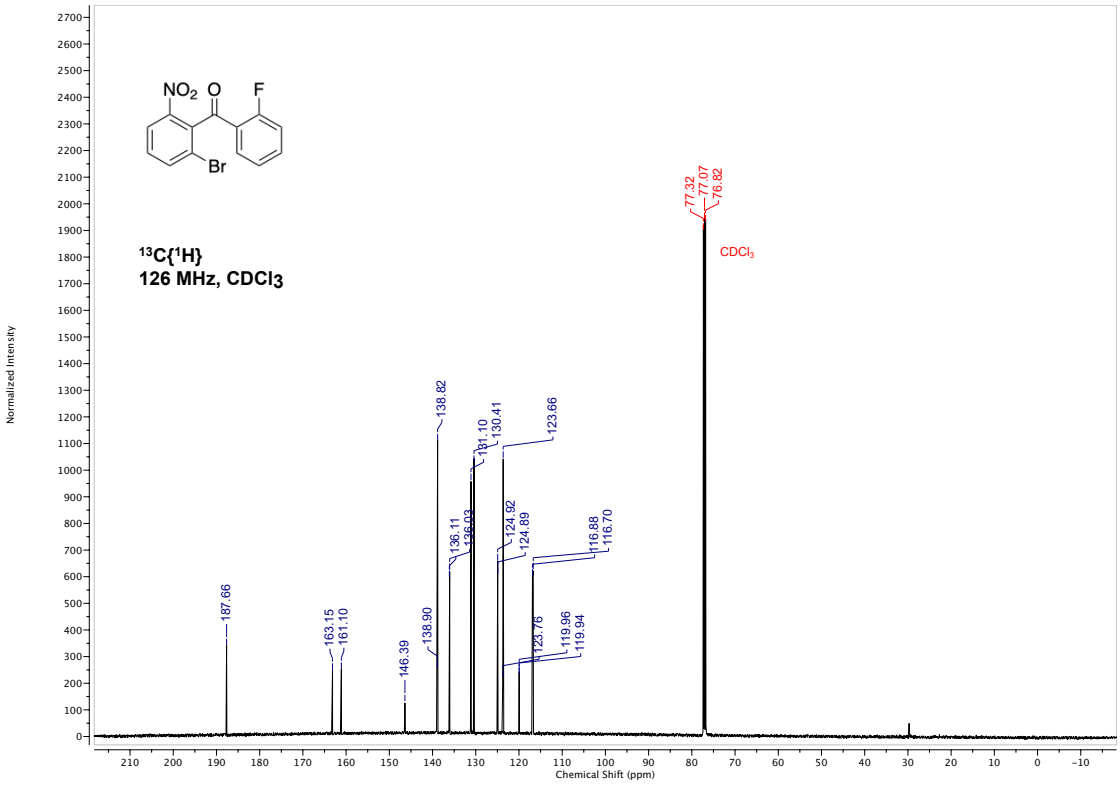
NO2 O F
Br
13C{1H}
126 MHz, CDCl3
77.32
77.07
76.82
CDCl3
138.82
131.10
130.41
123.66
136.11
136.03
124.92
124.89
116.88
116.70
187.66
163.15
161.10
146.39
138.90
123.76
119.96
119.94
Normalized Intensity
Chemical Shift (ppm)

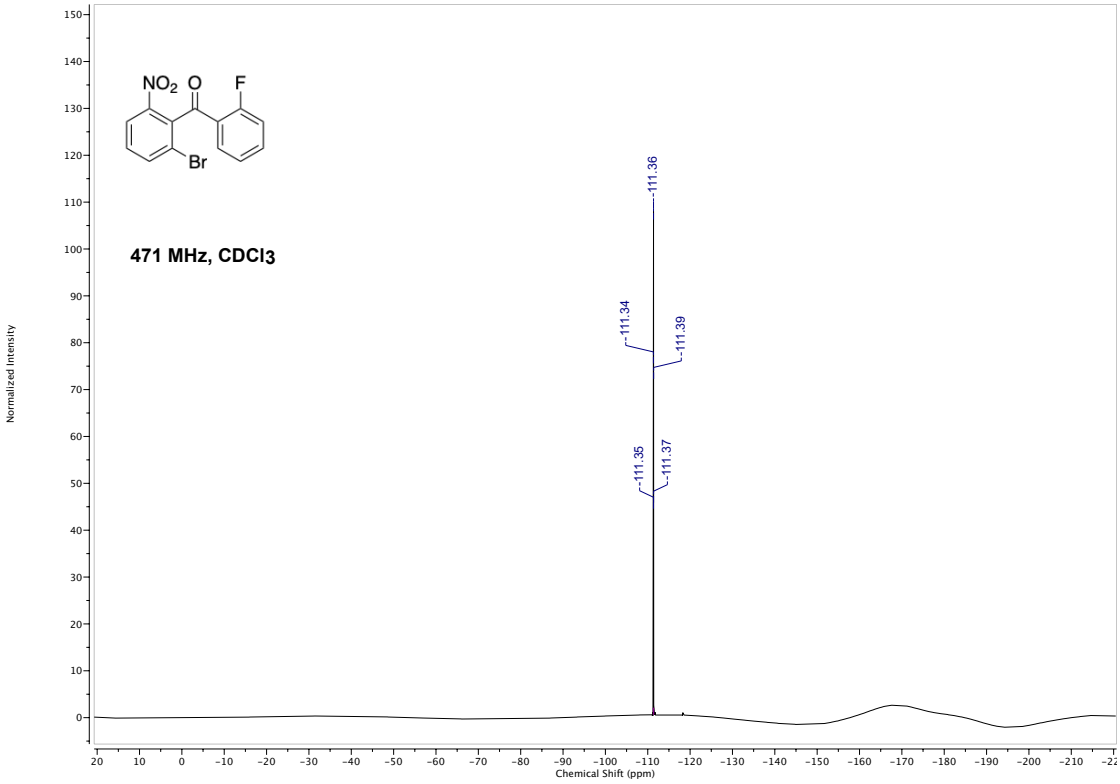
NO2 O F
Br
471 MHz, CDCl3
111.36
111.34
111.39
111.35
111.37
Normalized Intensity
Chemical Shift (ppm)

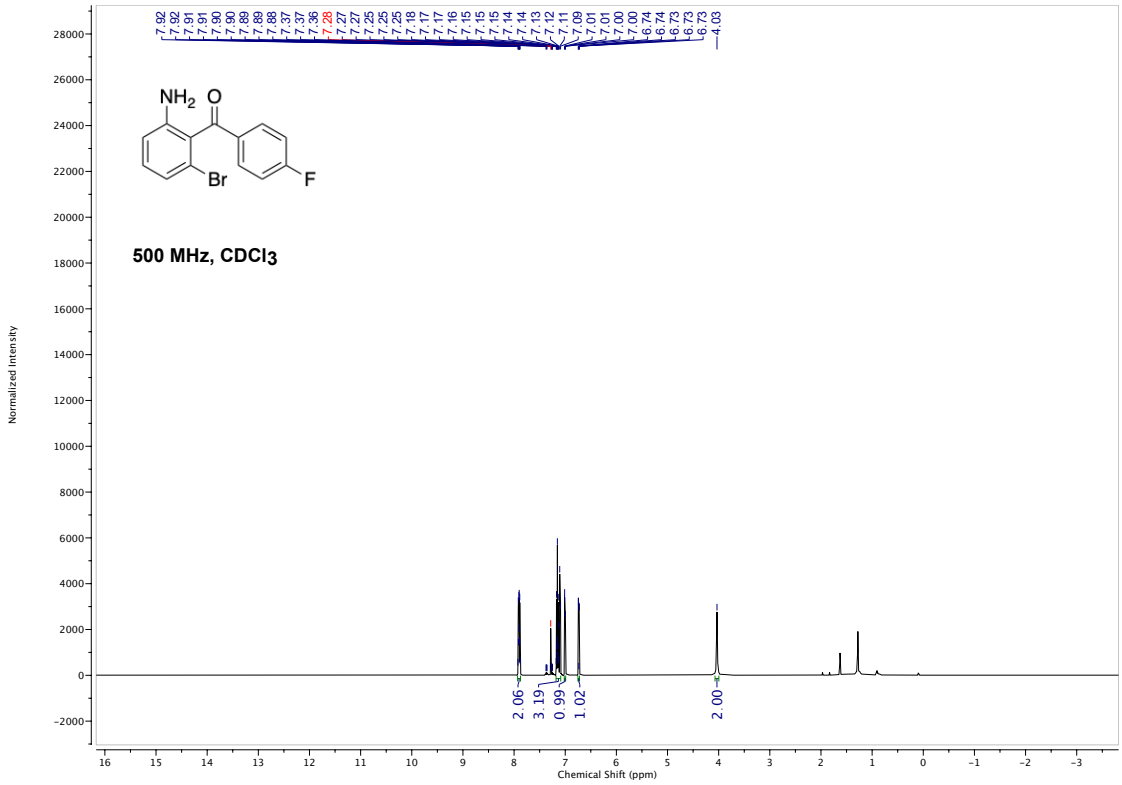
7.92
7.92
7.91
7.91
7.90
7.90
7.89
7.89
7.37
7.36
7.28
7.27
7.27
7.25
7.25
7.18
7.17
7.17
7.16
7.15
7.15
7.14
7.14
7.13
7.12
7.11
7.09
7.01
7.01
7.00
7.00
6.74
6.74
6.73
6.73
6.73
4.03
NH2
O
Br
F
500 MHz, CDCl3
Normalized Intensity
2.06
3.19
0.99
1.02
2.00
Chemical Shift (ppm)

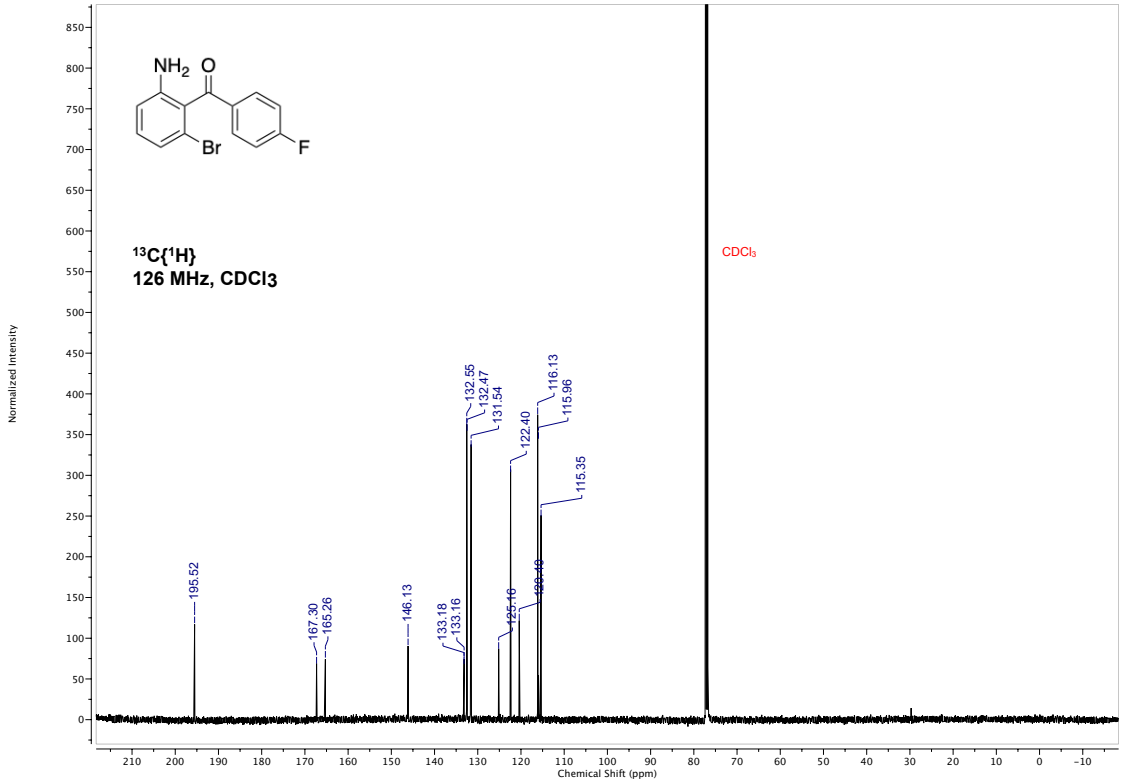
NH2
O
Br
F
13C{1H}
126 MHz, CDCl3
CDCl3
Normalized Intensity
195.52
167.30
165.26
146.13
133.18
133.16
132.55
132.47
131.54
125.16
122.40
116.13
115.96
115.35
Chemical Shift (ppm)

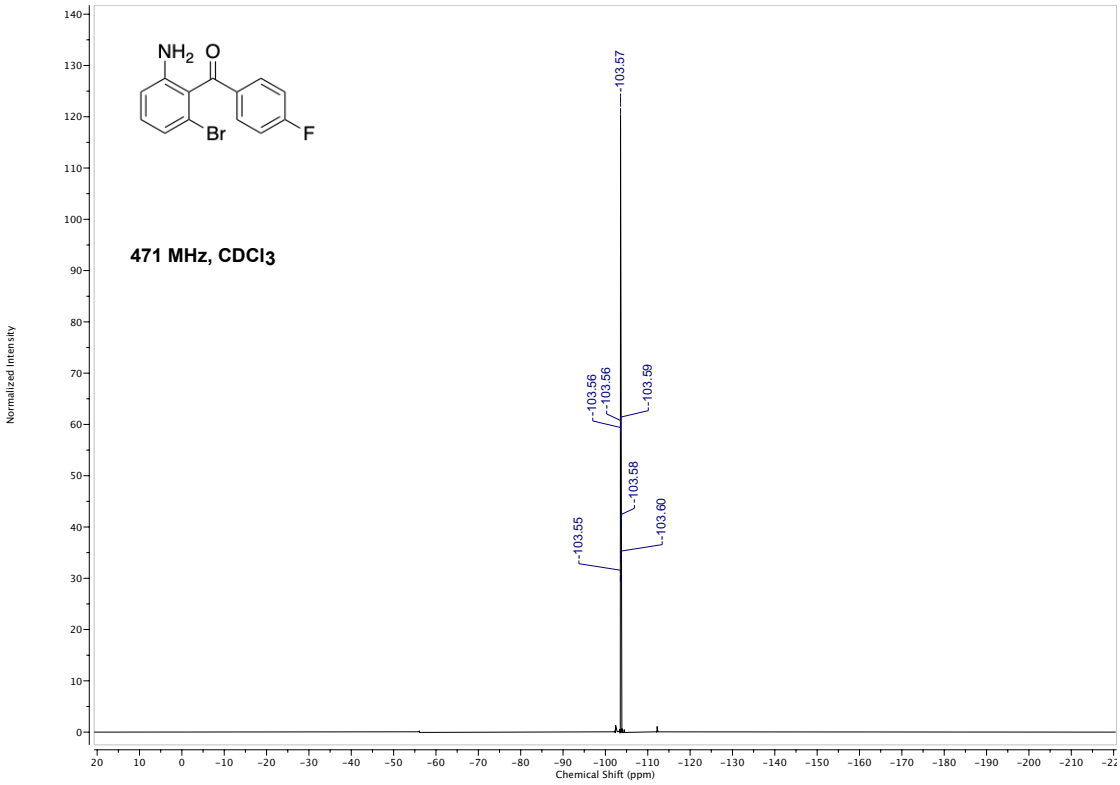
NH2 O
Br
F
471 MHz, CDCl3
Normalized Intensity
Chemical Shift (ppm)
103.57
103.56
103.56
103.59
103.58
103.60
103.55

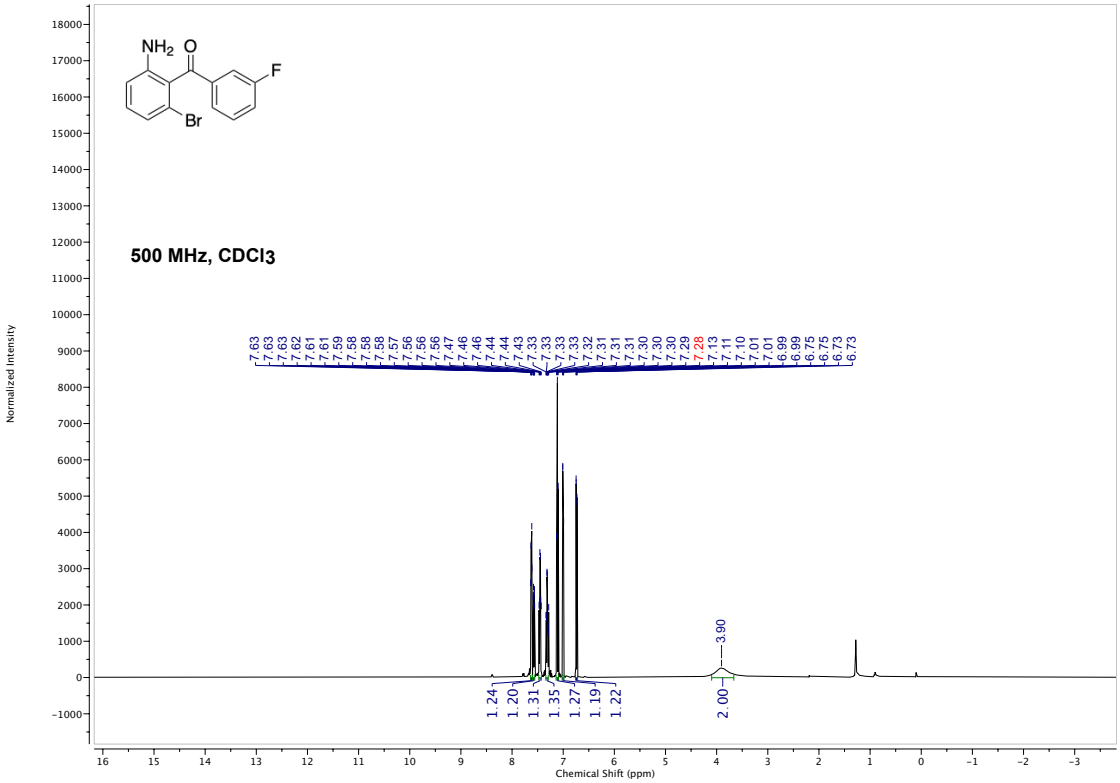
NH2 O
Br
F
500 MHz, CDCl3
Normalized Intensity
Chemical Shift (ppm)
7.63
7.63
7.63
7.62
7.61
7.59
7.58
7.58
7.58
7.57
7.56
7.56
7.56
7.47
7.46
7.46
7.44
7.44
7.43
7.33
7.33
7.33
7.33
7.32
7.31
7.31
7.31
7.30
7.30
7.30
7.29
7.28
7.13
7.11
7.10
7.01
7.01
6.99
6.99
6.75
6.75
6.73
6.73
3.90
1.24
1.20
1.31
1.35
1.27
1.19
1.22
2.00

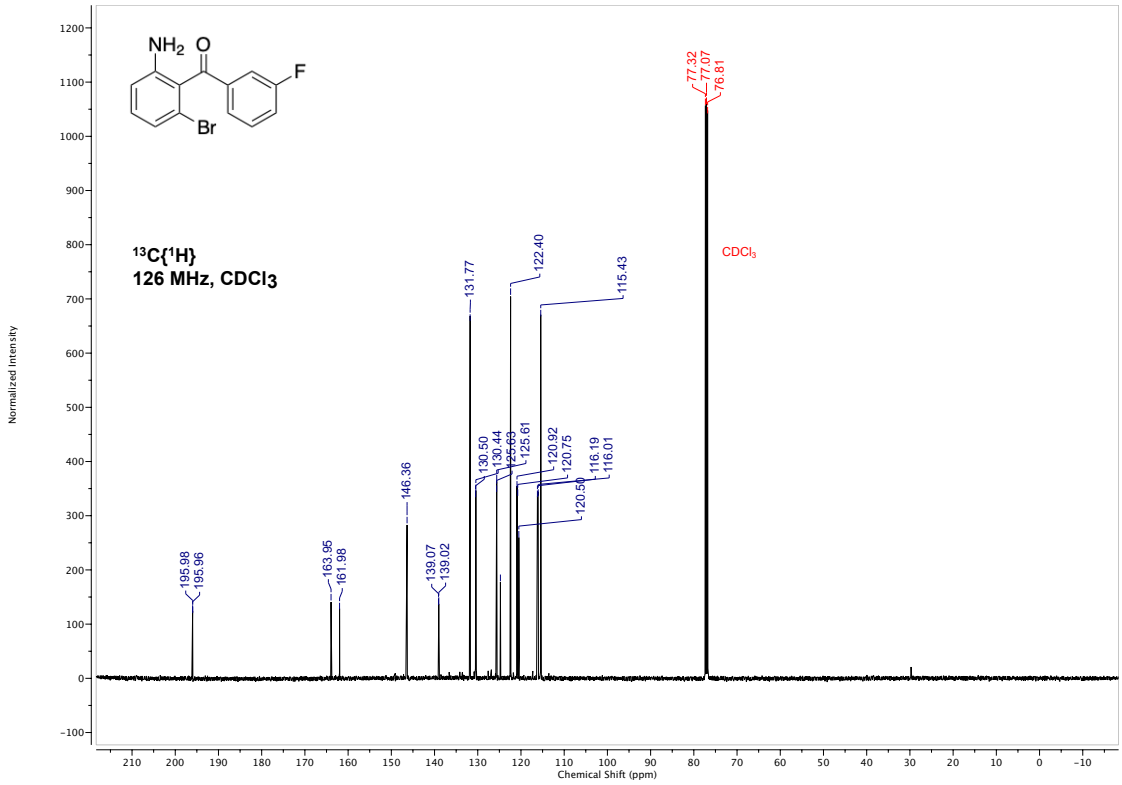
NH2 O
F
Br
13C{1H}
126 MHz, CDCl3
CDCl3
77.32
77.07
76.81
131.77
122.40
115.43
130.50
130.44
125.63
125.61
120.92
120.75
116.19
116.01
120.56
146.36
139.07
139.02
163.95
161.98
195.98
195.96
Normalized Intensity
Chemical Shift (ppm)

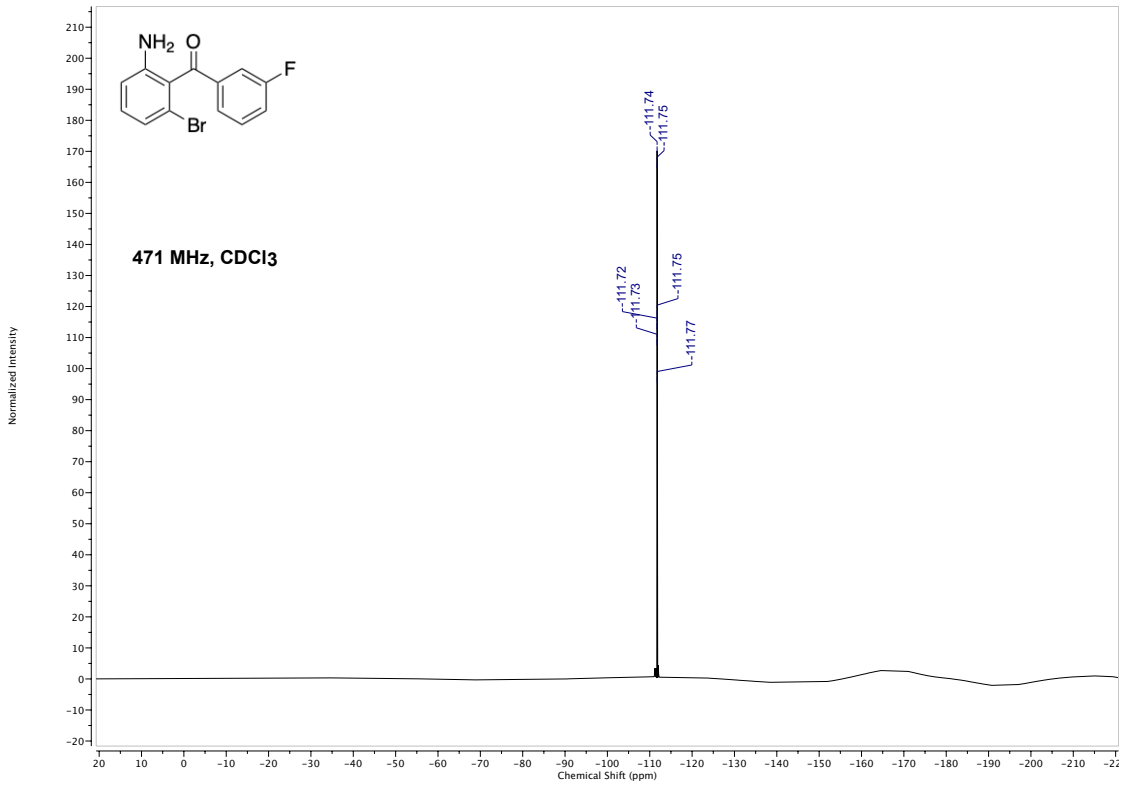
NH2 O
F
Br
471 MHz, CDCl3
111.74
111.75
111.72
111.73
111.75
111.77
Normalized Intensity
Chemical Shift (ppm)

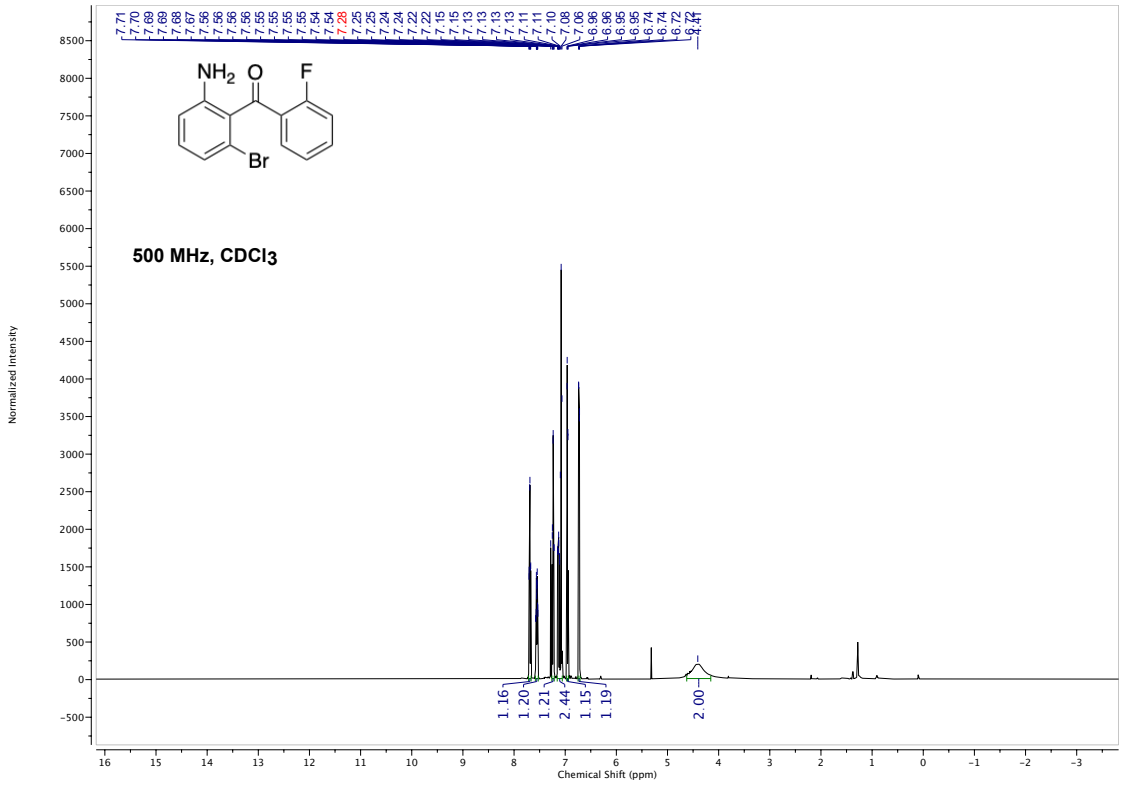
7.71
7.70
7.69
7.69
7.68
7.67
7.56
7.56
7.56
7.56
7.55
7.55
7.55
7.55
7.54
7.54
7.28
7.25
7.25
7.24
7.24
7.22
7.22
7.15
7.13
7.13
7.13
7.13
7.11
7.11
7.10
7.08
7.06
6.96
6.96
6.95
6.95
6.74
6.72
4.41
NH2
O
F
Br
500 MHz, CDCl3
Normalized Intensity
1.16
1.20
1.21
2.44
1.15
1.19
2.00
Chemical Shift (ppm)

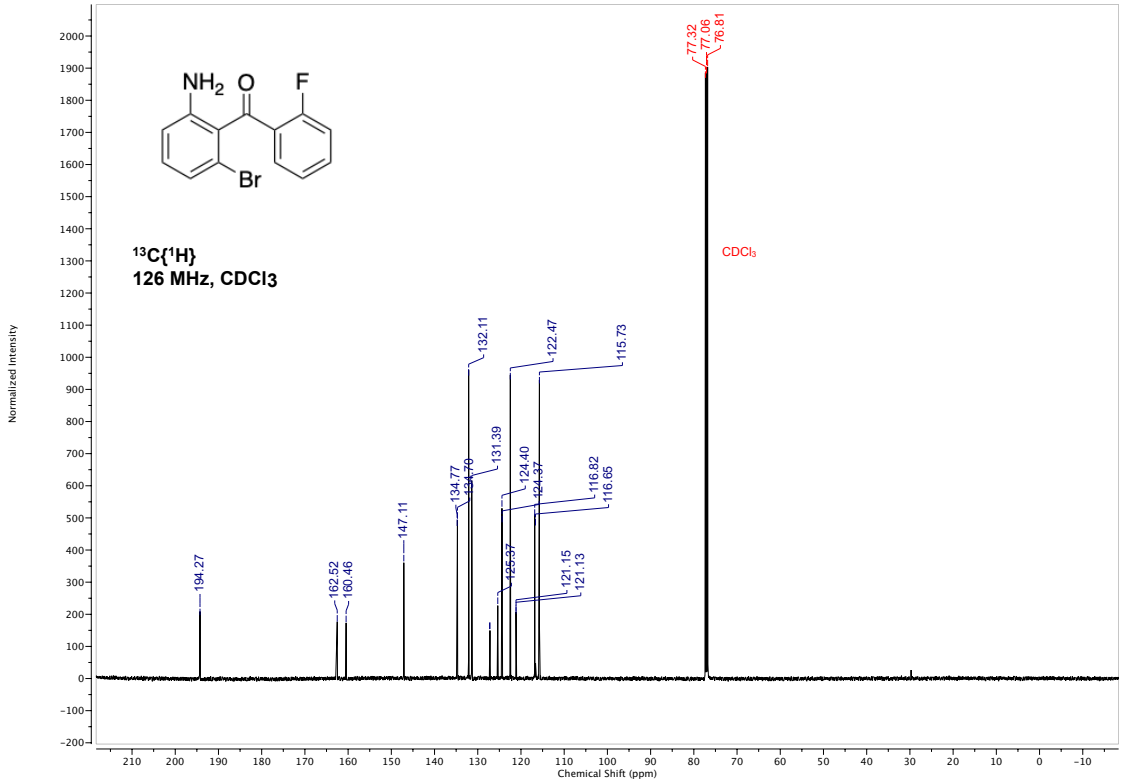
NH2
O
F
Br
13C{1H}
126 MHz, CDCl3
Normalized Intensity
77.32
77.06
76.81
CDCl3
132.11
122.47
115.73
131.39
124.40
124.37
116.82
116.65
134.77
134.70
147.11
194.27
162.52
160.46
125.37
121.15
121.13
Chemical Shift (ppm)

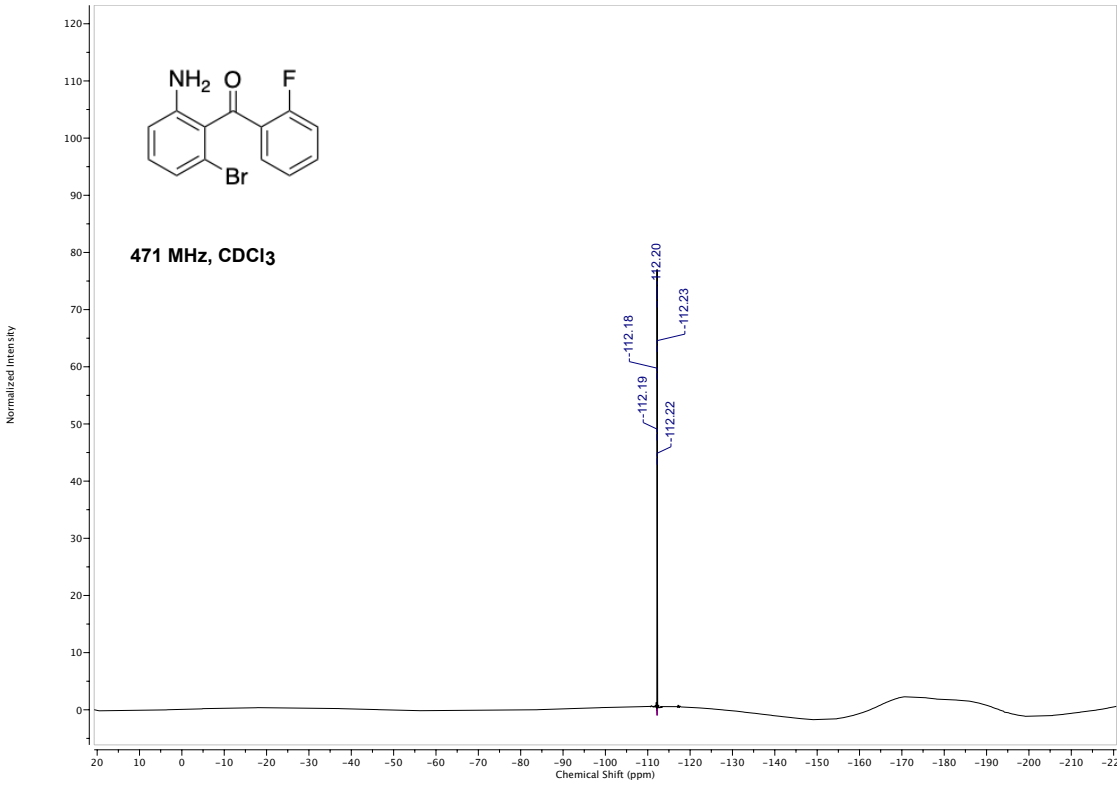
NH2 O F
Br
471 MHz, CDCl3
112.20
112.23
112.18
112.19
112.22
Normalized Intensity
Chemical Shift (ppm)

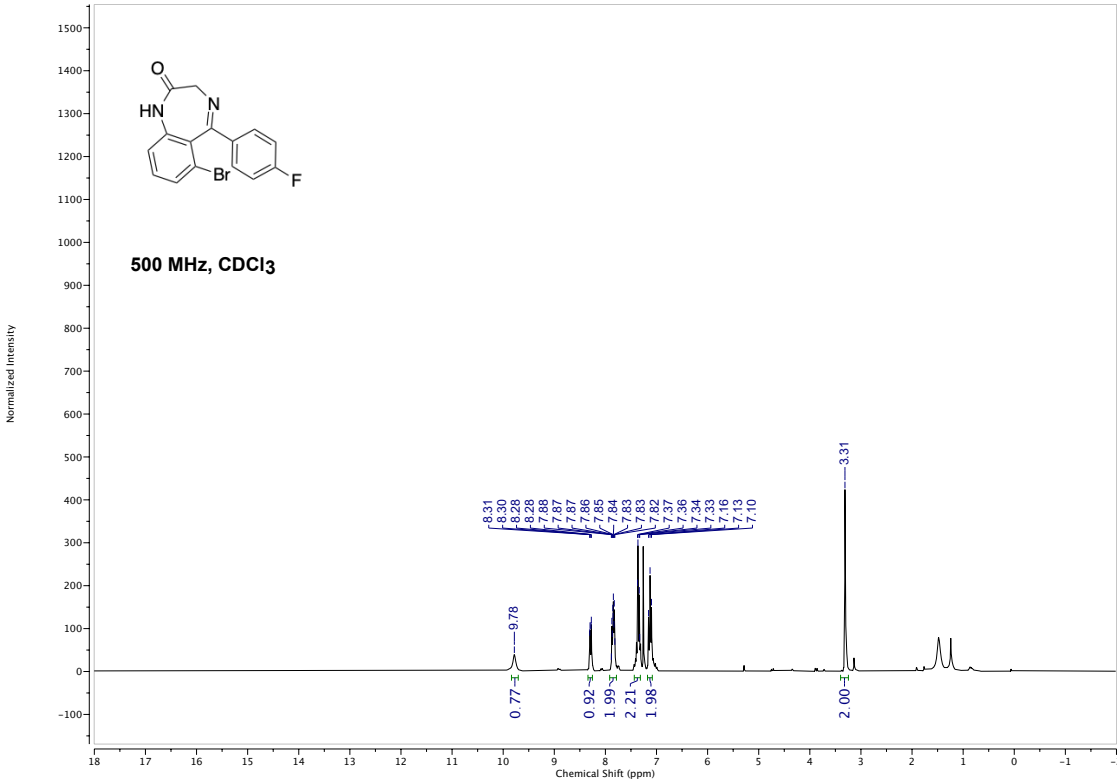
O
HN
N
Br
F
500 MHz, CDCl3
8.31
8.30
8.28
8.28
8.28
7.88
7.87
7.87
7.86
7.85
7.84
7.83
7.83
7.82
7.37
7.36
7.34
7.33
7.16
7.13
7.10
3.31
9.78
0.77
0.92
1.99
2.21
1.98
2.00
Normalized Intensity
Chemical Shift (ppm)

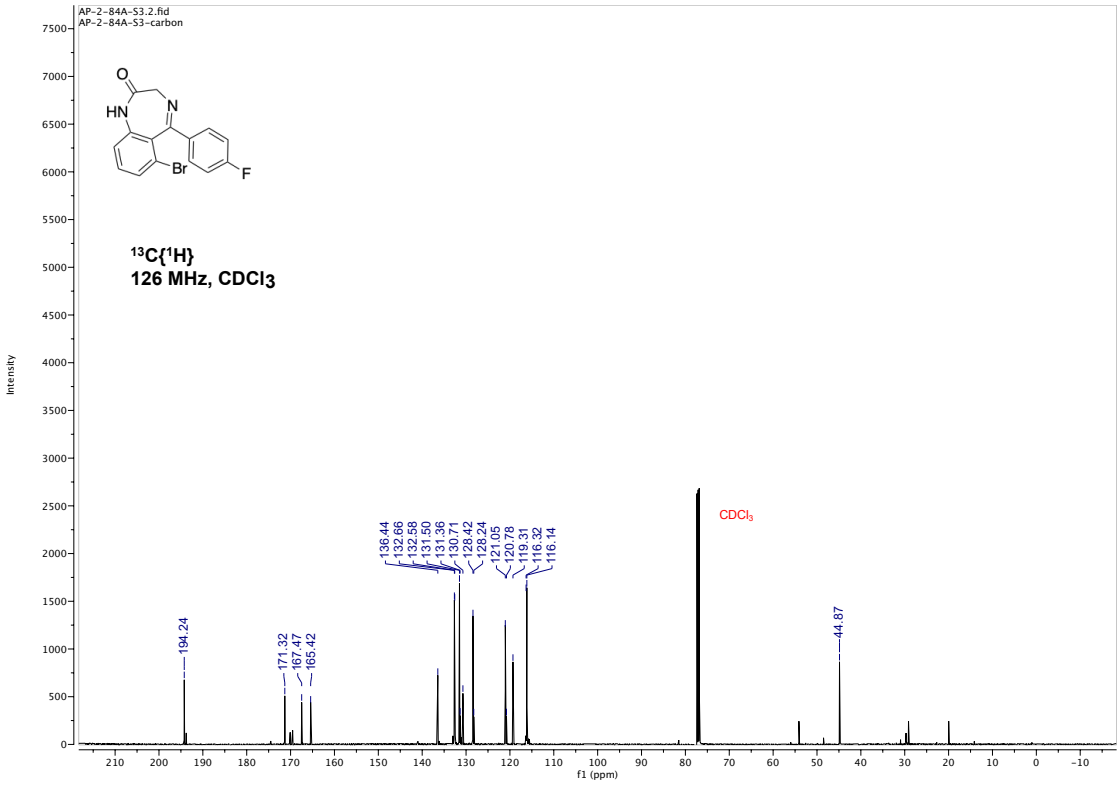
AP-2-84A-S3.2.fid
AP-2-84A-S3-carbon
$^{13}C\{^{1}H\}$
126 MHz, $CDCl_3$
Intensity
f1 (ppm)
194.24
171.32
167.47
165.42
136.44
132.66
132.58
131.50
131.36
130.71
128.42
128.24
121.05
120.78
119.31
116.32
116.14
$CDCl_3$
44.87

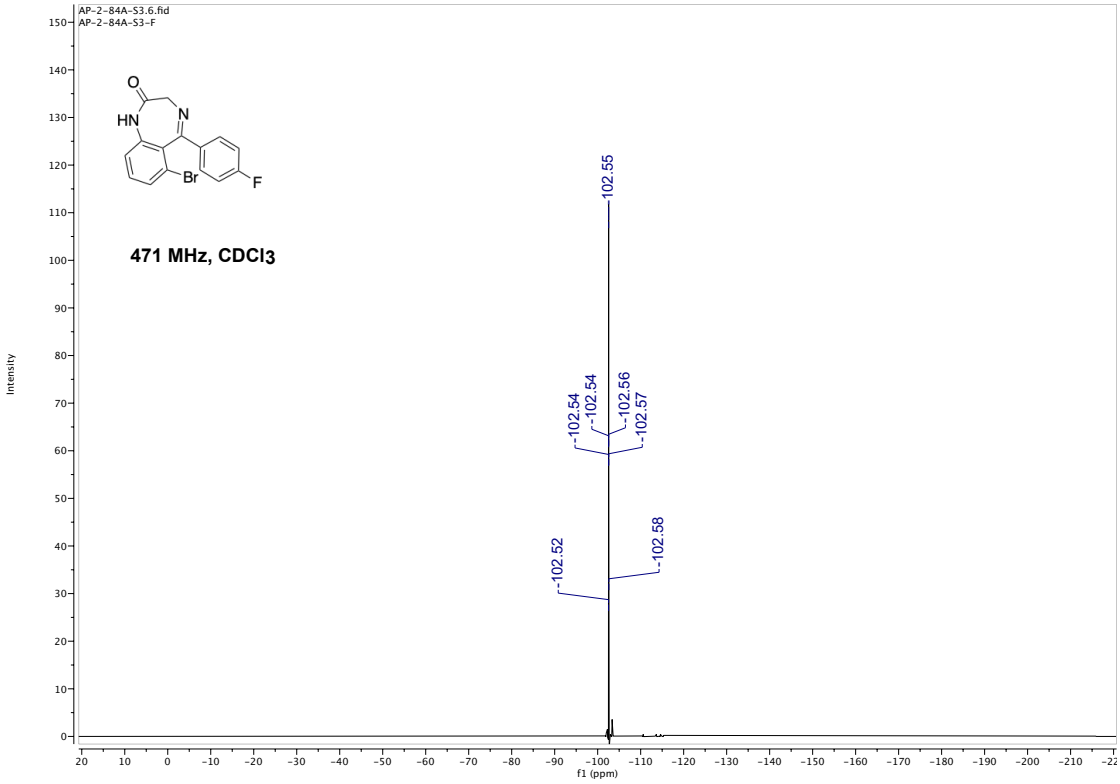
AP-2-84A-S3.6.fid
AP-2-84A-S3-F
471 MHz, $CDCl_3$
Intensity
f1 (ppm)
102.55
102.54
102.54
102.56
102.57
102.52
102.58

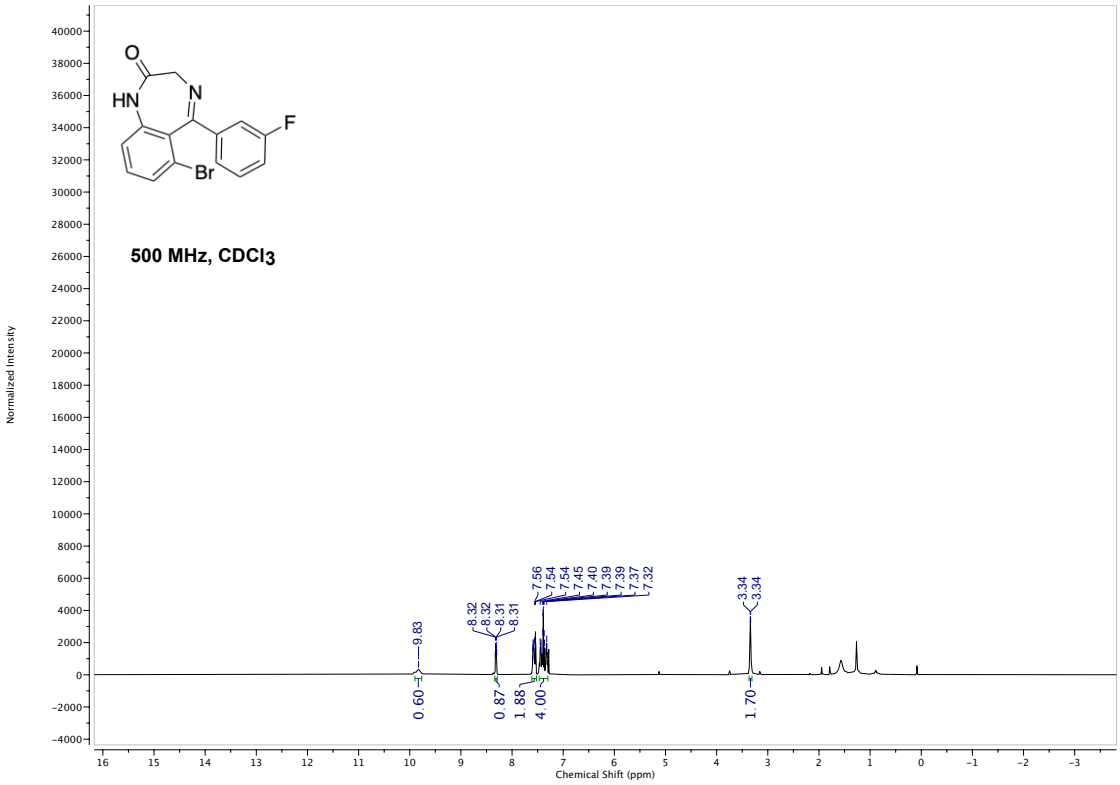
500 MHz, CDCl3
Normalized Intensity
Chemical Shift (ppm)
9.83
8.32
8.32
8.31
8.31
7.56
7.54
7.54
7.45
7.40
7.39
7.39
7.37
7.32
3.34
3.34
0.60
0.87
1.88
4.00
1.70

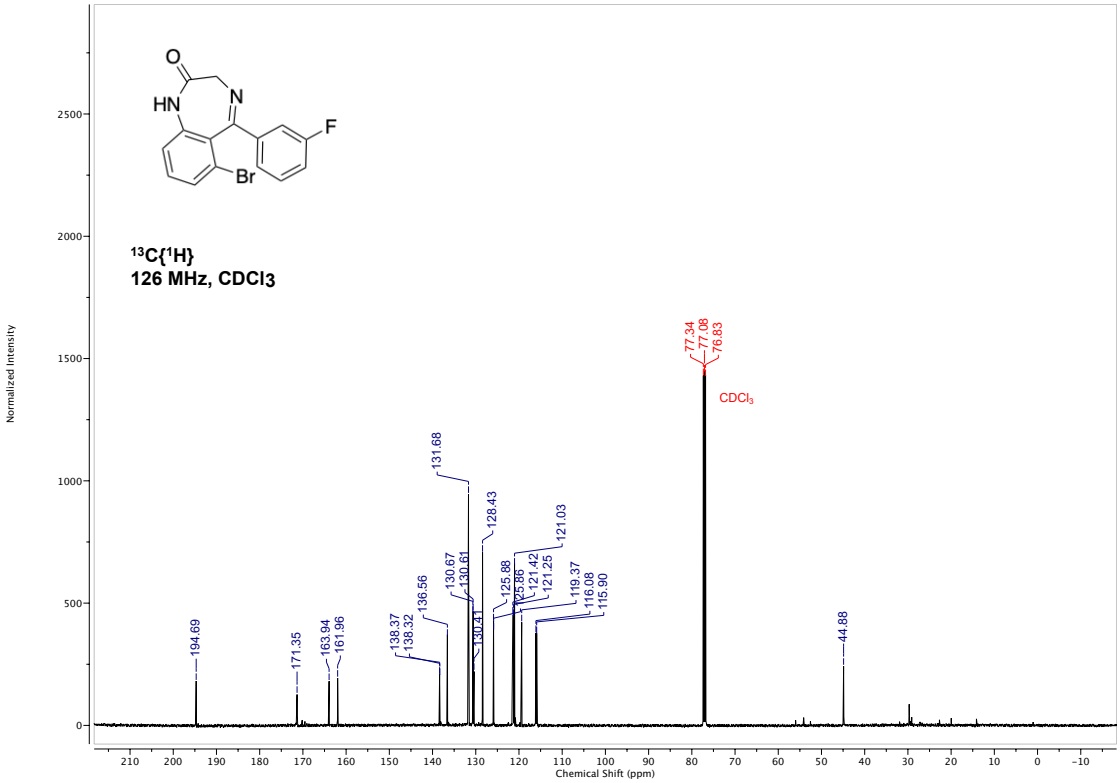
13C{1H}
126 MHz, CDCl3
Normalized Intensity
Chemical Shift (ppm)
194.69
171.35
163.94
161.96
138.37
138.32
136.56
131.68
130.67
130.61
130.41
128.43
125.88
125.86
121.42
121.25
121.03
119.37
116.08
115.90
77.34
77.08
76.83
CDCl3
44.88

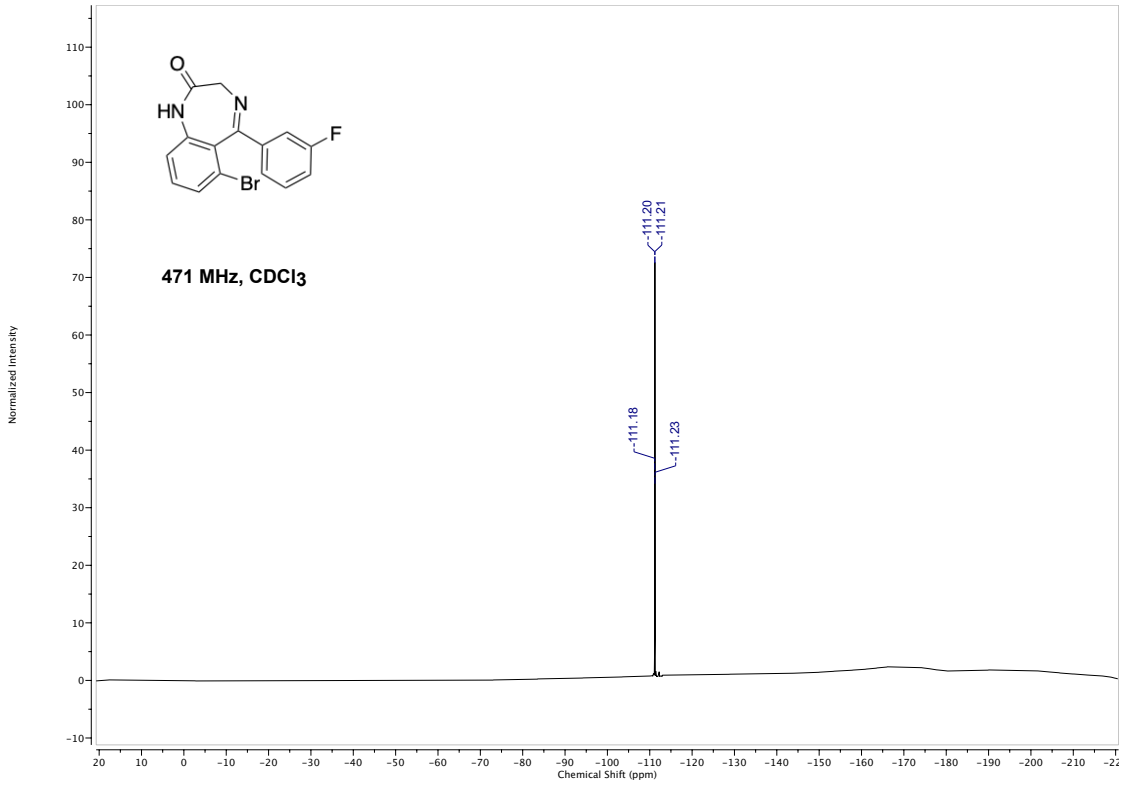
O
HN
N
F
Br
471 MHz, CDCl3
111.20
111.21
111.18
111.23
Normalized Intensity
Chemical Shift (ppm)

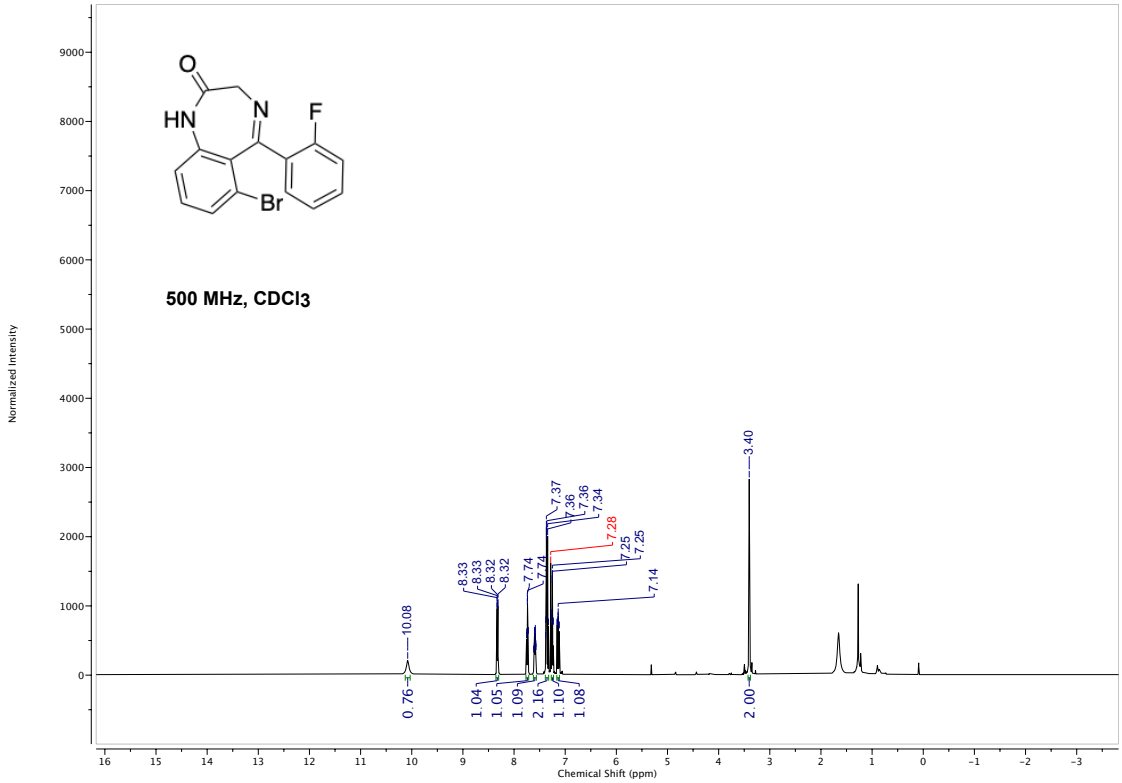
O
HN
N
F
Br
500 MHz, CDCl3
10.08
8.33
8.33
8.32
8.32
7.74
7.74
7.37
7.36
7.36
7.34
7.28
7.25
7.25
7.14
3.40
0.76
1.04
1.05
1.09
2.16
1.10
1.08
2.00
Normalized Intensity
Chemical Shift (ppm)

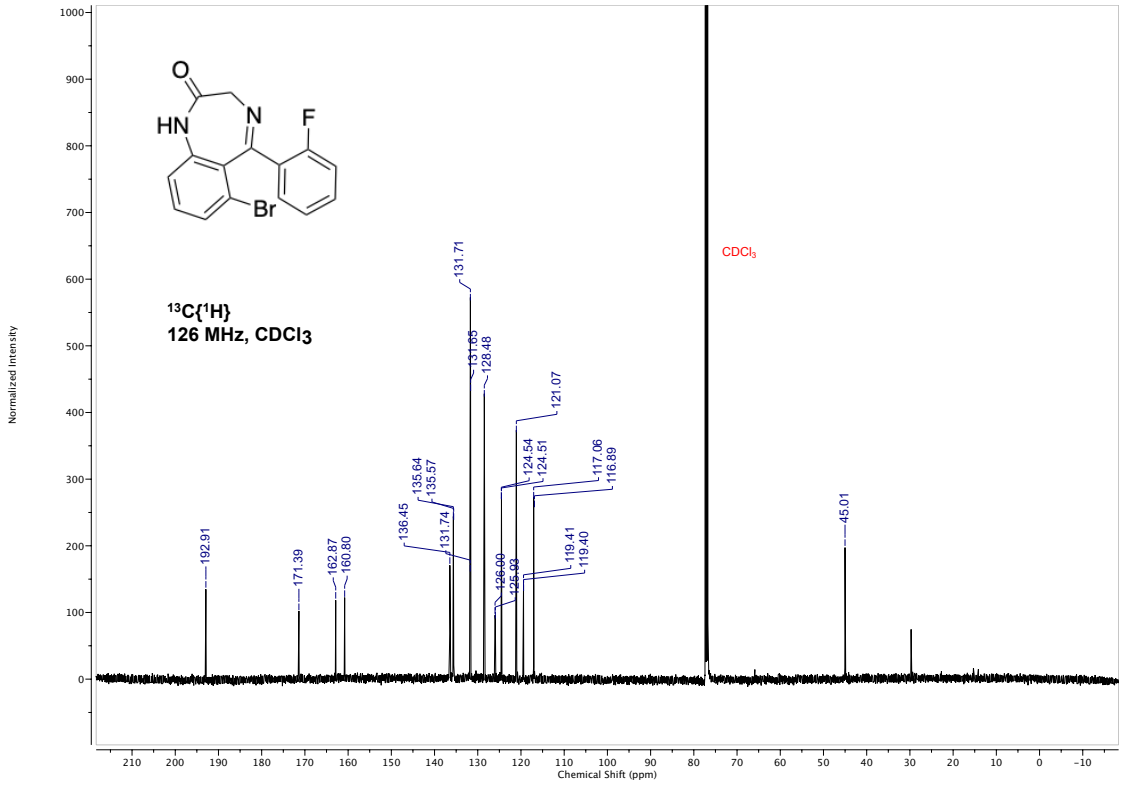
O
HN
N
F
Br
$^{13}C\{^{1}H\}$
126 MHz, $CDCl_3$
$CDCl_3$
Normalized Intensity
Chemical Shift (ppm)
192.91
171.39
162.87
160.80
136.45
135.64
135.57
131.74
131.71
131.65
128.48
126.00
125.93
124.54
124.51
121.07
119.41
119.40
117.06
116.89
45.01

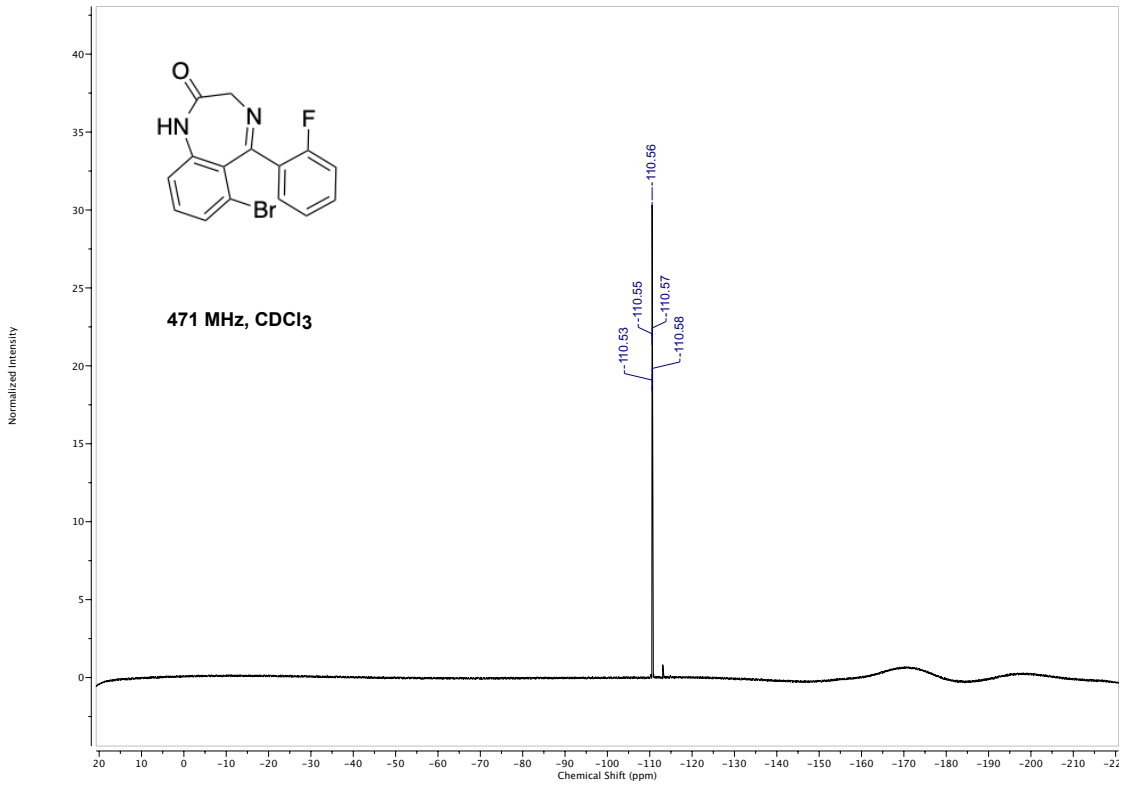
O
HN
N
F
Br
471 MHz, $CDCl_3$
Normalized Intensity
Chemical Shift (ppm)
110.56
110.55
110.57
110.53
110.58

3.9 References

(1) (a) Schifano, F. Recent Changes in Drug Abuse Scenarios: The New/Novel Psychoactive Substances (NPS) Phenomenon. *Brain Sciences*. Multidisciplinary Digital Publishing Institute December 13, 2018, p 221. (b) Sellers, E. M. Deconstructing Designer Drugs. *Clin. Pharmacol. Ther.* **2017**, *101* (2), 167–169.

(2) NIDA. "The science behind designer drugs." *National Institute on Drug Abuse*, 9 Feb. 2015, https://archives.drugabuse.gov/news-events/latest-science/science-behind-designer-drugs. Accessed 8 Nov. 2021.

(3) Baumeister, D.; Tojo, L. M.; Tracy, D. K. Legal Highs: Staying on Top of the Flood of Novel Psychoactive Substances. *Therapeutic Advances in Psychopharmacology*. **2015**, 97–132.

(4) United Nations Office of Drugs and Crime (UNODC). *Current NPS Threats*. 2020, Vol. II. https://www.unodc.org/documents/scientific/Current_NPS_Threats_Volume_II_Web.pdf. Accessed 9 Nov. 2021

(5) Shafi, A.; Berry, A. J.; Sumnall, H.; Wood, D. M.; Tracy, D. K. New Psychoactive Substances: A Review and Updates. *Ther. Adv. Psychopharmacol.* **2020**, *10*.

(6) (a) Schmitz, A. Benzodiazepine Use, Misuse, and Abuse: A Review. *Ment. Heal. Clin.* **2016**, *6* (3), 120–126; (b) Manchester, K. R.; Lomas, E. C.; Waters, L.; Dempsey, F. C.; Maskell, P. D. The Emergence of New Psychoactive Substance (NPS) Benzodiazepines: A Review. *Drug Testing and Analysis*. **2018**, *10,* 37–53; (c) Wick, J. Y.

The History of Benzodiazepines. *Consult. Pharm.* **2013**, *28* (9), 538–548; (d) Abouchedid, R.; Gilks, T.; Dargan, P. I.; Archer, J. R. H.; Wood, D. M. Assessment of the Availability, Cost, and Motivations for Use over Time of the New Psychoactive Substances-Benzodiazepines Diclazepam, Flubromazepam, and Pyrazolam-in the UK. *J. Med. Toxicol*. **2018**, *14*, 134-143

(7) Griffin, C. E.; Kaye, A. M.; Bueno, F. R.; Kaye, A. D. Benzodiazepine Pharmacology and Central Nervous System-mediated Effects. Ochsner J. 2013, 13, 214−223.

(8) Cascade, E.; Kalali, A. H. Use of Benzodiazepines in the Treatment of Anxiety. *Psychiatry (Edgmont).* **2008**, *5* (9), 21–22.

(9) Zhdanova, I. V. Advances in the Management of Insomnia. *Expert Opinion on Pharmacotherapy*. Taylor & Francis July 2004, pp 1573–1579.

(10) Browne, T. R.; Penry, J. K. Benzodiazepines in the Treatment of Epilepsy A Review. *Epilepsia* **1973**, *14* (3), 277–310.

(11) Longo, L. P.; Johnson, B. Addiction: Part I. Benzodiazepines - Side Effects, Abuse Risk and Alternatives. *American Family Physician*. **2000**, *61,* 2121–2128.

(12) Benzodiazepines. Drug Enforcement Administration. Office of Diversion Control. Drug & Chemical Evaluation Section. Dec. 2019.

(13) Emerging Threat Report, Annual 2017. Drug Enforcement Administration: Special Testing and Research Laboratory.

https://cesar.umd.edu/sites/cesar.umd.edu/files/pubs/dea-emerging-threat-report-2017-annual.pdf

(14) Emerging Threat Report, Annual 2018. Drug Enforcement Administration: Special Testing and Research Laboratory. https://cesar.umd.edu/sites/cesar.umd.edu/files/pubs/DEA-Emerging-Threat-Report-2018-Annual.pdf. (b) Emerging Threat Report, Annual 2019. Drug Enforcement Administration: Special Testing and Research Laboratory. https://cesar.umd.edu/sites/cesar.umd.edu/files/pubs/DEA-Emerging-Threat-Report-2019-Annual.pdf. (c) Emerging Threat Report, Annual 2020. Drug Enforcement Administration: Special Testing and Research Laboratory. https://cesar.umd.edu/sites/cesar.umd.edu/files/pubs/DEA-Emerging-Threat-Report-2020-Annual.pdf

(15) (a) Moosmann, B.; Huppertz, L. M.; Hutter, M.; Buchwald, A.; Ferlaino, S.; Auwärter, V. Detection and identification of the designer benzodiazepine flubromazepam and preliminary data on its metabolism and pharmacokinetics. *J. Mass Spectrom*. **2013**, *48*, 1150-1159; (b) Riss, J.; Cloyd, J.; Gates, J.; Collins, S. Benzodiazepines in Epilepsy: Pharmacology and Pharmacokinetics. *Acta Neurol. Scand.* **2008**, *118* (2), 69–86; (c) Moosmann, B.; Bisel, P.; Auwärter, V. Characterization of the Designer Benzodiazepine Diclazepam and Preliminary Data on Its Metabolism and Pharmacokinetics. *Drug Test. Anal.* **2014**, *6* (7–8), 757–763; (d) Huppertz, L. M.; Moosmann, B.; Auwärter, V. Flubromazolam – Basic Pharmacokinetic Evaluation of a Highly Potent Designer Benzodiazepine. *Drug Test. Anal.* **2018**, *10* (1), 206–211.

(16) Drug Enforcement Adminstration (DEA), Department of Justice. Definition of "positional isomer" as it pertains to the control of schedule I controlled substances. Final rule. *Fed Regist*. **2007**, *72*, 67850.

(17) Treatment of controlled substance analogues. U.S. Code, Section 813, Title 21, 2006; (b) Controlled Substances Act. Public Law 91-513, 1970. For details, visit: U.S. Drug Enforcement Administration. https://www. dea.gov/druginfo/csa.shtml

(18) Høiseth, G.; Tuv, S. S.; Karinen, R. Blood Concentrations of New Designer Benzodiazepines in Forensic Cases. *Forensic Sci. Int.* **2016**, *268*, 35–38.

(19) Persona, K.; Madej, K.; Knihnicki, P.; Piekoszewski, W. Analytical Methodologies for the Determination of Benzodiazepines in Biological Samples. *J. Pharm. Biomed. Anal.* **2015**, *113*, 239–264.

(20) (a) Koch, K.; Auwärter, V.; Hermanns-Clausen, M.; Wilde, M.; Neukamm, M. A. Mixed intoxication by the synthetic opioid U-47700 and the benzodiazepine flubromazepam with lethal outcome: Pharmacokinetic data. *Drug Test. Anal.* **2018,** *10*, 1336-1341; (b) Valli, A.; Lonati, D.; Locatelli, C. A.; Buscaglia, E.; Tuccio, M. Di; Papa, P. Analytically Diagnosed Intoxication by 2-Methoxphenidine and Flubromazepam Mimicking an Ischemic Cerebral Disease. *Clin. Toxicol.* **2017**, *55* (6), 611–612; (c) Garg, U.; Krumsick, R.; Frazee, C. C.; Pietak, R.; Peterson, D. C. Chapter 8.3 - A Death Involving Flubromazepam and Methadone. In *Toxicology Cases for the Clinical and Forensic Laboratory*; Ketha, H., Garg, U., Eds.; Academic Press, 2020; pp 117–119.

(21) Ligon, E. S.; Nawyn, J.; Jones, L. V.; Allred, B. M.; Reinhardt, D. V.; France, S. Synthesis of Flubromazepam Positional Isomers for Forensic Analysis. *J. Org. Chem.* **2019**, *84*, 10280-10291.

(22) Sternbach, L. H.; Fryer, R. I.; Metlesics, W.; Reeder, E.; Sach, G.; Stempel, A. Quinazolines and 1,4-Benzodiazepines. V. o-Aminobenzophenones. *J. Org. Chem*. **1962**, *27*, 3781-3788.

(23) The IUPAC name for the parent flubromazepam is 7-Bromo-5-(2-fluorophenyl)-1,3-dihydro-2H-benzo[e][1,4]diazepin-2-one. In order to simply the discussion, we have established the following formalism based on the IUPAC name to represent each flubromazepam isomer: (X,X')-isomer, where X represent the position of the bromine atom and X' represents the position of the fluorine atom. Thus, the parent compound represents the (7,2')-isomer.

(24) Huntress, E. H.; Pfister, K.; Pfister, K. H. T. Fluorenones and Diphenic Acids. IX.1 Establishment of Authentic 1-Bromo- and 4-Bromofluorenones. *J. Am. Chem. Soc*. **1942**, *64*, 2845-2849.

(25) Miller, H. F.; Bachman, G. B. The Higher Benzenoid Hydrocarbons. II. The Isomeric Bromofluorenones1. *J. Am. Chem. Soc*. **1935**, *57*, 2443-2446.

(26) Stephens, H. N. THE FRIEDEL AND CRAFTS' REACTION. BROMOPHTHALIC ANHYDRIDES, BENZENE AND ALUMINUM CHLORIDE. *J. Am. Chem. Soc.* **1921,** *43*, 1950-1956.

(27) Smith, P. A. S. "The Curtius reaction". *Org. React.* **1946**, *3*, 337–449; (b) Curtius, T. Ueber Stickstoffwasserstoffsäure (Azoimid) N3H. *Chem. Ber.* **1890**, *23*, 3023-3033.

(28) For selected examples, see: (a) Nagahora, N.; Tanaka, R.; Tada, T.; Yasuda, A.; Yamada, Y.; Shioji, K.; Okuma, K. Thiopyrylium Scaffolds from the Lewis/Brønsted-Acid-Promoted Cyclization of Thioethers. *Org. Lett.* **2020,** *22*, 6192-6196; (b) Tran, P. H.; Nguyen, H. T.; Hansen, P. E.; Le, T. N. Greener Friedel-Crafts Acylation Using Microwave-Enhanced Reactivity of Bismuth Triflate in the Friedel-Crafts Benzoylation of Aromatic Compounds with Benzoic Anhydride. *ChemistrySelect* **2017**, *2*, 571-575; (c) Yadav, G. D.; Bhagat, R. D. Experimental and theoretical analysis of Friedel–Crafts acylation of thioanisole to 4-(methylthio)acetophenone using solid acids. *J. Mol. Catal. A Chem.* **2005**, *235*, 98-107.

(29) For representative reviews and articles on thioethers as directing groups for C-H functionalization, see: (a) Xuchong, T.; Yingwei, Z. A Review on Sulfur-Directed C−H Bond Activation. *Mini Rev. Org. Chem.* **2020,** *17*, 1-23; (b) Thioether-Directed Peri-Selective C-H Arylation under Rhodium Catalysis: Synthesis of Arene-Fused Thioxanthenes. *Org. Lett*. **2019**, *21*, 233-236; (c) Sambiagio, C.; Schönbauer, D.; Blieck, R.; Dao-Huy, T.; Pototschnig, G.; Schaaf, P.; Wiesinger, T.; Zia, M. F.; Wencel-Delord, J.; Besset, T.et al. A comprehensive overview of directing groups applied in metal-catalysed C–H functionalisation chemistry. *Chem. Soc. Rev.* **2018,** *47*, 6603-6743; (d) Yu, M.; Xie, Y.; Xie, C.; Zhang, Y. Palladium-Catalyzed C–H Alkenylation of Arenes Using Thioethers as Directing Groups. *Org. Lett*. **2012**, *14*, 2164-2167; (e) Shabashov, D.; Daugulis, O. Auxiliary-Assisted Palladium-Catalyzed Arylation and Alkylation of sp2 and sp3 Carbon−Hydrogen Bonds. *J. Am. Chem. Soc*. **2010**, *132*, 3965-3972.

(30) (a) Park, S. J.; Buschmann, H.; Bolm, C. Bioactive sulfoximines: Syntheses and properties of Vioxx® analogs. *Bioorg. Med. Chem. Lett*. **2011**, *21*, 4888-4890; (b) Thérien, M.; Gauthier, J. Y.; Leblanc, Y.; Léger, S.; Perrier, H.; Prasit, P.; Wang, Z. Synthesis of Rofecoxib, (MK 0966, Vioxx® 4-(4-Methylsulfonylphenyl)-3-Phenyl-2(5H)-Furanone), a Selective and Orally Active Inhibitor of Cyclooxygenase-2. *Synthesis* **2001**, 1778-1779.

(31) Ghosh, A. K.; Brindisi, M.; Sarkar, A. The Curtius Rearrangement: Applications in Modern Drug Discovery and Medicinal Chemistry. *ChemMedChem* **2018**, *13* (22), 2351–2373.

(32) For selected desulfuration examples, see: (a) Matsumura, T.; Niwa, T.; Nakada, M. Pd-catalyzed reductive cleavage of alkyl aryl sulfides with triethylsilane that is accelerated by trialkylsilyl chloride. *Tetrahedron Lett*. **2012**, *53*, 4313-4316; (b) Barbero, N.; Martin, R. Ligand-Free Ni-Catalyzed Reductive Cleavage of Inert Carbon–Sulfur Bonds. *Org. Lett*. **2012**, *14*, 796-799; (c) Graham, T. H.; Liu, W.; Shen, D.-M. A Method for the Reductive Scission of Heterocyclic Thioethers. *Org. Lett*. **2011**, *13*, 6232-6235.

(33) It has been shown that for the analogous 3-fluoroanisole, Friedel-Crafts alkylation occurs ortho to the ether with low yield. For examples, see: (a) Mtashobya, L. Insights on tert-butyl alkylation effects on fluorobenzene. *Sci. Afr.* **2021**, *11*, e00659; (b) Olah, G. A.; Yamato, T.; Hashimoto, T.; Shih, J. G.; Trivedi, N.; Singh, B. P.; Piteau, M.; Olah, J. A. Aromatic substitution. 53. Electrophilic nitration, halogenation, acylation, and alkylation of (.alpha.,.alpha.,.alpha.-trifluoromethoxy)benzene. *J. Am. Chem. Soc*. **1987**, *109*, 3708-3713; (c) Olah G.A. (Ed.), *Friedel–Crafts and Related Reactions*, Wiley Interscience, New York (1964).

(34) Pricing obtained from compound commercial availability search using Scifinder. SciFinder; Chemical Abstracts Service: Columbus, OH; https://scifinder.cas.org (accessed September 30, 2021).

(35) Ashburn, B. O.; Carter, R. G.; Zakharov, L. N. Synthesis of Tetra-ortho-substituted, Phosphorus-Containing and Carbonyl-Containing Biaryls Utilizing a Diels−Alder Approach. *J. Am. Chem. Soc*. **2007**, *129*, 9109-9116.

(36) Vetelino, M. G.; Coe, J. W. A mild method for the conversion of activated aryl methyl groups to carboxaldehydes via the uncatalyzed periodate cleavage of enamines. *Tetrahedron Lett*. **1994**, *35*, 219-222.

(37) Zhang, J.; Zhu, D.; Yu, C.; Wan, C.; Wang, Z. A Simple and Efficient Approach to the Synthesis of 2-Phenylquinazolines via sp3 C−H Functionalization. *Org. Lett*. **2010**, *12*, 2841-2843.

CHAPTER 4. FORENSIC ANAYLSIS AND DIFFERENCIATION OF THE (6,X')-FLUBROMAZEPAM POSITIONAL ISOMERS*

4.1 Forensic Differentiation

4.1.1 Purpose

As discussed previously in Chapter 3, positional isomers of designer benzodiazepines are structurally similar analogous to their federally controlled parent benzodiazepines that are anticipated to display comparable physiological outcomes. Due to the Federal Analogue Act, positional isomers of designer benzodiazepines must be scheduled individually as many drugs of this class fall under Schedule IV. As more drugs become scheduled, distributors often look to positional isomers as technically legal alternatives. The speed in which these new drugs are being synthesis often makes it difficult for forensic examiners and other agencies to stay up to date with new developments. To stay on top of this, the 12 positional isomers of flubromazepam, were synthesized to aid in accruing analytical data to differentiate between illicit designer benzodiazepines. In this study, traditional forensic analysis techniques such as mass spectroscopy (MS), infrared spectroscopy (IR), and proton, carbon, and fluorine nuclear magnetic resonance (^{1}H, ^{13}C, ^{19}F NMR) were used for the structural identification and validation of the three newly synthesized (6,X')-flubromazepam isomers. The characterization data of the 3 isomers will be used to compared to the parent in hopes that each isomer presents a unique analytical profile for the purpose of differentiation.

*Work performed in collaboration with the Defense Forensic Science Center (DFSC)

Differentiation through Traditional Forensic Analysis Techniques

4.1.2 LC-MS/MS Analysis

Mass spectrometry (MS) has been widely acknowledged as the "gold standard" in forensic analysis. Through MS, the precise molecular mass of ions as determined by their mass to charge ratio is measured.[1] Usually, MS is coupled with various separation techniques such as gas chromatography (GC), liquid chromatography (LC), or capillary electrophoresis (CE) which assists in identifying, quantifying, and/or elucidating the structures of substances in a complex sample.[2] Liquid chromatography (LC) is a technique used to separate non-volatile compounds. Separation through this technique occurs based on the interaction of the sample with the mobile and stationary phases. Once separated, the analyte reaches a detector for identification. In recent years, MS has evolved and become the detector of choice for chromatographic techniques as the use of MS allows for the unambiguous identification of analytes. The recent advances in tandem MS (MS/MS) coupled with LC have provided additional dimensions in the analysis of substances like 1) higher specificity and sensitivity which allows for lower limits of detection and 2) the ability to "multiplex" or identify and quantify several analytes of interest concurrently.[3] Thus, LC-MS/MS has been used in numerous forensic cases and studies to analyse, identify, and quantify drug samples.[4] To contribute to the many applications of this analytical technique herein, LC-MS/MS analysis was used as a potential means of isometric differentiation for the (6,X')-isomers from the parent flubromazepam isomer.

For all (6,X')-isomers, the expected molecular ion peak $[M+H]^+$ was present (m/z 333.0) which was consistent with the parent isomer. Other major fragments include loss of

bromine, [M-79] (m/z = 253); loss of CO and bromine, [M-106] (m/z = 226); loss of HF (m/z = 208) for previous fragment (m/z = 226); fragmentation with chemical composition C_7H_7BrN (m/z = 184). Table 4.1 shows the elemental composition for common MS fragments for the (6,X')-isomers. Based on data obtained by the Defense Forensic Science Center on the parent (7,2') and the other 8 isomers, peaks present at 287, 253, and 198 m/z are unique to (6,X')-isomers only.

Table 4.1 Elemental Composition of (6,X')-Flubromazepam Fragments

Formula	Mass Observed	ppm
$C_{14}H_{11}N_2BrF$	305.0083	-0.281
$C_{14}H_8NBrF$	287.9818	-0.405
$C_{15}H_{10}ON_2F$	253.0771	-0.307
$C_{14}H_{11}N_2F$	226.09	-0.434
$C_{14}H_{10}NF$	211.0792	-0.09
$C_8H_6N_2Br$	208.9709	0.06
$C_{13}H_9NF$	198.0714	-0.021
C_7H_7NBr	183.9756	0.063
$C_9H_6ON_2$	158.0475	-0.091
C_7H_6F	109.0451	2.981
C_7H_7N	105.0576	3.324

Based on the data presented, MS/MS has the potential to aid in differentiating the (6,X')-isomers from the parent by way of the distinguishing fragmentation patterns highlighted in Table 4.1. Comparing the MS data of all 12 isomers to one another will truly tell if MS/MS is an appropriate diagnostic tool for isomeric differentiation.

LC retention times are hypothesized to be a distinguishing analytical tool for the identity of flubromazepam isomers. The retention times for the (6,X')-isomers are shown in Table 4.2. Based on the average retention time and standard deviation, there is a clear

difference in the time it takes for each isomer to elute. However, isomeric differentiation from the parent may not be possible for the (6,3')-isomer as they would potentially elute around the same time (parent retention time = 4.39). A comparison of all 12 isomers and more rigorous statistical analysis is needed to accurately compare and support or deny this hypothesis.

Table 4.2 LC Retention Times of (6,X')-Flubromazepam Isomers

	Peak time Averages and Std				
	Run				
Isomer	1	2	3	Average	Standard Deviation
6,2'	4.01	4.02	4.05	4.03	0.021
6,3'	4.43	4.36	4.67	4.49	0.163
6,4'	4.19	4.16	4.16	4.17	0.017

4.1.3 FTIR Analysis

Infrared Spectroscopy (IR) is considered a highly discriminatory method for the forensic analysis of illicit substances. Interpretation of an IR spectra allows for determination of molecular functional groups within a substance.[1] For a pure compound, an IR spectrum provides a distinct fingerprint that can be easily differentiated from other compounds, including molecules with the same chemical formula, or positional isomers. Unknown samples and mixtures of compounds can pose issues for analysis; however, most compounds can be unambiguously identified when reference standards are available.

The IR data obtained for the (6,X')-flubromazepam positional isomers is shown in the Experimental Section. Functional groups in the 4000-1600 cm^{-1} region for each (6,X')-isomer resembled the (7,2')-parent flubromazepam isomer with a N-H stretch

corresponding to the amide around 3200 cm^{-1}, sp^2- and sp^3-C-H stretches around 3060 cm^{-1} and 2920 cm^{-1} respectively, and two strong peaks consistent with amide C=O (~1670 cm^{-1}) and imine C=N (~1560 cm^{-1}) stretches.

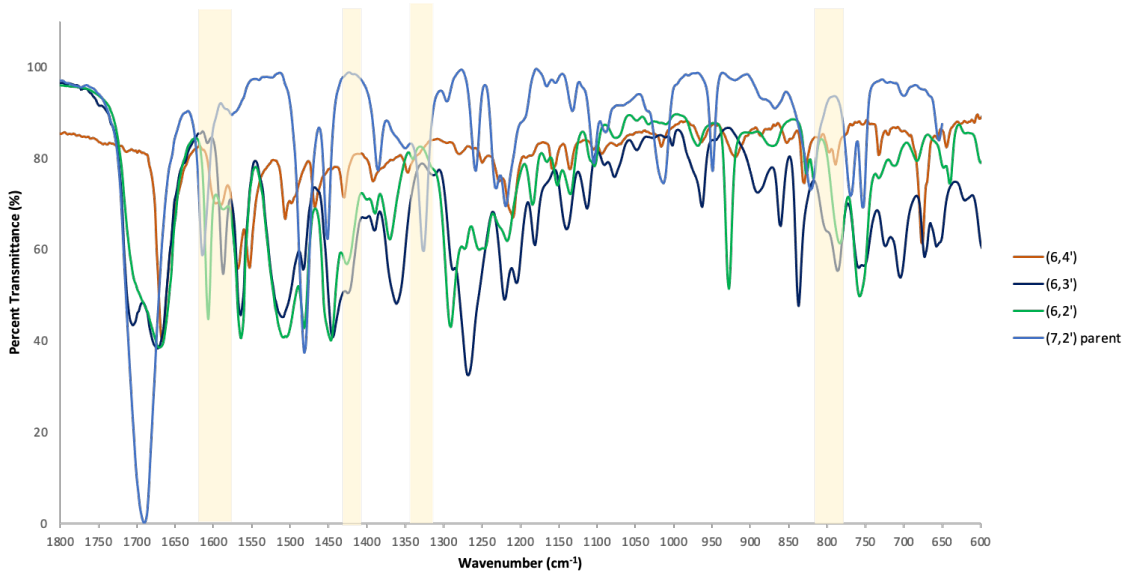

Figure 4.1 Fingerprint Region Comparison

The area known as the fingerprint region falls between 1500-400 cm^{-1}. It usually contains a large number of peaks which makes it difficult to identify anything specific with the naked eye. However, the fingerprint region is important because each compound produces a unique pattern even if the compounds contain the same bonds. In the case of the flubromazepam positional isomers, the fingerprint region shows patterns consistent with C-Br and C-F stretching and C-H aromatic bending frequencies. Figure 4.1 shows an overlay of the fingerprint regions of the (6,X')-isomers compared to the parent with points of potential distinguishability. This is extremely hard to see with the naked eye, therefore, statistical analysis is needed. Now that there is IR reference data for all twelve positional isomers of flubromazepam, with the help of forensic spectral libraries such as NIST, the

fingerprint regions, as well as the spectra as a whole, can be used to differentiate between isomers and aid in identifying these isomers in unknown samples.[5]

4.1.4 NMR Analysis

Nuclear Magnetic Resonance (NMR) is one of the most powerful techniques used for structure elucidation in the fields of chemistry and biology. In forensic science, NMR as an analytical technique is still in its infancy; however, when used, it is largely applied to the identification and quantification of controlled substances.[6] Here, we use NMR as a means for structure identification and differentiation between flubromazepam positional isomers, with hopes that the data obtained will be useful in the field should positional isomers of flubromazepam appear in unknown forensic samples.

4.1.4.1 ^{1}H NMR

For each (6,X')-flubromazepam isomer, ^{1}H NMR revealed a sharp singlet between 10.1-9.7 ppm corresponding to the NH functional group and also a sharp singlet around 3.2-4.1 ppm consistent with deshielded CH_2 protons. The aromatic region exhibited the expected 7 aromatic protons based on integration as well as the anticipated splitting and coupling constants associated with having *ortho*- and *meta*- protons around the benzene rings. In addition, the positional changes of the fluorine atom give each isomer a distinct splitting pattern beneficial for both structural identification and isomeric differentiation.

Upon comparing the parent **(7,2')**-flubromazepam[7] to the **(6,X')**-isomers, a clear differentiation in the ^{1}H NMR spectra is evident (Figure 4.2). For the benzodiazepine amide proton (Figure 4.2A), the parent has a signal at 10.73 ppm, whereas the **(6,X')**-isomers

have signals that appear at chemical shifts below 10 ppm. Similarly, the **(6,X')**-isomers show aromatic proton signals between 7.75 and 8.5 ppm, whereas the parent compound does not (Figure 4.2B). Thus, differentiation by ^{1}H NMR is a plausible approach to forensic analysis and compound identification.

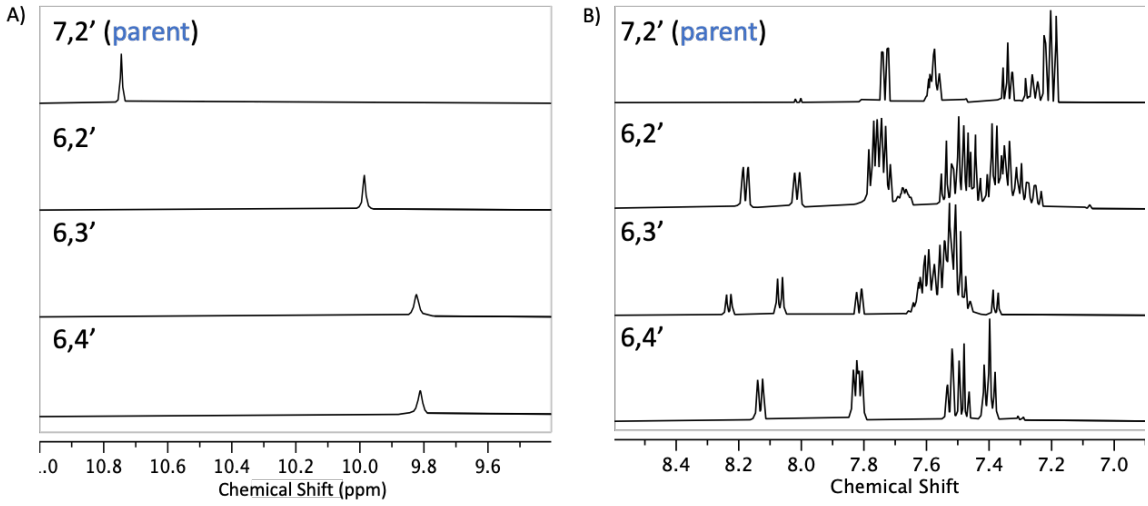

Figure 4.2 ^{1}H NMR comparison of the parent (7,2')-flubromazepam to the (6,2')-, (6,3')-, and (6,4')-positional isomers.

4.1.4.2 ^{13}C NMR

In terms of structural identification, the most easily distinguishable functional groups in the ^{13}C NMR spectra for the (6,X')-flubromazepam isomers are the amide carbonyl carbon (C=O) between 192-194 ppm, the imine carbon (C=N) around 171 ppm, and the aliphatic carbon (CH_2) between 44-45 ppm. The aromatic region contains the remaining corresponding carbons in addition to the peaks derived from splitting due to the fluorine atom. As expected, the carbons on the fluoro-phenyl ring are split into doublets with coupling constants consistent with typical short- and long-range values.

A few major point of differentiation for the (6,X')-isomers compared to the parent (7,2')-isomer is the chemical shifts of the amide carbonyl carbon, the imine carbon and the aliphatic carbon (Scheme 4.3). In the parent isomer, these peaks occur at 169.59 ppm (C=O), 165.10 (C=N) ppm, and 57.06 ppm (CH_2) while the (6,X')-isomers display peaks between 192-194 ppm (C=O), around 171 ppm (C=N), and between 44-45 ppm (CH_2) (Figure 4.3). This rather drastic difference in chemical shift for the (C=O) peak is likely attributed to the bromine in the 6-position inducing conformational strain compared to the parent isomer. This could also be the reason for 1) the differences in (C=N) and (CH_2) chemical shifts as orbital interactions of adjacent carbons will have likely been altered and 2) the instability of each isomer. A deeper investigation on the conformational analysis of these isomers is needed to support this hypothesis. Although ^{13}C NMR is considered a less sensitive technique resulting in longer run times and the need for adequately concentrated samples, it proves to be a useful technique in identifying the (6,X')-isomers and differentiating them from the (7,2')-parent flubromazepam isomer.

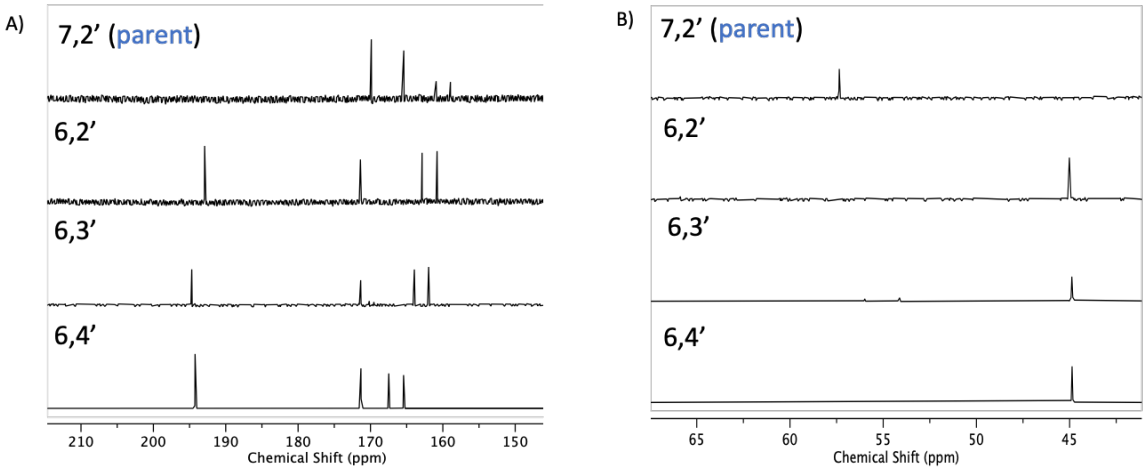

Figure 4.3 ^{13}C NMR comparison of the parent (7,2')-flubromazepam to the (6,2')-, (6,3')-, and (6,4')-positional isomers.

4.1.4.3 ^{19}F NMR

Of the NMR techniques mentioned, ^{19}F NMR analysis shows the greatest potential for isomeric differentiation. This technique offers the greatest sensitivity as ^{19}F is present in 100% abundance and acquisition times are under a minute. The are no clear trends among the (6,X') isomers, but compared to the parent flubromazepam isomer, the chemical shifts and splitting patterns differ significantly (Table X).

Table 4.3 ^{19}F NMR comparison of the parent (7,2')-flubromazepam to the (6,2')-, (6,3')-, and (6,4')-positional isomers.

Isomer	Chemical Shift (ppm) (Multiplicity, J value)
7,2' (parent)	-113.91 – -114.01 (m)
6,2'	-110.56 (dt, J = 11.4, 5.9 Hz)
6,3'	-111.21 (q, J = 8.0 Hz)
6,4'	-102.56 (td, J = 8.9, 8.5, 4.6 Hz)

4.2 Summary

Using traditional forensic analysis techniques, characterization data for the three newly synthesized (6,X')-flubromazepam positional isomers was acquired for the purpose of structural identification and isomeric differentiation from the parent (7,2')-isomer. From this study, we begin to see trends that can be further accessed upon comparison of all 12 positional isomers of flubromazepam. Upon rigorous statistical analysis of the data a standard protocol to distinguish between isomers and potentially other benzodiazepines can be developed.

4.3 Experimental

4.3.1 Analytical Methods

4.3.1.1 LCMS

The Thermo Fisher Scientific (Waltham, MA) Vanquish™ ultrahigh pressure liquid chromatograph (UHPLC) was used to chromatographically separate isomers with a C18 reverse phase column (2.1 x 50 mm, 1.7 µm particles, 130 Å pores). Flow rate was set to 0.7µL/min, and the mobile phases were 0.1 mM ammonium acetate in water (A) and acetonitrile (B). The method began at 5 % B and was ramped up to 95 % over 10 minutes and then held for 2 minutes. The Q Exactive™ Hybrid Quadrupole-Orbitrap Mass Spectrometer (MS) from Thermo Fisher Scientific (Waltham, MA) used to detect flubromazepam had a positive ionization spray voltage was set at 3500 V, 250 °C capillary, 50 °C probe and the sheath gas was set to 10 (unknown units). The data dependent acquisition (DDA) had a full scan resolution of 140,000 between m/z 200 and m/z 2000, and dd-Ms2 resolution of 35,000 with an isolation window of m/z 0.4 and normalized collision energy (NCE) of 50. Data was collected and analyzed using XclaiburTM ver4.1.21.9 and Qual Browser from Thermo Fisher Scientific (Waltham, MA), respectively.

4.3.1.2 NMR

Proton and carbon and fluorine nuclear magnetic resonance spectra (^{1}H NMR and ^{13}C NMR) were recorded on a Bruker 500 MHz spectrometer with solvent resonances as the internal standard (^{1}H NMR: $CDCl_3$ at 7.26 ppm or DMSO-d_6 at 2.50; ^{13}C NMR: $CDCl_3$ at

77.0 ppm or DMSO-d_6 at 39.5; ^{19}F NMR: locked to $CDCl_3$ or DMSO-d_6). NMR signals from prep TLC binders appear between 0.6 and 1.3 ppm in ^{1}H NMR and ~29.7 ppm in ^{13}C NMR. ^{1}H NMR data are reported as follows: chemical shift (ppm), multiplicity (s = singlet, d = doublet, dd = doublet of doublets, dt = doublet of triplets, ddd = doublet of doublet of doublets, t = triplet, m = multiplet, br = broad), coupling constants (Hz), and integration.

4.3.2 MS Data

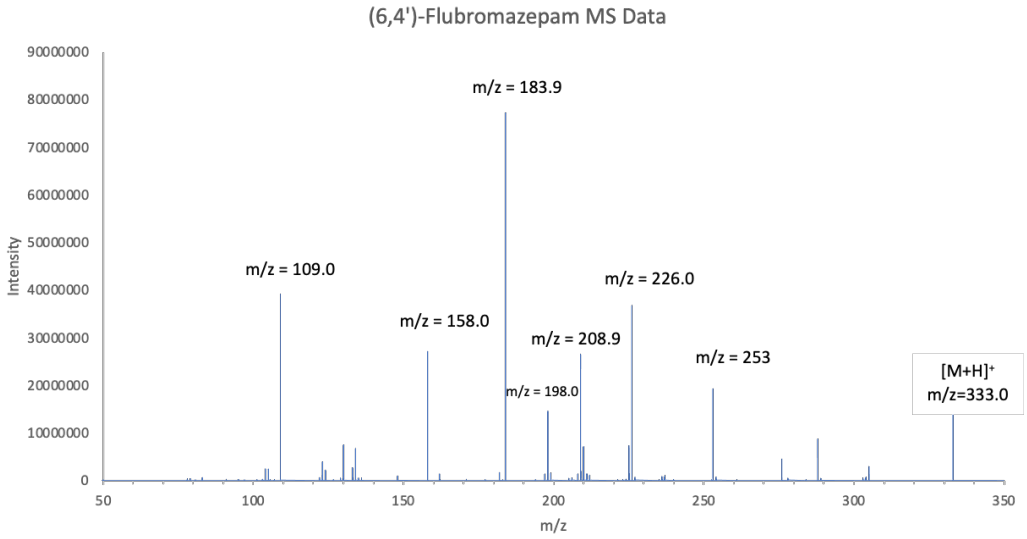

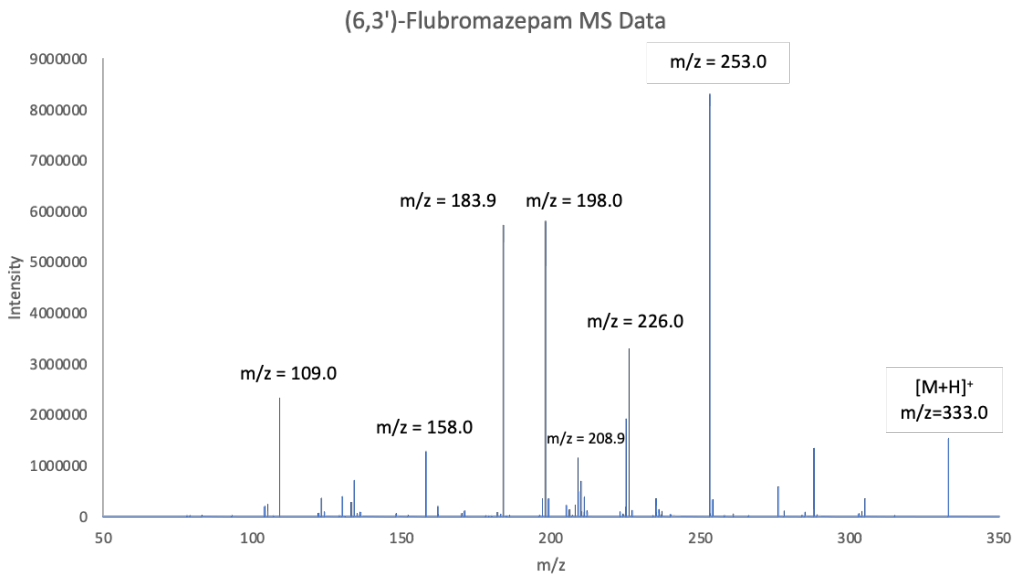
(6,3')-Flubromazepam MS Data
m/z = 253.0
m/z = 183.9
m/z = 198.0
m/z = 226.0
m/z = 109.0
m/z = 158.0
m/z = 208.9
[M+H]+
m/z=333.0
Intensity
m/z

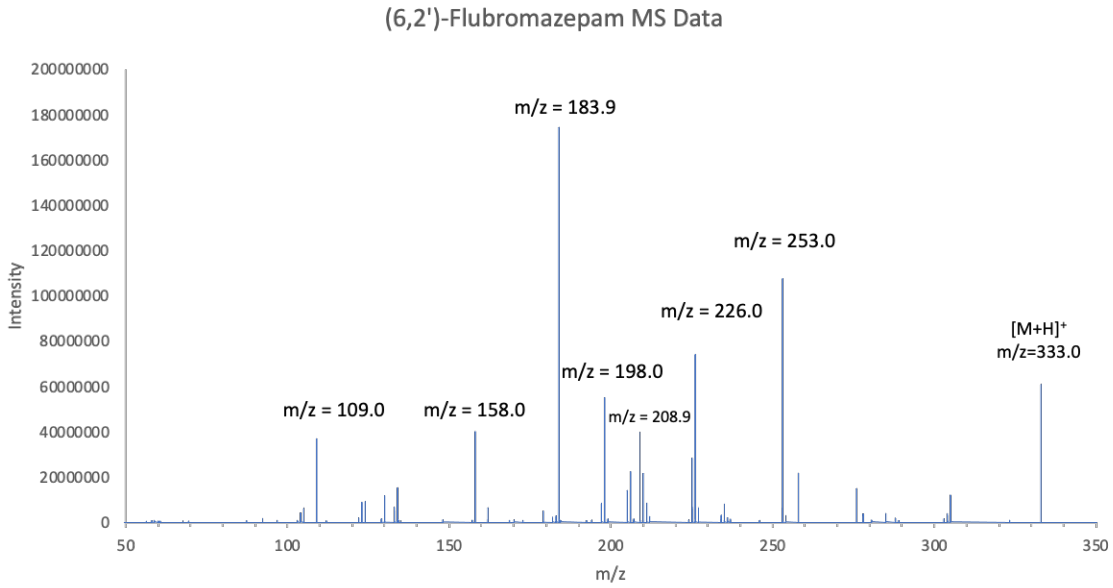
(6,2')-Flubromazepam MS Data
m/z = 183.9
m/z = 253.0
m/z = 226.0
m/z = 198.0
[M+H]+
m/z=333.0
m/z = 109.0
m/z = 158.0
m/z = 208.9
Intensity
m/z

4.3.3 LC Data

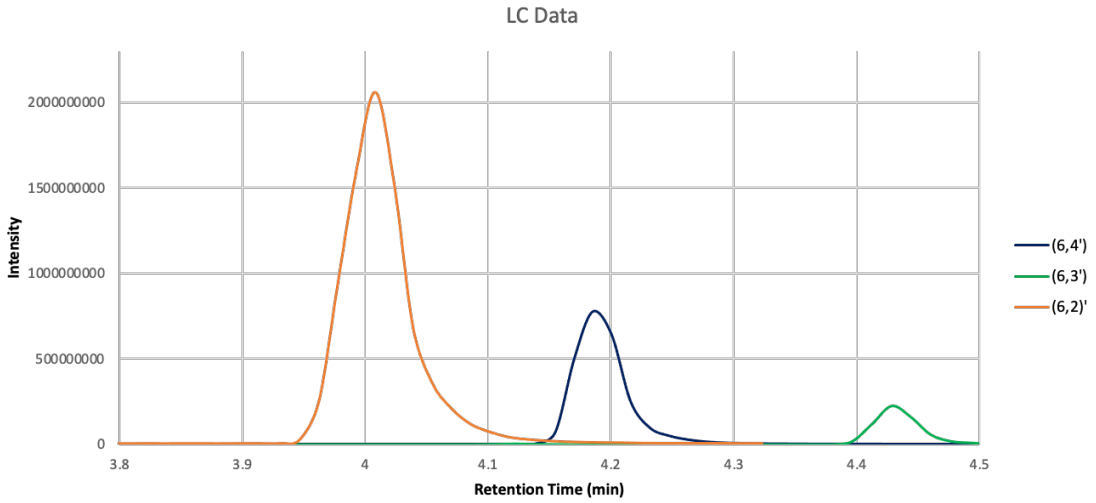

4.3.4 IR Spectra

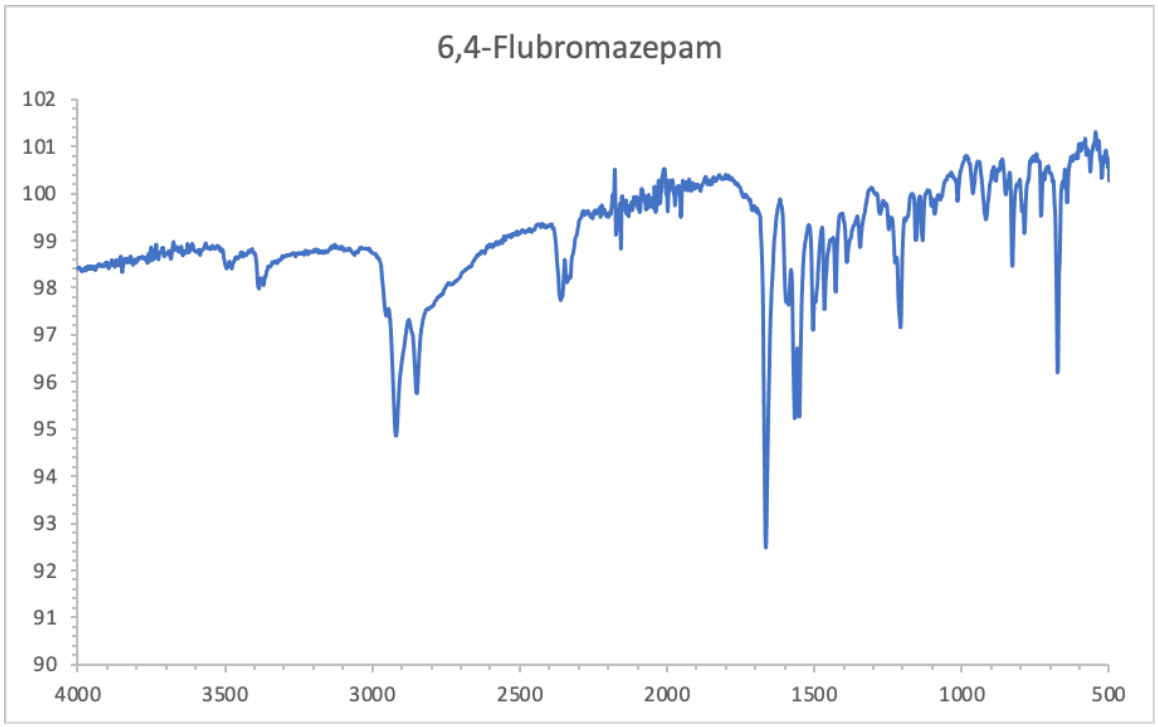

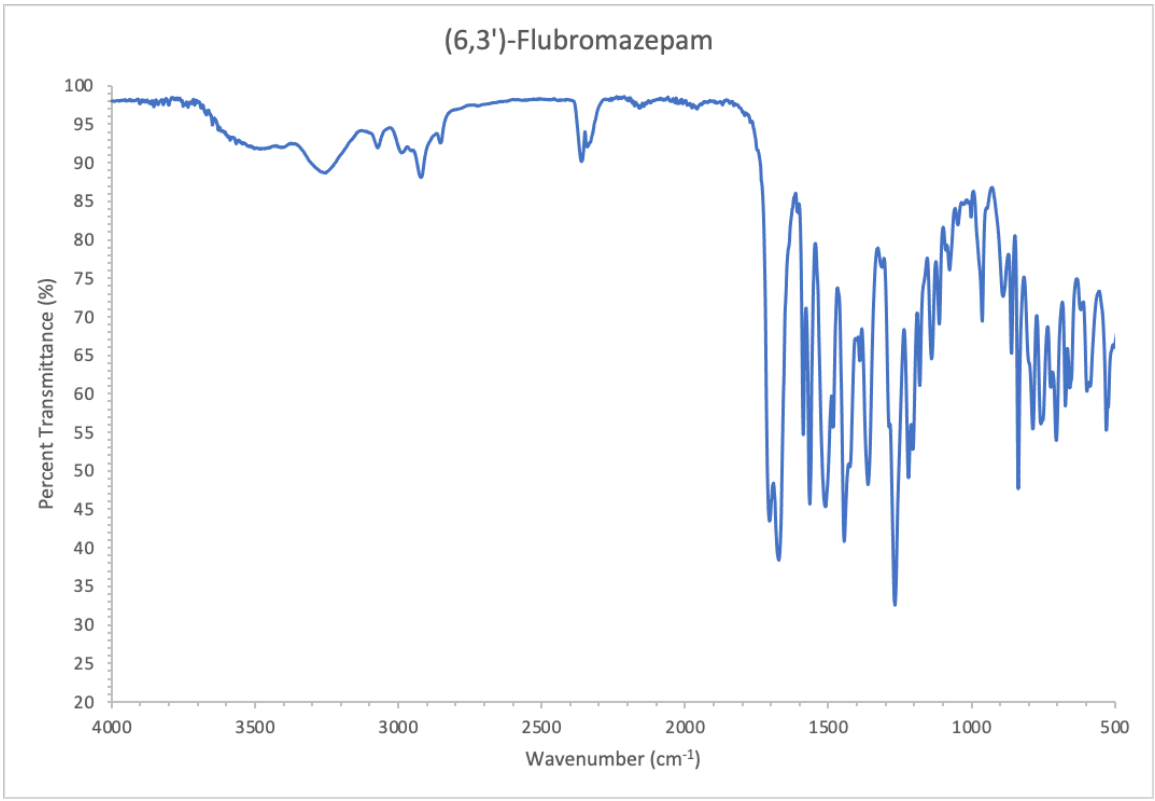
(6,3')-Flubromazepam
Percent Transmittance (%)
100
95
90
85
80
75
70
65
60
55
50
45
40
35
30
25
20
4000
3500
3000
2500
2000
1500
1000
500
Wavenumber (cm-1)

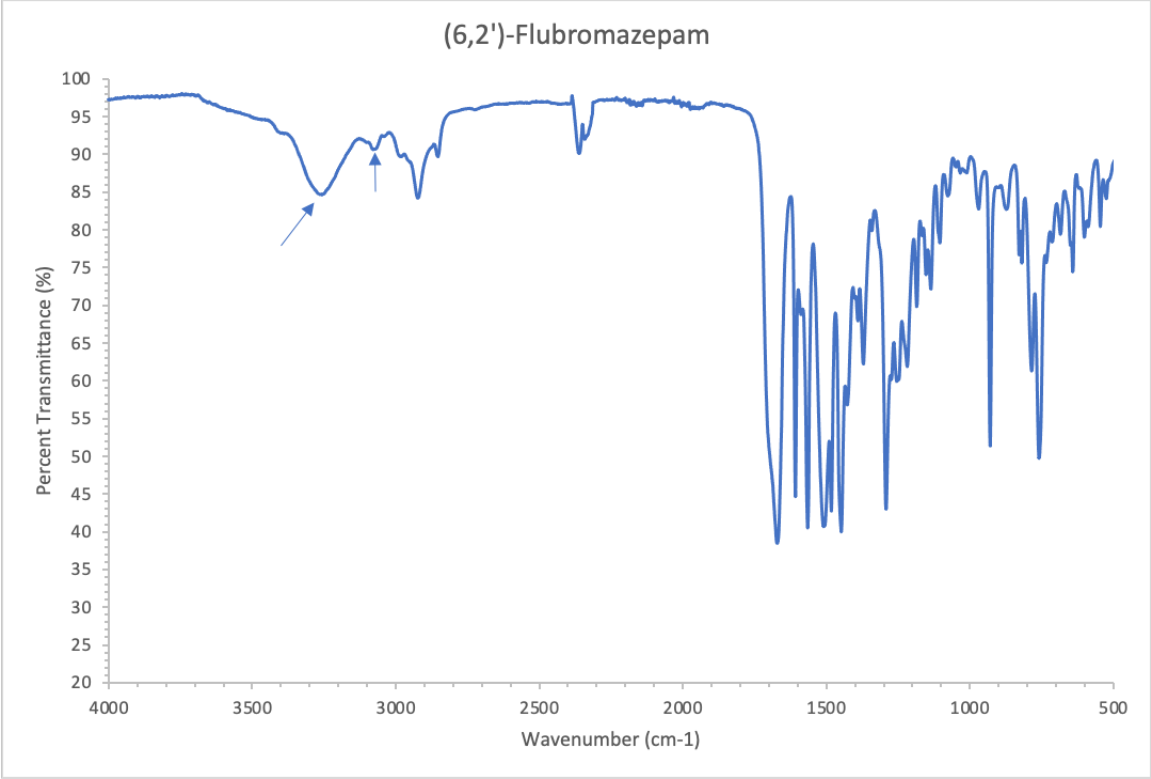
(6,2')-Flubromazepam
Percent Transmittance (%)
100
95
90
85
80
75
70
65
60
55
50
45
40
35
30
25
20
4000
3500
3000
2500
2000
1500
1000
500
Wavenumber (cm-1)

4.4 References

(1) Harper, L.; Powell, J.; Pijl, E. M. An Overview of Forensic Drug Testing Methods and Their Suitability for Harm Reduction Point-of-Care Services. *Harm Reduct. J.* **2017**, *14* (1), 52.

(2) Tsai JSC, Lin GL. Drug-testing technologies and applications. In: Wong RC, Tse HY, editors. Drug-testing technologies and applications. Totowa: Humana Press; 2005. p. 29–69.

(3) Gallardo, E.; Barroso, M.; Queiroz, J. A. LC-MS: A Powerful Tool in Workplace Drug Testing. *Drug Test. Anal.* **2009**, *1* (3), 109–115.

(4) (a) Chèze, M.; Villain, M.; Pépin, G. Determination of Bromazepam, Clonazepam and Metabolites after a Single Intake in Urine and Hair by LC–MS/MS: Application to Forensic Cases of Drug Facilitated Crimes. *Forensic Sci. Int.* **2004**, *145* (2), 123–130. (b) Rice, K.; Hikin, L.; Lawson, A.; Smith, P. R.; Morley, S. Quantification of Flualprazolam in Blood by LC–MS-MS: A Case Series of Nine Deaths. *J. Anal. Toxicol.* **2021**, *45* (4), 410–416. (c) Pettersson Bergstrand, M.; Helander, A.; Beck, O. Development and Application of a Multi-Component LC–MS/MS Method for Determination of Designer Benzodiazepines in Urine. *J. Chromatogr. B* **2016**, *1035*, 104–110. (d) Moosmann, B.; Bisel, P.; Auwärter, V. Characterization of the Designer Benzodiazepine Diclazepam and Preliminary Data on Its Metabolism and Pharmacokinetics. *Drug Test. Anal.* **2014**, *6* (7–8), 757–763.

(5) Bartick, E. G. Applications of Vibrational Spectroscopy in Criminal Forensic Analysis. In *Handbook of Vibrational Spectroscopy*; 2002; pp 1–13.

(6) (a) Zhong, Y.; Huang, K.; Luo, Q.; Yao, S.; Liu, X.; Yang, N.; Lin, C.; Luo, X. The Application of a Desktop NMR Spectrometer in Drug Analysis. *Int. J. Anal. Chem.* **2018**, *2018*. (b) Reitzel, L. A.; Dalsgaard, P. W.; Müller, I. B.; Cornett, C. Identification of Ten New Designer Drugs by GC-MS, UPLC-QTOF-MS, and NMR as Part of a Police Investigation of a Danish Internet Company. *Drug Test. Anal.* **2012**, *4* (5), 342–354. (c) Duffy, J.; Urbas, A.; Niemitz, M.; Lippa, K.; Marginean, I. Differentiation of Fentanyl Analogues by Low-Field NMR Spectroscopy. *Anal. Chim. Acta* **2019**, *1049*, 161–169. (d) Keizers, P. H. J.; Bakker, F.; Ferreira, J.; Wackers, P. F. K.; van Kollenburg, D.; van der Aa, E.; van Beers, A. Benchtop NMR Spectroscopy in the Analysis of Substandard and Falsified Medicines as Well as Illegal Drugs. *J. Pharm. Biomed. Anal.* **2020**, *178*, 112939. (e) Huppertz, L. M.; Bisel, P.; Westphal, F.; Franz, F.; Auwärter, V.; Moosmann, B. Characterization of the Four Designer Benzodiazepines Clonazolam, Deschloroetizolam, Flubromazolam, and Meclonazepam, and Identification of Their in Vitro Metabolites. *Forensic Toxicol.* **2015**, *33* (2), 388–395.

(7) (b) Kirby, A. J.; Komarov, I. V; Feeder, N. Synthesis, Structure and Reactions of the Most Twisted Amide. *J. Chem. Soc. Perkin Trans. 2* **2001**, No. 4, 522–529. (b) J. Kirby, A.; V. Komarov, I.; Kowski, K.; Rademacher, P. Distortion of the Amide Bond in Amides and Lactams. Photoelectron-Spectrum and Electronic Structure of 3,5,7-Trimethyl-Azaadamantan-2-One, the Most Twisted Amide. *J. Chem. Soc. Perkin Trans. 2* **1999**, No. 7, 1313–1316.

CHAPTER 5. FURTURE OUTLOOKS AND CONCLUSION

5.1 Conclusion

Highlighted in this thesis are synthetic strategies established to access a library of privileged scaffolds pertaining to the heterocyclic seven-membered ring systems for medicinal chemistry and forensic analysis. This work expands the synthetic "toolbox" and gives access to cyclohepta[*b*]indoles and the 1,4-benzodiazepine, flubromazepam. In route to cyclohepta[*b*]indoles, we found that the catalytic formal [5+2] cycloaddition reaction tolerates a broad scope. Thus, leading to an unexpected pathway and the discovery of novel bicyclo[3.2.2]nonane cyclohepta[*b*]indole derivatives though a proposed divinyl iminium intermediate. Regarding flubromazepam, we have successfully prepared the once elusive (6,X')-isomers to complete the set of possible flubromazepam positional isomers. This was done through the investigation of two different modular approaches toward the key *ortho*-aminobenzophenone intermediate. Through this methodology, proof of concept was established for use of a thioether as a removable directing group for Friedel-Crafts acylation but ultimately was unsuccessful toward the (6,X')-isomers. Gratifyingly, we achieved the key *ortho*-aminobenzophenone precursors through an aryl Grignard attack on a *o*-nitrobenzaldehyde followed by an oxidation-reduction sequence. This modular strategy can now be applied to the synthesis of other halogen-containing designer benzodiazepines and their isomers. Lastly, we were able to obtain characterization data for the newly synthesized (6,X')-flubromazepam positional isomers. The analytical profile established for each (6,X')-isomer through LCMS, FTIR, and NMR was compared to the parent flubromazepam isomer and a forensic protocol to differentiate between each has been

demonstrated. It is my hope that the completed work and concepts described herein lead to a better understanding of medicinal chemistry and forensic science.

5.2 Exploring the Synthetic Utility of the Divinyl Iminium Intermediate

Chapter 2 explored the formal [5+2]-cycloaddition methodology toward the formation of cyclohepta[*b*]indoles, a privileged scaffold found in many natural products and pharmaceutically relevant compounds. This methodology tolerated a broad scope using mono- and disubstituted aryl alkenes to give a variety of highly functionalized cyclohepta[*b*]indole derivatives in moderate to excellent yields. In addition, when either phenyl vinyl sulfide or ether were employed, an unanticipated chemodivergence was observed affording bicyclo[3.2.2]nonane cyclohepta[*b*]indoles. Products of this type were presumably formed from the expected [5 + 2] cycloaddition product following PhXH elimination to form a divinyl iminium intermediate, which undergoes an unprecedented [5 + 2] cycloaddition. This divinyl iminium intermediate is interesting because of the way in which it is formed off the indole moiety. Most instances of the formation of this type of intermediate occur through the reaction of a divinyl ketone with an amine. Thus, we envisioned recreating this reactive intermediate in order to investigate its synthetic utility.

Based on previous cyclopropane studies established by the France lab and the findings from the work discussed in Chapter 2, it is hypothesized that this intermediate can be recreated through the reaction presented in Scheme 5.1A. Upon activating the alpha heteroatom alkenyl phenyl (thio)ether cyclopropyl ketoester **1** with a Lewis acid, cyclopropane ring opening will occur to give carbocation **I.** Carbocation **I** will then be trapped through an intramolecular Friedel Crafts type alkylation, then through assumed

Lewis acid activation of the phenyl (thio)ether, C-X bond cleavage will follow providing the cationic divinyl iminium intermediate **II**. Through the addition of an olefin, we hope to trap intermediate **II** through a subsequent [5+2] cycloaddition to produce **2** (Scheme 5.1B).

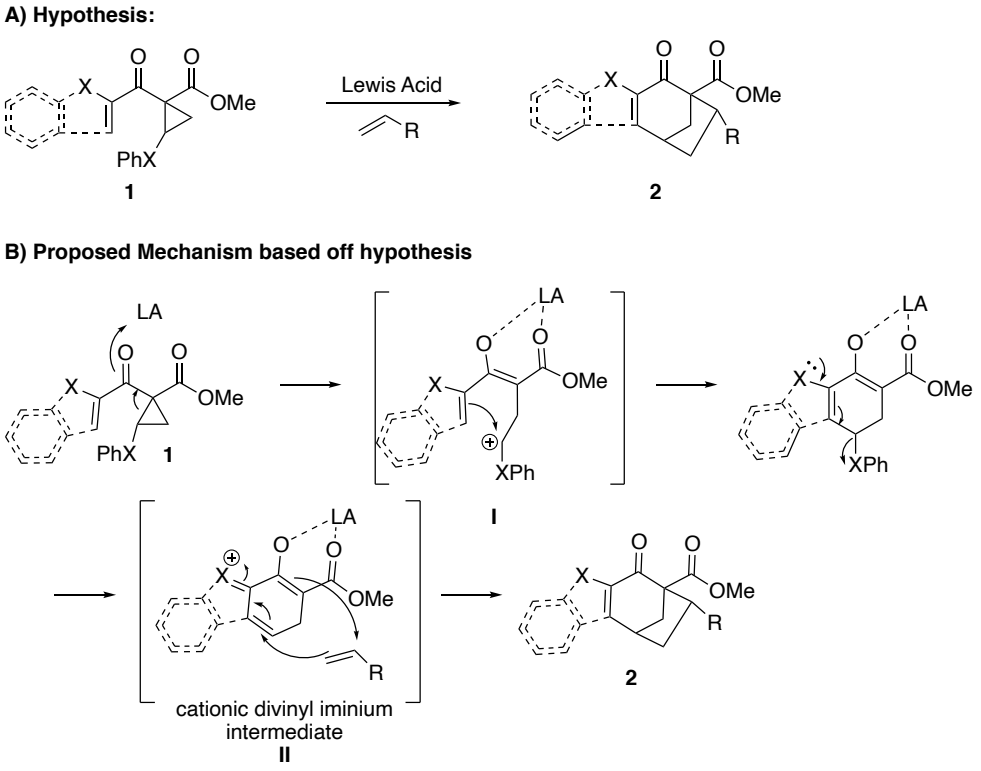

Scheme 5.1 Proposed Synthetic Strategy to Investigate the Divinyl Iminium Intermediate

5.3 Staying ahead of the Game: Proposed Synthesis of Flubromazolam from Flubromazepam

Flubromazolam is a triazole analogue of the designer benzodiazepine, flubromazepam. Currently, flubromazolam can simply be purchased on the internet and is used as a recreational drug in the United States except in the state of Virginia where it is classified under Schedule I. As a result, flubromazepam has been identified in an increasing number of drug overdose deaths and law enforcement seizures. A Federal Register Notice

(Vol. 86, No. 31) dated February 18, 2021, invited people to submit comments on whether this substance among others should be evaluated for scheduling (federal control). The parent drug could soon become federally regulated and depending on the Schedule it falls under; it's positional isomers could still be technically legal alternatives. Synthesizing and obtaining analytical reference data would help keep forensic institutions "ahead of the game". It is envisioned that flubromazolam can be achieved through a one pot reaction from flubromazepam from one or both methods shown in Scheme 5.7. Upon the successful synthesis of flubromazolam and its positional isomers investigating the general pharmacology, toxicology, and obtaining analytical characterizations through traditional forensic techniques would further expand the knowledge of this substance.

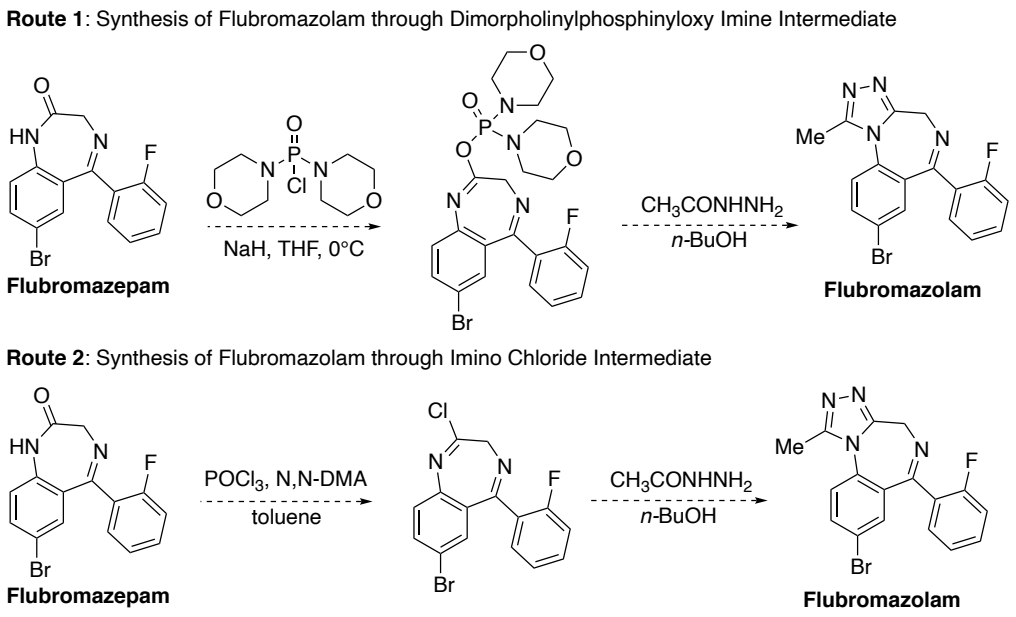

Scheme 5.2 Proposed Syntheses of Flubromazolam

5.4 Future Outlook for Forensic Differentiation of Flubromazepam

To date, all 12 of the positional isomers of flubromazepam have been prepared and characterized by using traditional forensic analytical techniques, including gas chromatography–electron ionization mass spectrometry (GC-EI-MS), gas chromatography–solid phase infrared spectroscopy (GC-IR), liquid chromatography mass spectrometry, Fourier Transform Infrared Spectroscopy (FTIR), and less conventional nuclear magnetic resonance (NMR). This data for each isomer is currently being analyzed in hopes that each isomer presents a unique analytical profile for the purpose of differentiation. Through this model study we hope to implement a standard analytical protocol for the differentiation of positional isomers of known designer benzodiazepines through routine forensic drug analysis.

APPENDIX I. EXPLORATION OF THE DIVINYL IMINIUM INTERMEDIATE: ATTEMPTED SYNTHESES OF THE MODEL SUBSTRATE

I. Background

The divinyl iminium intermediate proposed in Chapter 2 was envisioned to be recreated through the hypothesized reaction presented in Scheme 5.1A. This hypothesis is based on previously established cyclopropane methodology by the France lab[1] where they describe a catalytic homo-Nazarov cyclization of cyclopropyl heteroaryl ketones and the chemodivergent findings in Chapter 2. Throughout the literature, the divinyl iminium intermediate is typically formed through the reaction of a divinyl ketone with an amine[2] conversely, we envision studying the divinyl iminium intermediate through the reaction of a cyclopropane and an alkene.

II. Attempted Syntheses Toward the Model Substrate

Toward this end, attempts at synthesizing the desired cyclopropane starting material to establish proof of concept has proven to be challenging. There are many efficient ways to synthesis cyclopropanes, and in this case, we must find the appropriate conditions that tolerate the -XPh group off the donor-acceptor-acceptor cyclopropane system we desire. The methods attempted regarding the desired model substrate are displayed herein. We first sought to prepare the desired cyclopropane substrate through the Corey-Chaykovsky reaction.[3] This method proceeds through the generation of a sulfonium ylide that then nucleophilically attacks highly polarized double bonds to produce cyclopropanes. The

desired precursor **7** was synthesized through the synthetic approach in Scheme I.2 and subjected to the Corey-Chaykovsky conditions, but unfortunately resulted in no desired product being formed. This is likely due to the strong electron donating ability of the thiophenyl group decreasing the required electrophility of the system for cyclization.

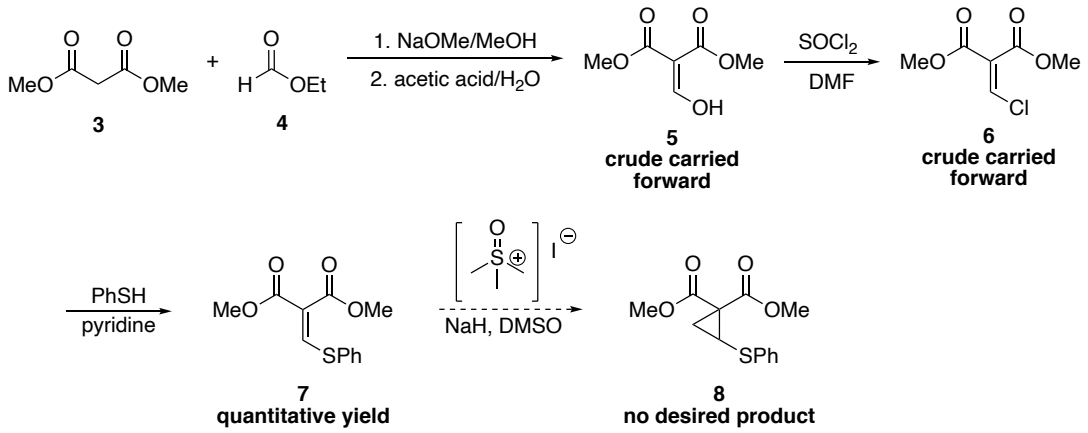

Scheme I.1 Attempted Synthesis of Cyclopropane Model Substrate Through Corey-Chaykovsky Reaction

The donor-acceptor-acceptor cyclopropane precursor envisioned for this transformation is thought to be more reactive than the aryl substituted cyclopropane precursors used in previous France lab methodologies.[4] In order to temper this increased reactivity, we sought to employ the *gem*-dimethyl effect which is known to decrease the ring strain energy of small rings and in turn decrease the reactivity.[5] We sought to prepare the desired cyclopropane through the synthesis shown in Scheme I.2A. The formation of cyclopropane **12** was successful resulting in a 30% yield, unfortunately this reaction didn't tolerate scale-up and ultimately was abandoned. Instead, we attempted to directly synthesis the desired cyclopropane off the indole moiety. Regrettably, upon bromination, no brominated product was observed, instead cyclized product **16** was formed (Scheme I.2B).

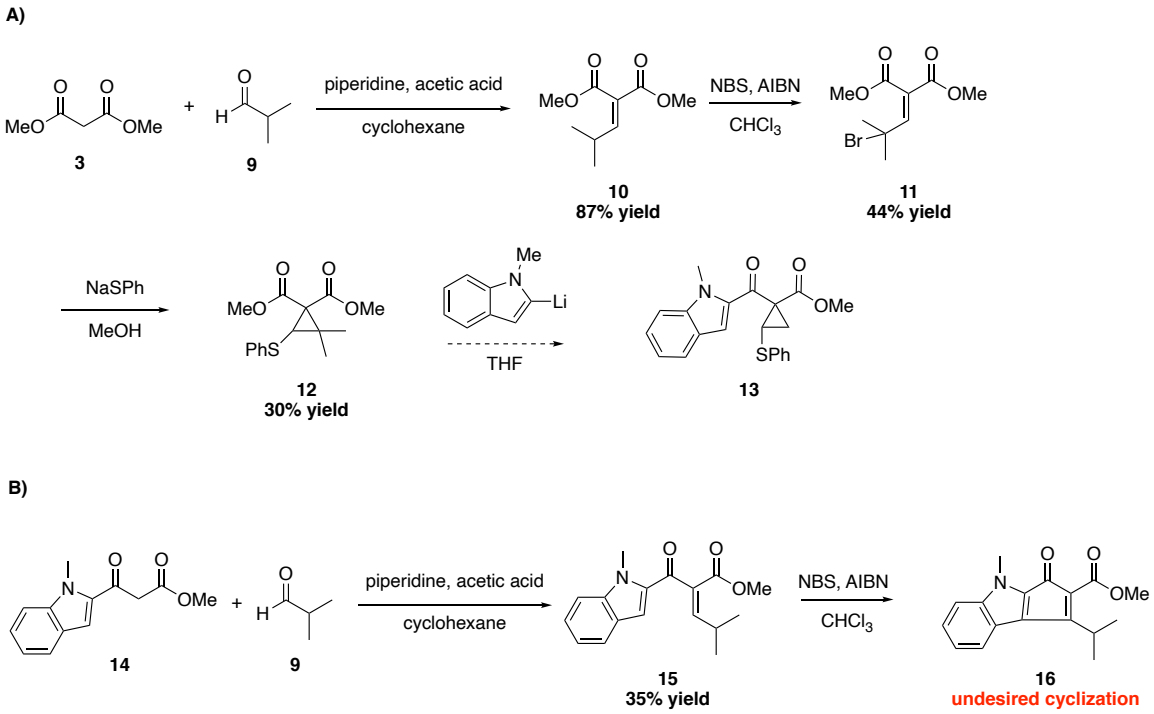

Scheme I.2 Attempted Synthesis of *Gem*-dimethyl Cyclopropane Model Substrate

One of the most popular methods to generate cyclopropanes is through the diazo degradation to form metal carbenoids.[6] The diazo method is advantageous due to 1) high functional group tolerance 2) low catalyst loading and 3) ease of setup. There is also literature precedent for the cyclopropanation with phenyl vinyl ether of diazodimethylmalonate[7] and as the literature suggested we were able to achieve the desired cyclopropane precursor **18** in 41% yield (Scheme I.3A). However, in route to the model substrate, lithiate addition of the indole to the dimethylmalontate cyclopropane system failed as only starting material was recovered. It is believed that the lack of reactivity is due to the quenching of the lithiate by the relatively acidic proton on the cyclopropane ring because of the -OPh substituent. To circumvent this issue, we attempted to first tether the diazo to the indole beta-keto ester **20** then cyclize, but this method failed to give any desired product also (Scheme I.3B).

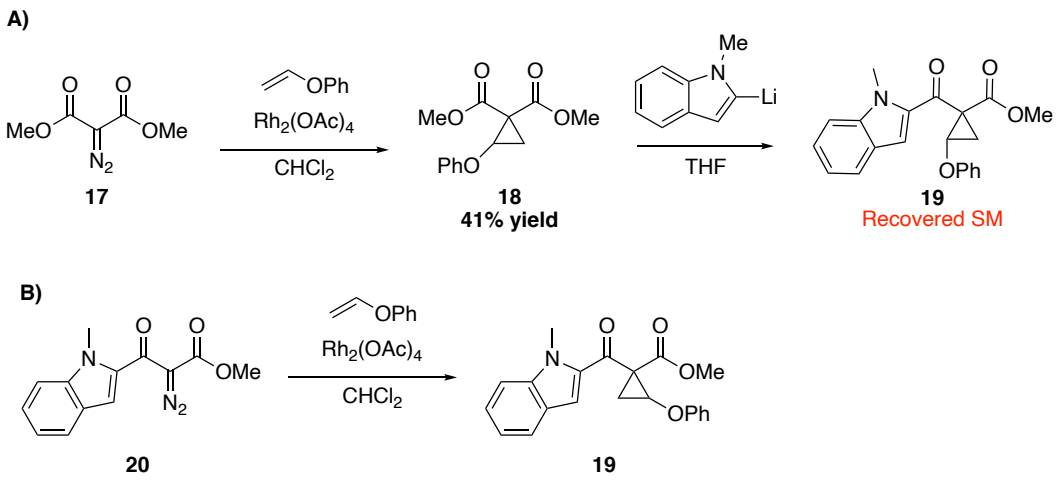

Scheme I.3 Attempted Synthesis of Cyclopropane Model Substrate Through Diazo Chemistry

Tethering the cyclopropane precursor to the indole moiety in the previous synthetic sequence proved to be unsuccessful resulting in recovered starting material. As a last effort to get around this issue, an adapted synthesis of Nishii's Reformatsky reaction[8] described in Scheme I.4 could be applied. This method would eliminate the need to use a highly reactive and basic lithiate and instead utilize an indolyl acid chloride **23**. The success of this reaction would expand the scope of the Reformastsky reaction and after many attempts provide the model substrate for the desired methodology. If this methodology is viable through the cyclopropane model substrate, it would expand the range and reactivity of cyclopropane ring-opening/ring-closing cyclizations and contribute another reactive intermediate to the synthetic community.

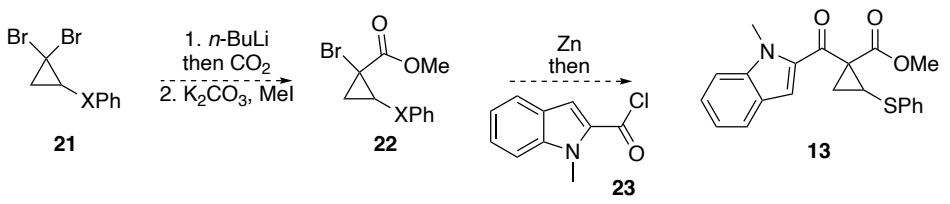

Scheme I.4 Proposed Synthetic Route Toward the Model Cyclopropane Substrate

Although the synthesis of the desired cyclopropane substrate envisioned for this study has presented various challenges, there are other ways to investigate the synthetic utility of the divinyl iminium intermediate. One way is by testing various vinyl (thio)-ether substrates with the indolyl alkylidene beta ketoester system in order to understand which substrates are best suited for this transformation (Scheme I.5). It would also be interesting to see if this transformation is tolerant of other heteroatoms. This investigation could provide an expansion of scope for the formal [5+2] cycloaddition reaction as well as give a better understanding of the reactivity of the divinyl iminium intermediate.

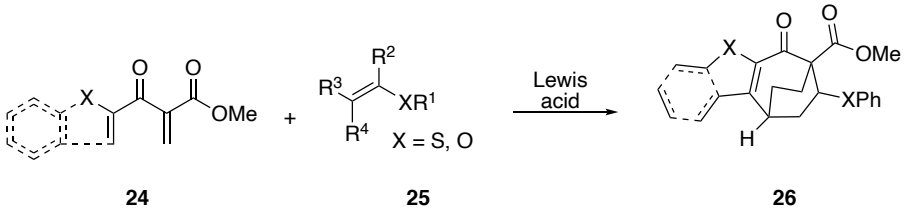

Scheme I.5 Proposed Exploration of Divinyl Iminium Intermediated Through Formal [5+2] Cycloaddition Using Substituted Vinyl (Thio)-ethers

III. Summary

In conclusion, we show initial results for the synthesis of the model cyclopropane substrate in route to the exploration of the synthetic utility of the divinyl iminium

intermediate. Although many were unsuccessful, a new synthetic scheme has been proposed that will potentially mitigate the issue described herein.

IV. Reference

(1) Phun, L. H.; Patil, D. V; Cavitt, M. A.; France, S. A Catalytic Homo-Nazarov Cyclization Protocol for the Synthesis of Heteroaromatic Ring-Fused Cyclohexanones. *Org. Lett.* **2011**, *13* (8), 1952–1955.

(2) Hamilton, J. Z.; Kadunce, N. T.; McDonald, M. D.; Rios, L.; Matlin, A. R. Hydroxylamine Catalyzed Nazarov Cyclizations of Divinyl Ketones. *Tetrahedron Lett.* **2015**, *56* (47), 6622–6624.

(3) Corey, E. J.; Chaykovsky, M. Dimethyloxosulfonium Methylide ((CH3)2SOCH2) and Dimethylsulfonium Methylide ((CH3)2SCH2). Formation and Application to Organic Synthesis. *J. Am. Chem. Soc.* **1965**, *87* (6), 1353–1364.

(4) (a) Martin, M. C.; Patil, D. V; France, S. Functionalized 4-Carboxy- and 4-Keto-2,3-Dihydropyrroles via Ni(II)-Catalyzed Nucleophilic Amine Ring-Opening Cyclizations of Cyclopropanes. *J. Org. Chem.* **2014**, *79* (7), 3030–3039. (b) Patil, D. V; Cavitt, M. A.; Grzybowski, P.; France, S. An Efficient Synthesis of Hydropyrido[1,2-a]Indole-6(7H)-Ones via an In(Iii)-Catalyzed Tandem Cyclopropane Ring-Opening/Friedel–Crafts Alkylation Sequence. *Chem. Commun.* **2011**, *47* (37), 10278–10280. (c) Patil, D. V; Phun, L. H.; France, S. Indium-Catalyzed Homo-Nazarov Cyclizations of Alkenyl Cyclopropyl Ketones. *Org. Lett.* **2010**, *12* (24), 5684–5687.

(5) Bachrach, S. M. The Gem-Dimethyl Effect Revisited. *J. Org. Chem.* **2008**, *73* (6), 2466–2468.

(6) Davies, H. M. L.; Antoulinakis, E. G. Intermolecular Metal-Catalyzed Carbenoid Cyclopropanations. *Organic Reactions*. April 15, 2004, pp 1–326.

(7) Wallbaum, J.; Garve, L. K. B.; Jones, P. G.; Werz, D. B. Ring-Opening 1, 3-Halochalcogenation of Cyclopropane Dicarboxylates. *Org. Lett.* **2017**, *19* (1), 98–101.

(8) Sakuma, D.; Yamada, K.; Sasazawa, K.; Nishii, Y. Highly Stereoselective Carbon–Carbon Bond-Forming Reactions on Cyclopropane Rings Using 1-(Methoxycarbonyl) Cyclopropylzinc Bromides. Chem. Lett. **2015**, 44 (6), 818–820.